

Dissertation zur Erlangung des Doktorgrades der  
Fakultät für Chemie und Pharmazie der  
Ludwig-Maximilians-Universität München

**The Immunogenicity of Protein Aggregates:  
Studies on a Murine Monoclonal Antibody  
in Wild-Type Mice**

**Angelika Juliane Freitag**

aus Zwickau

**2012**

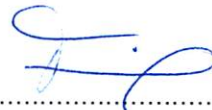
### **Erklärung**

Diese Dissertation wurde im Sinne von § 7 der Promotionsordnung vom 28. November 2011 von Herrn Prof. Dr. G. Winter betreut.

### **Eidesstattliche Versicherung**

Diese Dissertation wurde eigenständig und ohne unerlaubte Hilfe erarbeitet.

München, den 16.08. 2012



.....  
Angelika Freitag

Dissertation eingereicht am: 02.10.2012

1. Gutachter: Prof. Dr. G. Winter

2. Gutachter: Prof. Dr. W. Frieß

Mündliche Prüfung am: 09.11.2012

**For my parents and  
my brother**



# ACKNOWLEDGEMENTS

---

The present thesis was prepared at the Department of Pharmacy, Pharmaceutical Technology and Biopharmaceutics at the Ludwig-Maximilians-University (LMU) in Munich, Germany under the supervision of Prof. Dr. Gerhard Winter.

First and foremost, I would like to express my deepest gratitude to my supervisor Prof. Dr. Gerhard Winter, who gave me the opportunity to join his research group and to work in the fascinating field of protein pharmaceuticals. I want to thank him for his outstanding professional and enthusiastic guidance throughout this study and all the valuable advices that always encouraged and inspired me. I very much appreciated the numerous opportunities to present my work on congresses all over the world and the realization of my research stay in Colorado.

I want to thank Prof. Dr. Wolfgang Frieß for his continuous enthusiasm and interest in my work, the scientific input and advice over the last years and for kindly being co-referee of this thesis.

I would like to thank both of you, Prof. Winter and Prof. Frieß for the great efforts to provide excellent technical equipment and a pleasant working climate that made the development of this thesis not just possible, but a fulfilling and exciting time.

I want to thank Dr. Sandra Schulze for her supervision and great support during the first months of this work. She excellently introduced me in the numerous analytical techniques and provided dedicated guidance at any time.

I am indebted to Dr. Julia Myschik, who took over the supervision and was great help during preparation and performance of the animal studies.

Many thanks to my cooperation partners from the University of Colorado: Prof. Dr. Theodore W. Randolph, Prof. Dr. John F. Carpenter and Maliheh Shomali for the cooperation and scientific input and thank you for the warm welcome during my research stay.

Abbott GmbH & Co. KG is gratefully acknowledged for scientific and financial support, providing materials and enabling the realization of animal studies in Ludwigshafen. I am deeply grateful to Dr. Michael Siedler, Dr. Zehra Kaymakcalan and Dr. Hans-Jürgen Krause for their continuous support during this project. Besides I want to thank all colleagues that contributed to this thesis and assisted the study in Ludwigshafen; especially Dr. Ralf Löbbert, Ernst-Friedrich Spilger, Dr. Silke Weber, Dr. Günter Blaich, Ute Dressler, Karl-Heinrich Bolz and Dr. Julia Pieh.

From the Department of Pharmacology of the LMU in Munich, I would like to thank Prof. Dr. Martin Biel and Dr. Stylianos Michalakis for the great collaboration with the animal studies.

From the Department of Pharmaceutical Biology of the LMU in Munich, I would like to thank Prof. Dr. A. Vollmar for her scientific support and the possibility of conducting FACS measurements in her laboratories.

The student assistants Katharina Wittmann, Isabell Immohr and Susanne Anzer are acknowledged for the good job they have done. It was a pleasure to work with you.

Many thanks are expressed to all the colleagues from the research groups of Prof. Winter and Prof. Frieß who shared the time here in Munich with me, for support and numerous activities in daylight and night time. I want to deeply thank my lab-mate Thomas Bosch for the exciting time we had, for the music, for all the help during day and night sessions in the lab, for many fruitful discussions, making jokes, always providing a pleasant atmosphere and becoming a very close friend. Special thanks to Elsa Etzl, Markus Hofer, Sebastian Hertel, Raimund Geidobler, Veronika Spalthoff and Gerhard Sax, for all the help and support, the great time in the labs and for the numerous activities also outside university.

I want to thank my friends at home, from studying and from Badminton for their continuous friendship during the last years: Katja, André, Franziska, André, Anja, Silvia, Marina, Sepp and all others.

Finally, and most important I want to thank my wonderful family and especially my parents and grandmother for their love, their dedicated encouragement, and support throughout my entire life. Many thanks to my brother and best friend Eckehard, your support and faith in me always encouraged me to go this way. Thanks to all of you for being a part of me.

Steffen, thanks a lot for your support and your patience over the past years, and most important for your continuous love. You are the best thing that ever happened to me.

# TABLE OF CONTENTS

---

<b>1 Objectives of the Thesis .....</b>	<b>1</b>
<b>2 Introduction.....</b>	<b>3</b>
2.1.1 Stability of therapeutic protein formulations .....	4
2.2.1 Mechanisms of protein aggregation .....	4
2.2.2 Factors inducing protein aggregation .....	6
2.2.3 Classification and conformation of protein aggregates .....	7
2.3.1 Detection of insoluble protein aggregates.....	9
2.3.1.1 Light obscuration .....	9
2.3.1.2 Microscopic methods.....	10
2.3.1.3 Light scattering methods.....	11
2.3.2 Detection of soluble protein aggregates .....	11
2.3.2.1 High performance size exclusion chromatography .....	12
2.3.2.2 Asymmetrical flow field-flow fractionation .....	12
2.3.2.3 Sodium dodecyl sulfate - polyacrylamide gel electrophoresis .....	15
2.3.2.4 Dynamic light scattering.....	15
2.4.1 Factors influencing immunogenicity .....	16
2.4.2 Responses of the immune system to therapeutic proteins .....	17
2.4.3 Impact of antibody induction .....	19
2.5.1 Structure of monoclonal antibodies .....	20
2.5.2 The pharmacokinetics of monoclonal antibodies .....	21
2.5.3 The market of monoclonal antibodies.....	22
<b>3 Aggregation Studies on A Human Monoclonal Antibody .....</b>	<b>33</b>
3.1.1 Temperature .....	33
3.1.2 Mechanical stress.....	34
3.1.3 Freeze-thaw stress .....	34
3.1.4 Light exposure .....	35
3.2.1 Materials.....	36
3.2.1.1 Human IgG1 antibody (huAb) .....	36
3.2.2 Methods to provoke protein instability .....	36

3.2.2.1	Stirring stress .....	36
3.2.2.2	Shaking stress.....	36
3.2.2.3	Freeze-thaw stress .....	36
3.2.2.4	Light exposure.....	37
3.2.2.5	Temperature stress .....	37
3.2.3	Methods to determine protein stability .....	37
3.2.3.1	Light obscuration .....	37
3.2.3.2	Dynamic light scattering.....	37
3.2.3.3	Turbidity .....	38
3.2.3.4	Size exclusion chromatography .....	38
3.2.3.5	Intrinsic protein fluorescence spectroscopy .....	38
3.2.3.6	Extrinsic protein fluorescence spectroscopy.....	38
3.2.3.7	Fourier transform infrared spectroscopy (FTIR).....	39
3.2.3.8	High resolution UV absorbance spectroscopy .....	39
3.3.1	Mechanical stability of Human IgG1 antibody (huAb).....	40
3.3.2	Stability of huAb against freeze-thawing.....	47
3.3.3	Stability of huAb against light exposure .....	49
3.3.4	Stability of huAb against storage at elevated temperatures.....	56
<b>4</b>	<b>Aggregation Studies on A Murine Monoclonal Antibody .....</b>	<b>71</b>
4.2.1	Materials.....	72
4.2.1.1	Murine IgG2c antibody (muAb) samples .....	72
4.2.2	Methods to provoke protein instability .....	72
4.2.2.1	Stirring stress .....	72
4.2.2.2	Shaking stress.....	72
4.2.2.3	Light exposure.....	73
4.2.2.4	Temperature stress .....	73
4.2.3	Methods to determine protein stability .....	73
4.2.3.1	Light obscuration .....	73
4.2.3.2	Turbidity .....	73
4.2.3.3	Size exclusion chromatography .....	74
4.2.3.4	Intrinsic protein fluorescence spectroscopy .....	74
4.2.3.5	Extrinsic protein fluorescence spectroscopy.....	74



4.2.3.6	Fourier transform infrared spectroscopy (FTIR).....	74
4.2.3.7	High resolution UV absorbance spectroscopy .....	74
4.3.1	Formation of subvisible particles of the murine IgG2c antibody (muAb) .....	74
4.3.2	Formation of soluble aggregates of the murine IgG2c antibody (muAb) .....	76
4.3.3	Modifications in the structure of the murine IgG2c antibody (muAb).....	80
4.3.3.1	Structural modifications of muAb after stirring and shaking .....	80
4.3.3.2	Structural modifications of muAb after storage at 50°C .....	81
4.3.3.3	Structural modifications of muAb after light exposure .....	81
<b>5</b>	<b>Fractionation of Protein Aggregates of a Human Monoclonal Antibody by AF4 .....</b>	<b>87</b>
5.1.1	The use of asymmetrical flow field-flow fractionation (AF4) to separate protein aggregates .....	87
5.2.1	Sample preparation .....	89
5.2.2	Asymmetrical flow field-flow fractionation .....	89
5.2.3	Protein concentration by centrifugation .....	91
5.2.4	Micro BCA™ Protein Assay Kit .....	91
5.2.5	Sodium dodecyl sulfate – polyacrylamide gel electrophoresis .....	92
5.2.6	Size exclusion chromatography .....	92
5.3.1	Characterization of the samples .....	92
5.3.2	Collection of protein species after field-flow fractionation .....	96
5.3.3	Increasing protein concentration within the fractions.....	98
<b>6</b>	<b>The Preparative Use of AF4 to Obtain Endotoxin-free Protein Species .....</b>	<b>109</b>
6.2.2	Asymmetrical flow field-flow fractionation .....	111
6.2.3	Protein concentration by centrifugation .....	111
6.2.4	Determination of endotoxin level .....	112
6.3.1	Preparation of instrument, samples and buffer solutions.....	112
6.3.2	Field-flow fractionation of mouse IgG2c .....	113
6.3.3	Collection and concentration of protein species after AF4 separation .....	114
<b>7</b>	<b>The Need for Immune Complex Dissociation in Anti-Drug Antibody Detection .....</b>	<b>121</b>
7.2.1	Generation of protein aggregate test items.....	122
7.2.2	Size exclusion chromatography .....	123
7.2.3	Light obscuration .....	123
7.2.4	Endotoxin testing .....	123

7.2.5	Animals .....	123
7.2.6	Immunization protocol.....	124
7.2.7	Collection of blood samples .....	124
7.2.8	Determination of Anti-Drug Antibodies (ADAs) .....	124
7.2.8.1	Method A.....	125
7.2.8.2	Method B.....	125
7.2.9	Determination of drug levels in serum (pharmacokinetics, PK) .....	126
7.3.1	SEC Analysis of murine IgG2c after light exposure.....	126
7.3.2	Analysis of anti-drug antibody levels using two ELISA formats .....	127
7.3.3	Detection of serum levels of muAb – pharmacokinetics .....	135
<b>8</b>	<b>Investigations on the immunogenicity of protein aggregates of a murine monoclonal antibody in wild-type mice .....</b>	<b>143</b>
8.2.1	Materials.....	144
8.2.1.1	Murine IgG2c antibody (muAb) .....	144
8.2.1.2	Animals .....	144
8.2.2	Methods .....	144
8.2.2.1	Sample preparation .....	144
8.2.2.3	Asymmetrical flow field-flow fractionation (AF4) .....	146
8.2.2.4	Light obscuration (LO) .....	146
8.2.2.5	Turbidity measurements .....	146
8.2.2.6	Endotoxin testing.....	146
8.2.2.7	Fourier transform infrared spectroscopy (FTIR).....	146
8.2.2.8	Ultraviolet (UV) absorbance spectroscopy at 280 nm .....	146
8.2.2.9	Immunization protocol .....	146
8.2.2.10	Collection of blood samples .....	147
8.2.2.11	Determination of anti-drug antibodies (ADAs) .....	147
8.2.2.12	Determination of drug levels in serum (pharmacokinetics, PK) .....	147
8.2.2.13	Statistical analysis .....	147
8.3.1	Preparation and analysis of aggregates .....	148
8.3.2	Preparation and analysis of the adjuvant samples.....	150
8.3.3	Testing of the samples for the presence of endotoxins .....	150
8.3.4	Detection of immune response – Anti-drug antibodies towards muAb.....	150

8.3.4.1	anti-muAb antibodies in C57BL/6 mice .....	151
8.3.4.2	anti-muAb antibodies in BALB/c mice .....	154
8.3.4.3	Comparison of C57BL/6 mice and BALB/c mice .....	157
8.3.5	Detection of muAb circulating in the blood stream – pharmacokinetics .....	159
8.4.1	Pharmacokinetics of muAb .....	162
8.4.2	Immunogenicity of muAb in the control groups .....	163
8.4.3	Soluble aggregates of muAb .....	163
8.4.4	Insoluble aggregates of muAb.....	164
8.4.4.1	Aggregation by light exposure.....	165
8.4.4.2	Aggregation by mechanical stress .....	165
8.4.4.3	Aggregation by elevated temperature .....	166
8.4.5	Species differences .....	166
<b>9</b>	<b>Final Summary and Conclusions .....</b>	<b>171</b>
	<b>List of Abbreviations .....</b>	<b>I</b>
	<b>List of Presentations and Publications.....</b>	<b>VII</b>
	<b>Curriculum Vitae .....</b>	<b>IX</b>



# 1 OBJECTIVES OF THE THESIS

---

The overall aim of this thesis was to investigate the immunogenicity of antibody aggregates in wild-type animals.

This work dealt only with homogeneous aggregates, meaning aggregates that consist only of protein drug but not of foreign substances such as glass particles or silicone oil droplets. With regard to anti-drug antibody formation some crucial points of protein aggregation were touched: the size of aggregates, the conformation and structural changes of the protein were investigated with regard to the induced immune response.

First of all, stress methods that can trigger aggregation of the protein drug had to be evaluated. The work focused on monoclonal antibodies, which currently are the largest category of biopharmaceuticals. Antibodies seem to be more stable than many other proteins, thus suitable conditions for aggregation had to be found. On the one side the applied conditions needed to be relevant for processing and handling steps a protein might suffer from. Therefore, methods resembling steps during production (such as stirring), during shipment and storage (such as freeze-thawing, light exposure, and elevated temperatures), and during handling (such as shaking) were chosen to induce aggregation. The suitability of the methods had to be estimated according to the amount of generated aggregates provoked by the respective stress. Since the immune response to the aggregates should be investigated, not the immunogenicity of the native drug or its fragments, a sufficient amount of aggregates had to be generated to enable separation from concomitant native protein species.

The separation of aggregates was the second major aim of this thesis. If sufficient amounts of soluble aggregates are gained by any stress method, a method to fractionate them from the monomeric protein needed to be established. Ideally, asymmetric flow field-flow fractionation (AF4) or size exclusion chromatography would be used. Particulate aggregates have to be separated from soluble species as well. The separated aggregates had to be physicochemically characterized to the extent possible before being used in animal studies.

The final and pivotal aim of this work was the immunogenicity investigation of separated aggregates of a monoclonal antibody *in vivo*. Therefore, a proper animal model had to be found and suitable analytical methods to detect immune responses had to be developed. A murine monoclonal antibody was used in a mouse model, thus no transgenic animals were needed. It was aimed to relate the immune response to the characteristics of the aggregates. If differences in the immunogenic potential of aggregates would be detected, a classification of protein aggregates of a monoclonal antibody with respect to their immunogenicity would be possible for the first time.



## 2 INTRODUCTION

---

### 2.1 BIOPHARMACEUTICALS

The outstanding advances in recombinant DNA techniques and biotechnology during the last decades enabled the large-scale production and facilitated the development of highly purified recombinant therapeutic proteins, a new class of drugs. In 1982, human insulin (Humulin, Genentech), the first recombinant engineered protein for therapeutic use, was approved. Since that time numerous products of biotechnological origin entered the market and now make up to 30% of the marketed drugs [Brinks *et al.*, 2011]. Furthermore, large numbers of protein drugs are in development [Leader *et al.*, 2008]. The market for “biopharmaceuticals” is still fast growing and their chance of success is estimated to be much higher compared to conventional synthetic chemical drugs [Pavlou *et al.*, 2005; Pavlou *et al.*, 2004]. In general, biopharmaceuticals encompass products based on cell or tissue-engineering as well as nucleic-acid products, besides the above mentioned recombinant therapeutic proteins [Walsh, 2010]. For the purpose of this work the term “biopharmaceutical” is referred to as therapeutic proteins.

Therapeutic proteins benefit from their extremely high activity and specificity at low concentrations [Wang, W., 1999], thus resulting in minimized side effects. These promising molecules are nowadays widely used as therapeutics, mainly in the treatment of life-threatening and severe diseases particularly in the field of oncology, auto-immunogenicity, and inflammation [Berger *et al.*, 2002; Walsh, 2006]. They should either modify a disease process or adjust a deficiency of a native human protein; either inherited or acquired [Van Regenmortel, 2001].

The main difference of therapeutic proteins to the conventional chemical drugs is their molecular weight. Therapeutic proteins consist of long polypeptide chains and usually possess molar masses of several kDa, whereas the molar mass of chemical drugs is usually below 1 kDa. The complex and delicate structure of protein therapeutics is subject to a variety of instabilities and degradation pathways that may occur during development, production, and handling. This implicates a wealth of engineering challenges to achieve a convenient, stable, and safe formulation [Frokjaer *et al.*, 2005; Randolph *et al.*, 2007]. The most obvious challenge concerns the insufficient oral availability of protein drugs. Firstly, proteins are not resistant against enzymatic and hydrolytic degradation in the gastrointestinal (GI) tract. Secondly, due to their features of a hydrophilic surface and a high molar mass, proteins are not able to pass the membranes in the GI-tract and therefore resorption and bioavailability are poor. Except very few products, proteins are administered parenterally in form of aqueous solutions or suspensions.

### 2.1.1 Stability of therapeutic protein formulations

The poor stability of the proteins' structural composition pose challenges to maintain stability throughout their shelf-life which is typically between 18 - 24 months at 2-8°C [Chang *et al.*, 2002; Randolph *et al.*, 2007]. The possible degradation pathways proteins can undergo are manifold and are generally subdivided in chemical and physical degradation [Bee *et al.*, 2011; Mahler *et al.*, 2009; Manning *et al.*, 1989; Wang, W., 1999]. Changes of the structure of the protein including the loss or the formation of new covalent bonds are referred to as chemical degradation [Liu *et al.*, 2008; Manning *et al.*, 1989]. The large numbers of functional groups within the amino acid sequence make proteins prone to various chemical reactions. The most common chemical degradation pathways proteins can undergo are deamidation, oxidation, aspartate isomerization, disulfide bond formation, and breakage, and hydrolysis of the peptide bonds [Liu *et al.*, 2008; Shahrokh *et al.*, 1994; Wakankar *et al.*, 2007; Wang, 2005; Wang, W. *et al.*, 2006a; Yang *et al.*, 2007]. Besides the primary structure of the molecules, the therapeutic protein additionally has to maintain its native steric conformation in the higher order structure (secondary and above) to assure the correct binding to the site of action. Biological activity and efficacy essentially require a definite conformation. Physical degradation of proteins often leads to unfolding and misfolding of the protein, altering this conformation [Manning *et al.*, 1989; Wang, W., 1999]. Moreover, these partially or fully unfolded molecules are prone to interactions and can easily aggregate [Chi *et al.*, 2003a].

However, both types of protein degradation depend on each other and a clear classification is not always possible [Wang, 2005]. During the manufacturing and handling processes of therapeutic proteins many stages, such as production, filling, storage and shipping have to be passed. It is of utmost importance for the pharmaceutical industry and for the authorities to avoid any kind of degradation, assure chemical and conformational stability and finally to achieve stable formulations.

## 2.2 PROTEIN AGGREGATION

### 2.2.1 Mechanisms of protein aggregation

Aggregation is the most common physical instability of biopharmaceutical products and a major problem during their formulation, shipping and handling processes. Aggregation was first investigated and described more than 50 years ago by the Lumry-Eyring model [Lumry *et al.*, 1954]. In general, two different phenomena can be differentiated. "Protein aggregation" denotes the formation of irreversible oligomers from non-native species. The "self-association" of proteins merely includes the formation of small oligomers from native species, which are soluble and reversible upon dilution [Saluja *et al.*, 2008]. However, in general the term "protein aggregation" refers to any type of interaction between the protein molecules that lead to self-associated oligomers of higher molecular weight than the requested species [Singh, S.K. *et al.*,



2010]. Throughout this thesis the latter mentioned and more general definition will form the basis of the investigation and discussion.

According to the Lumry-Eyring model self-association is proposed to be linked to the existence of even low amounts of partially unfolded intermediate states of proteins (Figure 2-1), since the aggregation of such intermediate states of proteins are energetically favored [Wang, 2005].

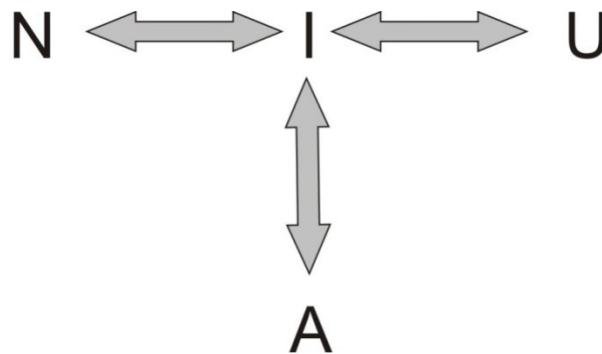


**Figure 2-1 – Lumry-Eyring model of protein self-association.**

The native protein (N) can form reversible unfolding intermediate states (I) which then can either form reversible unfolded states (U) or irreversible/reversible aggregates (A). [Manning *et al.*, 1989; Wang, 2005]

The transitional/intermediate species can be prone to association and aggregation [Lumry *et al.*, 1954]. The latter can be facilitated by (partial) unfolding, because patterns of contiguous hydrophobic side chains can initiate the process [Wang, 2005].

The pathways that protein aggregation underlies were investigated in more detail during the last decades. Five important aggregation mechanisms (1 – 5) were described by Philo and Arakawa [Philo *et al.*, 2009]. They classified these mechanisms concerning the conformation of the interacting protein molecules and the process of interaction. The first pathway (1) is based on a high propensity of the native monomer to reversibly associate in order to form small oligomers which might grow larger over time. Powered by the law of mass action, especially high protein concentration can accelerate oligomer growth and the formation of potentially irreversible larger aggregates can occur [Philo *et al.*, 2009]. Insulin is known to associate in this manner [Pekar *et al.*, 1972]. In the second pathway (2), the monomer has no clear tendency to associate in the native state. However, slight transient changes like partial unfolding (see Figure 1) can lead to an immense aggregation of the conformationally altered monomer. Factors that may precede and initially trigger the conformational alteration can be e.g. shearing or heating. This most dominant pathway of aggregation [Chi *et al.*, 2003a; Krishnamurthy *et al.*, 2002; Wang, 2005] was exemplarily shown to appear in G-CSF [Krishnan *et al.*, 2002] and interferon- $\gamma$  formulations [Kendrick *et al.*, 1998]. If the initial conformational alteration implies different covalent structures another pathway (3) can occur. The onset of this mechanism is based on chemical degradations, like deamidation, proteolysis or oxidation of tryptophan or methionine [Philo *et al.*, 2009; Roy *et al.*, 2009]. Similarly to the process of

crystal-growth, protein aggregates can also originate from nucleation processes (4). Nucleation is independent of the initial conformation of the interacting molecules and describes the increase in size and number of aggregates. At the same time the population of the monomer is decreasing. The growth of a “critical nucleus” of sufficient size can be very fast, due to a thermodynamically favored addition of monomers to these species [Philo *et al.*, 2009]. Therefore, a rapid formation of very large aggregates, which eventually might precipitate and form visible particles, is possible [Chi *et al.*, 2003a]. Usually, the formation of such large particles exhibits a lag-phase. Meanwhile, subvisible small oligomers arise. But when a certain size of the nucleus has been reached they appear rather suddenly [Philo *et al.*, 2009]. Such nucleation-controlled processes can either be “homogeneous” if the nucleus consists of protein molecules or “heterogeneous” if the nucleus is made from an impurity or contaminant such as stainless steel particles [Tyagi *et al.*, 2009], silica particles [Chi *et al.*, 2005] or silicone oil droplets [Jones *et al.*, 2005; Thirumangalathu *et al.*, 2009]. In general, the interaction of monomer molecules with such nuclei could be considered as interaction with a surface. Aggregation at interfaces (5) is another phenomenon that can occur in protein solutions during manufacturing. The trigger can either be an air-liquid interface, ice-water interface or a container surface [Cleland *et al.*, 1993; Mahler *et al.*, 2005; Wang, W., 1999].

### 2.2.2 Factors inducing protein aggregation

The aggregation phenomenon can be induced or affected by certain environmental conditions or simply with time. Wei Wang reviewed several key biopharmaceutical processes that are linked to protein aggregation. The phenomenon was observed in upstream processes, such as fermentation, downstream processes, such as purification, formulation process, such as drying and reconstitution, as well as during storage [Kiese, 2008; Wang, 2005]. The underlying physical stress principles the protein can be exposed to during manufacturing are manifold. Besides others, temperature variations during freezing and thawing [Cao *et al.*, 2003; Kuelto *et al.*, 2008], UV-light exposure during purification [Kerwin *et al.*, 2007; Qi *et al.*, 2009; Roy *et al.*, 2009] and the interactions with different types of solid surfaces [Mollmann *et al.*, 2005; Randolph *et al.*, 2007] or air-liquid interfaces [Chang *et al.*, 1996; Kiese, 2008] can trigger aggregation.

Each stress principle can result in different forms of aggregates. Temperature is the major factor affecting protein stability. In general proteins have melting temperatures ( $T_m$ ) between 40°C and 80°C [Wang, W., 1999]. When exposed to temperatures close to  $T_m$  the protein can become partially or completely unfolded and more prone to aggregation. Chemical degradation can be increased as well since the amino acid sequence can be altered by heat. Furthermore, Brownian motion, hydrophobic interactions and reaction kinetics are enhanced [Chi *et al.*, 2003a; Wang, 2005]. Generally it can be stated that an increase in temperature goes along with a decrease in protein stability. Thus, protein formulations are typically stored clearly below the unfolding temperature, meaning frozen or at 2 – 8°C [Kiese, 2008].

The exposure to light can occur at several stages during manufacturing. Chromatographic purification is usually monitored by absorption to UV light at 280 nm and every molecule of the eluting protein is exposed to that wavelength for a short period of time. During formulation and inspection operations the protein can be exposed to daylight or ambient light as well [Roy *et al.*, 2009]. Finally, the self-administration from patients entails insecurity of storage conditions including inadvertent light exposure. The chemical and physical stability of a protein can be affected by the absorption of light [Davies *et al.*, 2001; Kerwin *et al.*, 2007]. Aggregation and conformational changes of proteins are known to be triggered by light in the UV-B range (280 nm – 320 nm) [Kim *et al.*, 2007; Miller *et al.*, 2003; Prompers *et al.*, 1999]. The photoreactions within these studies mainly based on the irradiation of tryptophan (Trp) since it is the chromophore that is able to absorb light most efficiently in this region [Lakowicz, 1983]. Subsequently to the irradiation of Trp, disulfide bonds can be reduced and cleaved enabling the formation of new intermolecular bonds and crosslinking [Prompers *et al.*, 1999]. The underlying mechanism is not yet fully understood. However, the spatial proximity between the disulfide bond forming cysteine and aromatic residues like Trp is found in many proteins and can attribute to these observations [Petersen *et al.*, 1999].

Agitation stresses such as shaking, stirring, and pumping can lead to different types of aggregates as well [Kiese, 2008]. Volkin and Klibanov showed that shaking creates air/water interfaces. Due to their hydrophobicity protein molecules align at the interface, expose hydrophobic areas by unfolding and eventually aggregate [Volkin *et al.*, 1989]. Besides creating air/water interfaces stirring and pumping operations expose solid surfaces to the protein as well. Furthermore, these shearing processes may also change protein conformation and lead to transitional exposure of hydrophobic patches of the protein. Such mechanical stress leads often to the formation of non-covalent and native oligomers that can either be soluble or insoluble.

The amphiphilic properties of protein molecules cause a strong propensity to accumulate at interfaces. The air-water interface is very hydrophobic and the most important during manufacturing processes like agitation, pumping and filtration [Jones *et al.*, 1997; Kiese, 2008]. The majority of therapeutic proteins tend to adsorb at hydrophobic surfaces by partial unfolding. The interaction with a hydrophobic surface may entail the exposition of parts the hydrophobic core of the protein resulting in conformational changes [Chi *et al.*, 2005; Wang, W., 1999]. Vermeer *et al.* showed that the secondary structure of an immunoglobulin G significantly changed by adsorption to a surface [Vermeer *et al.*, 1998]. The high concentration of protein molecules with altered structures near/at the interface, can result in destabilization, and finally in aggregation processes [Carpenter, John F. *et al.*, 1999; Randolph *et al.*, 2002]

### **2.2.3 Classification and conformation of protein aggregates**

Depending on the aggregation mechanism and the type of protein, the properties of the resulting aggregates can strongly differ. A generally accepted classification of such protein aggregates differentiates between:

- a) covalent and non-covalent aggregates
- b) reversible and irreversible aggregates
- c) soluble and insoluble aggregates
- d) native and non-native aggregates [Cromwell *et al.*, 2006; Kiese, 2008; Liu *et al.*, 2007; Mahler *et al.*, 2009]

Covalent aggregates originate from the formation of chemical bonds such as disulfide bridges between the native protein molecules, whereas non-covalent aggregates are formed by weak electrostatic or hydrophobic interactions, or hydrogen bonding [Demeule *et al.*, 2007]. During heat stress the formation of intermolecular anti-parallel  $\beta$ -sheet structures was observed in various proteins [Wang, 2005]. The underlying formation of hydrogen bonds between the molecules occurred independent from the initially existing secondary structure of the native molecule [Dong *et al.*, 1995]. During aggregation some amino acid chains and molecular regions of the protein might become accessible to the formation of new intermolecular interactions. Hydrophobic regions or free thiol-groups might be exposed at the proteins surface enabling association through non-covalent or disulfide bonds.

Especially the weak non-covalent interactions often lead to the formation of reversible protein aggregates, which might appear in equilibrium with the monomer depending on the environmental conditions in the formulation [Cromwell *et al.*, 2006]. Occasionally, these reversible self-association processes come along with an increase in viscosity of the solution [Liu *et al.*, 2005]. Reversible oligomers usually can be dissolved by dilution with buffer or during application. Instead, irreversible aggregates cannot be dissolved by dilution and no equilibrium with the monomer exists. Reversibility was shown by Patro and Przybycien 1996 to depend on the surface characteristics and the distribution of hydrophobic and hydrophilic patches of the protein [Patro *et al.*, 1996]. Soluble aggregates are mainly defined by a small size. Thus, they can be defined as non-visible and cannot be removed by a sterile filter having a 0.22  $\mu\text{m}$  pore size [Cromwell *et al.*, 2006]. In contrast, insoluble aggregates can be visible under specified inspection conditions and may be removed by filtration. However, there is no consistent borderline between these two types of aggregates [Cromwell *et al.*, 2006; Narhi *et al.*, 2009]. Aggregates that arose from an association of the native monomer usually form small reversible oligomers that are difficult to detect and quantify due to possible disruption of the oligomers during analysis [Demeule *et al.*, 2007; Philo *et al.*, 2009]. If the conformation of the underlying monomer is altered or it is chemically modified non-native aggregates might originate.

Though there is no distinct specification in the guidelines of USP or PhEur, the presence of even small amounts (> 1%) of any non-native protein species can be considered unacceptable for product release [Randolph *et al.*, 2007].

## 2.3 ANALYTICAL METHODS TO DETECT PROTEIN AGGREGATES

The sizes of protein aggregates cover a wide range: from small oligomers in nanometer range, starting with dimers, to large visible aggregates or precipitates of several  $\mu\text{m}$ . This makes it obviously impossible to find the one and only analytical tool that will give the complete answer about the product in all situations. However, controlling the aggregation process is of major concern for all biopharmaceutical products and therefore the development of reliable analytical methods is of utmost importance. The most critical problem with such methods is that many of these techniques have the potential to perturb the distribution of aggregates, altering their size and structure. Aggregates can be either destroyed or created for example by dilution or shear forces.

### 2.3.1 Detection of insoluble protein aggregates

Insoluble protein aggregates are large assemblies of protein species and for the purpose of this thesis defined as aggregates that are larger than  $0.1\ \mu\text{m}$  and therefore are usually not detectable during analysis like size exclusion chromatography (SEC) [Mahler *et al.*, 2009]. Zöls *et al.* and Narhi *et al.* defined species above  $0.1\ \mu\text{m}$  as particles [Narhi *et al.*, 2009; Zoells *et al.*, 2012]. Moreover, these large oligomers are subdivided in visible and subvisible particles. For the unaided eye particles of  $100\ \mu\text{m}$  and larger in size are visible. The resulting gap between  $0.1\ \mu\text{m}$  and  $100\ \mu\text{m}$  is commonly referred to the size of subvisible particles [Carpenter *et al.*, 2009; Narhi *et al.*, 2009; Sharma *et al.*, 2010; Singh, S.K. *et al.*, 2010; Zoells *et al.*, 2012]. The presence of visible aggregates is unacceptable for product release in general. For example the European Pharmacopoeia (PhEur) requires labels claiming "...without visible particles" or "...practically free from particles" and the Pharmacopoeia of the United States (USP) requests drug formulations "...essentially free from visible particulates". Besides, both Pharmacopoeias require clear limitations on subvisible particle numbers of  $\geq 10\ \mu\text{m}$  and  $\geq 25\ \mu\text{m}$  in size in parenteral pharmaceutical preparations [PhEur 2.9.19., 2011; USP/NF, 2008]. These guidelines originally evolved from potential safety issues like the occlusion of blood vessels after administration and immunogenicity, which may appear from the presence of larger particulates [Carpenter *et al.*, 2009; Narhi *et al.*, 2009].

#### 2.3.1.1 Light obscuration

The most widely used method to quantify subvisible particles is light obscuration (LO). The very fast and simple method is not capable of distinguishing between proteinaceous and non-proteinaceous particles or air bubbles but can be utilized to quantify particles between  $1$  and  $600\ \mu\text{m}$  [Zoells *et al.*, 2012]. Light obscuration instruments create a laser beam irradiating through a flow cell where particles are passing by. Each particle blocks part of the laser light depending on its cross-sectional area. Finally, a photo diode detector collects the residual light of the beam. This principle entails a restricted particle concentration within the sample, since overloading would lead to interference of the particles and miscounting. Another downside of

LO analysis of therapeutic protein formulations for quality control, is the huge required volume of 25 mL per analysis in PhEur as well as USP [PhEur 2.9.19., 2011; USP/NF, 2008]. That usually entails pooling of several vials and makes the measurement cost-intensive. In general, the instruments are calibrated by polystyrene beads calculating the equivalent circular diameter of the analytes. However, these synthetic beads differ a lot from protein particles, concerning refractive index, shape and transparency. Thus, translucent analytes can even be missed, because parts of light still pass through these particles reaching the detector [Huang *et al.*, 2009].

#### 2.3.1.2 Microscopic methods

Several different microscopic techniques are available to detect and visualize particulate materials and protein aggregates. Due to the drawback of all microscopic methods to visualize only small fractions of the sample, the results of these methods are only representative when large volumes are analyzed, which makes this technique rather time consuming. The widely spread optical microscopy is limited to species larger than 1  $\mu\text{m}$  [Zoells *et al.*, 2012]. The PhEur and the USP have approved this technique for the quantification of subvisible particles [PhEur 2.9.19., 2011; USP/NF, 2008]. The particles are isolated by filtration of the entire sample and subsequently the determination of size and counting is performed by microscopy [Narhi *et al.*, 2009]. The detection of unstained protein particles can be sophisticated since those particles are often translucent. Besides, it can be challenging to distinguish between foreign particles and intrinsic particles of proteinaceous origin on the filter material. Because of shear forces during the filtration step, proteinaceous particles can be dissociated into smaller species which might either pass through the filter or sink into the pores. This is probably one reason why optical microscopy usually results in much lower particle counts compared to light obscuration [Narhi *et al.*, 2009].

Other microscopic techniques to detect protein aggregates are fluorescence microscopy, atomic force microscopy or electron microscopy which will not be described in detail. A meaningful example was reported in 2009 by Demeule *et al.*: The combination of fluorescence microscopy and transmission electron microscopy (TEM) was shown to be a valuable tool to detect protein aggregates of different (but not overlapping) size ranges, covering large parts of the nm and  $\mu\text{m}$  fields [Demeule *et al.*, 2009].

A method that recently has increasingly been used to detect protein aggregates especially in early stages of aggregation is flow imaging microscopy (FIM); commonly also known as Micro-Flow Imaging (MFI) [Barnard *et al.*, 2011]. The particles are not isolated by a filter but instead pass a flow cell where they are illuminated and visualized by a camera. Particles sized from approximately 1 to 400  $\mu\text{m}$  can be counted and additional information about shape, size and special features like transparency can be obtained. The latter enables the distinction between proteinaceous and non-proteinaceous particles such as silicone oil droplets [Sharma *et al.*, 2010; Strehl *et al.*, 2011]. A disadvantage of these methods is the

necessity of dilution, thereby possibly altering the sample properties when particle count limits are reached. Additionally, like all light-based techniques, flow imaging microscopy requires a substantial difference of refractive index between the surrounding liquid and the particles [Demeule *et al.*, 2010; Zoells *et al.*, 2012].

#### 2.3.1.3 Light scattering methods

Traditionally turbidimetry is also used to detect subvisible particles. This technique relies on the measurement of the optical density of the sample, but is not able to quantify the species of interest.

The methods to detect subvisible particles are currently subject of debate since it has been shown that light obscuration underestimates proteinaceous particles due to their non-spherical shape and their transparency [Sharma *et al.*, 2010]. Light obscuration determines the equivalent circular diameter (ECD) of all particles and is not able to distinguish between different species like silicone oil droplets or air bubbles which might be present as well. The interest in alternative methods steadily increased in the last years and several publications showed that especially Micro-Flow Imaging seems to be a suitable technique to complementary monitor subvisible particles in addition to light obscuration [Huang *et al.*, 2009; Narhi *et al.*, 2009; Sharma *et al.*, 2010; Singh, S.K. *et al.*, 2010]. However, more experience is needed to confirm the capabilities of MFI. One advantage of MFI is the possibility of discrimination between particles of different origin based on their translucency and particle shape. In general, proteinaceous particles appear more translucent and possess a more irregular shape than for example silicone oil droplets. Another innovative technique which is capable of distinguishing between particles of different origin is the Archimedes method, developed by Affinity biosensors. The particle size determination is based on resonant mass measurements. Furthermore, Coulter counter and nanoparticle tracking analysis (NTA) should be mentioned as alternative methods to determine subvisible particles in nm and  $\mu\text{m}$  range.

### 2.3.2 Detection of soluble protein aggregates

For the detection of soluble protein aggregates several analytical methods have been established. The most important ones are

- High performance size exclusion chromatography (HP-SEC)
- Asymmetrical flow field-flow fractionation (AF4)
- Sedimentation velocity analytical ultracentrifugation (SV-AUC)
- Sodium dodecyl sulfate - polyacrylamide gel electrophoresis (SDS-PAGE)
- Dynamic light scattering (DLS).

[Mahler *et al.*, 2009; Wang, 2005]

Throughout this thesis only HP-SEC, AF4, SDS-PAGE, and DLS were utilized for qualitative and quantitative determination of protein aggregates. Hence, these three techniques are solely taken into consideration.

#### 2.3.2.1 High performance size exclusion chromatography

The most commonly used technique to detect and quantify small oligomers is HP-SEC, also referred as gel permeation chromatography (GPC). Due to the usually prepended filter of 0.1 to 0.22  $\mu\text{m}$  pore size to avoid clogging of the column, any particle larger will be removed and HP-SEC is limited to the determination of soluble aggregates. The separation is based on size since the different molecules permeate in the pores exposed by the inert, stationary phase in the column [Gabrielson *et al.*, 2006]. The separation depends on a globular shape of a protein or its aggregates. The analytes are separated concerning their hydrodynamic radii ( $R_h$ ). Therefore, the size of a protein species can be overestimated if the hydrodynamic radius exceeds that of a spherical shaped protein due to for example highly coiled structures. The steric extension of two species of the same molar mass is decisive for the correct determination of the molecular weight simply based on elution profile. When using on-line light scattering detection combined with refractive index determination the size determination is independent of the elution time [Wang, 2005; Wen *et al.*, 1996]. Additionally, coupling to ultraviolet-visible (UV-Vis) spectroscopy detectors and fluorescence spectroscopy detectors is widely used to determine concentrations of proteins and aggregates. It was recently reported, that HP-SEC can also be coupled to mass spectrometry (MS) to accurately determine the molecular mass of the protein species [Brady *et al.*, 2008; Kuekrer *et al.*, 2010]. HP-SEC is the “gold-standard” in the analysis of protein aggregates, since it can cover a wide range of polarities and molecular weights. Considering the numerous different materials of the solid phase, the fractionation range is approximately in between 5 and 1000 kDa [Unger, 1983]. Analytes which are too large to penetrate into the pores of the solid matrix will quickly be eluted within the void volume, without being separated [Barth *et al.*, 2006; Mahler *et al.*, 2009]. For a good precision a difference in molecular weight of 50 – 100% is typically required [Goetz *et al.*, 2004]. However, the HP-SEC technique has also some essential drawbacks in the analysis of protein aggregates. First, the sample is highly diluted by the mobile phase possibly dissociating reversible or loosely associated aggregates [Philo, 2006]. Second, the species of interest can more or less interact with the material of the solid phase. This might change the conformation of the analytes and result in an altered elution profile and an inaccurate determination of the molecular weight of the initial species [Wen *et al.*, 1996].

#### 2.3.2.2 Asymmetrical flow field-flow fractionation

The latter disadvantage of HP-SEC can be excluded when using orthogonal techniques. Field-flow fractionation (FFF) is one of these methods and is meanwhile widely used to detect protein aggregates. It was first conceptualized in the 1960s by Giddings *et al.* [Giddings *et al.*, 1976]. Instead of the packed column in HP-SEC the component separation



takes place in is an empty, narrow, elongated flow chamber (also referred to as “channel”). The establishment of a laminar flow profile within that channel is the mutual feature of all FFF variants (channel flow). In flow field-flow fractionation (FFFF) the underlying force to separate the species, the so called cross flow, is a physical field directed perpendicular to the laminar flow of the mobile phase [Fraunhofer *et al.*, 2004; Reschiglian *et al.*, 2005]. Across the resulting parabolic profile the different components of the sample distribute according to their diffusion coefficients and by that to their hydrodynamic radii [Litzen *et al.*, 1993]. The separation principle is shown in Figure 2-2. Two contrarily directed forces are created in the chamber: the cross flow accumulating the analytes at the membrane/accumulation wall, versus the diffusion of the analytes back to the center of the channel. Before elution is starting, the sample is injected in the channel and subsequently focused in a narrow band at the accumulation wall. In normal elution mode, the smaller diffusion coefficients of large species entail their accumulation near the ultrafiltration membrane with slow flow rates of the channel flow. In contrast, smaller species tend to diffuse to the center of the parabolic flow profile with a faster flow rate. This principle results in the elution of species according to their size with those species of lower molecular weight eluting first and large species eluting subsequently [Arakawa *et al.*, 2007; Fraunhofer *et al.*, 2004; Jonsson, 2001].

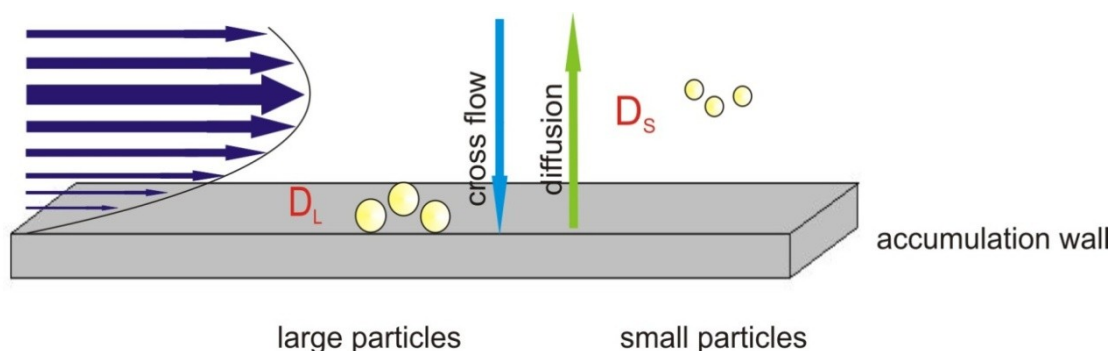


**Figure 2-2 – Separation principle of flow field-flow fractionation. (Adopted from Fraunhofer *et al.*, 2004)**

The separation principle is based on two contrarily directed forces: cross flow and diffusion.  
Normal operation mode.

In case the sample components are larger than a critical size, the operating mode might invert. This critical size strongly depends on the channel height and is usually reached in the range between 0.5 and 1  $\mu\text{m}$  channel height. The so called steric mode is characterized by an inversed elution profile; larger species elute prior to smaller ones. This inversion is caused by the large radius of the particles impeding the approximation near the wall. The centers of gravity protrude in faster fractions of the laminar flow profile leading to faster elution [Fraunhofer *et al.*, 2004].

FFFF has the ability to separate very broad ranges of size since the lower limit is determined by the molecular weight cut-off of the ultrafiltration membrane that is 300 Da (Postnova Analytics, Landsberg am Lech, Germany), and the upper limit is around 50 – 100  $\mu\text{m}$  depending on the channel height which is defined by a spacer [Fraunhofer *et al.*, 2004; Litzen *et al.*, 1991; Liu *et al.*, 2006]. This entails the versatile field's application FFFF is used for, such as the detection of macromolecules, polymers, colloids and solid particles of various origins [Fraunhofer *et al.*, 2004; Giddings, 1993; Qureshi *et al.*, 2011; Reschiglian *et al.*, 2005; Schimpf, 2000].

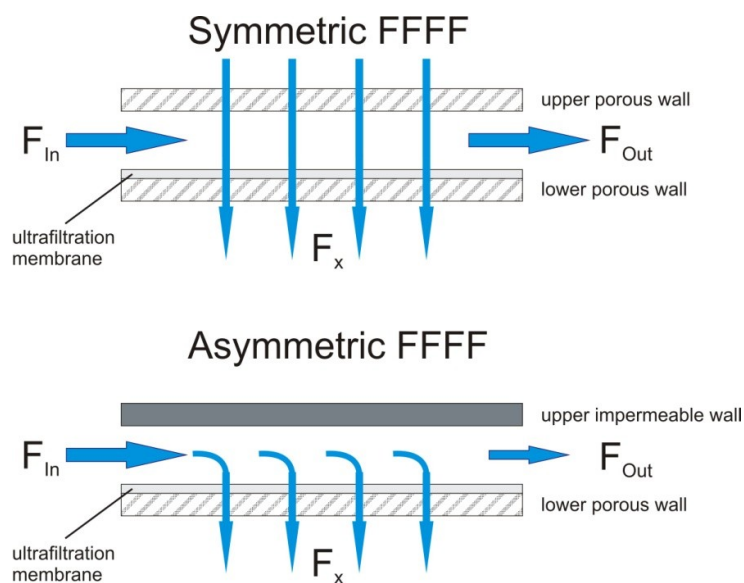


**Figure 2-3 – Comparison of separation principles of symmetric and asymmetric flow field-flow fractionation. (Adopted from Qureshi *et al.*, 2011)**

In symmetric FFFF both channel walls are porous and a second pump initiates a flow of the same carrier liquid perpendicular to the channel flow through both walls. In asymmetric FFFF the upper wall of the channel is solid and impermeable for liquids. Only one pump is needed to create the flow of carrier liquid through the system ( $F_{\text{In}}$ ), since this flow is split in two parts. The channel flow ( $F_{\text{Out}}$ ) is axially flushed through the channel towards the detection outlet; whereas the cross flow ( $F_x$ ) leaves the channel through the ultrafiltration membrane and the porous wall.

Most commonly used is asymmetrical flow field-flow fractionation (AF4), where the channel possesses only one wall permeable for the carrier liquid. Hence, the cross flow is generated as part of the inlet channel flow. This technique is well established for the separation of protein aggregates [Arakawa *et al.*, 2007; Liu *et al.*, 2006; Williams *et al.*, 2006] and reported to be successful for various biomolecules [Caldwell *et al.*, 2005; Giddings, 1993; Wahlund, 2002].

When comparing AF4 to HP-SEC, in AF4 the analytes should theoretically interact with almost no solid matrix. However, the AF4 method relies on a membrane that is permeable for the mobile phase, the so called accumulation wall (see Figure 2-3). That gives rise to a much smaller interfacial area between solid and liquid than in HP-SEC, though the possibility of interactions cannot be totally excluded. The samples do not necessarily have to be filtered

before injection since no porous stationary phase can be clogged [Augsten *et al.*, 2008]. In addition, AF4 is distinguished by much lower shear forces and lower pressures than HP-SEC. These characteristics appear to be advantageous for the analysis of protein aggregates since structural changes and probable dissolving of weak bonds of the species should be reduced [Jonsson, 2001]. Moreover, the separation can be performed in various buffer conditions, probably even in the formulation buffer [Liu *et al.*, 2006]. Undesirable limitations of AF4 are for example the possible artificial association of protein molecules during analysis since the sample is accumulated in a narrow band near the ultrafiltration membrane before separation and elution. Besides, the dilution of the samples of interest is still high during analysis facilitating probable dissolving of aggregates.

#### 2.3.2.3 Sodium dodecyl sulfate - polyacrylamide gel electrophoresis

Traditionally, polyacrylamide gel electrophoresis (PAGE) was used to determine protein aggregation. A molecular weight range of 5 to 500 kDa can be covered with this technique [Mahler *et al.*, 2009]. It is a rather simple technique and in most cases it is run under denaturing conditions by adding sodium dodecyl sulfate (SDS-PAGE). The presence of this anionic surfactant dissociates loose aggregates and is only useful to detect covalently linked aggregates. Alternatively, a native PAGE can be performed particularly if non-covalent aggregates associated by weak bonds shall be investigated. Utilizing PAGE under reducing and non-reducing conditions one has the ability to differentiate between aggregates originating from disulfide bridges and those that originate from other bindings [Wang, 2005]. SDS-PAGE is first and foremost employed for qualitative analysis. However, quantification is possible by UV detection after staining the separated protein bands. SDS-PAGE is a valuable method to detect protein aggregates and to discriminate between those associated by disulfide bonds and those that are associated in another way. However, like in HP-SEC and AF4, subtle conformational or oxidative alterations cannot be differentiated.

#### 2.3.2.4 Dynamic light scattering

Dynamic light scattering (DLS) is a valuable tool to determine the diffusion coefficients and hydrodynamic radii of proteins, their aggregates and particles in solution in the size range of 1 nm to 10  $\mu\text{m}$  [Arakawa *et al.*, 2006]. DLS is also referred to quasi-elastic light scattering (QELS) and photon correlation spectroscopy (PCS) and can be performed in cuvette or plate reader based systems [Zoells *et al.*, 2012]. The analytes are moving in Brownian motion and thereby scatter the light of a monochromatic laser beam. Hence, a time-dependent fluctuation of the laser light intensity is observed, which correlates to the diffusion coefficient and thus the size of the analytes [Schmidt, 2010]. The measurements strongly depend on temperature and viscosity of the samples. Beside the mean diameter of the analyte (Z-average diameter) information on the polydispersity of the sample can be achieved by this non-destructive and quick analytical method.

## 2.4 IMMUNOGENICITY OF BIOPHARMACEUTICALS

The implementation of proteins as therapeutics is very much dependent on their potential to circumvent any recognition by the immune system (excluding those drugs that are supposed to inhibit or stimulate specific immune reactions) [Foged *et al.*, 2008]. Most biopharmaceuticals approved for clinical use are known to be immunogenic and provoke the formation of antibodies in a significant fraction of patients [Chirino *et al.*, 2004; Porter, 2001]. The formation of antibodies can be associated with minor or major adverse reactions and therapeutic failure by reducing the drug's efficacy and potency [Bendtzen, 2011; Chirino *et al.*, 2004]. With the possibility of the recombinant production of "self" proteins with a near identity to human counterparts it was hoped to solve the immunogenicity problem, because those biopharmaceuticals should theoretically be accepted as self-molecules by the immune system and thus should be tolerated [De Groot *et al.*, 2007; Foged *et al.*, 2008]. However, interestingly, those proteins that have an identical or nearly identical amino acid sequence to endogenous human proteins were shown to be immunogenic as well although the incidence of immune reactions is much lower [Chirino *et al.*, 2004; Patten *et al.*, 2003; van Regenmortel *et al.*, 2005]. A second aspect that is considered to be the cause of immunogenicity is a lack of tolerance, either in patients with an inherent immune deficiency (minor immune competence) or in healthy individuals [Hermeling *et al.*, 2004; Rosenberg, 2003]. But, the overall immunogenicity problem is more complex and cannot simply be explained by a "self" versus "nonself" model and a lacking tolerance to endogenous proteins existing in minor concentrations [Patten *et al.*, 2003; Rosenberg, 2003]. The underlying processes of immune responses to biopharmaceuticals are still elusive. Numerous other factors attributable to host and product may cause the immunogenicity of those molecules, some of them are yet unknown [Rosenberg, 2006; Schellekens, 2002; Scott *et al.*, 2010].

### 2.4.1 Factors influencing immunogenicity

Alterations in the molecular structure of the protein, such as variations in the amino acid sequence or different glycosylation patterns, most comprehensibly - though not necessarily - result in immunogenicity [Hermeling *et al.*, 2004]. Biopharmaceuticals that are known to be subject to these triggers are salmon calcitonin [Grauer *et al.*, 1994], granulocyte-macrophage colony-stimulating factor (GM-CSF) and streptokinase [Malucchi *et al.*, 2008; Rosenschein *et al.*, 1991]. However, there are also some converse examples like interferon- $\alpha$ 2a [Kontsek *et al.*, 1999], where alterations in the molecular pattern did not result in an increased immunogenicity. The glycosylation pattern strongly depends on the host cell used for the production of the protein. Products derived from bacteria, like *Escherichia coli*, are generally non-glycosylated, reduce shielding effects and expose unknown patches of the proteins which might act as antigen. Instead, mammalian cell lines such as Chinese Hamster Ovary (CHO) cell lines produce glycosylated molecules that have to be purified since initially the result of this posttranslational modification can be very heterogeneous. Since the glycosylation pattern also

depends on the culture conditions Hermeling *et al.* hypothesized that recombinant human glycoproteins, such as monoclonal antibodies, will always differ more or less from their endogenous counterparts [Hermeling *et al.*, 2004].

In general, the subcutaneous and intramuscular administrations have been shown to be more immunogenic than other administration routes [Perini *et al.*, 2001; Schellekens, 2002; Wierda *et al.*, 2001]. In comparison, intravenous administration is much less immunogenic [Peng *et al.*, 2009]. Nevertheless, many therapeutic proteins, such as the large group of monoclonal antibodies, are commonly applied via the subcutaneous route. Besides, also the frequency of the administration and the dose are associated with immunogenicity [Hwang *et al.*, 2005; Kuus-Reichel *et al.*, 1994]. Chronic administration of a therapeutic protein generally is more likely related to immunogenic side effects than one acute application [Ross *et al.*, 2000].

Product-related impurities or contaminants such as host-cell proteins, arising from the formulation of biopharmaceuticals, may mimic pathogen-associated molecular patterns (PAMPs) [Foged *et al.*, 2008] and have shown to be linked to immunogenicity [Hermeling *et al.*, 2004; Schellekens, 2002; Singh, 2011]. Due to the increasing purity of manufacturing processes and the final products these risks could be minimized by purification procedures, but some are still of relevance. Crucial factors for immunogenicity are considered to be particulate structures existent in the formulation of the biopharmaceuticals [Carpenter *et al.*, 2009; Rosenberg, 2006]. Such materials can for instance be subvisible or visible particles in the micron range and smaller protein aggregates in the nanometer range. Several studies were published indicating an enhanced immunogenicity of therapeutic protein formulations containing aggregates [Braun *et al.*, 1997; Fradkin *et al.*, 2009; Hermeling *et al.*, 2006; Perini *et al.*, 2004; Ring *et al.*, 1979; Rosenberg, 2006]. Protein aggregates as a special type of particulate impurities can also activate immune reactions by imitation of PAMPs. In 2006 Rosenberg stated that protein aggregates and their repetitive structures might resemble the repetitive characteristics of external surfaces of microbial pathogens [Rosenberg, 2006]. However, the exact mode of activation of the immune system by aggregates is still unclear [Barbosa *et al.*, 2007; De Groot *et al.*, 2007]. In addition, there is uncertainty whether only some aggregates or aggregates in general can be made responsible for unwanted immune responses [Hermeling *et al.*, 2004]. Therefore it is a major challenge for development and approval of biopharmaceuticals to prevent aggregation and to establish reliable, sensitive, and suitable analytical methods for detection and quantitation of trace amounts of aggregated proteins [Arakawa *et al.*, 2006; Chi *et al.*, 2003b; John P. Gabrielson, 2007].

#### **2.4.2 Responses of the immune system to therapeutic proteins**

A therapeutic protein interacts with several types of immune cells such as antigen presenting cells (APCs), B-cells and T-cells, to trigger an immune response. Each interaction step is based on distinct antigen properties.

First of all, the protein has to be recognized by the immune system (see Figure 2-4). This recognition can proceed by different cells of the immune system. APCs will first encounter the molecules and incorporate them by receptor-mediated endocytosis, pinocytosis or phagocytosis. Dendritic cells (DC) will be the first responders if the protein is administered subcutaneously since they numerously are present in the skin. After this uptake of the antigen, dendritic cells migrate from the peripheral tissues to the lymphatic organs spleen and lymph nodes. The cells will subsequently break the molecules down and present the resulting peptides by major histocompatibility complexes class II (MHC-II) on their surface to other cells of the immune system. Some co-stimulating signals have to be presented as well and are decisive for the recognition by specific T cells present in the lymph nodes. Due to the concurrent production and release of cytokines of the dendritic cells, these T cells are activated and start to proliferate. Dendritic cells are thus able to efficiently stimulate the production of CD4+ cells (T helper cells,  $T_H1$  and  $T_H2$ ) [Janeway *et al.*, 2004; Vollmar, 2005]. Proliferating helper T cells can differentiate into two subtypes. The  $T_H1$  cells are involved in the cellular immune response, whereas  $T_H2$  cells promote the stimulation of the humoral immune response by activating B cells. Those B cells express B cell receptors directed against the antigen on their surface and start to proliferate into antibody-secreting plasma B cells, once they are activated by the corresponding antigen [Sauerborn *et al.*, 2010].

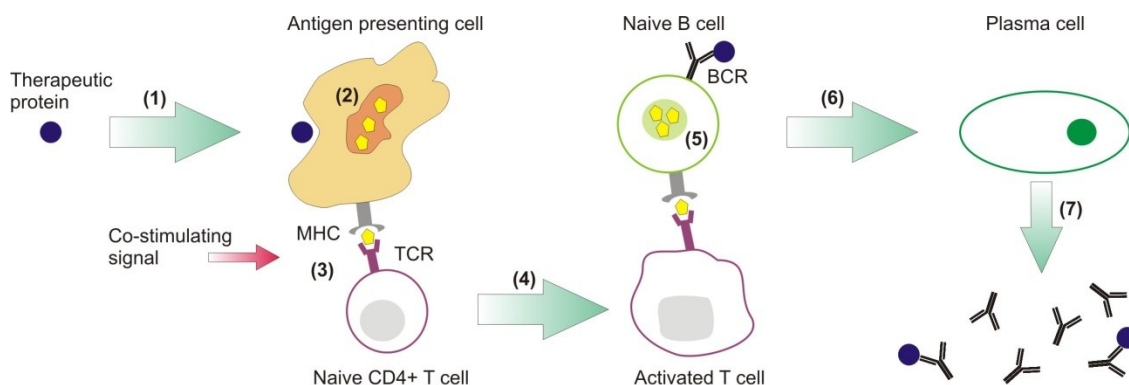


**Figure 2-4 – Immune recognition of therapeutic proteins**

(1) The protein is taken up by APCs, (2) the molecules are processed to peptides, (3) in presence of co-stimulating molecules e.g. from inflammation complexes are formed between peptide, major histocompatibility complex and T cell receptor, (4) maturation of the T cells, (5) interaction of B cells and T cells, comprising the peptide-MHC-TCR complexes and the therapeutic protein binding to BCRs, (6) maturation of the B cells, (7) release of specific antibodies binding the protein molecules.

In vaccines, particulate materials are often used as adjuvants, to enhance the immune response towards the antigens. These structures can on the one hand side bind the antigen and entail a sustained release of it. On the other hand side, particulate adjuvants are taken up by macrophages and DCs. Adjuvants are, at least in part, needed to fully activate dendritic cells to the antigen-presenting status and thus initiate a strong, unspecific, adaptive immune response, although an infection is absent [Janeway *et al.*, 2004]. The prolonged exposure of particulate materials to APCs such as DCs, and T cells, is thought to play an important role in

eliciting immunogenicity [Chirino *et al.*, 2004]. This mechanism might be at least part of the processes underlying the immunogenicity of protein aggregates, although it is likely that other factors play an important part as well.

The elicitation of antibodies towards antigens can also be independent of T cells. Polyvalent antigens such as viral capsids and lipopolysaccharides from bacteria are able to crosslink B cell receptors (BCRs) due to repetitive epitopes on their surface that are arranged in certain steric distance [De Groot *et al.*, 2007; Rosenberg, 2006]. Dintzis *et al.* defined clusters of polymers that fit to this model and thus are able to induce T cell-independent immune responses as “immunons” [Dintzis *et al.*, 1976]. Protein aggregates can, due to their high molecular weight and the composition of multiple monomeric molecules, possess multivalent surface structures resembling bacteria or viruses and crosslink BCRs [Sauerborn *et al.*, 2010]. Especially protein aggregates of high molecular weight and proteins adsorbed on particles from impurities are thought to elicit antibody responses that way. The difference of both immunological mechanisms to elicit antibody responses is the subclass switching and affinity maturation. The T cell-dependent activation of B cells generally leads to a more robust antibody response and the generation of memory B cells [De Groot *et al.*, 2007]. This implies the switching of immunoglobulin subclasses by changing the constant part of the antibody but the variable region, and hence the antigen specificity, remains the same. Therefore, the antibodies can interact with different effector molecules, resulting in versatile activations or inhibitions of proteins in the immune system. Affinity maturation occurs in B cells after repeated exposures to the antigen and a T cell-dependent activation. In the secondary response these cells are able to elicit antibodies of greater affinity to the antigen and thus show an enhanced reaction and high effectiveness upon re-exposure of the antigen [Hermeling *et al.*, 2004].

#### **2.4.3 Impact of antibody induction**

The clinical consequences of the induction of antibodies against the therapeutic protein can be various, depending on the epitopes the immune response is directed to. The antibodies can be directed towards an epitope which is specific for the recombinant protein variation. These antibodies can be either neutralizing or non-neutralizing. The latter will merely interact with the therapeutic protein by forming immune complexes and possibly induce a quick elimination and reduced bioavailability of the drug [Pendley *et al.*, 2003; Schellekens, 2003]. Neutralizing antibodies usually bind to the protein as well, but are furthermore either able to inhibit the interaction with the molecules responsible for the biological effect or to neutralize the effect subsequently. Pharmacokinetics and efficacy of the therapeutic protein can be influenced [Pendley *et al.*, 2003]. Serious clinical consequences can arise if the immune response is directed toward an epitope which is also present in the endogenous counterpart. The occurrence of pure red cell aplasia in numerous patients treated with recombinant erythropoietin is one tremendous example for that [Casadevall *et al.*, 2002; Schellekens, 2005]. Other safety concerns like allergic or anaphylactic reactions can also be related to antibody generation and might occur as well.

## 2.5 MONOCLONAL ANTIBODIES

In 1975 Kohler and Milstein developed the first monoclonal antibodies (mAbs) leading to a revolution in immunology [Koehler *et al.*, 1975]. This discovery initiated an impressive development of plethora of drugs. Today monoclonal antibodies are an important class of protein-based drugs due to their ability of antibodies to specifically identify and eliminate a certain antigen within the immune system [Harris *et al.*, 2004; Roque *et al.*, 2004] and coevally implying a desirable marginal off-target toxicity [Wang, W. *et al.*, 2008].

### 2.5.1 Structure of monoclonal antibodies

Due to the structural similarity with human antibodies mAbs are classified into murine, chimeric, humanized and human antibodies [Pendley *et al.*, 2003; Reichert, Janice M., 2001; Reichert, Janice M. *et al.*, 2005]. The first therapeutic antibodies developed were of murine origin generated by the use of hybridoma technology and entered the market in 1980s [Walsh, 2005]. Muromonab-CD3 (Orthoclone, OKT3<sup>®</sup>) was approved by the FDA in 1986 for the treatment of acute rejection of transplanted organs. Based on the foreign origin, up to 80% of the patients treated with murine antibodies generated human anti-mouse antibodies (HAMA) potentially influencing safety, efficacy and pharmacokinetics of these drugs [Aksentijevich *et al.*, 2002; Walsh, 2004]. To reduce this antigenicity the molecules were altered by exchanging the murine parts in the constant region to constant regions of human origin [Boulianne *et al.*, 1984; Morrison *et al.*, 1984]. Such modified mAbs are called chimeric antibodies and many of those are already therapeutically used. Significant research efforts were devoted to further reduce the amount of murine part, developing humanized and human antibodies for use in human patients [Berger *et al.*, 2002]. Humanized antibodies are mostly of human origin and solely include the hyper variable CDR-regions (complementary determining regions) from mice. Fully human antibodies can be produced by phage display technology or by using human hybridoma cells, instead of murine ones [Roque *et al.*, 2004]. They are completely made of human sequences. Humanized mAbs as well as human mAbs showed reduced immunogenicity in humans in contrast to the murine and chimeric mAbs [Clark, 2000; Reichert, Janice M. *et al.*, 2005].

In 2006 the first entirely human recombinant monoclonal antibody was approved. Adalimumab (Humira<sup>®</sup>) is of IgG1 subtype and targets the inhibition of tumor necrosis factor alpha (TNF $\alpha$ ) in rheumatoid arthritis patients. Most mAbs in therapeutic use are of immunoglobulin isotype IgG [Piggee, 2008]. The general structure of IgG antibodies is displayed in Figure 2-5.



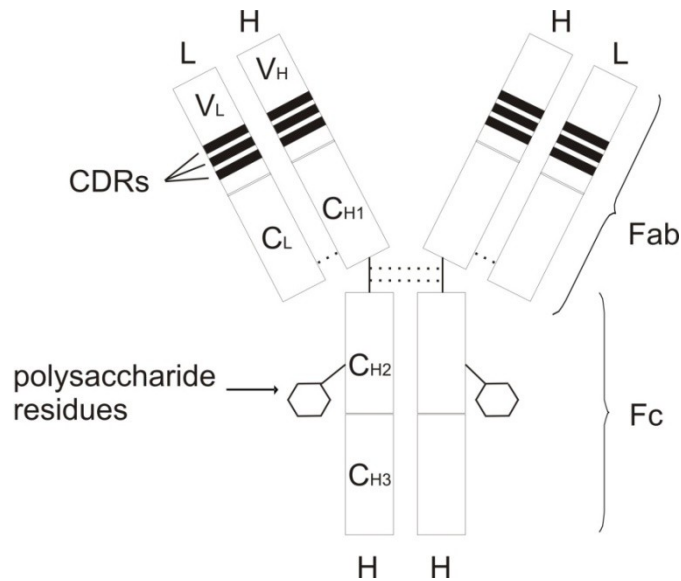


**Figure 2-5 – General structure of immunoglobulin G.**

The molar mass of an IgG is approximately 150 kDa since the molecule is composed of two identical light chains (L, 25 kDa) and heavy chains (H, 50 kDa). The subunits are linked by disulfide bonds. The two antigen binding regions are situated in the Fab parts and consist of the variable regions of light (V<sub>L</sub>) and heavy (V<sub>H</sub>) chain. The three CDR-regions per variable chain entail the particular surface structure and assure the high specificity of the antigen binding [Wang, W. *et al.*, 2006b].

The family of immunoglobulin G can be subdivided into four subclasses: IgG1, IgG2, IgG3 and IgG4. The structural differences between these are in the heavy chains in the Fc part of the molecules. The relevant part for binding to cell surfaces and the resulting induction of a cellular response is the Fc part. It is composed of the constant domains C<sub>H2</sub> and C<sub>H3</sub> of the two heavy chains. Besides, the C<sub>H2</sub> domains usually are glycosylated. The glycosylation pattern is of importance for modulating the effector functions and strongly depends on the expression system used for production [Chadd *et al.*, 2001; Harris *et al.*, 2004; Roque *et al.*, 2004; Wright *et al.*, 1997].

### 2.5.2 The pharmacokinetics of monoclonal antibodies

Several pharmacokinetic properties of monoclonal antibodies entail the utility of these molecules as therapeutics. The half-life of entire recombinant human monoclonal antibody is usually relatively long. It varies according to the subclass of the antibody but is very similar between different patients [Roskos *et al.*, 2004]. For example the most important isotype in humans, IgG1, has a half-life of 3 weeks [Waldmann *et al.*, 1970]. This allows infrequent administrations to the patient and enhances patient compliance. The bioavailability and half-lives of mAbs are determined by the catabolism of the antibody, such as the interaction with the FcRn receptor. This receptor protects immunoglobulins from intracellular catabolism by recycling them to the cell surface after endocytotic uptake and therefore impeding its degradation in the lysosomes. The currently marketed antibodies are administered either intravenously (IV), subcutaneously (SC) or intramuscularly (IM). IV administration allows the

absorption of larger volumes. But it is not very convenient for the patient, since hospitalization is often required. The absorption after SC and IM administration usually proceeds slowly by the lymphatic system, implying that the time to reach maximal plasma concentrations lasts several days. However, the absolute bioavailability of these administration routes typically lies between 50 and 100% [Lobo *et al.*, 2004]. These properties in particular qualify such extravascular administrations for therapies where slow absorption is desired. The downside of IM and SC dosing is the limitation on the volume that can be injected, which is ~5 mL for IM and 2.5 mL for SC administration. Besides, the solubility of monoclonal antibodies in solution is relatively limited to ~ 100-200 mg/mL and therefore large doses of mAbs cannot be injected IM or SC. The antibodies administered in such a way need to have high dose potency or repeated injections are necessary [Wang, W. *et al.*, 2008].

### 2.5.3 The market of monoclonal antibodies

In 2005, mAbs provided about 50% of the biopharmaceuticals in development. Recent numbers from March 2011 showed 32 therapeutic antibodies in total, that were already approved or in review in the United States and the European Union [Reichert, 2011]. Nearly three-quarters are either humanized or human mAbs. The major indications mAbs are used for are autoimmune diseases, such as arthritis, and oncology [Berger *et al.*, 2002]. As probably most important group of biopharmaceuticals, monoclonal antibodies have proven to be economically very successful drugs. Their sales are forecast to annually grow by 9.5% between 2009 and 2015 [Datamonitor, 2010]. Accordingly, the sales of other therapeutic proteins, vaccines and small molecule drugs are outpaced. These impressive forecast numbers especially will be commanded by the “Big 5” therapeutic antibodies on the market (Adalimumab, Bevacizumab, Infliximab, Rituximab and Trastuzumab). Each of them has sales of over US \$ 1 billion/year worldwide [IMS Health, 2010]. This profitability and the versatility of monoclonal antibodies as therapeutics give reason to the current high efforts and investments in research and development of mAbs that are realized by the manufacturing biopharmaceutical industry.

## 2.6 REFERENCES

[Aksentijevich *et al.*, 2002], Monoclonal antibody therapy with autologous peripheral blood stem cell transplantation for non-Hodgkin's lymphoma, *Cancer control : journal of the Moffitt Cancer Center*, 9, 99-105

[Arakawa *et al.*, 2007], Aggregation analysis of therapeutic proteins, part 3: principles and optimization of field-flow fractionation (FFF), *BioProcess International*, 5, 52-70

[Arakawa *et al.*, 2006], Aggregation analysis of therapeutic proteins, part 1: General aspects and techniques for assessment, *BioProcess International*, 4, 32-43

[Augsten *et al.*, 2008], Characterizing molar mass distributions and molecule structures of different chitosans using asymmetrical flow field-flow fractionation combined with multi-angle light scattering, *International Journal of Pharmaceutics*, 351, 23-30

[Barbosa *et al.*, 2007], Immunogenicity of protein therapeutics and the interplay between tolerance and antibody responses, *Drug Discovery Today*, 12, 674-681

[Barnard *et al.*, 2011], Subvisible particle counting provides a sensitive method of detecting and quantifying aggregation of monoclonal antibody caused by freeze-thawing: Insights into the roles of particles in the protein aggregation pathway, *J. Pharm. Sci.*, 100, 492-503

[Barth *et al.*, 2006], High-performance SEC column technology, *LCGC North America*, 24, 38-43

[Bee *et al.*, 2011], Effects of surfaces and leachables on the stability of biopharmaceuticals, *J. Pharm. Sci.*, 100, 4158-4170

[Bendtsen, 2011], Is there a need for immunopharmacologic guidance of anti-tumor necrosis factor therapies?, *Arthritis and rheumatism*, 63, 867-870

[Berger *et al.*, 2002], Therapeutic applications of monoclonal antibodies, *The American journal of the medical sciences*, 324, 14-30

[Boulianne *et al.*, 1984], Production of functional chimaeric mouse/human antibody, *Nature*, 312, 643-646

[Brady *et al.*, 2008], Molecular Mass Analysis of Antibodies by On-Line SEC-MS, *Journal of the American Society for Mass Spectrometry*, 19, 502-509

[Braun *et al.*, 1997], Protein aggregates seem to play a key role among the parameters influencing the antigenicity of interferon alpha (IFN-alpha ) in normal and transgenic mice, *Pharmaceutical Research*, 14, 1472-1478

[Brinks *et al.*, 2011], Immunogenicity of Therapeutic Proteins: The Use of Animal Models, *Pharmaceutical Research*, 28, 2379-2385

[Caldwell *et al.*, 2005], Field-flow fractionation, *Biotechnology: Pharmaceutical Aspects*, 3, 413-433

[Cao *et al.*, 2003], Effect of freezing and thawing rates on denaturation of proteins in aqueous solutions, *Biotechnology and Bioengineering*, 82, 684-690

[Carpenter *et al.*, 1999], Inhibition of stress-induced aggregation of protein therapeutics, *Methods in Enzymology*, 309, 236-255

[Carpenter *et al.*, 2009], Overlooking subvisible particles in therapeutic protein products: gaps that may compromise product quality, *J. Pharm. Sci.*, 98, 1201-1205

[Casadevall *et al.*, 2002], Pure red-cell aplasia and antierythropoietin antibodies in patients treated with recombinant erythropoietin, *New England Journal of Medicine*, 346, 469-475

[Chadd *et al.*, 2001], Therapeutic antibody expression technology, *Current Opinion in Biotechnology*, 12, 188-194

[Chang *et al.*, 2002], Practical approaches to protein formulation development, *Pharmaceutical Biotechnology*, 13, 1-25

[Chang *et al.*, 1996], Surface-Induced Denaturation of Proteins during Freezing and Its Inhibition by Surfactants, *J. Pharm. Sci.*, 85, 1325-1330

[Chi *et al.*, 2003a], Roles of conformational stability and colloidal stability in the aggregation of recombinant human granulocyte colony-stimulating factor, *Protein Science*, 12, 903-913

[Chi *et al.*, 2003b], Physical Stability of Proteins in Aqueous Solution: Mechanism and Driving Forces in Nonnative Protein Aggregation, *Pharmaceutical Research*, 20, 1325-1336

[Chi *et al.*, 2005], Heterogeneous nucleation-controlled particulate formation of recombinant human platelet-activating factor acetylhydrolase in pharmaceutical formulation, *J. Pharm. Sci.*, 94, 256-274

[Chirino *et al.*, 2004], Minimizing the immunogenicity of protein therapeutics, *Drug Discovery Today*, 9, 82-90

[Clark, 2000], Antibody humanization: a case of the 'Emperor's new clothes'?, *Immunology Today*, 21, 397-402

[Cleland *et al.*, 1993], The development of stable protein formulations: a close look at protein aggregation, deamidation, and oxidation, *Critical Reviews in Therapeutic Drug Carrier Systems*, 10, 307-377

[Cromwell *et al.*, 2006], Protein aggregation and bioprocessing, *AAPS Journal*, 8, E572-E579

[Datamonitor, 2010] Monoclonal Antibodies: 2010, [http://www.datamonitor.com/store/Product/monoclonal\\_antibodies\\_2010?productid=HC00029-00002](http://www.datamonitor.com/store/Product/monoclonal_antibodies_2010?productid=HC00029-00002)

[Davies *et al.*, 2001], Photo-oxidation of proteins and its role in cataractogenesis, *Journal of Photochemistry and Photobiology, B: Biology*, 63, 114-125

[De Groot *et al.*, 2007], Immunogenicity of protein therapeutics, *Trends in Immunology*, 28, 482-490

[Demeule *et al.*, 2007], Characterization of protein aggregation: The case of a therapeutic immunoglobulin, *Biochimica et Biophysica Acta, Proteins and Proteomics*, 1774, 146-153

[Demeule *et al.*, 2010], Characterization of Particles in Protein Solutions: Reaching the Limits of Current Technologies, *AAPS Journal*, 12, 708-715

[Demeule *et al.*, 2009], New methods allowing the detection of protein aggregates: a case study on trastuzumab, *mAbs*, 1, 142-150

[Dintzis *et al.*, 1976], Molecular determinants of immunogenicity: The immunon model of immune response, *Proceedings of the National Academy of Sciences of the United States of America*, 73, 3671-3675

[Dong *et al.*, 1995], Infrared spectroscopic studies of lyophilization- and temperature-induced protein aggregation, *J Pharm Sci*, 84, 415-424

[Foged *et al.*, 2008], Immune reactions towards biopharmaceuticals - a general, mechanistic overview, *Biotechnology: Pharmaceutical Aspects*, 8, 1-25

[Fradkin *et al.*, 2009], Immunogenicity of aggregates of recombinant human growth hormone in mouse models, *J Pharm Sci*, 98, 3247-3264

[Fraunhofer *et al.*, 2004], The use of asymmetrical flow field-flow fractionation in pharmaceuticals and biopharmaceuticals, *European Journal of Pharmaceutics and Biopharmaceutics*, 58, 369-383

[Frokjaer *et al.*, 2005], Protein drug stability: a formulation challenge, *Nature Reviews Drug Discovery*, 4, 298-306

[Gabrielson *et al.*, 2006], Quantitation of aggregate levels in a recombinant humanized monoclonal antibody formulation by size-exclusion chromatography, asymmetrical flow field flow fractionation, and sedimentation velocity, *J. Pharm. Sci.*, 96, 268-279

[Giddings, 1993], Field-flow fractionation: analysis of macromolecular, colloidal, and particulate materials, *Science (Washington, DC, United States)*, 260, 1456-1465

[Giddings *et al.*, 1976], Flow field-flow fractionation: a versatile new separation method, *Science*, 193, 1244-1245

[Goetz *et al.*, 2004], Comparison of selected analytical techniques for protein sizing, quantitation and molecular weight determination, *Journal of Biochemical and Biophysical Methods*, 60, 281-293

[Grauer *et al.*, 1994] Neutralizing antibodies against salmon calcitonin. The cause of a treatment failure in Paget's disease, 507-510

[Harris *et al.*, 2004], Commercial manufacturing scale formulation and analytical characterization of therapeutic recombinant antibodies, *Drug Development Research*, 61, 137-154

[Hermeling *et al.*, 2004], Structure-Immunogenicity Relationships of Therapeutic Proteins, *Pharmaceutical Research*, 21, 897-903

[Hermeling *et al.*, 2006], Antibody response to aggregated human interferon alpha2b in wild-type and transgenic immune tolerant mice depends on type and level of aggregation, *J. Pharm. Sci.*, 95, 1084-1096

[Huang *et al.*, 2009], Quantitation of protein particles in parenteral solutions using micro-flow imaging, *J. Pharm. Sci.*, 98, 3058-3071

[Hwang *et al.*, 2005], Immunogenicity of engineered antibodies, *Methods (San Diego, CA, United States)*, 36, 3-10

[IMS Health, 2010] Top 20 Global Products, 2010, Total Audited Markets, [http://www.imshealth.com/deployedfiles/ims/Global/Content/Corporate/Press%20Room/Top-line%20Market%20Data/2010%2020Topline%2020Market%2020Data/Top\\_2020\\_Global\\_Products.pdf](http://www.imshealth.com/deployedfiles/ims/Global/Content/Corporate/Press%20Room/Top-line%20Market%20Data/2010%2020Topline%2020Market%2020Data/Top_2020_Global_Products.pdf)

[Janeway *et al.*, 2004], Immunobiology: The Immune System in Health and Disease, 6th Edition,

[John P. Gabrielson, 2007], Quantitation of aggregate levels in a recombinant humanized monoclonal antibody formulation by size-exclusion chromatography, asymmetrical flow field flow fractionation, and sedimentation velocity, *Journal of Pharmaceutical Sciences*, 96, 268-279

[Jones *et al.*, 1997], Surfactant-stabilized protein formulations: a review of protein-surfactant interactions and novel analytical methodologies, *ACS Symposium Series*, 675, 206-222

[Jones *et al.*, 2005], Silicone oil induced aggregation of proteins, *J. Pharm. Sci.*, 94, 918-927

[Jonsson, 2001], Field-Flow Fractionation Handbook, 1st Edition,

[Kendrick *et al.*, 1998], Aggregation of Recombinant Human Interferon Gamma: Kinetics and Structural Transitions, *J. Pharm. Sci.*, 87, 1069-1076

[Kerwin *et al.*, 2007], Protect from light: Photodegradation and protein biologics, *J. Pharm. Sci.*, 96, 1468-1479

[Kiese, 2008], Shaken, not stirred: Mechanical stress testing of an IgG1 antibody, *Journal of Pharmaceutical Sciences*,

[Kim *et al.*, 2007], Photodegradation mechanism and reaction kinetics of recombinant human interferon- $\alpha$ 2a, *Photochemical & Photobiological Sciences*, 6, 171-180

[Koehler *et al.*, 1975], Continuous cultures of fused cells secreting antibody of predefined specificity, *Nature (London, United Kingdom)*, 256, 495-497

[Kontsek *et al.*, 1999], Immunogenicity of interferon-alpha2 in therapy: structural and physiological aspects, *Acta Virologica (English Edition)*, 43, 63-70

[Krishnamurthy *et al.*, 2002], The stability factor: importance in formulation development, *Current Pharmaceutical Biotechnology*, 3, 361-371

[Krishnan *et al.*, 2002], Aggregation of Granulocyte Colony Stimulating Factor under Physiological Conditions: Characterization and Thermodynamic Inhibition, *Biochemistry*, 41, 6422-6431

[Kuekrer *et al.*, 2010], Mass Spectrometric Analysis of Intact Human Monoclonal Antibody Aggregates Fractionated by Size-Exclusion Chromatography, *Pharmaceutical Research*, 27, 2197-2204

[Kueltzo *et al.*, 2008], Effects of solution conditions, processing parameters, and container materials on aggregation of a monoclonal antibody during freeze-thawing, *J. Pharm. Sci.*, 97, 1801-1812

[Kuus-Reichel *et al.*, 1994], Will immunogenicity limit the use, efficacy, and future development of therapeutic monoclonal antibodies?, *Clinical and diagnostic laboratory immunology*, 1, 365-372

[Lakowicz, 1983], Principles of Fluorescence Spectroscopy, 2nd Edition, *Plenum Press*, 496 pp,

[Leader *et al.*, 2008], Protein therapeutics: a summary and pharmacological classification, *Nature Reviews Drug Discovery*, 7, 21-39

[Litzen *et al.*, 1991], Zone broadening and dilution in rectangular and trapezoidal asymmetrical flow field-flow fractionation channels, *Analytical Chemistry*, 63, 1001-1007

[Litzen *et al.*, 1993], Separation and quantitation of monoclonal antibody aggregates by asymmetrical flow field-flow fractionation and comparison to gel permeation chromatography, *Analytical Biochemistry*, 212, 469-480

[Liu *et al.*, 2006], A critical review of analytical ultracentrifugation and field flow fractionation methods for measuring protein aggregation, *AAPS Journal*, 8, E580-E589

[Liu *et al.*, 2007], Characterization of lower molecular weight artifact bands of recombinant monoclonal IgG1 antibodies on non-reducing SDS-PAGE, *Biotechnology Letters*, 29, 1611-1622

[Liu *et al.*, 2008], Heterogeneity of monoclonal antibodies, *J. Pharm. Sci.*, 97, 2426-2447

[Liu *et al.*, 2005], Reversible self-association increases the viscosity of a concentrated monoclonal antibody in aqueous solution. [Erratum to document cited in CA144:345313], *J. Pharm. Sci.*, 95, 234-235

[Lobo *et al.*, 2004], Antibody pharmacokinetics and pharmacodynamics, *Journal of Pharmaceutical Sciences*, 93, 2645-2668

[Lumry *et al.*, 1954], Conformation changes of proteins, *Journal of Physical Chemistry*, 58, 110-120

[Mahler *et al.*, 2009], Protein aggregation: Pathways, induction factors and analysis, *J. Pharm. Sci.*, 98, 2909-2934

[Mahler *et al.*, 2005], Induction and analysis of aggregates in a liquid IgG1-antibody formulation, *European Journal of Pharmaceutics and Biopharmaceutics*, 59, 407-417

[Malucchi *et al.*, 2008], Clinical aspects of immunogenicity to biopharmaceuticals, *Biotechnology: Pharmaceutical Aspects*, 8, 27-56

[Manning *et al.*, 1989], Stability of protein pharmaceuticals, *Pharmaceutical Research*, 6, 903-918

[Miller *et al.*, 2003], Solid-state photodegradation of bovine somatotropin (bovine growth hormone): Evidence for tryptophan-mediated photooxidation of disulfide bonds, *J. Pharm. Sci.*, 92, 1698-1709

[Mollmann *et al.*, 2005], Adsorption of human insulin and AspB28 insulin on a PTFE-like surface, *Journal of Colloid and Interface Science*, 286, 28-35

[Morrison *et al.*, 1984], Chimeric human antibody molecules: mouse antigen-binding domains with human constant region domains, *Proceedings of the National Academy of Sciences of the United States of America*, 81, 6851-6855

[Narhi *et al.*, 2009], A critical review of analytical methods for subvisible and visible particles, *Current Pharmaceutical Biotechnology*, 10, 373-381

[Patro *et al.*, 1996], Simulations of reversible protein aggregate and crystal structure, *Biophysical Journal*, 70, 2888-2902

[Patten *et al.*, 2003], The immunogenicity of biopharmaceuticals: Lessons learned and consequences for protein drug development, *Developments in Biologicals (Basel, Switzerland)*, 112, 81-97

[Pavlou *et al.*, 2005], The therapeutic antibodies market to 2008, *European journal of pharmaceutics and biopharmaceutics : official journal of Arbeitsgemeinschaft fur Pharmazeutische Verfahrenstechnik e.V.*, 59, 389-396

[Pavlou *et al.*, 2004], Recombinant protein therapeutics--success rates, market trends and values to 2010, *Nat Biotechnol*, 22, 1513-1519

[Pekar *et al.*, 1972], Conformation of proinsulin. Comparison of insulin and proinsulin self-association at neutral pH, *Biochemistry*, 11, 4013-4016

[Pendley *et al.*, 2003], Immunogenicity of therapeutic monoclonal antibodies, *Current Opinion in Molecular Therapeutics*, 5, 172-179

[Peng *et al.*, 2009], Effect of route of administration of human recombinant factor VIII on its immunogenicity in Hemophilia A mice, *J. Pharm. Sci.*, 98, 4480-4484



[Perini *et al.*, 2004], The clinical impact of interferon beta antibodies in relapsing-remitting MS, *Journal of Neurology*, 251, 305-309

[Perini *et al.*, 2001], Interferon-beta (IFN- $\beta$ ) antibodies in interferon- $\beta$ 1a- and interferon- $\beta$ 1b-treated multiple sclerosis patients. Prevalence, kinetics, cross-reactivity, and factors enhancing interferon- $\beta$  immunogenicity in vivo, *European Cytokine Network*, 12, 56-61

[Petersen *et al.*, 1999], Amino acid neighbours and detailed conformational analysis of cysteines in proteins, *Protein Engineering*, 12, 535-548

[PhEur 2.9.19., 2011], Particulate contamination: Sub-visible particles, *European Directorate for the Quality of Medicine (EDQM)*, 7th edition,

[Philo, 2006], Is any measurement method optimal for all aggregate sizes and types?, *AAPS Journal*, 8, E564-E571

[Philo *et al.*, 2009], Mechanisms of protein aggregation, *Current Pharmaceutical Biotechnology*, 10, 348-351

[Piggee, 2008], Therapeutic antibodies coming through the pipeline, *Analytical Chemistry (Washington, DC, United States)*, 80, 2305-2310

[Porter, 2001], Human immune response to recombinant human proteins, *J. Pharm. Sci.*, 90, 1-11

[Prompers *et al.*, 1999], Tryptophan mediated photoreduction of disulfide bond causes unusual fluorescence behavior of *Fusarium solani* pisi cutinase, *FEBS Letters*, 456, 409-416

[Qi *et al.*, 2009], Characterization of the photodegradation of a human IgG1 monoclonal antibody formulated as a high-concentration liquid dosage form, *J. Pharm. Sci.*, 98, 3117-3130

[Qureshi *et al.*, 2011], Optimization of asymmetrical flow field-flow fractionation, *LCGC North America*, 29, 76-83

[Randolph *et al.*, 2007], Engineering challenges of protein formulations, *AIChE Journal*, 53, 1902-1907

[Randolph *et al.*, 2002], Surfactant-protein interactions, *Pharmaceutical Biotechnology*, 13, 159-175

[Reichert, 2001], Monoclonal antibodies in the clinic, *Nature Biotechnology*, 19, 819-822

[Reichert, 2011], Antibody-based therapeutics to watch in 2011, *mAbs*, 3, 76-99

[Reichert *et al.*, 2005], Monoclonal antibody successes in the clinic, *Nature Biotechnology*, 23, 1073-1078

[Reschiglian *et al.*, 2005], Field-flow fractionation and biotechnology, *Trends in Biotechnology*, 23, 475-483

[Ring *et al.*, 1979], Anaphylactoid reactions to infusions of plasma protein and human serum albumin. Role of aggregated proteins and of stabilizers added during production, *Clinical allergy*, 9, 89-97

[Roque *et al.*, 2004], Antibodies and Genetically Engineered Related Molecules: Production and Purification, *Biotechnology Progress*, 20, 639-654

[Rosenberg, 2003], Immunogenicity of biological therapeutics: A hierarchy of concerns, *Developments in Biologicals (Basel, Switzerland)*, 112, 15-21

[Rosenberg, 2006], Effects of protein aggregates: an immunologic perspective, *The AAPS Journal* 2006, 8, E501-E507

[Rosenschein *et al.*, 1991], Streptokinase immunogenicity in thrombolytic therapy for acute myocardial infarction, *Israel journal of medical sciences*, 27, 541-545

[Roskos *et al.*, 2004], The clinical pharmacology of therapeutic monoclonal antibodies, *Drug Development Research*, 61, 108-120

[Ross *et al.*, 2000], Immunogenicity of interferon- $\beta$  in multiple sclerosis patients: influence of preparation, dosage, dose frequency, and route of administration, *Annals of Neurology*, 48, 706-712

[Roy *et al.*, 2009], Light-induced aggregation of type I soluble tumor necrosis factor receptor, *J. Pharm. Sci.*, 98, 3182-3199

[Saluja *et al.*, 2008], Nature and consequences of protein-protein interactions in high protein concentration solutions, *Int J Pharm*, 358, 1-15

[Sauerborn *et al.*, 2010], Immunological mechanism underlying the immune response to recombinant human protein therapeutics, *Trends in Pharmacological Sciences*, 31, 53-59

[Schellekens, 2002], Bioequivalence and the immunogenicity of biopharmaceuticals, *Nature Reviews Drug Discovery*, 1, 457-462

[Schellekens, 2003], Immunogenicity of therapeutic proteins, *Nephrology, Dialysis, Transplantation*, 18, 1257-1259

[Schellekens, 2005], Immunologic mechanisms of EPO-associated pure red cell aplasia, *Best Practice & Research, Clinical Haematology*, 18, 473-480

[Schimpf, 2000], Field Flow Fractionation Handbook, 1st Edition, *Wiley-Interscience*, 560 pp,

[Schmidt, 2010] Dynamic Light Scattering for Protein Characterization.,

[Scott *et al.*, 2010], Can we prevent immunogenicity of human protein drugs?, *Annals of the Rheumatic Diseases*, 69, i72-i76

[Shahrokh *et al.*, 1994], Probing the conformation of protein (bFGF) precipitates by fluorescence spectroscopy, *Journal of Pharmaceutical and Biomedical Analysis*, 12, 1035-1041

[Sharma *et al.*, 2010], Micro-flow imaging: flow microscopy applied to sub-visible particulate analysis in protein formulations, *AAPS Journal*, 12, 455-464

[Singh, 2011], Impact of product-related factors on immunogenicity of biotherapeutics, *J. Pharm. Sci.*, 100, 354-387

[Singh *et al.*, 2010], An industry perspective on the monitoring of subvisible particles as a quality attribute for protein therapeutics, *J. Pharm. Sci.*, 99, 3302-3321

[Strehl *et al.*, 2011], Discrimination Between Silicone Oil Droplets and Protein Aggregates in Biopharmaceuticals: A Novel Multiparametric Image Filter for Sub-visible Particles in Microflow Imaging Analysis, *Pharmaceutical Research*, No pp yet given

[Thirumangalathu *et al.*, 2009], Silicone oil- and agitation-induced aggregation of a monoclonal antibody in aqueous solution, *J. Pharm. Sci.*, 98, 3167-3181

[Tyagi *et al.*, 2009], IgG particle formation during filling pump operation: a case study of heterogeneous nucleation on stainless steel nanoparticles, *J. Pharm. Sci.*, 98, 94-104

[Unger, 1983], The application of size exclusion chromatography to the analysis of biopolymers, *TrAC, Trends in Analytical Chemistry*, 2, 271-274

[USP/NF, 2008], general chapter <788> particulate matter in injections, *Ed. Rockville, MD: United States Pharmacopoeial Convention*,

[Van Regenmortel, 2001], Antigenicity and immunogenicity of synthetic peptides, *Biologicals*, 29, 209-213

[van Regenmortel *et al.*, 2005], Immunogenicity of biopharmaceuticals: an example from erythropoietin, *BioPharm International*, 18, 36-52

[Vermeer *et al.*, 1998], Structural changes of IgG induced by heat treatment and by adsorption onto a hydrophobic Teflon surface studied by circular dichroism spectroscopy, *Biochimica et Biophysica Acta, General Subjects*, 1425, 1-12

[Volkin *et al.*, 1989], Mechanism of thermoinactivation of immobilized glucose isomerase, *Biotechnology and Bioengineering*, 33, 1104-1111

[Vollmar, 2005], Immunologie - Grundlagen und Wirkstoffe, 1st Edition, *Wissenschaftliche Verlagsgesellschaft mbH Stuttgart*, 455 pp,

[Wahlund, 2002], Field-flow fractionation for molar mass characterization of polysaccharides, *Journal of Chromatography Library*, 66, 573-594

[Wakankar *et al.*, 2007], Aspartate Isomerization in the Complementarity-Determining Regions of Two Closely Related Monoclonal Antibodies, *Biochemistry*, 46, 1534-1544

[Waldmann *et al.*, 1970], Variations in the metabolism of immunoglobulins measured by turnover rates, *Immunoglobulins, Proc. Conf. Biol. Aspects Clin. Uses Immunoglobulins*, 33-51

[Walsh, 2004], Modern antibody-based therapeutics, *BioPharm International*, 17, 18-20, 22-25

[Walsh, 2005], Biopharmaceuticals: recent approvals and likely directions, *Trends in Biotechnology*, 23, 553-558

[Walsh, 2006], Biopharmaceutical benchmarks 2006, *Nature Biotechnology*, 24, 769-776

[Walsh, 2010], Biopharmaceutical benchmarks 2010, *Nat Biotechnol*, 28, 917-924

[Wang, 1999], Instability, stabilization, and formulation of liquid protein pharmaceuticals, *International Journal of Pharmaceutics*, 185, 129-188

[Wang, 2005], Protein aggregation and its inhibition in biopharmaceuticals, *International Journal of Pharmaceutics*, 289, 1-30

[Wang *et al.*, 2006a], Antibody structure, instability, and formulation, *J. Pharm. Sci.*, 96, 1-26

[Wang *et al.*, 2006b], Antibody structure, instability, and formulation, *J. Pharm. Sci.*, 96, 1-26

[Wang *et al.*, 2008], Monoclonal Antibody Pharmacokinetics and Pharmacodynamics, *Clinical Pharmacology & Therapeutics (New York, NY, United States)*, 84, 548-558

[Wen *et al.*, 1996], Size-exclusion chromatography with on-line light-scattering, absorbance, and refractive index detectors for studying proteins and their interactions, *Anal Biochem*, 240, 155-166

[Wierda *et al.*, 2001], Immunogenicity of biopharmaceuticals in laboratory animals, *Toxicology*, 158, 71-74

[Williams *et al.*, 2006], Field-flow fractionation of proteins, polysaccharides, synthetic polymers, and supramolecular assemblies, *Journal of Separation Science*, 29, 1720-1732

[Wright *et al.*, 1997], Effect of glycosylation on antibody function: implications for genetic engineering, *Trends in Biotechnology*, 15, 26-32

[Yang *et al.*, 2007], Determination of tryptophan oxidation of monoclonal antibody by reversed phase high performance liquid chromatography, *Journal of Chromatography, A*, 1156, 174-182

[Zoells *et al.*, 2012], Particles in therapeutic protein formulations, Part 1: Overview of analytical methods, *J. Pharm. Sci.*, 101, 914 - 935

## 3 AGGREGATION STUDIES ON A HUMAN MONOCLONAL ANTIBODY

---

### 3.1 INTRODUCTION

According to the aggregation subject elaborately discussed in the previous chapter an immense versatility of aggregate structures is feasible, depending on the environmental conditions triggering the aggregation process. Considerable differences in the properties of aggregates of monoclonal antibodies in diverging stress studies were exemplarily reported by Kiese *et al.* and Hawe *et al.* [Hawe *et al.*, 2009; Kiese *et al.*, 2010].

This chapter aims to distinguish between the physicochemical characteristics of a monoclonal human antibody formulation, serving as model protein for follow-up studies after exposure to selective stress conditions. A variety of stress conditions is applied to the model antibody and the resulting aggregate pattern is analyzed quantitatively as well as qualitatively. Thus, meticulous analytics of the stressed antibody formulations will be performed and a critical evaluation of promising stress conditions will be performed based on these results. The objective is to obtain sufficient amounts of aggregates of well-defined physicochemical properties and structural conformation. Later on, the selected stress conditions shall be transferred to a murine monoclonal antibody in preparation of *in vivo* studies.

#### 3.1.1 Temperature

Temperature is the most common and most critical factor in affecting protein stability. In general an increase in temperature lowers the protein stability. Several proteins are most stable in a certain temperature range, indicating that both high and low temperatures outside this range may destabilize or unfold the protein. This unfolding is often promptly followed by aggregation. At low temperatures, beneath the specific temperature range, hydrophobic interactions are weakened. Thus, the hydrophobic regions may become more exposed to solvent and may lead to an increase in intermolecular interactions and aggregation [Brandts *et al.*, 1970; Privalov, 1990]. The denaturation of proteins at high temperatures is a more broadly known phenomenon, usually starting with an endothermic process of unfolding of the native protein. Upon unfolding the hydrophobic residues of the protein become exposed to the surface, while the tertiary structure degrades. Additionally, higher temperature leads to a strengthening of hydrophobic interactions. Both, the exposure of hydrophobic patches and the enhancement of hydrophobic interactions trigger the formation of different aggregates by intermolecular hydrophobic binding. [Vermeer *et al.*, 2000]. Furthermore an increased temperature implies an acceleration of the Brownian movement of the formulation ingredients, enhancing the incidence of protein-protein contact [Speed *et al.*, 1997]. Typically, heat stress causes irreversible denaturation of a protein, perturbing the native conformation [Chi *et al.*, 2003b]. Several studies investigated the resulting structure of aggregates after heating.

Augener *et al.* determined aggregation by non-covalent interaction as well as disulfide bond formation in a human IgG formulation [Augener *et al.*, 1970]. Examples of thermally induced irreversible unfolding and aggregation are immunoglobulines, human interferon- $\gamma$ , and streptokinase [Azuaga *et al.*, 2002; Mulkerrin *et al.*, 1989; Vermeer *et al.*, 2000; Zlateva *et al.*, 1999].

### 3.1.2 Mechanical stress

Mechanical stresses, such as shaking and stirring, create new interfaces within the protein formulation. The most common one is the air/water interface which is created by shaking as well as stirring. However, stirring studies have already been performed with Teflon<sup>®</sup> coated stirring bars, which create an additional hydrophobic Teflon<sup>®</sup> surface [Kiese, 2008; Mahler *et al.*, 2005]. Due to the amphiphilic structure of proteins and the hydrophobic surface of the air respectively Teflon<sup>®</sup>, protein molecules strongly tend to accumulate and align at this new interface exposing their hydrophobic patches to the more hydrophobic area of the interface. This highly concentrated rearrangement at the interface can lead to hydrophobic interactions and unfolding since the protein exposes parts of its hydrophobic core. The proximity to similar molecules at the new interface increases the incidence of protein-protein interactions leading to substantial aggregation [Carpenter, John F. *et al.*, 1999; Mahler *et al.*, 2010b]. Numerous proteins were shown to be prone to aggregation induced by agitation, including monoclonal antibodies [Bam *et al.*, 1998; Carpenter, John F. *et al.*, 1999; Colombie *et al.*, 2001; Mahler *et al.*, 2009]. However, the aggregation characteristics already strongly differ within the class of monoclonal antibodies. Some mAbs were reported to quickly aggregate within hours of mechanical stress exposure [Fesinmeyer *et al.*, 2009; Kiese, 2008]. In comparison, other IgGs were reported to be remarkably resistant to agitation stress and the exposure to air-water interfaces [Mahler *et al.*, 2009; Paborji *et al.*, 1994]. For the development of new therapeutic proteins, surface-induced aggregation has to be circumvented to reduce potential implications concerning efficacy and safety. Approaches for an avoidance of agitation induced aggregates should involve processing steps, like stirring and shaking, as well as the properties of the drug candidate itself.

### 3.1.3 Freeze-thaw stress

Freeze-thawing can accidentally or by design arise to the protein during many stages in production, storing and shipping. Proteins that are formulated by lyophilization are dried in a frozen state, whereas proteins formulated as liquids are sometimes frozen for long-term storage and thawed prior to use [Arakawa *et al.*, 2001]. The formation of ice is the most crucial step during freezing, since the protein is excluded from the ice phase and thus concentration of all solutes in the liquid phase increases strongly. This artificial concentration can additionally involve pH changes, as reported for phosphate buffers, for example [van den Berg *et al.*, 1959]. The complexity of environmental changes during freezing can have a major impact on protein stability and lead to aggregation and denaturation [Carpenter, John F. *et al.*, 1988]. Therefore, a maximum stability of the protein in non-frozen aqueous solution should be chosen during

formulation development, since it is qualitatively related to stability during freezing and thawing [Arakawa *et al.*, 2001]. The use of cryoprotectants can stabilize proteins with low inherent stability to freeze-thaw stress [Arakawa *et al.*, 1991]. Cryoprotectants are of great chemical diversity including sugars, amino acids, polyols, polymers, and salts. Besides others, the most important underlying stabilizing effect is preferential exclusion, a mechanism described in detail by Timasheff and his colleagues [Arakawa *et al.*, 1982; Timasheff, 1995]. They reported that substances like sucrose and glycerol are preferentially excluded from the immediate environment of a protein in aqueous systems, thereby stabilizing the protein in solution. Thus solutes which are preferentially excluded from the surface of the protein are capable of preventing protein denaturation during freezing and thawing [Arakawa *et al.*, 2001].

#### 3.1.4 Light exposure

Therapeutic proteins typically are exposed to light numerous times amongst their production process and the administration to the patient. Almost all proteins are subject to chromatographic purification, which includes detection by absorption of UV light after elution from the column. In general, these columns are made of glass. Therefore, protein molecules located near the glass wall can be continually exposed to room light or daylight during the entire process [Kerwin *et al.*, 2007]. Furthermore, light exposure might occur during bulk storage, when the storage container is transparent for light, during fill and finish operations, and visual inspections. Finally, the intravenously administration of therapeutic proteins requires the use of IV bags, enabling the exposure to light irradiation while delivery [Kerwin *et al.*, 2007; Roy *et al.*, 2009]. The expression of recombinant proteins by mammalian cell lines often implicates viral contamination. This entails requirements by FDA dealing with viral reduction. One excellent option is the inactivation of viruses by ultraviolet C (UV-C) light, though its application to biopharmaceuticals is controversial, due to photodegradation of proteins [Lorenz *et al.*, 2009]. The most prominent amino acids for photodegradation are Phenylalanine, Tryptophan, and Tyrosine. The different pathways of photoreactions in proteins were reported in numerous publications and shall not be discussed in more detail [Davies *et al.*, 2001; Hovorka *et al.*, 2001; Kerwin *et al.*, 2007; Parker *et al.*, 2007; Prompers *et al.*, 1999; Roy *et al.*, 2009; Vanhooren *et al.*, 2002]. The regulatory agencies are aware of the potentially occurring degradation of proteins by light exposure and published guidelines on photostability testing of new active substances at the International Conference on Harmonization (ICH) [ICH Q1B, 1998]. The consequences of light absorbance by proteins vary from conformational changes, aggregation, to loss of efficacy and biological activity. Light induced degradation of proteins is a well-known phenomenon *in vivo*. The damage of proteins in the skin and in the eyes is of great concern in aging [Mizdrak *et al.*, 2008; Parker *et al.*, 2007]. This study omits the implications on chemical stability, but investigates the physical stability of monoclonal antibodies by light exposure.

## **3.2 MATERIALS AND METHODS**

### **3.2.1 Materials**

#### **3.2.1.1 Human IgG1 antibody (huAb)**

A recombinant human monoclonal IgG1 antibody (huAb) was kindly provided by Abbott GmbH & Co. KG and used as a model protein for these separation studies. The antibody solution applied in the experiments was diluted to a concentration of 4 mg/mL in a formulation buffer containing 1.2 mM citrate, 14 mM phosphate, 105 mM sodium chloride and 66 mM mannitol at pH 5.2. The IgG1 stock solution had an initial concentration of 70 mg/mL and was stored at -80 °C in the deep freezer. Prior to use, the formulation buffer was filtrated using a 0.2 µm sterile syringe filter made of cellulose acetate (VWR International, Darmstadt, Germany). 3 mL of the antibody solution was filled into cleaned and sterilized 6 R vials made from glass type 1 (Schott AG, Mainz, Germany), sealed with Teflon<sup>®</sup>-faced rubber stoppers (West Pharmaceuticals Services, Eschweiler, Germany) and crimped. All antibody samples were prepared under aseptic conditions. Highly purified water generated in-house was used for the preparation of samples and buffers (PURELAB Plus instrument (USF Elga, Celle, Germany)). All substances used were of analytical grade.

### **3.2.2 Methods to provoke protein instability**

#### **3.2.2.1 Stirring stress**

Stirring stress of the huAb was performed in 6 R glass vials filled with 3 mL of a 4 mg/mL antibody solution. A 6 x 3 mm sized Teflon<sup>®</sup> (PTFE)-coated stir bar (VWR International, Darmstadt, Germany) was used on a Variomag Telesystem 60.07 multipoint stirrer (Thermo Fisher Scientific, Schwerte, Germany). Speed was set to 240 rounds per minute (rpm) and a temperature of 25°C was fixed by stirring in a cabinet dryer. For control experiments, the pure buffer solution was stirred under the same conditions as well.

#### **3.2.2.2 Shaking stress**

Shaking stress of the antibodies was performed in 6 R glass vials filled with 3 mL of a 4 mg/mL antibody solution. A VWR Microplate Shaker (VWR International, Darmstadt, Germany) was used for shaking the vials at 240 rpm. Therefore, the vials were arranged upright in a non-transparent box and the shaker moves in horizontal circles and with an orbit size of 3 mm.

#### **3.2.2.3 Freeze-thaw stress**

Freeze-thaw stress was conducted in 6 R glass vials filled with 3 mL of a 4 mg/mL antibody solution. The vials were placed in the deep freezer at -80°C for 2 hours and subsequently thawed at 25°C in a cabinet dryer for 2 hours. The cycle was repeated up to eight times.



#### 3.2.2.4 Light exposure

A Suntest CPS radiation chamber (Heraeus Holding, Hanau, Germany) was used to expose the samples to light. Radiation intensity was set to  $55 \pm 5 \text{ W/m}^2$ . The light source was a xenon lamp emitting light of the whole sunlight spectrum. A filter made of sheet glass was incorporated to obtain a radiation spectrum close to that to which an antibody formulation might be exposed to during storage and handling. 3 mL of the samples containing 4 mg/mL of protein were filled in 6 R glass vials and placed in the center of the radiation chamber in an upright position. Sampling was performed after 1 day, 4 days, 6 days and 7 days by withdrawal of three vials. Additionally, the formulation buffer was exposed to light as well and sampled at the same time points. For control experiments, a triplicate of vials completely shielded with aluminum foil was included in the study, serving as control on final sampling date for the slight temperature increase ( $35 \pm 2^\circ\text{C}$ ) during radiation.

#### 3.2.2.5 Temperature stress

Heating was performed 6 R glass vials filled with 3 mL of a 4 mg/mL antibody solution. The vials were incubated in cabinet dryers of a fixed temperature of  $50^\circ\text{C}$  for up to 4 weeks. Sampling was performed weekly. The melting temperature ( $T_m$ ) of the human IgG1 was  $75^\circ\text{C}$ , thus several degrees above the incubation temperature.

### 3.2.3 Methods to determine protein stability

#### 3.2.3.1 Light obscuration

Light obscuration (LO) measurements were conducted with a PAMAS-SVSS-C Sensor HCB-LD 25/25 (Partikelmess- und Analysensysteme GmbH, Rutesheim, Germany) to quantify subvisible particles between 1 and  $200 \mu\text{m}$ . Three aliquots of 0.3 mL of each sample were analyzed. Before each measurement, 0.3 mL of the sample was flushed through the system and discarded. Between the sample measurements the system was rinsed with highly purified water until the system was free of particles. The results of the particle counts were calculate as mean value out of three measurements, referring to a sample volume of 1.0 mL. If necessary the samples were diluted with highly purified water to reach the linear range of the instrument.

#### 3.2.3.2 Dynamic light scattering

Dynamic light scattering on a Malvern Zetasizer Nano ZS (Malvern, Herrenberg, Germany) was used to investigate the size distribution of particles and molecules in the protein samples in the sub-visible range between 1 nm and  $1 \mu\text{m}$ . Non-invasive backscattering at an angle of  $173^\circ$  was performed at  $25^\circ\text{C}$  using a Helium-Neon-Laser at 633 nm. Each sample was analyzed twice. The refractive index for aqueous protein solution was set to 1.45. 700  $\mu\text{L}$  of the undiluted protein samples were measured in half-micro cuvettes made of polystyrene (Fisher Scientific, Schwerte, Germany). Each sample was measured in triplicate. Using the Dispersion Technology Software (version 6.1, Malvern) the polydispersity index (PDI) and the Z-average diameter ( $Z_{\text{ave}}$ ) were calculated from the correlation function.

### 3.2.3.3 Turbidity

The turbidity was measured by 90° light scattering at  $\lambda = 860$  nm using a NEPHLA turbidimeter (Dr. Lange, Düsseldorf, Germany). Approximately 1.8 ml of the final samples were analyzed according to the European Pharmacopoeia and the results are reported in formazine nephelometric units (FNU) [PhEur 2.9.19., 2011].

### 3.2.3.4 Size exclusion chromatography

Concentrations of soluble aggregates, fragments, and monomeric protein were measured by size exclusion chromatography on an Agilent system with RI and UV detection (Agilent Technologies, Palo Alto, USA). A Superdex 200 10/300 GL column (GE Healthcare, Little Chalfont, UK) was used as the solid phase. Phosphate buffered saline (PBS) at pH 7.4 (12 mM phosphate, 137 mM sodium chloride, 2.7 mM potassium chloride) with a flow rate of 0.5 ml/min was used as a mobile phase. Before injection the samples were centrifuged at 5000 x g for 10 minutes to remove insoluble species, probably clogging the column. Each sample was analyzed in duplicate, using an injection volume of 50  $\mu$ l. The protein recovery was calculated using either the refractive index signal or the UV absorbance signal at 280 nm. The area under the curve (AUC) of the unstressed sample was defined as 100%.

### 3.2.3.5 Intrinsic protein fluorescence spectroscopy

A Varian Cary Eclipse fluorescence spectrometer (Varian, Inc., Darmstadt, Germany) was used to monitor intrinsic protein fluorescence and thus to analyze the tertiary structure of the protein. The temperature was set to 20°C for all measurements. Samples were centrifuged and supernatant was measured in triplicate in white 96-well plates (Nunc, Roskilde, Denmark) using a volume of 200  $\mu$ L for each well. Excitation wavelength was set to 295 nm and the excitation slit was fixed at 5 nm. Emission was recorded from 300 to 500 nm using a 5 nm emission slit. The sample concentration was 0.5 mg/mL, unless otherwise mentioned. The scanning rate was set to 20 nm/min and the voltage of the photomultiplier was set to 800 V. The "Scan application" of the Cary Eclipse Software (version 1.0, Varian, Inc., Darmstadt, Germany) was utilized to record the spectra. The mean spectrum of each triplicate was calculated after recording. All samples were buffer corrected. Smoothing was performed by OriginLab 8.0 DataAnalysis Software (OriginLab Corporation, Northampton, USA) on 99 points according to the Savitzky-Golay algorithm.

### 3.2.3.6 Extrinsic protein fluorescence spectroscopy

A Varian Cary Eclipse fluorescence spectrometer (Varian, Inc., Darmstadt, Germany) was used to monitor extrinsic protein fluorescence and thus to analyze the conformational structure of the protein. ANS (1-Anilinonaphthalene-8-sulfonic acid) at 20  $\mu$ M concentration was used as fluorescent dye. ANS is hardly fluorescent in a polar, aqueous environment, but in a non-polar, hydrophobic environment it becomes highly fluorescent [Weber et al., 1954]. However, ANS itself might induce structural alterations of proteins due to electrostatic

interactions [Ali et al., 1999]. Besides electrostatic interactions between protein and ANS, hydrophobic interactions are discussed to be involved in the binding mechanisms between both [Laurence, 1952]. Several studies reported the ability of ANS to interact with hydrophobic sites of proteins accompanied with an increase of fluorescence intensity and an blue shift of the emission maximum [De Filippis et al., 1996; Stryer, 1965].

The temperature was set to 20°C for all ANS fluorescence measurements. Samples were measured in triplicate in white 96-well plates (Nunc, Roskilde, Denmark) using a volume of 200 µL for each well. Excitation wavelength was set to 350 nm and the excitation slit was fixed at 5 nm. Emission was recorded from 360 to 600 nm using a 5 nm emission slit. The sample concentration was 0.5 mg/mL, unless otherwise mentioned. The scanning rate was set to 20 nm/min and the voltage of the photomultiplier was set to 800 V. The “Scan application” of the Cary Eclipse Software (version 1.0, Varian, Inc., Darmstadt, Germany) was utilized to record the spectra. The mean spectrum of each triplicate was calculated and buffer corrected after recording. Smoothing was performed by OriginLab 8.0 DataAnalysis Software (OriginLab Corporation, Northampton, USA) on 99 points according to the Savitzky-Golay algorithm.

#### 3.2.3.7 Fourier transform infrared spectroscopy (FTIR)

For the determination of changes in secondary structure of proteins, native and aggregated formulation samples were analyzed at 1 mg/mL by FTIR in ATR mode, unless otherwise mentioned. The temperature of the Bio-ATR II unit of a Tensor 27 spectrometer (Bruker Optics GmbH, Ettlingen, Germany) was set to 20°C. Spectra were collected from 4000 cm<sup>-1</sup> to 850 cm<sup>-1</sup> with a resolution of 4 cm<sup>-1</sup>. 120 scans were averaged for each sample measurement. Each spectrum was background corrected and vector normalized on the amide I band using the Opus software (version 6.5, Bruker Optics, Ettlingen, Germany). Finally, the second derivatives of the spectra were calculated and smoothened on 17 points (according to the Savitzky-Golay algorithm).

#### 3.2.3.8 High resolution UV absorbance spectroscopy

The tertiary structure of the samples was analyzed by high-resolution UV absorbance spectroscopy in a quartz cuvette at 25°C using an Agilent 8453 UV-visible spectrophotometer (Agilent Technologies, Waldbronn, Germany). Spectra were recorded from 190 to 400 nm at a resolution of 1 nm and a protein concentration of 0.5 mg/mL. Finally, the second derivatives of the spectra were calculated and fitted to a cubic function with 99 interpolated points per raw data point [Kuelto et al., 2003]. The final resolution resulting from this procedure was 0.01 nm. The *a/b* ratio was calculated from the peak to peak distances between the minimum around 283 nm and the maximum around 287 nm (referring to *a*), as well as the peak to peak distance between the minimum around 290 nm and the maximum around 295 nm (referring to *b*). The determination of peaks and *a/b* ratios was performed by OriginLab 8.0 Data Analysis Software (OriginLab Corporation, Northampton, USA).

### 3.3 RESULTS

#### 3.3.1 Mechanical stability of Human IgG1 antibody (huAb)

The formation of particles in the huAb formulation in the micrometer range was determined by light obscuration. Stirring and shaking at 240 rpm quickly lead to the formation of numerous particles larger than 1  $\mu\text{m}$  and an increase in turbidity (see Table 3-1).

**Table 3-1 – Results of light obscuration and turbidity measurements of huAb after agitation stress.**

Stirring 240 rpm		huAb			buffer
Duration	0 h	4 h	24h	72h	72h
# of particles $\geq 1 \mu\text{m}$	1479	263,041	272,490	329,476	16,234
# of particles $\geq 10 \mu\text{m}$	20	327	16,557	15,284	150
# of particles $\geq 25 \mu\text{m}$	2	1	7	403	13
Turbidity [FNU]	1.5	28.8	191.1	> 1300	0.9
Shaking 240 rpm		huAb			buffer
Duration	0 h	4 h	24h	72h	72h
# of particles $\geq 1 \mu\text{m}$	1479	16,346	43,852	75,574	8549
# of particles $\geq 10 \mu\text{m}$	20	216	228	3,223	107
# of particles $\geq 25 \mu\text{m}$	2	9	15	87	32
Turbidity [FNU]	1.5	4.9	9.1	12.2	0.8

These results indicate that especially prolonged stirring of several hours results in the formation of numerous aggregates in the upper  $\mu\text{m}$ -range. A particle growth on the cost of low  $\mu\text{m}$  sized initial species, generated within the first hours of stirring is suggested. 72 h of stirring of the buffer solution was additionally performed to verify that the enhanced particle loading originates from protein. The total particle counts within the formulation buffer increased due to stirring, though particle numbers far below those in protein containing solutions were detected. About 16,200 particles  $\geq 1 \mu\text{m}$  per mL were detected in the buffer sample. Thus, a minor fraction ( $\sim 1\text{-}5\%$ ) of generated particles can at least partially consist of abrasive PTFE (Teflon®) particles.

Another valuable and simple method to detect insoluble aggregates in protein solutions is turbidity measurement [Wang, John *et al.*, 1996]. Using a laser wavelength of 860 nm especially large particles will impact the results, since large particles more effectively scatter light of long wavelengths than light of short wavelengths [Mahler *et al.*, 2005]. Turbidity measurements using the nephelometric set-up resulted in significantly increasing formazine nephelometric unit (FNU) values during stirring. Already after 4 h of stirring the samples were visually observed to be turbid, represented by a value of 28.8 FNU. After one day, 191.1 FNU were measured within the stirred samples. Finally, the turbidity of the samples exceeded the limitations of the turbidimeter after 72 h of stirring. These elevated turbidity values indicate the existence of large particles/aggregates and precipitation. For control, the buffer formulation

was stirred under the same conditions for 72 h as well. The resulting turbidity was 0.9 FNU, which is considered to be a clear solution, according to the PhEur [PhEur 2.2.1., 2011].

Dynamic light scattering measurements resulted in the determination of two peaks of different size after 4 hours. The main peak exhibited a diameter of 9.2 nm, and a second minor peak arises around 1000 nm (data not shown). After 72 hours, one peak around 1000 nm was detected. The dynamic light scattering results were heavily influenced by precipitation appearing already after 4 hours of stirring. Thus the parameters characterizing the size distribution in the nanometer range are not evaluated for the stirred samples.

Shaking the protein samples also induces particle formation in micrometer range. Furthermore, a constantly increasing turbidity was measured referring to shaking time. In the end, 12.2 FNU were determined in the antibody samples shaken for three days. After 24 hours of shaking the samples started to visibly appear turbid as well, whereas the buffer remained clear after shaking up to 72 hours. After 4 hours of shaking the sample appeared still monodispers (PDI 0.09) in DLS measurements, with one peak around 9.4 nm (diameter). Increasing shaking time to 72 h resulted in two species and a PDI of ~0.3. The major peak appeared at a diameter of 10.9 nm and a minor one around 950 nm (data not shown). The shaken samples slightly started to precipitate after 72 h. The elevated PDI indicates the formation of species of different sizes within the samples. Additionally the Z-average diameter increased with shaking duration too, suggesting that especially larger species/ aggregates are formed. Table 3-2 summarizes the  $Z_{ave}$  and PDI results of the shaken samples.

**Table 3-2 – Results of Z-average diameter and polydispersity index of huAb samples after shaking.**

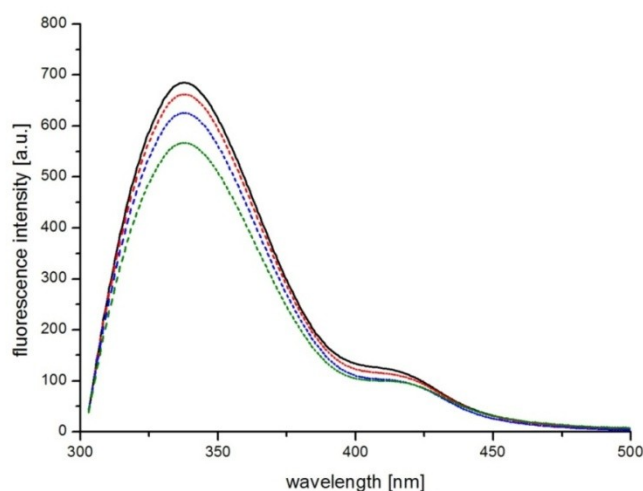
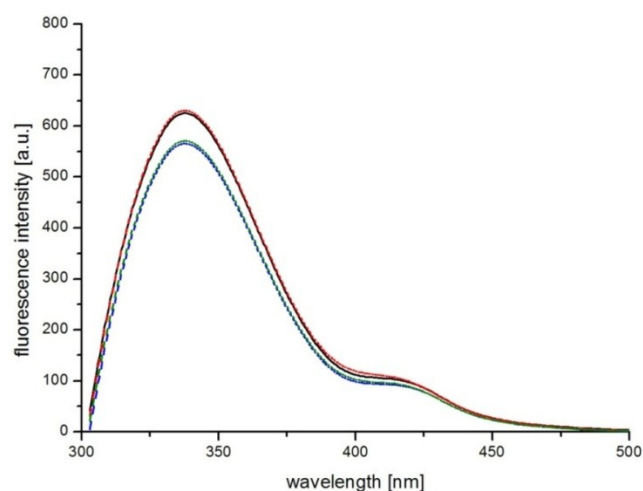
Shaking 240 rpm	0 h	4 h	24 h	72 h
$Z_{ave}$	11.5	11.3	17.8	30.6
PDI	0.04	0.09	0.31	0.29

Size exclusion chromatography (SEC) was performed after centrifugation of the mechanically stressed samples. The insoluble species that obviously appeared within the samples were separated and the size distribution of soluble protein species was determined by UV-detection at 280 nm. After 4 hours of stirring  $96 \pm 1.9$  % of total protein content compared to the unstressed sample was recovered. The total recovery further decreases to  $94 \pm 2.5$  % after 24 hours and finally after 72 hours of stirring merely  $80.3 \pm 4.5$  % of the original protein content were found. These data confirm the results from the previous experiments, showing that stirring induces a strong formation of insoluble aggregates, expressed by the significant reduction of total protein recovery. The huAb samples that were shaken revealed a decreasing protein recovery within the three days of investigation too. After 72 hours  $89.8 \pm 2.6$  % of the protein content were recovered, compared to the unstressed sample. All chromatograms of shaken and stirred samples consisted of only one peak eluting around 66 minutes representing the monomeric protein. No additional soluble species like fragments or aggregates were detected by SEC (data not shown).

To determine alterations in the tertiary structure of the human IgG1 samples intrinsic protein fluorescence was utilized. The emission spectra of the samples after stirring are shown in Figure 3-1, A. The position of the maximum fluorescence intensity around 340 nm did not change in any of the stirred samples. But the intensity of emitting fluorescence decreases about 17 % (from 690 arbitrary units (a.u.) of the unstressed sample to 570 a.u. after 72 h of stirring) with prolonged stirring time. Similar results were obtained of the samples after shaking (see Figure 3-1, B). No wavelength shift of the emission maxima was detected (data not shown). A reduction of fluorescence intensity was first detected after 24 hours of shaking. It finally decreases about 9 % while 72 h of shaking.

Intrinsic fluorescence of a protein is provoked by the aromatic amino acids phenylalanine, tryptophan and tyrosine [Jiskoot et al., 2005]. The emission spectra shown in Figure 3-1 solely represent the emission of tryptophan (Trp), due to the excitation at 295 nm. The fluorescence of the hydrophobic amino acid tryptophan is especially dependent on the environmental conditions surrounding the protein. Thus, changes in the local environment of Trp can be investigated by intrinsic fluorescence. Depending on the characteristics of the original surrounding, alterations can either lead to decreases or increases of the fluorescence intensity. For example, polar conditions can decrease fluorescence intensity by quenching [Jiskoot et al., 2005]. When quenching amino acids will be removed from the micro-environment of Trp due to unfolding, intensity might also increase [Hawe et al., 2008]. As a typical application area unfolding processes of proteins should be mentioned, which might expose the hydrophobic core of a protein to the aqueous solvent. Thus, the aromatic amino acids will change their interaction with neighboring amino acids leading to changes in the fluorescence intensity [Chen et al., 1998]. If the maximum of the fluorescence intensity changes its wavelength position as well, a pronounced alteration of the environment of tryptophan can be assumed.

The maxima of all emission spectra arise around 340 nm thereby indicating that the tertiary structure of the IgG1 did not considerably change while stirring. A complete unfolding would entail contact of tryptophan to water molecules in the aqueous surrounding and is reported to shift the emission maximum to 350 nm [Ladokhin, 2006]. However, both stress methods reduced the fluorescence intensity, indicating that unfolding processes occurred in the non-precipitated protein species and the fluorescence of Trp is quenched. Comparing both agitation methods at the same duration, stirring leads to stronger alterations in the neighborhood of Trp than shaking.

**A)****B)**

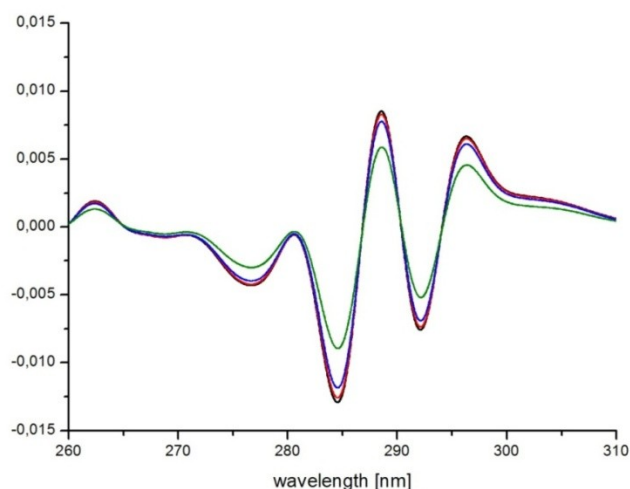
**Figure 3-1 – Intrinsic protein fluorescence emission spectra of 0.5 mg/mL human IgG1 after excitation at 295 nm. A) Spectra of stirred samples B) spectra of shaken samples**

The solid black lines represent the spectra of the unstressed huAb sample. The dashed red lines represent the spectra after 4 hours of stirring/shaking, the dashed blue lines after 24 h of stirring/shaking and the dashed green lines after 72 hours of stirring/shaking.

Another spectroscopic method to investigate the tertiary structure of proteins is UV/Vis absorbance spectroscopy. It was additionally utilized to assess the conformational stability of the human IgG1 antibody. The zero-order spectra are typically consisting of the overlapping absorbance of phenylalanine (between 245 and 270 nm), tryptophan (between 265 and 295 nm), and tyrosine (between 265 and 285 nm). The second derivative of UV absorbance is commonly used to enhance the resolution compared to the zero-order spectra [Kuelzto et al., 2003]. The resulting spectra obtain peaks whose positions are sensitive to the polarity of the environment of the absorbing amino acids. A peak shift to shorter wavelengths generally indicates an increase in polarity of the amino acid's environment [Mach et al., 1994]. The

$a/b$  ratio is often used to determine the exposure of tyrosine and tryptophane residues to the surrounding environment [Kuiltzo et al., 2005].

A)



B)

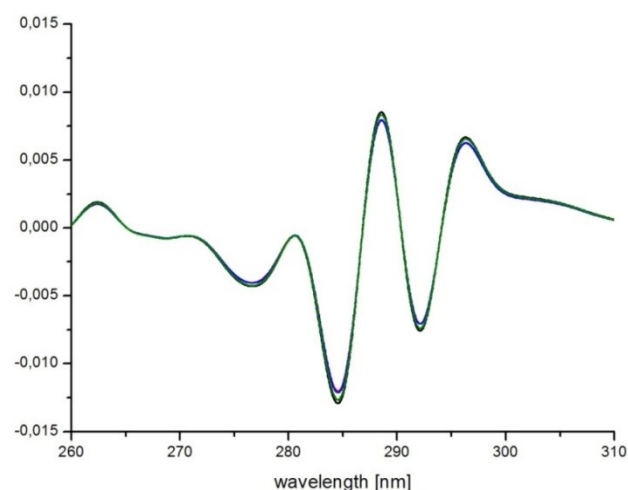


**Figure 3-2 – UV 2<sup>nd</sup> derivative spectra of 0.5 mg/mL human IgG1.**

**A) Spectra of stirred samples    B) spectra of shaken samples**

The solid black lines represent the spectra of the unstressed huAb sample. The dashed red lines represent the spectra after 4 hours of stirring/shaking, the dashed blue lines after 24 h of stirring/shaking and the dashed green lines after 72 hours of stirring/shaking.

The 2<sup>nd</sup> derivative spectra recorded between 260 and 310 nm after stirring and shaking procedures are displayed in Figure 3-2. The spectra showed no significant peak shift, neither after stirring, nor after shaking the human IgG1 formulation. The mean values of the triplicate measurements of the  $a/b$  ratios determined in the 2<sup>nd</sup> derivative spectra are summarized in Table 3-3. Stirring slightly increases the  $a/b$  ratio, whereas shaking does not affect the ratio at all. Thus, UV absorbance spectroscopy enabled the detection of slight changes in the environment of tyrosine and tryptophane of soluble species after stirring, but not after shaking. But these unfolding processes are suggested to be weak.



**Table 3-3 – Results of a/b ratio determination from UV 2<sup>nd</sup> derivative spectroscopy of huAb.**

Agitation	Unstressed	Stirred 72 h	Shaken 72 h
a/b ratio	1.516	1.535	1.516

The conformational state of the human IgG1 after agitation was further analyzed by extrinsic fluorescence spectroscopy and ATR-FTIR spectroscopy. 1-Anilinonaphthalene-8-sulfonic acid (ANS) in 20  $\mu\text{M}$  concentration was used as fluorescent dye for the determination of the extrinsic fluorescence of the protein. Significant increases of ANS-fluorescence intensity were determined after stirring as well as after shaking.

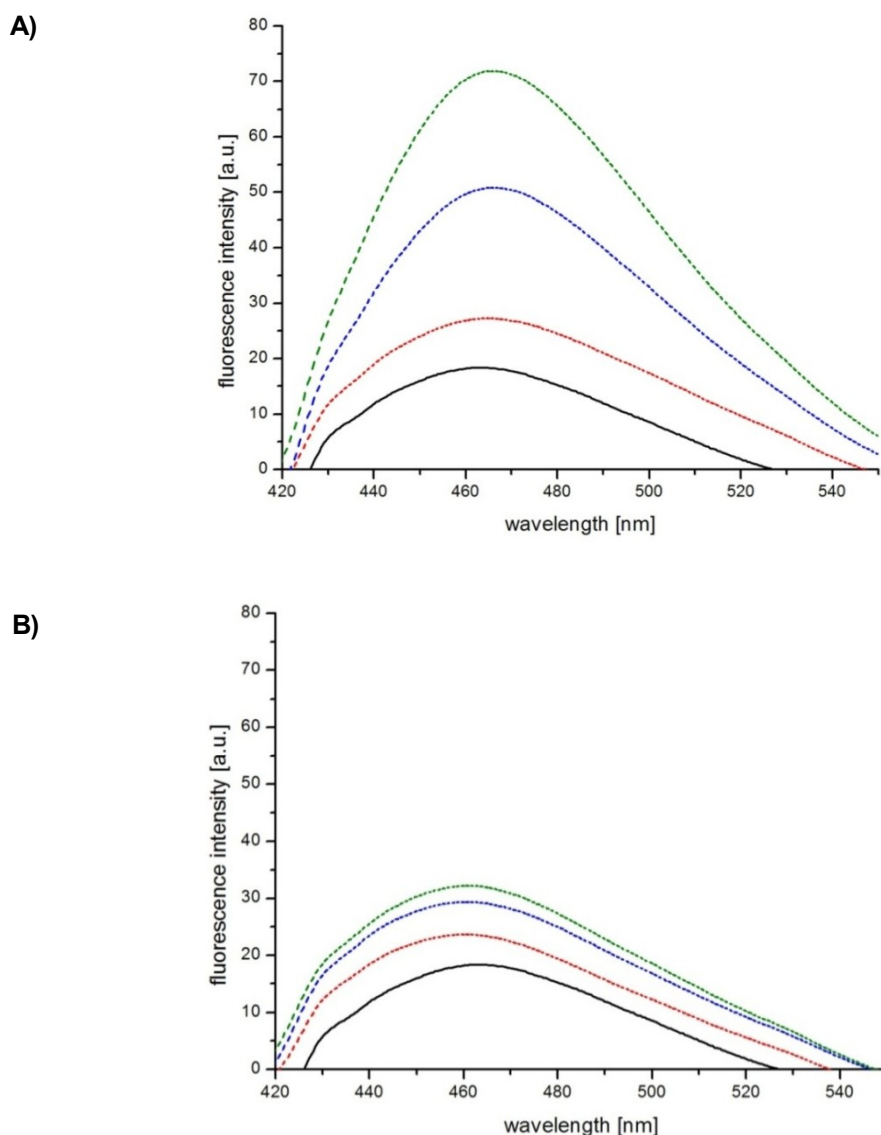


**Figure 3-3 – Extrinsic fluorescence emission spectra of 0.5 mg/mL human IgG1 and 20  $\mu\text{M}$  ANS after excitation at 350 nm. A) Spectra of stirred samples B) spectra of shaken samples**

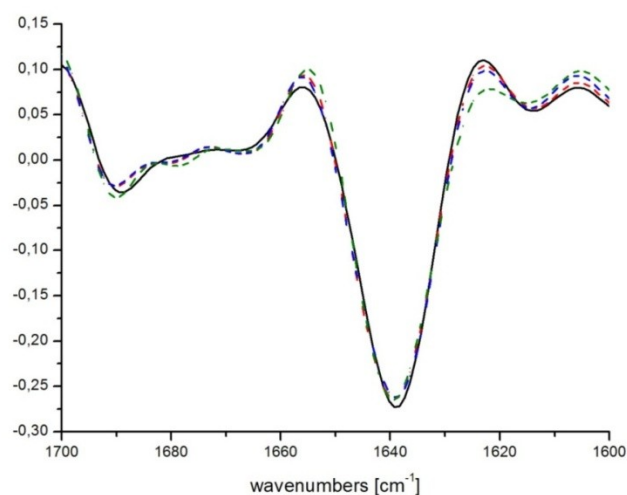
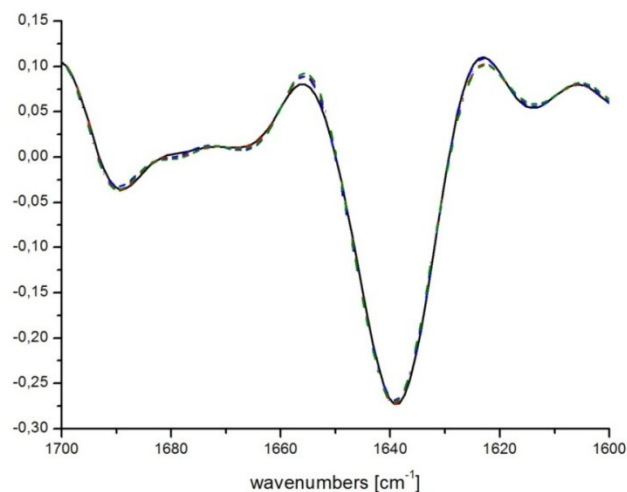
The solid black lines represent the spectra of the unstressed huAb sample. The dashed red lines represent the spectra after 4 hours of stirring/shaking, the dashed blue lines after 24 h of stirring/shaking and the dashed green lines after 72 hours of stirring/shaking.

The emission spectra of huAb after agitation stress after background subtraction are shown in Figure 3-3. The intensity of the emitting light is continuously increasing with prolonged stirring time. Starting with a weak ANS fluorescence intensity of ~18 a.u. for the native protein sample, a nearly four times higher intensity of more than 70 a.u. is finally emitted after 72 h of stirring. Shaking resulted in only minor increases in ANS fluorescence intensity. After the same duration of agitation the peak maximum possessed an intensity of 32 a.u.. It can be suggested that during shaking and stirring unfolding the protein underwent processes that enabled an enhanced interaction with ANS. The peak maxima are summarized in Table 3-4. The determined wavelength shifts are weak. A red shift to higher wavelengths of 3 nm was determined after 72 h of shaking. After the same duration of shaking, instead, a blue shift of nearly 2 nm was found. The shaken and the stirred samples showed an increased capability to bind ANS, indicating that unfolding occurred [Hawe *et al.*, 2008; Jiskoot *et al.*, 2005]. But the characteristics of the secondary structure of shaken and stirred huAb and their interaction with ANS differ.

**Table 3-4 – Results of peak position from ANS fluorescence emission spectra of 0.5 mg/mL huAb.**

Agitation	Unstressed	Stirring 72 h	Shaking 72 h
Peak position	462.98 nm	465.97 nm	461.04 nm

FTIR spectroscopy was consulted to assess the influence of mechanical stress on the secondary structure of the human antibody. The 2<sup>nd</sup> derivative spectra of the samples (after removal of particles) before and after agitation are shown in Figure 3-4. The spectra are dominated by the strong valley at 1638 cm<sup>-1</sup>, associated with the typical intramolecular  $\beta$ -sheet structure of antibodies [Byler *et al.*, 1998; Costantino *et al.*, 1997]. Figure 3-4, A depicts the effect of stirring on the secondary structure of huAb. Slight decreases of the intramolecular  $\beta$ -sheet band were detected, coming along with minor changes at band positions around 1622 - 1615 cm<sup>-1</sup>, representing intermolecular  $\beta$ -sheets. The weak alterations in the spectra suggest that minor unfolding and aggregation was induced by stirring. However, the predominant  $\beta$ -sheet structure of the IgG1 was maintained in the soluble species. No substantial difference in second derivative ATR-FTIR spectra was detectable between the soluble fraction of the shaken and non-shaken antibody formulations (Figure 3-4, B). These data indicate that the secondary structure did not change in the non-particulate fraction after shaking.

**A)****B)**

**Figure 3-4 – Second derivative ATR-FTIR spectra of amide I band of 1 mg/mL human IgG1**

**A) Spectra of stirred samples    B) spectra of shaken samples**

The solid black lines represent the spectra of the unstressed huAb sample. The dashed red lines represent the spectra after 4 hours of stirring/shaking, the dashed blue lines after 24 h of stirring/shaking and the dashed green lines after 72 hours of stirring/shaking.

### 3.3.2 Stability of huAb against freeze-thawing

Most therapeutic proteins undergo freeze-thaw processes during production or storage, either in bulk formulation, or in the final formulation for lyophilization or final storage. The influence of up to eight freeze-thaw cycles alternating between -80°C and +25°C were investigated with the human IgG1 antibody. Light obscuration detected no significant increasing numbers of particles  $\geq 1 \mu\text{m}$  per mL (data not shown). The numbers of particles larger than 10  $\mu\text{m}$  slightly increased within 8 freeze-thaw cycles. The unstressed material obtained 37 particles of this size per mL, and after eight times freezing and thawing 149 particles per mL were counted. Turbidity measurements resulted in 1.9 FNU after eight freeze-thaw cycles and

dynamic light scattering determined one single peak obtaining a diameter of 11.5 nm (data not shown). The data suggest that no substantial formation of subvisible particles was induced by freeze-thawing.

To detect potentially generated soluble protein aggregates or fragments, the samples were investigated by size exclusion chromatography. The chromatograms revealed a total protein recovery of  $107.8 \pm 13.2$  %, indicating that no precipitation occurred while freeze-thawing. The distribution of soluble protein species in the chromatograms detected by UV absorbance showed no increase in fragmented or aggregated species (data not shown). Neither soluble nor insoluble aggregates were generated by freeze-thawing of huAb.

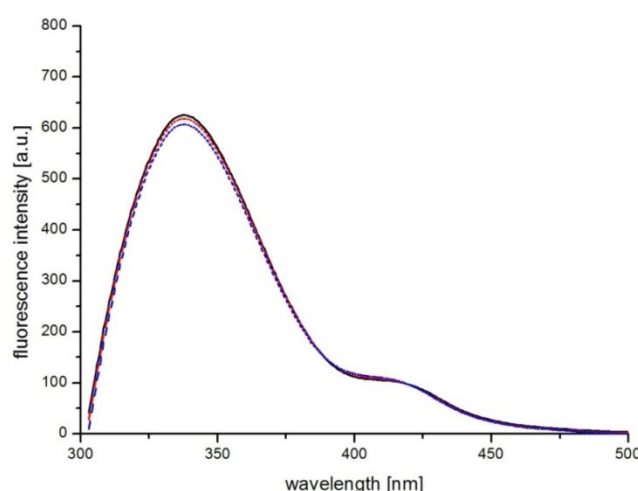


**Figure 3-5 – Intrinsic protein fluorescence emission spectra of 0.5 mg/mL human IgG1 after excitation at 295 nm.**

The solid black line represents the mean spectrum of the unstressed huAb sample. The dashed red line represents the mean spectrum after 4 freeze-thaw cycles and the dashed blue line after 8 freeze-thaw cycles.

The tertiary structure of huAb after freeze-thawing was monitored by intrinsic protein fluorescence measurements (see Figure 3-5). Neither a significant change in fluorescence intensity nor a peak shift was determined in the emission spectra. Each spectrum represents the mean of three measurements.

As orthogonal methods for the determination of changes in tertiary structure UV/Vis absorbance spectroscopy and extrinsic fluorescence spectroscopy were utilized. The 2<sup>nd</sup> derivative spectra of UV absorbance between 260 and 310 nm revealed no differences of either peak position or *a/b* ratio between the unstressed antibody formulation and that after eight freeze-thaw cycles (data not shown). Analyses of potential conformational changes using 20  $\mu$ M ANS as fluorescent dye confirmed these results. The emission spectra obtained from the human IgG1 antibody samples before and after freeze-thaw stress showed no differences in

ANS fluorescence intensity or peak position (data not shown). Repetitive freeze-thawing did not alter the conformational state of the human monoclonal antibody.

Finally, the investigations on alterations of the secondary structure were performed by ATR-FTIR spectroscopy. The unmodified spectra of the amide I band revealed neither a difference in absorbance nor in the wavenumbers of the peaks. Furthermore, no differences between the spectra after vector normalization and the 2<sup>nd</sup> derivative spectra were distinguished (data not shown). Freeze-thawing also does not influence the secondary structure of the human IgG1 antibody.

### 3.3.3 Stability of huAb against light exposure

Light exposure was included as stress condition potentially inducing chemical modifications of the protein, followed by aggregation [Schoeneich, 2010]. The used light source emitted a spectrum ranging from 200 to 1000 nm, thus consequences on protein stability cannot be referred to a certain wavelength or the range of UV light.

Particle formation soared after day 4 (see Figure 3-6). The total numbers of particles in the  $\mu\text{m}$ -range exponentially increased from approximately  $3 \times 10^3$  to  $2 \times 10^5$  between day 4 and day 6.

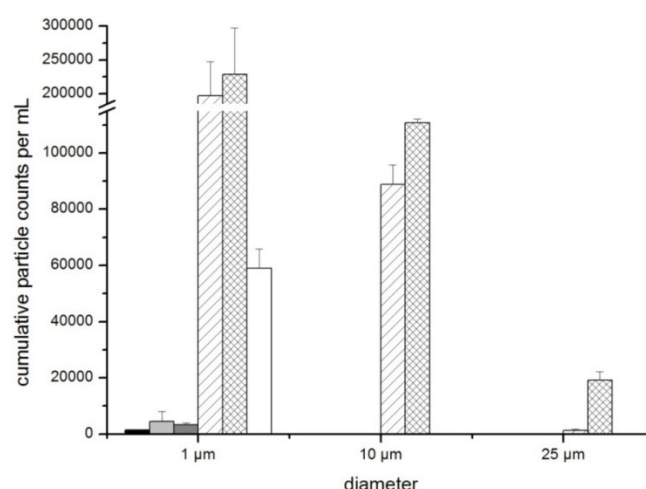


**Figure 3-6 – Particle counts of light exposed huAb by light obscuration.**

Cumulative particle numbers  $\geq$  diameter per mL of unstressed sample (■), 1 day light exposed sample (□), 4 days light exposed sample (▒), 6 days light exposed sample (▨), 7 days light exposed sample (▩), and control sample shielded from light after 7 days (□). Error bars represent standard deviation of at least two measurements.

Turbidity measurements confirmed these observations. The formazine nephelometric units (FNU) of the irradiated samples slightly increased until day 4. The turbidity of 3.7 FNU on day 4 exceeded the benchmark of 3.2 FNU of the PhEur, below which samples are considered to be clear [PhEur 2.2.1., 2011]. This slightly increased turbidity is not caused by particles

$\leq 10 \mu\text{m}$ , since the counts of these larger particles were not significantly increased after 4 days of light exposure. Prolonging the radiation time leads to visible precipitation, enhanced formation of particles  $\geq 10 \mu\text{m}$  and  $\geq 25 \mu\text{m}$  and thus an escalation of turbidity. It immediately reaches the limit of detection of the method at 1300 FNU (see Figure 3-7).

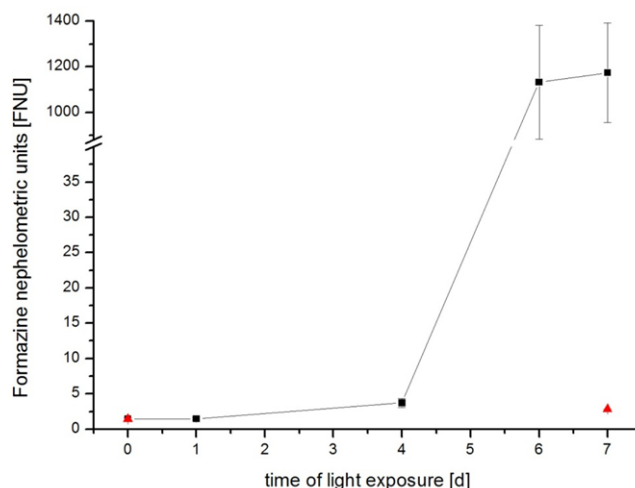


**Figure 3-7 – Results of turbidity measurements of human IgG1 after light exposure.**

The graph shows the formazine nephelometric units of the light exposed samples (black squares) and the shielded control samples (red triangles). The error bars represent the standard deviation of three samples per time point. Within the first 4 days of irradiation turbidity slightly increased, but later on the samples on day 6 and 7 got extremely turbid. The turbidity of the control samples slightly increased within 7 days.

The total particle counts of the shielded control samples showed an increase of the species  $\geq 1.0 \mu\text{m}$ , which exceeded the particle load after 4 days of light exposure, but no enhanced formation of larger particles. Therefore, the sample appeared to be clear after 7 d incubation in the radiation chamber and resulted in a slightly increased turbidity of 2.9 FNU.

The buffer formulations stressed under the same conditions showed no significant increase in total particle numbers and turbidity over 7 days of light exposure (data not shown). The generation of particles is therefore related to the light exposure of the protein.

Dynamic light scattering of the light exposed samples showed similar results. Until 4 days of light exposure small and medium sized subvisible species were detected. The occurring heavy precipitation hindered the dynamic light scattering measurements of the samples exposed to light for 6 or 7 days. Therefore, Figure 3-8 shows only the mean particle size distribution in the nanometer range of the samples up to four days of light exposure.

The particle size distribution determined by DLS show constantly increasing  $Z_{\text{ave}}$  and PDI values over radiation time. The native huAb sample initially revealed a monodispers

distribution with a  $Z_{ave}$  value of 11.48 nm, and a polydispersity index (PDI) of 0.042. After four days of light exposure  $Z_{ave}$  resulted in 49.31 nm and the mean PDI was 0.208. The enhanced polydispersity of these samples is represented by the additional peaks rising between 20 and 100 nm in Figure 3-8. A slight increase was also observed measuring the turbidity of these samples. 3.7 FNU were detected after 4 days of light exposure, implying that the samples are considered not to be clear anymore [PhEur 2.2.1., 2011].

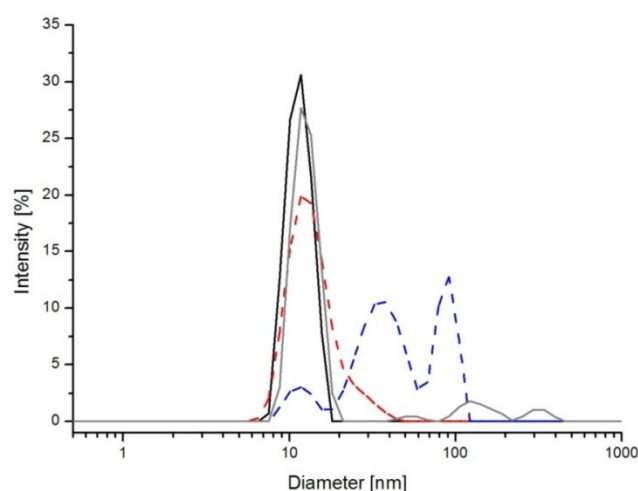


**Figure 3-8 – Particle size distribution of light exposed huAb samples determined by DLS.**

The scattering intensity of the irradiated IgG1 samples and their diameter in nm is plotted. Each line represents the mean out of three samples, each measured in duplicate. The black solid line represents the native human IgG1 sample, the grey solid line represents the shielded control sample after 7 days, the red dashed line represents the sample after 1 day of light exposure and the blue dashed line represents the sample after 4 days of light exposure.

Within the control sample, shielded from light, a mean  $Z_{ave}$  of 47.61 nm and a PDI of 0.186 were determined after 7 days. The control samples show the formation of new particles of diameters between 30 and 400 nm with weak scattering intensities, which contribute to the slightly increase turbidity. The original peak around 11 nm represents still the main compound in this sample, maintaining more than 27 % of scattering intensity.

Besides particle formation of sub-visible and visible size range, smaller protein species like fragments or aggregates might be induced by light exposure too. Size exclusion chromatography is the most important method to detect soluble protein species and separate them concerning to their size. The results of UV detection after SEC separation of the light exposed samples of the human IgG1 antibody are summarized in Figure 3-9. The total recovery of all detected species dramatically starts to decrease on day 6 of radiation, and ends at approximately 32 % at day 7. This reduction is accompanied by the enhanced precipitation mentioned above. The recovery of monomeric species starts to decrease already on day 1, accompanied by an enhanced formation of fragments and small aggregates. On day 4, before strong formation of insoluble particles begins, 61 % of the total recovered species is composed

of monomeric protein species, followed by 19.7 % of intermediate molecular weight species. The relative majority of soluble high molecular weight aggregates appeared on day 6. Further radiation of the samples resulted in only half of the total recovery. Decreases in the relative amounts of all three differentiated soluble aggregate species accompanied by a constant amount of monomeric species and a slightly increasing relative amount of fragments were detected. The control samples shielded from light, maintained 97 % of total recovery over the whole study and no generation of soluble aggregates or fragments. Only an increase in subvisible particles in the size range  $> 1 \mu\text{m} < 10 \mu\text{m}$  was detected. Anyway, the tremendous formation of fragments as well as aggregates is attributed to the light exposure and not to the side effect of a slightly elevated temperature during incubation. The resulting distribution of fragments, monomeric species and the various aggregates is time dependent. Generally, with prolonged duration of irradiation, the amount and size of aggregates increases. A growth of aggregated species is suggested which sometime between day 4 and day 6 exceeds a critical size of several  $\mu\text{m}$  and subsequently start to precipitate. Besides aggregation, fragmentation was detected too, indicating that light exposure is also able to cleave the IgG1 molecules.

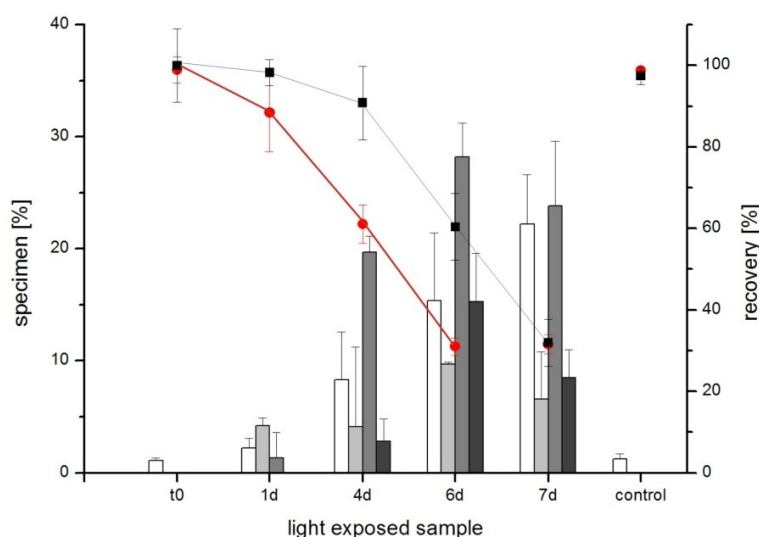


**Figure 3-9 – Distribution of soluble protein species in samples after light exposure determined by UV detection after SEC.**

The content of the species is ranked on the left y-axis. The white bars represent the amount of fragments, the light grey bars represent the amount of dimers/trimers, the grey bars represent the amount of intermediate molecular weight aggregates (IMW) and the dark grey bars represent the high molecular weight aggregates (HMW). The right y-axis ranks the total recovery (black squares) and the monomer recovery (red dots). The error bars represent the standard deviation of at least two samples.

The appearance of aggregation and fragmentation potentially implicates changes in the conformation of the protein, detectable by spectroscopic methods analyzing the secondary and tertiary structure of a protein. The tertiary structure describes the steric constitution of the protein's amino acid chain [Lottspeich, 2006]. Fluorescence spectroscopy and UV absorbance spectroscopy were utilized to investigate changes in the steric organization of the protein after light exposure. Intrinsic protein fluorescence was measured at 0.25 mg/mL protein



concentration for the light exposed samples, since huge amounts of protein precipitated after 6 days of radiation and the concentration in the supernatant was too low for all intended analytical investigations. The intrinsic protein fluorescence is reduced with increasing duration of light exposure (see Figure 3-10a). After 1 day of light exposure, the fluorescence intensity slightly dropped. Further irradiation led to strong attenuation of the emission intensities. However, no significant wavelength shift of the maximum emission peak around 337 nm was detected at any time point. The reduced intensities imply a quenching of Trp residues within the samples due to the exposure to more polar conditions, i.e. unfolding occurred.

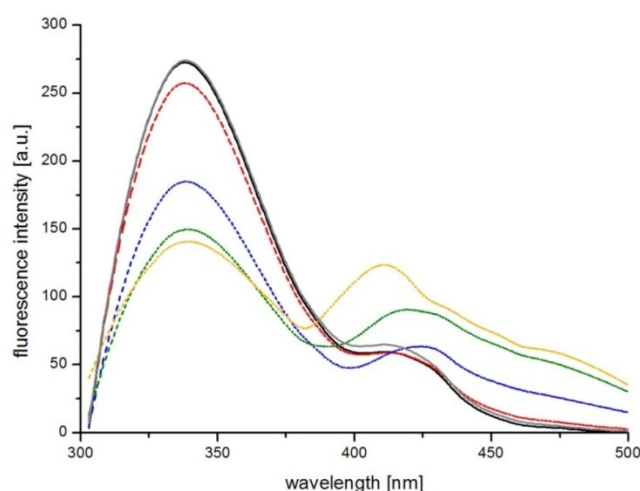


**Figure 3-10a – Intrinsic protein fluorescence of human IgG1 at 0.25 mg/mL after light exposure and excitation at 295 nm.**

The black solid line represents the unstressed huAb sample, the grey solid line represents the shielded control sample and the dashed lines represent the light exposed sample after 1 d (red), 4 d (blue), 6 d (green), and 7 d (yellow). Each line represents the mean of at least two spectra recordings.

Differences were additionally detected in the section of the spectra displaying wavelengths higher than 380 nm. The emitting fluorescence intensities of samples radiated 4 days or longer increased in this section. This new emerging peak indicates the enhanced formation of dityrosine due to oxidation caused by light irradiation [Malencik *et al.*, 1991; Malencik *et al.*, 1996]. Even more, a pronounced blue shift in wavelength of the dityrosine peak was monitored, proving that considerable changes in the polarity of the environment appeared additionally. The evident formation of novel species like dityrosine accompanied by the shift of peak position, emphasize that oxidation processes were induced by light exposure. The intrinsic protein fluorescence spectra also reveal that substantial structural changes started to appear at day 4 of light exposure, proceeding on days 6 and 7. The positions of dityrosine peak determined within the samples after several days light exposure are listed in Table 3-5.

**Table 3-5 – Results of secondary peak position from intrinsic protein fluorescence emission spectra of 0.25 mg/mL huAb after light exposure.**

Light exposure	Unstressed	4 d	6 d	7 d	Control
Peak position	411.5 nm	423.9 nm	419.1 nm	411.1 nm	410.5 nm

The second derivative UV absorbance spectra were additionally monitored to investigate the tertiary structure after light exposure. The resulting spectra showed no shift in the wavelengths of any minimum or maximum peak between 280 and 300 nm (data not shown). Differences were measured in the absorbance units of these minima and maxima. The *a/b* ratios calculated for the mean spectra are listed in Table 3-6. They show a significant trend to higher values with increasing duration of light exposure, suggesting that tyrosine residues are more and more exposed to the solvent [Ragone *et al.*, 1984]. This increased exposure to the solvent indicates the unfolding of the human antibody.

**Table 3-6 – Results of *a/b* ratio determination from UV 2<sup>nd</sup> derivative spectroscopy of huAb after light exposure.**

Light exposure	Unstressed	1 d	4 d	6 d	7 d	Control
<i>a/b</i> ratio	1.4937	1.5771	1.8611	1.9301	2.0499	1.5152

Alterations in the conformational structure of the human antibody after light exposure were also detected by extrinsic fluorescence spectroscopy using 20  $\mu$ M ANS and a protein concentration of 0.5 mg/mL. The emission spectra recorded of the supernatant of centrifuged samples are shown in Figure 3-10b.

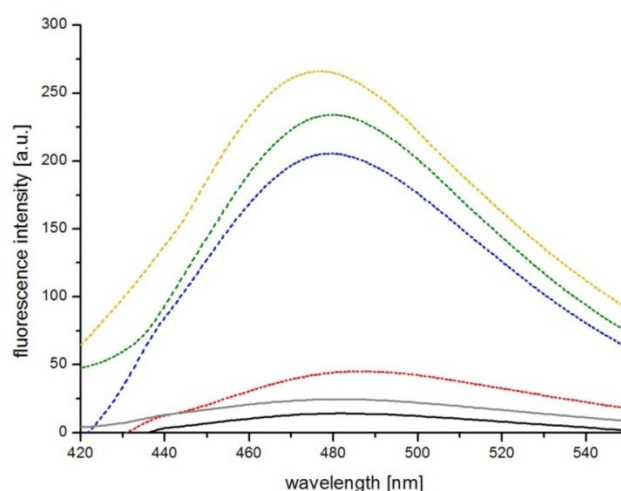


**Figure 3-10b – ANS fluorescence emission spectra of light exposed huAb samples at 0.25 mg/mL after excitation at 350 nm.**

The solid black line represents the unstressed huAb sample, and the solid grey line represents the control samples, shielded from light. The light exposed samples are shown in dashed lines: in red (1 d), in blue (4 d), in green (6 d) and in yellow (7 d).

Already after one day of light exposure the ANS fluorescence intensity is significantly enhanced. Between day 1 and day 4 the major enhancement of intensity was detected, whereas the further increases induced by the samples that were radiated even longer are relatively small. The positions of the ANS emission peaks are listed in Table 3-7. Ignoring the maximum intensity determined for the unstressed sample, a blue shift of the ANS-fluorescence maxima was detected. Between day 1 and day 7 a shift of nearly 10 nm was detected. The maximum detected in the unstressed sample might be imprecise due to the broad peak shape. The strong increase in intensity as well as the detected shift of the maximum peak to lower wavelengths indicates pronounced alterations in the protein structure and unfolding processes induced by light irradiation. Within the control samples shielded from light a marginal increase of ANS-fluorescence intensity was detected. The determination of the peak maximum of this sample was imprecise as well, due to the peak shape, and thus it is not mentioned in Table 3-7.

**Table 3-7 – Results of peak position from extrinsic ANS fluorescence emission spectra of 0.5 mg/mL huAb after light exposure and excitation at 350 nm.**

Light exposure	Unstressed	1 d	4 d	6 d	7 d	Control
Peak position	475.5 nm	486.6 nm	478.9 nm	478.5 nm	477.0 nm	481.9 nm

Potential changes in the secondary structure were analyzed by FTIR spectroscopy of the amide I band. The second derivate spectra of the normalized zero-order spectra are shown in Figure 3-11. The dominating valley at  $1638\text{ cm}^{-1}$  representing intramolecular  $\beta$ -sheets decreases with increasing light exposure. The decrease is first detectable on day 4 and accompanied by an increase in the range of  $1650 - 1660\text{ cm}^{-1}$ , an area that represents  $\alpha$ -helical structures [Mahler *et al.*, 2010a]. Even more, a second valley starts to form around  $1634\text{ cm}^{-1}$ , and the small dent at  $1614\text{ cm}^{-1}$  is deepened and shifted to lower wavenumbers. These alterations indicate the formation of intermolecular  $\beta$ -sheet structures [Van De Weert *et al.*, 2005]. The section of high wavenumbers (between  $1660$  and  $1690\text{ cm}^{-1}$ ) within the second derivative spectra heavily changes due to light exposure, but also in the control sample shielded from light radiation. These regions are assigned to various secondary structures like loops,  $\beta$ -turns, and unordered structures [Mahler *et al.*, 2010a; Van De Weert *et al.*, 2005]. The control samples show also the beginning formation of an additional band between  $1620$  and  $1630\text{ cm}^{-1}$ , which is attributed to the formation of intermolecular  $\beta$ -sheets.

Light exposure has a strong influence on the secondary structure of a protein leading to numerous alterations. In summary, the predominant  $\beta$ -sheet structures of the investigated monoclonal antibody are disturbed and accompanied by an increase in  $\alpha$ -helical structures

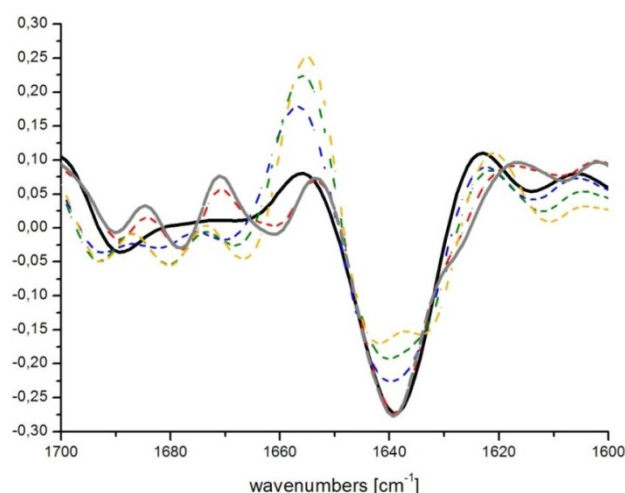


**Figure 3-11 – Second derivative ATR-FTIR spectra of light exposed huAb samples at 0.5 mg/mL.**

The spectrum of the native huAb is plotted in the black solid line. The grey solid line represents the control samples after 7 days of incubation. The light exposed samples are plotted in dashed lines. Red = 1 d of light exposure, blue = 4 d of light exposure, green = 6 d of light exposure, and yellow = 7 d of light exposure.

### 3.3.4 Stability of huAb against storage at elevated temperatures

To evaluate the influence of elevated temperatures on the stability of the human monoclonal antibody the samples were stored in drying a chamber at 50°C for up to 4 weeks. The particle numbers counted by light obscuration and the turbidity measurements are summarized in Table 3-8.

**Table 3-8 – Results of particle counts by light obscuration and turbidity measurements of huAb after storage at 50°C.**

Storage at 50°C	Unstressed	7 d	14 d	21 d	28 d
≥ 1 µm	1479	1037	863	1619	18,320
≥ 10 µm	20	56	16	30	313
≥ 25 µm	2	4	2	3	18
Turbidity [FNU]	1.5	1.8	1.6	1.2	4.3

Within the first three weeks of storage at 50°C, no consistent influence on the particle numbers of micron-sized species was detected by light obscuration. The predefined benchmarks of 1 µm, 10 µm, and 25 µm resulted in no significant increase. The generation of additional particles of those sizes was firstly detected after 28 days. Turbidity measurements confirmed these observations, since the turbidity remained on a nearly constant level of 1.5 ± 0.3 FNU within 21 days, before increasing to 4.3 after 28 days of storage at 50°C. Buffer samples were similarly incubated for 28 days, but neither enhanced particle numbers nor enhanced turbidity was detectable (data not shown). In contrast, dynamic light scattering indicated the enhanced formation of particles already on day 21, as the results of Z-average

diameter and polydispersity index in Table 3-9 show. Both parameters approximately remain on the same level within the first 14 days, but show an elevation on day 21. The  $Z_{ave}$  diameter increases to 64.1 nm on day 21 and 68.5 nm on day 28. The PDI increases to 0.19 on day 28. Incubation at 50°C does not show enhanced tendencies to formation of subvisible particles within the first four weeks of storage.

**Table 3-9 – Results of Z-average diameter and PDI of huAb after storage at 50°C.**

Storage at 50°C	Unstressed	7 d	14 d	21 d	28 d
$Z_{ave}$	11.5	12.1	11.9	64.1	68.5
PDI	0.04	0.03	0.09	0.18	0.19

The samples were also chromatographically analyzed after centrifugation by SEC to determine the distribution of soluble protein species potentially generated during storage at 50°C. The resulting chromatograms and the distribution of protein species are displayed in Figures 3-12 and 3-13.

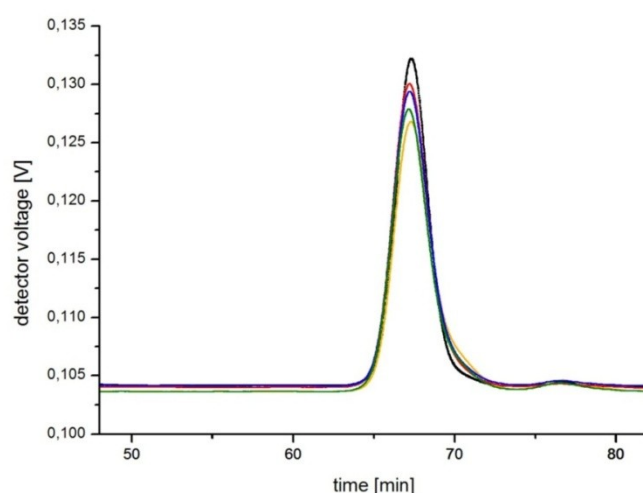


**Figure 3-12 – Refractive index - Size exclusion chromatograms of huAb samples stored at 50°C.**

Chromatograms of huAb samples after incubation at 50°C. The solid black line represents the unstressed sample. The stressed sample are displayed in red (after 7 days of storage), in blue (after 14 days of storage), in green (after 21 days of storage), and in yellow (after 28 days of storage).

The most obvious difference between the samples which can be detected from the chromatograms (Figure 3-12) is the constantly decreasing height of the monomer peak eluting around 66 minutes. At the same time, the amount of species eluting subsequent to the monomer being of smaller size increases. A shoulder coupled to the monomer peak rises around 70 minutes and the already existing fragment peak (eluting ~76 minutes) grows. The marginal amounts of aggregates can hardly be detected in this Figure, but became verifiable by increasing the resolution (data not shown). Figure 3-13 summarizes the results from RI detection including all soluble species that were unambiguously detectable. In the unstressed

samples of huAb > 96% or monomer were detected, accompanied by 2.5% of fragments and negligible amounts of aggregates (< 1% in total). After 7 and 14 days of storage the total recovery did not significantly change. The recovery of the monomer slightly decreased to ~ 93% after 14 days. At the same time the amount of fragments in the samples doubled to 5% (see green trend line). Furthermore, a minute increase of high molecular weight (HMW) aggregates was detected. After 14 days 1.6% of the soluble protein fraction was HMW aggregates.

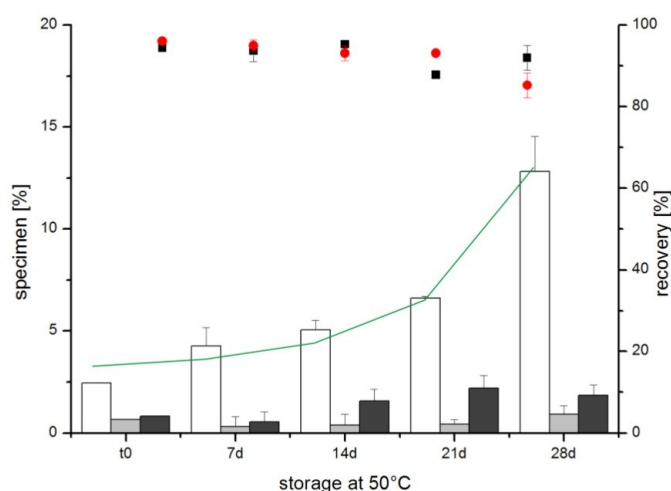


**Figure 3-13 – Distribution of soluble protein species in huAb samples stored at 50°C determined by RI detection after SEC.**

The content of the species is ranked on the left y-axis: the amount of fragments (□), the amount of dimers/trimers (▒) and the high molecular weight aggregates (HMW, ■). The right y-axis ranks the total recovery (black squares) and the monomer recovery (red dots). The error bars represent the standard deviation of 3 samples.

Numerous reports have shown that storage at elevated temperatures and heating triggers conformational changes of proteins [Carpenter, John F. *et al.*, 1999; Vermeer *et al.*, 2000]. Temperature is probably the most important factor which impacts protein stability, though there is no general mechanism to describe the influence of temperature on protein structure [Wang, W., 1999]. Potential structural changes of the investigated human IgG1 antibody due to storage at 50°C were monitored over 4 weeks by several spectroscopic techniques. Intrinsic protein fluorescence resulted in marginal decreases of the emission intensity (see Figure 3-14) but no wavelength shift (data not shown). The main reduction of intensity was achieved between day 21 and day 28. The magnitudes of intensity decrease monitored at the other sampling time points are rather small and inconsistent. Especially between day 14 and day 21 no substantial reduction of the emission intensity was detected. These observations suggest that significant unfolding processes might have started not until the last week of investigation, but for distinct assessment the incubation time was too short. However, 4 weeks at 50°C did not lead to substantial unfolding of the antibody, but slight quenching of Trp residues due to increasing polarity in the Trp surrounding was detected.

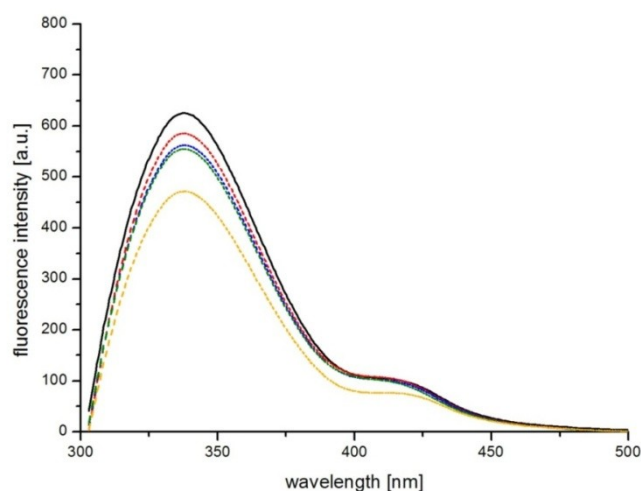


**Figure 3-14 – Intrinsic protein fluorescence of human IgG1 at 0.5 mg/mL after storage at 50°C and excitation at 295 nm.**

The black solid line represents the unstressed huAb sample. The dashed lines represent the heated sample after 7 d (red), 14 d (blue), 21 d (green), and 28 d (yellow). Each line represents the mean of at least two spectra recordings.

The 2<sup>nd</sup> derivative UV absorbance spectra point in the same direction as the results from intrinsic protein fluorescence. Marginal differences in the spectra and the decisive parameters were detected until day 21. After 4 weeks of incubation at 50°C the spectra featured significant differences compared to the spectra of native huAb. Figure 3-15 shows the 2<sup>nd</sup> derivative spectra between 260 and 310 nm.

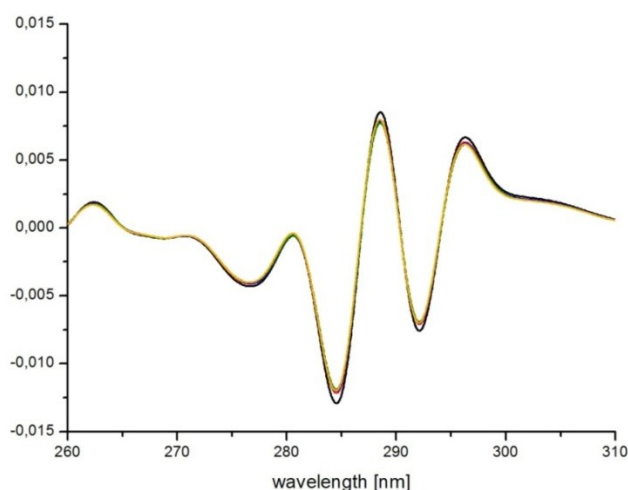


**Figure 3-15 – UV 2<sup>nd</sup> derivative spectra of 0.5 mg/mL human IgG1 after storage at 50°C.**

The solid black line represents the spectra of the unstressed huAb sample. The dashed red line represents the spectra after 7 days of storage at 50°C, the dashed blue line after 14 d, the dashed green line after 21 d, and the dashed yellow line after 28 d of storage at 50°C.

Slight variations in the peak height were observable and resulted in substantial differences in the  $a/b$  ratio, which are summarized in Table 3-10. The discrepancies between the  $a/b$  ratios of the unstressed sample and those samples incubated at 50°C up to 3 weeks are negligible, but follow the trend of reduced  $a/b$  ratios with prolonged storage. They range from 1.5305 for the unstressed material to 1.5232 for the material after 3 weeks of storage. On top of that, a distinctly diminished  $a/b$  ratio of 1.3562 was determined after 4 weeks of incubation.

**Table 3-10 – Results of  $a/b$  ratio determination from UV 2<sup>nd</sup> derivative spectroscopy of huAb after storage at 50°C.**

Storage @ 50°C	Unstressed	7d	14 d	21 d	28 d
<b><math>a/b</math> ratio</b>	1.5306	1.5258	1.5253	1.5232	1.3562

Changes of this value of tyrosine/tryptophane mixtures indicate alterations in solvent polarity, which are presumably induced by unfolding of the protein [Kueltzo *et al.*, 2005]. The high resolution of the UV absorbance spectroscopy method enables the determination of tiny peak shifts of up to 0.02 nm. The sensitivity of shifts on the wavelengths of derivative peaks to the environmental conditions of a protein and thus to conformational changes, was observed decades ago [Beaven *et al.*, 1952; Ichikawa *et al.*, 1979]. The two minima around 285 and 292 nm as well as the two maxima around 289 and 296 nm representing aromatic amino acids are typically considered. Storage at 50°C resulted in slight peak shifts to shorter wavelengths after 28 d of incubation (Table 3-11). A shift of up to 0.06 nm was detected potentially indicating a starting increase in the polarity of the environment of Tyr and Trp [Mach *et al.*, 1994]. However, a prolonged incubation would have been needed to confirm these findings.

**Table 3-11 – Results of wavelength shift of peaks from UV 2<sup>nd</sup> derivative spectroscopy of huAb after storage at 50°C.**

Storage @ 50°C	Unstressed	7d	14 d	21 d	28 d
<b>Minimum 1 [nm]</b>	284.58	284.56	284.56	284.56	284.50
<b>Maximum 1 [nm]</b>	288.53	288.52	288.52	288.52	288.49
<b>Minimum 2 [nm]</b>	292.15	292.14	292.14	292.13	292.08
<b>Maximum 2 [nm]</b>	296.24	296.25	296.25	296.25	296.24

Structural changes after several weeks of storing at elevated temperatures were also detected by ANS-fluorescence. The spectra displayed in Figure 3-16 show a constant increase of fluorescence intensity at the emission peak maximum. The highest magnitude of intensity elevation was detected between 21 and 28 days of incubation, confirming the results obtained from intrinsic fluorescence and 2<sup>nd</sup> derivative UV absorbance.



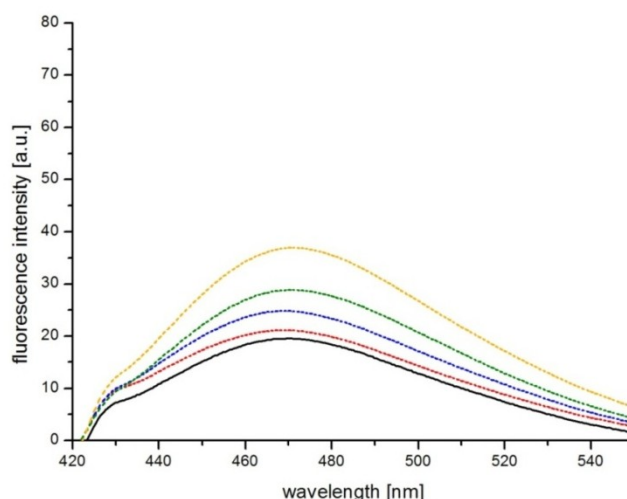


**Figure 3-16 – ANS fluorescence emission spectra of huAb samples stored at 50°C at 0.5 mg/mL after excitation at 350 nm.**

The solid black line represents the spectra of the unstressed huAb sample. The dashed red line represents the spectra after 7 days of storage at 50°C, the dashed blue line after 14 d, the dashed green line after 21 d, and the dashed yellow line after 28 d of storage at 50°C.

The emission peak maxima additionally revealed a slight peak shift to longer wavelengths with enhanced incubation time. The detected peak positions are summarized in Table 3-12. The peak did not show a wavelength shift within the first week of storage at 50°C, but starts to move to longer wavelengths after two weeks. A maximum red shift of 4.6 nm was detected after 3 weeks. The emission peak detected after 4 weeks was 4.0 nm red shifted from the unstressed sample.

**Table 3-12 – Results of peak position from extrinsic ANS fluorescence emission spectra of 0.5 mg/mL huAb after storage at 50°C and excitation at 350 nm.**

Storage @ 50°C	Unstressed	7d	14 d	21 d	28 d
Peak position	466.9 nm	466.9 nm	467.9 nm	470.5 nm	469.9 nm

The investigations on the tertiary structure of samples of the human IgG1 antibody after storage at 50°C for several weeks indicated that unfolding and structural alterations of the protein's conformation started. Analyzing the 2<sup>nd</sup> derivative spectra of ATR-FTIR spectroscopy no substantial alteration of the secondary structure of the immunoglobulin was detected during the first three weeks of storage (data not shown). A slight change in the intermolecular  $\beta$ -sheet band around 1622 cm<sup>-1</sup> was discovered after 4 weeks, suggesting structural changes in the molecule due to the unfolding processes determined e.g. also by fluorescence spectroscopy. However, the antibody revealed to be stable to storage at elevated temperatures, at least for several days.

### 3.4 DISCUSSION

The aim of this chapter was to investigate the effect of several extrinsic stress factors on folding and aggregation of a human monoclonal antibody (huAb), serving as a model protein. Agitation, freeze-thawing, light exposure and storage at elevated temperatures were chosen to evaluate the stability of huAb. Multiple methods were applied to the protein to gain deep insight in the influence of these factors on its structure. The formation of particles due to the stress methods was investigated by measurements of light obscuration, turbidity and dynamic light scattering. No subvisible particle formation at all was detected in the IgG1 samples after repetitive freeze-thawing. The by far fastest particle formation resulting in extreme numbers of subvisible particles was discovered after stirring using LO and turbidity measurements. The particles generated were too large for detection in dynamic light scattering since they precipitated and would entail miscalculation because of interfering with the Brownian movement. The control sample of stirred formulation buffer proved that the majority of generated particles were composed of protein, though abrasion of the PTFE-coated stir bar has to be considered a particle source as well. A slower but constant increase in particle numbers of nm- and  $\mu\text{m}$ -size was observed after shaking. All three methods to determine subvisible species showed consistent results, i.e. an increase in particle numbers and size. The light exposed samples initially do not include an enhanced subvisible particle numbers in the  $\mu\text{m}$ -range, but dramatically precipitate after 6 days of irradiation. Storage at 50°C possessed comparable characteristics of sustained particle formation, since the loading of subvisible particles remains on a low level within 3 weeks and subsequently starts to increase. However, during the predefined incubation time no precipitation occurred, indicating that the majority of induced particles were much smaller than those generated by prolonged light exposure. After 6 days of light exposure several thousand particles of  $\geq 10 \mu\text{m}$  and even  $\geq 25 \mu\text{m}$  were counted and turbidity reaches the upper limit of detection, whereas after 28 d storage at 50°C the numbers of two digit micrometer sized particles and turbidity are much less.

Based on the varying observations on particle formation it is suggested, that diverging mechanisms can be distinguished behind the stress methods. The particle growth after light exposure partly follows a nucleation controlled process. Within the first 4 days no enhanced loading of subvisible particles in  $\mu\text{m}$ -range was detectable. The slightly increasing turbidity of the sample is accompanied by enhanced values of  $Z_{\text{ave}}$  diameter and PDI, suggesting that these medium sized particles between 20 and 100 nm are attributed to the minor increases in turbidity [Mahler *et al.*, 2005]. Further continuation of irradiation provides numerous particles of several  $\mu\text{m}$  in size and heavy precipitation. These large and partly visible structures account for the tremendous turbidity increase detected in those samples. Initially, species in nm-range serving as nuclei are generated that become bigger and finally reach a size where precipitation occurs. This process of particle growth is often accelerated when the nucleus achieved a critical size [Philo *et al.*, 2009]. In the light exposed samples of human IgG1 this critical size is gained between day 4 and day 6. The increase in subvisible particles  $\geq 1 \mu\text{m}$  (but  $< 10 \mu\text{m}$ ) proves the accompanying influence of the slightly enhanced temperature ( $35 \pm 2^\circ\text{C}$ ) on the particle

formation. Unexpectedly, the impact of 7 d incubation at this temperature on particle formation is higher than that of 4 d incubation at this temperature plus the strong light exposure. However, after 7 d the particle numbers in the light exposed sample outreach the numbers in the control sample, indicating the additional influence of light radiation accompanied by strong conformational changes on the generation of particles. Furthermore, in the shielded sample only minor alterations in the secondary structure of the huAb and no formation of fragments or soluble aggregates have been detected. These results suggest that the entire vast modifications detected in the huAb samples after light exposure are mainly triggered by light irradiation. Though, a minor impact of the slightly elevated temperature in the radiation chamber has to be taken into consideration when evaluating the aggregation mechanisms behind.

Accessory phenomena of the particle formation are the structural changes detected after light irradiation. All spectroscopic methods employed to determine alterations in secondary or tertiary structure of huAb yielded in substantial changes in the spectra already after 1 day of light exposure, thus before mentionable subvisible particle formation was detected. It is suggested that light exposure induces the formation of growing particles in the human IgG1 model antibody formulation upon certain modification of the conformation of the model protein. Besides the conformational modifications, chemical modifications induced by light exposure, such as oxidations, are conceivable as well. The detection of the dityrosine peak in intrinsic protein fluorescence proves this indication. However, chemical alterations were not in detail investigated throughout this study. It is therefore speculative on what kind of initial modification in the monomer the subsequent particle growth is based on. In summary: besides nucleation, a second mechanism is suggested to be involved in the aggregation process after light exposure. The strong aggregation appearing after several days of irradiation could also result from the chemical and physical alterations in the initial structure of the protein [Philo *et al.*, 2009; Wang, 2005].

The mechanism considered to be involved in the aggregation process elicited by 4 weeks storage at elevated temperatures also requires conformational changes of the monomer. According to Philo *et al.* heat is a well-known stress that can promote the initial conformational change or partial unfolding of the monomer [Philo *et al.*, 2009]. No increase in the subvisible particle content was detected during the first 21 days of incubation at 50°C, but slight incremental alterations of the conformational structure were discovered. Reaching a certain level subvisible particles arose, firstly detectable on day 21 by an enhanced  $Z_{ave}$  and PDI, thus representing species in nm-range. These enhancements were not accompanied by increases in turbidity, indicating that the generated subvisible species were rather small and their content in the sample is low. At the next sampling time point also  $\mu$ m-sized species were detected and came along with an elevated turbidity, attributed to the increase in size and numbers of particles. Concomitantly to the beginning formation of subvisible particles the strongest alteration in tertiary structure of the antibody was detected in the supernatant. However, the unfolding is rather slow and no denaturation was observed. The melting temperature  $T_m$ , which is the temperature at which half of the protein molecules are unfolded

during a thermal transition [Mahler *et al.*, 2009], of the model antibody was beforehand determined by temperature dependent turbidity measurements using a UV-visible absorbance spectrophotometer (Agilent Technologies, Waldbronn, Germany) to be approximately 75°C (data not shown). Hence, the incubation was performed far below  $T_m$  of the human IgG1 and complete denaturation was not intended. However, partial unfolding and enhanced aggregation can occur to a protein when exposed to a temperature close to  $T_m$  [Chi *et al.*, 2003a]. McCarthy and Drake detected aggregates by light scattering after heating an IgG to 50°C [McCarthy *et al.*, 1989]. They furthermore stated that heating leads to unfolding especially in the Fab parts of immunoglobulins enabling aggregation. Instead, the Fc parts will be exposed to the hydrophilic environment [McCarthy *et al.*, 1989]. Heat might also enhance chemical degradation of proteins which can distort the protein conformation and amplify aggregation [Wang, 2005]. The most pronounced protein species that appeared from huAb after storage at 50°C were fragments. During this 4-week study the amount of antibody-fragments detected by SEC increased up to 13 %, indicating the degradation of the huAb molecule by temperature. Fragmentation by heat treatment is also a well-known phenomenon occurring in immunoglobulins [Harpel *et al.*, 1979; Lee, 2000]. Especially the IgG1 subclass has recently been shown to be more prone to fragmentation than other IgG subclasses [Ishikawa *et al.*, 2010].

Shaking and stirring are two mechanical stress conditions that were often reported to elicit aggregation in proteins [Kiese, 2008; Wang, W., 1999]. Comparing both agitation methods concerning protein stability, it was found that stirring can be much more harmful [Mahler *et al.*, 2005]. The resulting aggregate species generated by shaking and stirring vary substantially in terms of amount and size [Kiese, 2008]. Stirring and shaking of the huAb in this study provided similar results. The total particle numbers counted by light obscuration as well as the turbidity measurements indicate that shaking with a comparable agitation speed leads to weaker formation of particles than stirring. The size of the particles differs as well. Stirring results in larger particles, easily detectable by eye and by an elevated turbidity. The major step in protein aggregation caused by agitation is considered to be the collision of the protein molecules. Thus, it appears clear that especially the agitation speed and time influence the aggregation rate [Colombie *et al.*, 2001]. Though theoretically agitated at the same speed substantial differences between shaking and stirring were discovered. The overall mechanism behind both agitation methods is aggregation on new emerging surfaces [Philo *et al.*, 2009]. In case of shaking and stirring with Teflon® stir bars, the surface is hydrophobic. Therefore, the interaction of the protein with the new interface is mostly driven by hydrophobic binding and leads to partial unfolding. Accordingly, the subsequent aggregation is again based on modifications in protein structure [Philo *et al.*, 2009]. However, the detected variations in aggregate pattern after shaking and stirring are suggested to result on the one hand from the differences in hydrophobicity of the surfaces [Vermeer *et al.*, 1998], which is considered to be much higher in Teflon®. On the other hand, slight abrasion of particles from the surface of the stir bar might provide nuclei and thus amplify aggregation as well. Additional stress conditions which can be provoked by stirring as local heat and cavitation should also be taken into consideration. Thus, the detrimental effects on protein stability observed by stirring are caused by a combination of

occurring phenomena and various underlying mechanisms are conceivable. Instead, during shaking a constantly renewal of air/water interfaces was created in the vials and air bubbles were entrained into the solution. The protein potentially can adsorb or partially unfold at these interfaces and the modified molecules might be transported into the solution [Henson *et al.*, 1970; Maa *et al.*, 1997]. The air/water interface formation depends on the fill volume of the vial and aggregation caused by shaking can be heavily reduced by filling the container to the maximum diminishing the headspace [Kiese, 2008]. These observation indicate that aggregation during shaking solely relies on air/water interfaces and it can be suggested that the aggregation rate is therefore reduced, compared to stirring at the same speed.

Freeze-thawing cycles of the human antibody formulation served no increase in subvisible or visible particles and no substantial changes in protein conformation. The most critical phenomena that appear during freeze-thawing are concentration of the protein itself and osmolytes, resulting pH shifts and the formation of ice/water interfaces [Carpenter, John F. *et al.*, 1988; Kueltzo *et al.*, 2008; van den Berg *et al.*, 1959]. The IgG1 can be suggested to be very robust and stable to freeze-thawing and the meanwhile appearing stress conditions. The formulation buffer of huAb contained mannitol, a polyhydric alcohol and isomer of sorbitol. Polyhydric alcohols are well-known cryoprotective substances [Arakawa *et al.*, 1991; Carpenter, John F. *et al.*, 1988]. They were shown to preferentially being excluded from the protein's surface in aqueous solution [Timasheff, 1995]. This phenomenon accounts for their cryoprotective capacity [Carpenter, John F. *et al.*, 1988].

A summarizing overview of all stress methods and the resulting alterations in the amount of particles, aggregates and fragments as well as the conformational changes is provided in Table 3-13.

**Table 3-13 – Overview of resulting physico-chemical alterations in huAb after stress studies.**

<b>Stress method</b>	<b>Enhanced number of particles</b>	<b>Formation of soluble aggregates</b>	<b>Formation of fragments</b>	<b>Altered secondary structure</b>	<b>Altered tertiary structure / unfolding</b>
<b>Stirring</b>	++	-	-	-	+
<b>Shaking</b>	+	-	-	-	-
<b>Freeze-Thawing</b>	-	-	-	-	-
<b>Heat</b>	+	-	+	+	+
<b>Light</b>	++	+	+	++	++

- No substantial alterations detected

+ Moderate alterations detected

++ Strong alterations detected

### 3.5 CONCLUSION

A variety of stress conditions was investigated and found to induce structural modifications and the formation of aggregates in the human antibody. In perspective of the planned *in vivo* studies investigating the immunogenicity of protein aggregates, a huge spectrum of aggregates of different sizes and different conformational structures of a monoclonal antibody was requested. Stress conditions found to be capable to reproducibly generate a substantial amount of aggregates within a short time will now be transferred to a murine antibody.

The chosen stress conditions are all considered to be relevant for protein manufacturing processes. The aggregate pattern within the stress samples strongly differs according to applied conditions and time. Except repetitive freeze-thawing, all other stress methods were found to increase the number of subvisible particles in the antibody formulation and lead to structural changes of the protein. Therefore, freeze-thawing was decided to be omitted in the follow-up studies with the murine protein.

Subvisible particles are currently heavily discussed to be related to immunogenicity [Carpenter *et al.*, 2009; Cromwell *et al.*, 2006; Hermeling *et al.*, 2004; Rosenberg, 2006]. Stirring was found to be the fastest method to solely generate particles. In comparison to shaking, the numbers and sizes of particles generated were larger after stirring. Both agitation methods were found to result solely in the formation of insoluble species, without formation of smaller soluble aggregates detectable by SEC. However, stirring as well as shaking were decided to be valuable methods to generate aggregates for immunogenicity studies and thus should be transferred to the murine antibody.

Besides particle formation, during light exposure and storage at 50°C soluble species, were generated and discovered by size exclusion chromatography. Whereas in the heated samples the monomer was only accompanied by fragments, the light exposed samples contained soluble aggregates as well. Therefore light exposure of only a few days was the only stress condition to induce soluble aggregates. Furthermore, the most impressive modifications of secondary and tertiary structure were detected after light exposure, including oxidation products. Mass spectrometry as for example reported by Schöneich *et al.* potentially could provide detailed information about the primary structure of the resulting products [Schoeneich, Christian *et al.*, 2006]. Since protein aggregates induced by light oxidation are discussed to be immunogenic as well [Schoeneich, 2010], this method should also be transferred to the murine antibody. Though storage at elevated temperatures for 4 weeks did not reveal huge amounts of aggregates, heating should also be a method tested with the murine antibody. As for all other methods, the stress conditions might then be adapted.

### 3.6 REFERENCES

- [Arakawa *et al.*, 1991], Protein-solvent interactions in pharmaceutical formulations, *Pharmaceutical Research*, 8, 285-291
- [Arakawa *et al.*, 2001], Factors affecting short-term and long-term stabilities of proteins, *Advanced Drug Delivery Reviews*, 46, 307-326
- [Arakawa *et al.*, 1982], Preferential interactions of proteins with salts in concentrated solutions, *Biochemistry*, 21, 6545-6552
- [Augener *et al.*, 1970], Studies on the mechanism of heat aggregation of human gamma-G, *Journal of immunology (Baltimore, Md. : 1950)*, 105, 1024-1030
- [Azuaga *et al.*, 2002], Unfolding and aggregation during the thermal denaturation of streptokinase, *European Journal of Biochemistry*, 269, 4121-4133
- [Bam *et al.*, 1998], Tween Protects Recombinant Human Growth Hormone against Agitation-Induced Damage via Hydrophobic Interactions, *J. Pharm. Sci.*, 87, 1554-1559
- [Beaven *et al.*, 1952], Ultraviolet absorption spectra of proteins and amino acids, *Advances in Protein Chemistry (Academic Press Inc., New York, N.Y.)*, 7, 319-386
- [Brandts *et al.*, 1970], Low temperature denaturation of chymotrypsinogen in aqueous solution and in frozen aqueous solution, *Frozen Cell, Symp.*, 189-212
- [Byler *et al.*, 1998], Effect of sucrose on the thermal denaturation of a protein: an FTIR spectroscopic study of a monoclonal antibody, *AIP Conference Proceedings*, 430, 332-335
- [Carpenter *et al.*, 1988], The mechanism of cryoprotection of proteins by solutes, *Cryobiology*, 25, 244-255
- [Carpenter *et al.*, 1999], Inhibition of stress-induced aggregation of protein therapeutics, *Methods in Enzymology*, 309, 236-255
- [Carpenter *et al.*, 2009], Overlooking subvisible particles in therapeutic protein products: gaps that may compromise product quality, *J. Pharm. Sci.*, 98, 1201-1205
- [Chi *et al.*, 2003a], Roles of conformational stability and colloidal stability in the aggregation of recombinant human granulocyte colony-stimulating factor, *Protein Science*, 12, 903-913
- [Chi *et al.*, 2003b], Physical Stability of Proteins in Aqueous Solution: Mechanism and Driving Forces in Nonnative Protein Aggregation, *Pharmaceutical Research*, 20, 1325-1336
- [Colombie *et al.*, 2001], Lysozyme inactivation under mechanical stirring: effect of physical and molecular interfaces, *Enzyme and Microbial Technology*, 28, 820-826
- [Costantino *et al.*, 1997], Fourier-transform infrared spectroscopic analysis of the secondary structure of recombinant humanized immunoglobulin G, *Pharmaceutical Sciences*, 3, 121-128
- [Cromwell *et al.*, 2006], Protein aggregation and bioprocessing, *AAPS Journal*, 8, E572-E579
- [Davies *et al.*, 2001], Photo-oxidation of proteins and its role in cataractogenesis, *Journal of Photochemistry and Photobiology, B: Biology*, 63, 114-125
- [Fesinmeyer *et al.*, 2009], Effect of Ions on Agitation- and Temperature-Induced Aggregation Reactions of Antibodies, *Pharmaceutical Research*, 26, 903-913
- [Harpel *et al.*, 1979], Heat-induced fragmentation of human alpha 2-macroglobulin., *Journal of Biological Chemistry*, 254, 8669-8678

[Hawe *et al.*, 2009], Structural properties of monoclonal antibody aggregates induced by freeze-thawing and thermal stress, *European journal of pharmaceutical sciences : official journal of the European Federation for Pharmaceutical Sciences*, 38, 79-87

[Hawe *et al.*, 2008], Extrinsic Fluorescent Dyes as Tools for Protein Characterization, *Pharmaceutical Research*, 25, 1487-1499

[Henson *et al.*, 1970], The surface coagulation of proteins during shaking, *Journal of Colloid and Interface Science*, 32, 162-165

[Hermeling *et al.*, 2004], Structure-Immunogenicity Relationships of Therapeutic Proteins, *Pharmaceutical Research*, 21, 897-903

[Hovorka *et al.*, 2001], Oxidative degradation of pharmaceuticals: theory, mechanisms and inhibition, *J Pharm Sci*, 90, 253-269

[ICH Q1B, 1998], Photostability Testing of New Active Substances and Medicinal Products, *International Conference on Harmonization*,

[Ichikawa *et al.*, 1979], Estimation of state and amount of phenylalanine residues in proteins by second derivative spectrophotometry, *Biochimica et biophysica acta*, 580, 120-128

[Ishikawa *et al.*, 2010], Influence of pH on heat-induced aggregation and degradation of therapeutic monoclonal antibodies., *Biological and Pharmaceutical Bulletin*, 33, 1413-1417

[Jiskoot *et al.*, 2005], Fluorescence spectroscopy, *Biotechnology: Pharmaceutical Aspects*, 3, 27-82

[Kerwin *et al.*, 2007], Protect from light: Photodegradation and protein biologics, *J. Pharm. Sci.*, 96, 1468-1479

[Kiese, 2008], Shaken, not stirred: Mechanical stress testing of an IgG1 antibody, *Journal of Pharmaceutical Sciences*,

[Kiese *et al.*, 2010], Equilibrium studies of protein aggregates and homogeneous nucleation in protein formulation, *J. Pharm. Sci.*, 99, 632-644

[Kueltzo *et al.*, 2003], Derivative absorbance spectroscopy and protein phase diagrams as tools for comprehensive protein characterization: A bGCSF case study, *J. Pharm. Sci.*, 92, 1805-1820

[Kueltzo *et al.*, 2005], Ultraviolet absorption spectroscopy, *Biotechnology: Pharmaceutical Aspects*, 3, 1-25

[Kueltzo *et al.*, 2008], Effects of solution conditions, processing parameters, and container materials on aggregation of a monoclonal antibody during freeze-thawing, *J. Pharm. Sci.*, 97, 1801-1812

[Lee, 2000], High-performance sodium dodecyl sulfate-capillary gel electrophoresis of antibodies and antibody fragments, *Journal of Immunological Methods*, 234, 71-81

[Lorenz *et al.*, 2009], The effect of low intensity ultraviolet-C light on monoclonal antibodies, *Biotechnology Progress*, 25, 476-482

[Lottspeich, 2006], Bioanalytik, 2nd Edition, *Elsevier GmbH Spektrum Akademischer Verlag*, 1136 pp,

[Maa *et al.*, 1997], Protein denaturation by combined effect of shear and air-liquid interface, *Biotechnology and Bioengineering*, 54, 503-512



- [Mach *et al.*, 1994], Simultaneous monitoring of the environment of tryptophan, tyrosine, and phenylalanine residues in proteins by near-ultraviolet second-derivative spectroscopy, *Analytical Biochemistry*, 222, 323-331
- [Mahler *et al.*, 2010a], Protein Pharmaceuticals: Formulation, Analytics and Delivery, 1st Edition, *Editio Cantor Verlag*, 464 pp,
- [Mahler *et al.*, 2010b], Protein aggregation and particle formation: effects of formulation, interfaces, and drug product manufacturing operations, *Aggregation of Therapeutic Proteins*, 301-331
- [Mahler *et al.*, 2005], Induction and analysis of aggregates in a liquid IgG1-antibody formulation, *European Journal of Pharmaceutics and Biopharmaceutics*, 59, 407-417
- [Mahler *et al.*, 2009], Surface activity of a monoclonal antibody, *J. Pharm. Sci.*, 98, 4525-4533
- [Malencik *et al.*, 1991], Fluorometric characterization of dityrosine: complex formation with boric acid and borate ion, *Biochemical and Biophysical Research Communications*, 178, 60-67
- [Malencik *et al.*, 1996], Dityrosine: preparation, isolation, and analysis, *Analytical Biochemistry*, 242, 202-213
- [McCarthy *et al.*, 1989], Spectroscopic studies on IgG aggregate formation, *Molecular Immunology*, 26, 875-881
- [Mulkerrin *et al.*, 1989], pH dependence of the reversible and irreversible thermal denaturation of  $\gamma$  interferons, *Biochemistry*, 28, 6556-6561
- [Paborji *et al.*, 1994], Chemical and physical stability of chimeric L6, a mouse-human monoclonal antibody, *Pharmaceutical Research*, 11, 764-771
- [Parker *et al.*, 2007], Reversible binding of kynurenine to lens proteins: potential protection by glutathione in young lenses, *Investigative ophthalmology & visual science*, 48, 3705-3713
- [PhEur 2.2.1., 2011], Clarity and degree of opalescence of liquids, *European Directorate for the Quality of Medicine (EDQM)*, 7th edition,
- [PhEur 2.9.19., 2011], Particulate contamination: Sub-visible particles, *European Directorate for the Quality of Medicine (EDQM)*, 7th edition,
- [Philo *et al.*, 2009], Mechanisms of protein aggregation, *Current Pharmaceutical Biotechnology*, 10, 348-351
- [Privalov, 1990], Cold denaturation of proteins, *Critical Reviews in Biochemistry and Molecular Biology*, 25, 281-305
- [Prompers *et al.*, 1999], Tryptophan mediated photoreduction of disulfide bond causes unusual fluorescence behavior of *Fusarium solani* pisi cutinase, *FEBS Letters*, 456, 409-416
- [Ragone *et al.*, 1984], Determination of tyrosine exposure in proteins by second-derivative spectroscopy, *Biochemistry*, 23, 1871-1875
- [Rosenberg, 2006], Effects of protein aggregates: an immunologic perspective, *The AAPS Journal* 2006, 8, E501-E507
- [Roy *et al.*, 2009], Light-induced aggregation of type I soluble tumor necrosis factor receptor, *J. Pharm. Sci.*, 98, 3182-3199
- [Schoeneich, 2010] Light-induced oxidation and aggregation of proteins: potential immunogenicity consequences, *Workshop on Protein Aggregation and Immunogenicity*, Breckenridge, CO, July 20-22, 2010

[Schoeneich *et al.*, 2006], Mass spectrometry of protein modifications by reactive oxygen and nitrogen species, *Free Radical Biology & Medicine*, 41, 1507-1520

[Speed *et al.*, 1997], Polymerization mechanism of polypeptide chain aggregation, *Biotechnology and Bioengineering*, 54, 333-343

[Timasheff, 1995], Preferential interactions of water and cosolvents with proteins, *Protein-Solvent Interact.*, 445-482

[Van De Weert *et al.*, 2005], Fourier transform infrared spectroscopy, *Biotechnology: Pharmaceutical Aspects*, 3, 131-166

[van den Berg *et al.*, 1959], Effect of freezing on the pH and composition of sodium and potassium phosphate solutions: the reciprocal system  $\text{KH}_2\text{PO}_4\text{-Na}_2\text{HPO}_4\text{-H}_2\text{O}$ , *Archives of Biochemistry and Biophysics*, 81, 319-329

[Vanhooren *et al.*, 2002], Photoexcitation of tryptophan groups induces reduction of two disulfide bonds in goat  $\alpha$ -lactalbumin, *Biochemistry*, 41, 11035-11043

[Vermeer *et al.*, 1998], Structural changes of IgG induced by heat treatment and by adsorption onto a hydrophobic Teflon surface studied by circular dichroism spectroscopy, *Biochimica et Biophysica Acta, General Subjects*, 1425, 1-12

[Vermeer *et al.*, 2000], The thermal stability of immunoglobulin: unfolding and aggregation of a multi-domain protein, *Biophysical Journal*, 78, 394-404

[Wang, 1999], Instability, stabilization, and formulation of liquid protein pharmaceuticals, *International Journal of Pharmaceutics*, 185, 129-188

[Wang, 2005], Protein aggregation and its inhibition in biopharmaceutics, *International Journal of Pharmaceutics*, 289, 1-30

[Wang *et al.*, 1996], Characterization, stability, and formulations of basic fibroblast growth factor, *Pharmaceutical Biotechnology*, 9, 141-180

[Zlateva *et al.*, 1999], Factors affecting the dissociation and aggregation of human interferon gamma, *International Journal of Biological Macromolecules*, 26, 357-362

## 4 AGGREGATION STUDIES ON A MURINE MONOCLONAL ANTIBODY

---

### 4.1 INTRODUCTION

The structural diversity within the category of monoclonal antibodies is huge. Two major features of antibody structure should be mentioned: (i) The isotype of monoclonal antibodies, which depends on the glycosylation pattern of the Fc part of the molecule [Janeway *et al.*, 2004], varies between the market products. So far, all mAb products on the market belong to the immunoglobuline G subclass [Roskos *et al.*, 2004; Wang, W. *et al.*, 2006]. Most therapeutic mAbs are of IgG1 isotype, but IgG2 (Muromonab, Denosumab) and IgG4 (Natalizumab) subclasses are used as drug molecules as well [Datamonitor, 2010]. (ii) The structures of the monoclonal antibodies can also be classified according to the content of mouse protein in the molecules. Depending on the percentage of murine protein mAbs are classified in murine, chimeric, humanized and fully human antibodies. These two classifications provide only an extract of the manifold discriminative structures of mAbs. The discrepancies within the class of antibodies indicate that variations in the stability of the molecules, in their tendencies to aggregate, and finally in the resulting immunogenicity could appear.

It is the overall objective of this thesis to elucidate the immunogenicity of aggregates from a murine monoclonal antibody in mice. In this part of the work, the detailed aggregation studies on the human model antibody discussed in Chapter 3 will be transferred to the corresponding murine monoclonal antibody. Slight differences in aggregation between both molecules might be expected, since the fully human model antibody is of IgG1 subclass, whereas the murine antibody employed is of IgG2c subclass. However, the overall aggregation behaviors of both antibodies are expected to be rather similar. Thus, this chapter additionally aims to ensure similar aggregation patterns of both antibodies, confirming an appropriate transferability and prediction of immunogenicity results to a human antibody in human.

Another objective of this chapter is to implement methods to generate aggregates of the mouse muAb, which in the next step will be used in the preparation of an *in vivo* study on immunogenicity. A sufficient amount of aggregates reproducibly generated in a proper time were defined to be key parameters for the methods.

## **4.2 MATERIALS AND METHODS**

### **4.2.1 Materials**

#### **4.2.1.1 Murine IgG2c antibody (muAb) samples**

A murine monoclonal IgG2c antibody (muAb) was kindly provided by Abbott GmbH & Co. KG. The antibody solution applied in the experiments was diluted to a concentration of 10 mg/mL in a 20 mM histidine formulation buffer at pH 6.0. Compared to the aggregation studies on the human model antibody in Chapter 3, the concentration was enhanced from 4 to 10 mg/mL aiming to generate higher total amounts of aggregates sufficient for preparative separation from accompanying protein species. At the same time the sample volume was reduced from 3 mL in 6 R vials to 1 mL in 2 R vials. Both conditions should have comparable filling volume to head space volume ratios, that otherwise can strongly impact the aggregation behavior of the antibody at the air/water interface. The IgG2c stock solution had an initial concentration of 24 mg/mL and was stored at -80 °C in the deep freezer. Prior to use, the formulation buffer was filtrated using a 0.2 µm sterile syringe filter made of cellulose acetate (VWR International, Darmstadt, Germany). 1 mL of the antibody solution was filled into cleaned and sterilized 2 R vials made from glass type 1 (Schott AG, Mainz, Germany), sealed with Teflon<sup>®</sup>-faced rubber stoppers (West Pharmaceuticals Services, Eschweiler, Germany) and crimped. All antibody samples were prepared under aseptic conditions. Highly purified water generated in-house was used for the preparation of samples and buffers (PURELAB Plus instrument (USF Elga, Celle, Germany)). All substances used were of analytical grade.

### **4.2.2 Methods to provoke protein instability**

#### **4.2.2.1 Stirring stress**

Stirring stress of the muAb was performed in 2 R glass vials filled with 1 mL of a 10 mg/mL antibody solution. The same stirrer, stir bars and incubation temperature as in Chapter 3 were used to conduct this study. To accelerate the formation of particles speed was set to 400 rpm (instead of 240 rpm in huAb studies) and the final sampling time point was set to 24 hours of stirring. One vial was selected and removed after 4 h and another one after 6h of stirring. After the entire incubation time a triplicate of samples was left and used for more comprehensive analytics. For control experiments, the pure buffer solution was stirred for 24 h under the same conditions as well.

#### **4.2.2.2 Shaking stress**

Shaking stress of the antibodies was performed in 2 R glass vials filled with 1 mL of a 10 mg/mL antibody solution. A VWR Microplate Shaker (VWR International, Darmstadt, Germany) was used for shaking the vials up to 48 hours. One sample was additionally investigated after 24 h, whereas a triplicate of vials was analyzed after 48 hours. Like in the

stirring experiments the agitation was accelerated to 400 rpm, compared to the previous huAb studies. The arrangement of the vials on the shaker was identical to the huAb samples. For control experiments, the pure buffer solution was shaken for 48 h under the same conditions as well.

#### 4.2.2.3 Light exposure

The same settings of the Suntest CPS radiation chamber (Heraeus Holding, Hanau, Germany) as in the previous study were used for irradiation. 1 mL of the samples containing 10 mg/mL of protein were filled in 2 R glass vials and placed in the center of the radiation chamber in an upright position. Sampling of the vials was performed after 24 h and 48 h (n=1) and finally after 72 h (n=3). These time points were selected to focus the investigation on conformational alterations and the formation of soluble aggregates and fragments, since the huAb started to precipitate after 4 d (96 h) of light exposure. For size exclusion chromatography analysis 10  $\mu$ L of light exposed sample were withdrawn of the remaining three vials after 65 hours. Additionally, the formulation buffer was exposed to light as well and sampled at the same time points. For control experiments, a triplicate of vials completely shielded with aluminum foil was included in the study, serving as control for the slight temperature increase ( $35 \pm 3^\circ\text{C}$ ) during radiation and was sampled after 72 h of incubation.

#### 4.2.2.4 Temperature stress

Heating was performed in 2 R glass vials filled with 1 mL of a 10 mg/mL antibody solution. The vials were incubated in cabinet dryers of a fixed temperature of  $50^\circ\text{C}$  for up to 27 days. Every other week one vial was removed (after 7, 14, 21 days). Finally, a triplicate of vials was incubated 27 days. The melting temperature ( $T_m$ ) of the murine IgG2c was  $65.9^\circ\text{C}$  determined by micro differential scanning calorimetry ( $\mu$ -DSC) (data not shown) thus several degrees above the predefined incubation temperature. For control experiments, the pure buffer solution was incubated 27 days at  $50^\circ\text{C}$  as well.

### 4.2.3 Methods to determine protein stability

#### 4.2.3.1 Light obscuration

Light obscuration (LO) measurements were conducted with a PAMAS-SVSS-C Sensor HCB-LD 25/25 (Partikelmess- und Analysensysteme GmbH, Rutesheim, Germany) to quantify subvisible particles between 1 and 200  $\mu\text{m}$ . Due to limited volume, the muAb samples were diluted 1:5 using placebo formulation prior to analysis. Please refer to section 3.2.3.1 for detailed parameters of the LO measurements.

#### 4.2.3.2 Turbidity

The settings for turbidity measurements are described in section 3.2.3.3.

#### 4.2.3.3 Size exclusion chromatography

Concentrations of soluble aggregates, fragments, and monomeric protein were measured by size exclusion chromatography on an Agilent system equipped with RI and UV detection (Agilent Technologies, Palo Alto, USA) as well as a multi angle laser light scattering detector (MALLS) (DAWN EOS, Wyatt Technology Europe GmbH, Dernbach, Germany). A Superose 6 10/300 GL column (GE Healthcare, Little Chalfont, UK) was used as solid phase. Further settings to conduct SEC measurements are equal to those described in section 3.2.3.4 for the huAb studies.

#### 4.2.3.4 Intrinsic protein fluorescence spectroscopy

The settings for intrinsic protein fluorescence spectroscopy measurements are described in section 3.2.3.5. The sample concentration was changed to 0.1 mg/ml for muAb samples, unless otherwise mentioned.

#### 4.2.3.5 Extrinsic protein fluorescence spectroscopy

The settings for extrinsic protein fluorescence spectroscopy measurements with ANS are described in section 3.2.3.6.

#### 4.2.3.6 Fourier transform infrared spectroscopy (FTIR)

The settings for Fourier transform infrared spectroscopy measurements are described in section 3.2.3.7.

#### 4.2.3.7 High resolution UV absorbance spectroscopy

The settings for high resolution UV absorbance spectroscopy measurements are described in section 3.2.3.8.

### 4.3 RESULTS

#### 4.3.1 Formation of subvisible particles of the murine IgG2c antibody (muAb)

The formation of particles in the muAb formulation in the micrometer range was determined by light obscuration. One sample of each stress condition was measured after the entire incubation time. The highest numbers of subvisible particles  $\geq 1 \mu\text{m}$  were generated by stirring. The total particle numbers counted were three times higher than after shaking, and ten times higher than after heating. The overall increase in particle loading after stirring was accompanied by numerous particles larger than  $10 \mu\text{m}$  and  $25 \mu\text{m}$ . After 72 h of light exposure the detected total numbers of subvisible particles were on a comparable level to the total numbers after 48 h of shaking. However, the numbers of particles  $\geq 10 \mu\text{m}$  and  $\geq 25 \mu\text{m}$

exceeded those generated by shaking. Table 4-1 and Figure 4-1 summarize the cumulative particle counts in muAb samples. The particle numbers counted in the corresponding control samples containing the formulation buffer are not included. None of the stressed buffer samples resulted in a substantial increase in subvisible particles or turbidity.

**Table 4-1 – Numbers of subvisible particles in murine IgG2c samples counted by light obscuration.**

Sample	Number of Particles ≥ 1 µm	Number of Particles ≥ 10 µm	Number of Particles ≥ 25 µm
Unstressed	2,786	29	7
Stirring 24h	234,341	50,014	1,267
Shaking 48h	78,456	1,143	57
Light exposure 72h	61,617	1,650	372
Heat 27d	21,493	326	24

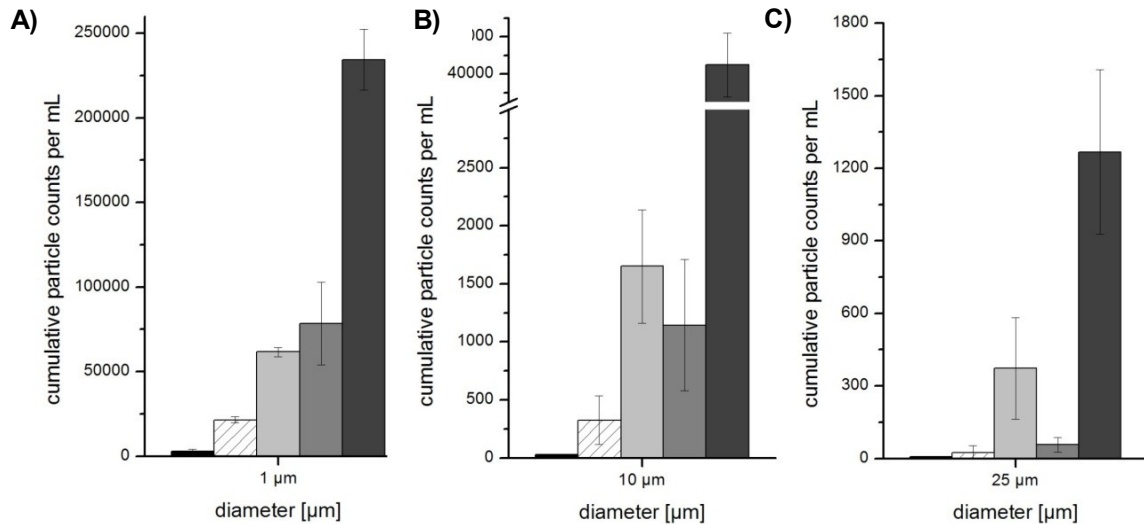


**Figure 4-1 – Particle size distribution of murine IgG2c samples detected by LO.**

**A) Particles ≥ 1 µm    B) Particles ≥ 10 µm    C) Particles ≥ 25 µm**

The unstressed samples are shown in black (■), the heated samples are shown striped (▨), the light exposed samples are shown in light grey (□), the shaken samples are shown in grey (▒) and the stirred samples are shown in dark grey (■). The error bars represent the standard deviation of 3 measurements.

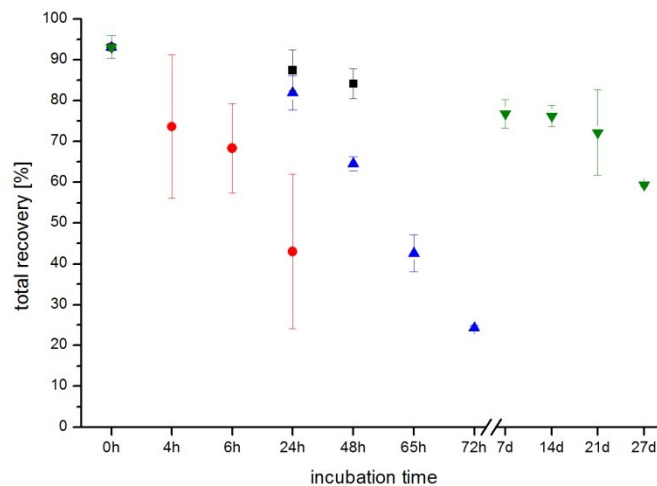
An overview of the determination of the turbidity of the samples is provided in Table 4-2. Confirming the results from light obscuration, the stirred samples were detected to be most turbid. After 24 hours of shaking the cloudiness of the samples slightly increased and a turbidity of  $7.55 \pm 2.86$  FNU was detected. 27 days of storage at 50°C did not increase the turbidity of the murine IgG2c antibody formulation and according to the European Pharmacopoeia the samples appeared clear [PhEur 2.2.1., 2011].

**Table 4-2 – Turbidity measurements of muAb samples after stressing.**

	Unstressed	Stirring 24h	Shaking 48h	Light exposure 72h	Heat 27d
<b>Turbidity [FNU]</b>	$1.20 \pm 0.12$	$87.62 \pm 31.48$	$7.55 \pm 2.86$	$4.40 \pm 2.31$	$1.27 \pm 0.30$

#### 4.3.2 Formation of soluble aggregates of the murine IgG2c antibody (muAb)

Size exclusion chromatography was used to identify and quantify non-particulate protein species accompanying the monomeric antibody, such as fragments and aggregates. Repeated samplings were performed for each chosen stress condition and hence the progress in size distribution of soluble species was monitored. Figure 4-2 provides an overview of the total recoveries after all stress conditions determined by SEC.

**Figure 4-2 – Recoveries of soluble protein species after stressing muAb – determined by SEC.**

The total recoveries after stirring (red), shaking (black), light exposure (blue) and heating (green) are shown compared to the incubation time (time axis not true to scale). A triplicate of samples was analyzed and the error bars represent the standard deviation of  $n=3$ .

Stirring the murine antibody with 400 rpm initiated a considerable loss of total protein recovery in SEC. After 24 hours of stirring  $43 \pm 19$  % of the original protein content was detected yet. Reviewing the tremendous increase in subvisible particles and turbidity in these samples, the formation of insoluble protein species is suggested. The centrifugation of the samples prior to injection to the SEC column separated these species from the solution finally injected.

The aggregation studies with the human IgG1 antibody previously described also revealed a formation of insoluble protein species from shaking, though not as incisive as from stirring. Shaking the murine antibody with 400 rpm also initiated a steady loss of total protein recovery in SEC. After 48 hours of shaking  $84 \pm 4$  % of the injected protein mass was detected



by UV absorption at 280 nm. Similarly to stirring, the formation of subvisible particles discovered by LO and turbidity measurements confirm the findings. Both methods, shaking and stirring, did not initiate the formation of fragments or soluble aggregates feasible to be separated by SEC. The UV 280 nm chromatograms did not show any new emerging peaks (data not shown).

During storage of the antibody at an elevated temperature of 50°C the total protein recovery decreased within the first week to  $77 \pm 4 \%$  (see Figure 4-2). Subsequently, it approximately remains on this level during the next two weeks, and further drops until day 27 reaching  $59 \pm 1 \%$  of total recovery.

The total recoveries determined in the light exposed samples revealed a constantly decreasing profile up to the final incubation time of 72 h.

Comparing the kinetics in the loss of total recovery between all stress conditions obviously stirring appears to be the fastest method to generate huge amounts of insoluble species which cannot be detected by SEC anymore. A drastic but slower loss of total recovery was determined after light exposure as well, whereas shaking and storage at 50°C revealed a very slow reduction of total recovery within the first days.

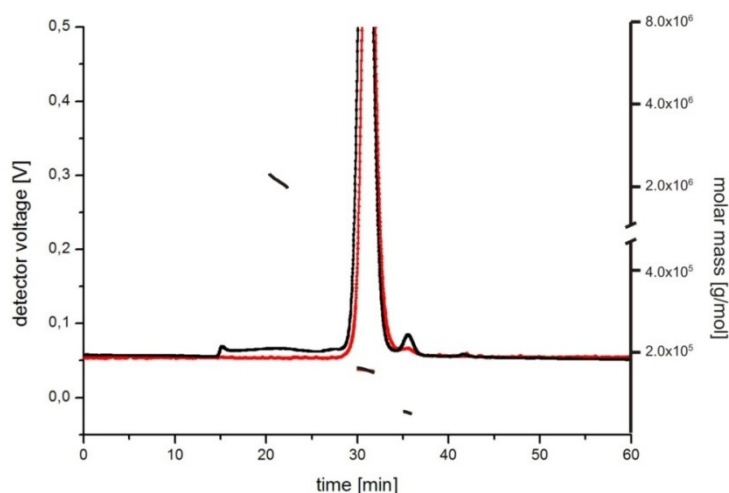


**Figure 4-3 – Distribution of soluble protein species in muAb samples stored at 50°C determined by UV detection after SEC separation.**

The UV chromatograms of the native muAb (red line) and the muAb after 27d of storage at 50°C (black line) are scaled on the left y-axis. The molar masses determined are scaled on the right axis.

The incubation at 50°C additionally led to the formation of additional species of lower and higher molecular weight detected by UV 280 nm. The molar mass determination of this peak indicated it to be formed by fragments (~42 kDa). The main peak comprised 85 % of the in total recovered soluble protein and represented the monomeric muAb approved by a molar mass determination of ~138 kDa. Furthermore, two species of higher molecular weight could be

differentiated due to retention time (see Figure 4-3). A small fraction eluting around 27 – 28 minutes was detected in UV and supposed to be dimers and/or trimers, though for molar mass determination by MALLS the peak was undersized. Besides, oligomers were detected, eluting in a broad peak prior to the dimers/trimers and the monomer. A molar mass of ~2 MDa was determined in a narrow section in the center of the peak. A broad size distribution of species is suggested to form this peak. Figure 4-4 provides the overview of the different species formed during storage at 50°C. The maximum of soluble aggregates was detected after 2 weeks of storage, subsequently dropping simultaneous to the loss of total recovery.

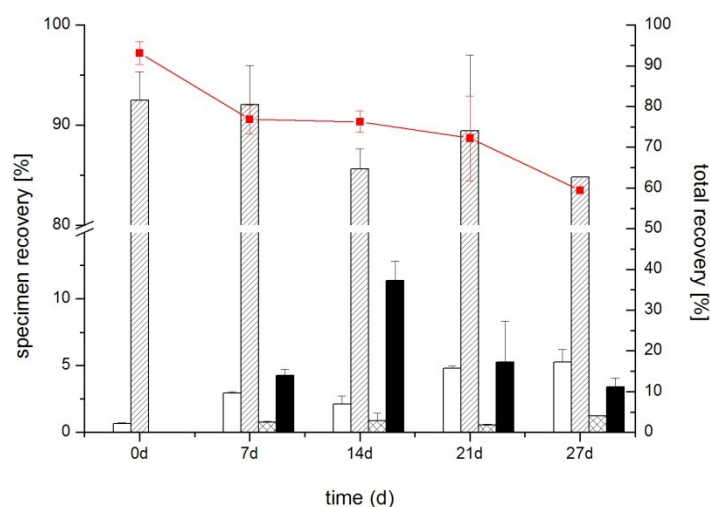


**Figure 4-4 – Distribution of soluble protein species after heating muAb – determined by SEC.**

The total recovery of soluble species is shown by the red squares, scaled on the right y-axis. The white bars represent the amount of species of lower molecular weight (fragments), the striped bars represent the monomer, the checkered bars represent small aggregates and the black bars represent oligomers. The error bars show the standard deviations of n=3 samples.

Soluble aggregates of the murine IgG2c antibody were as well generated by light exposure. The samples irradiated by light feature the quick formation of soluble species of both lower and higher molecular weight. The histidine containing formulation buffer implied the rising of a variety of peaks eluting between 38 and 52 minutes that are also seen in control samples of light exposed buffer. Figure 4-5 exemplarily displays the chromatogram after 72 h of light exposure overlaid to the native muAb sample and the shielded control sample. The formulation buffer degraded by light exposure is shown as well.

The majority of the total area under the curve after 72 h of light exposure eluted prior to the monomer peak. These larger molecular weight species are separated in a sharp peak eluting after 15 minutes and a broad peak eluting between 17 and 28 minutes. The molar mass within these peaks revealed approximations of 1.5 to 3 MDa (see Table 4-3). Besides the generation of huge amounts of aggregates, the originally detected peak representing fragments of muAb raised as well. Within the control samples (shielded from light but exposed to the

elevated temperature of ~35°C) 2.5 % lower molecular weight species but no species of higher molecular weight (aggregates) were detected.

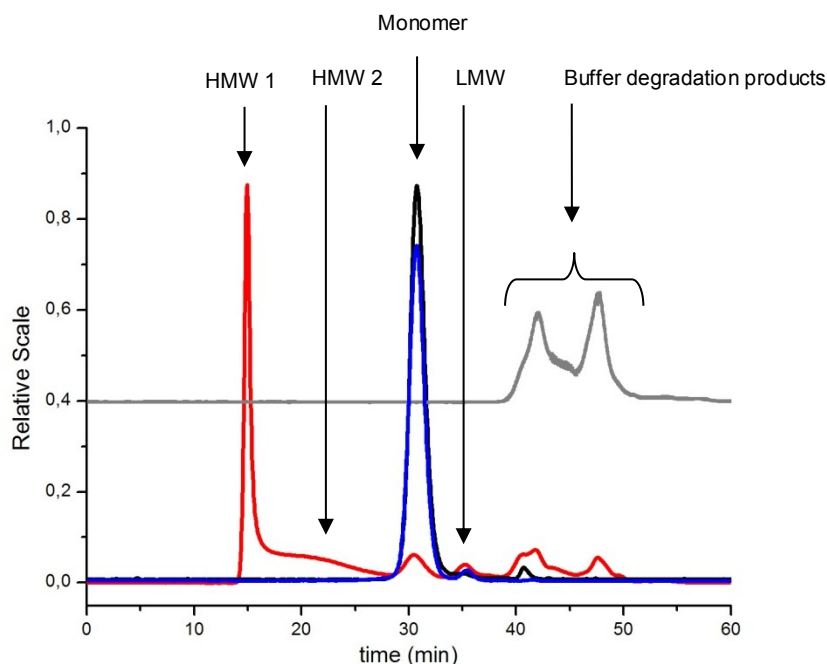


**Figure 4-5 – Distribution of soluble protein species of muAb samples after light exposure determined by UV detection after SEC separation.**

The UV 280 nm chromatograms represent the native murine antibody (black line), the control samples shielded from light but incubated 72h (blue line), and the sample after 72h of light exposure (red line). The grey line shows the chromatogram of light exposed formulation buffer (not true to scale).

**Table 4-3 – SEC: Molecular weight approximations and area percentages (UV) of muAb samples.**

Sample	LMW (Fragments)		Monomer		HMW 1		HMW 2	
	MW	%	MW	%	MW	%	MW	%
Native muAb	50 kDa	1.2 %	124 kDa	98.8 %	-	-	-	-
Control shielded from light	38 kDa	2.5 %	123 kDa	97.5 %	-	-	-	-
72 h light exposure	n/a	4.0 %	n/a	9.2 %	2.7 MDa	50.4 %	1.6 MDa	36.4 %

The distribution of soluble protein species as a function of incubation time is shown in Figure 4-6. Throughout the investigated 72h of light exposure the majority of remaining soluble protein species is represented by higher molecular weight species (aggregates) which were not detectable before irradiation. After the entire time of light exposure,  $88.5 \pm 0.2$  % of aggregates were detected within the  $24.3 \pm 0.7$  % of total protein that could be recovered. The rest was already precipitated into particles. The percentage of aggregates steadily increased during irradiation, whereas the monomer content coincidentally decreased. At the same time the amount of fragments in the samples remains more or less constant between 5.6 and 8.8 %.

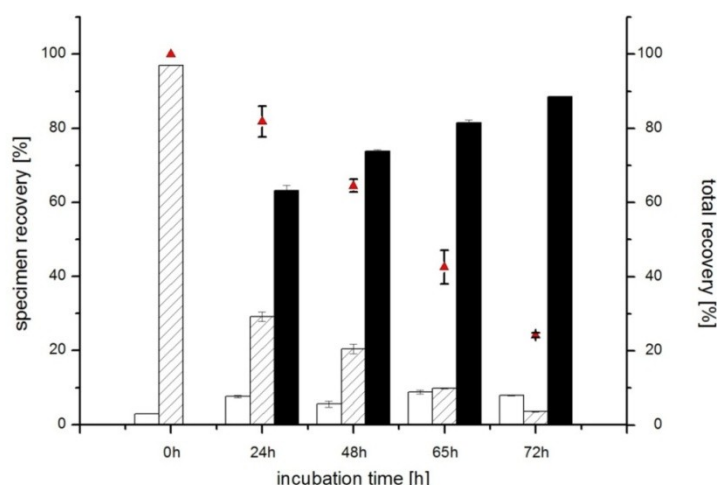


**Figure 4-6 – Time dependent distribution of soluble muAb species determined by SEC after light exposure.**

The left y-axis scales the recovery of the different species: fragments (white bars), monomer (striped bars) and aggregates (black bars). The right y-axis scales the total recovery displayed by the red triangles. The error bars represent the standard deviation of triplicate measurements.

### 4.3.3 Modifications in the structure of the murine IgG2c antibody (muAb)

In this section the structural investigations on muAb using spectroscopic methods such as 2<sup>nd</sup> derivative UV absorbance, intrinsic and extrinsic (ANS) fluorescence and FTIR spectroscopy are briefly described. Table 4-4 provides a short summary of the results from spectroscopic methods.

**Table 4-4 – Overview of results of spectroscopic investigations of stressed muAb.**

Stress method	2 <sup>nd</sup> derivative UV	Intrinsic fluorescence	ANS fluorescence	FTIR
Stirring	-	++	++	+
Shaking	-	+	-	+
Heat	+	++	++	++
Light	++	n/a	n/a	++

- No substantial alterations detected  
 + Moderate alterations detected  
 ++ Strong alterations detected

#### 4.3.3.1 Structural modifications of muAb after stirring and shaking

The detected alterations in the structure of muAb after stirring involve three categories:  
 (i) Minor changes in the tertiary structure of muAb were detected after 24h of stirring by reduced intrinsic fluorescence intensities but at the same time no remarkable changes in 2<sup>nd</sup> derivative

UV absorbance spectroscopy were detected. (ii) A significantly enhanced probability of hydrophobic interactions with ANS after stirring was shown by extrinsic fluorescence. (iii) The susceptibility of the secondary structure of muAb to stirring was indicated by a decrease of intramolecular  $\beta$ -sheet structures in FTIR spectroscopy data.

In comparison, after shaking also a slightly decreased intensity of intrinsic fluorescence and changes in the 2<sup>nd</sup> derivative FTIR spectra were detected, but no increase in ANS fluorescence spectroscopy. Thus, the conformational changes and unfolding procedures after stirring of muAb are more pronounced than after shaking muAb. However, both stress methods entail modifications in the secondary and tertiary structure of the antibody.

#### 4.3.3.2 Structural modifications of muAb after storage at 50°C

Several weeks of storage at 50°C led to enhanced changes in the structure of the murine antibody. The impact of heat on the tertiary structure was detected by a reduced intrinsic protein fluorescence as well as by changes in the *a/b* ratio of the 2<sup>nd</sup> derivative UV absorbance spectra. These changes in tertiary structure were accompanied by an increase in ANS fluorescence with a minute blue shift of the peak maximum, that indicate unfolding of the antibody and hydrophobic surface. By FTIR spectroscopy distinct changes in the secondary structure of the muAb were shown.

#### 4.3.3.3 Structural modifications of muAb after light exposure

The exposure of the murine antibody formulated in 20 mM histidine to light entailed an increasing yellow staining of the samples. The staining derived from the placebo formulation, since the control samples of placebo solution exposed to light were equally colored. With prolonged incubation time the intensity of the staining increased. Since this phenomenon was not observed in the human antibody samples that were formulated in a citrate-phosphate buffer with mannitol, it can be assumed that the coloring is related to oxidation of the histidine in the placebo formulation. This side effect of the irradiation interfered with several analytical methods, like fluorescence and UV absorbance spectroscopy measurements. Fluorescence measurements could not be conducted at all, whereas 2<sup>nd</sup> derivative UV absorbance spectroscopy was possible for the samples after 24 h and 48 h of light exposure. Already within this incubation time a tremendous alteration in the *a/b* ratio was detected suggesting a distinct modification in tertiary structure of light exposed muAb. Furthermore, 2<sup>nd</sup> derivative FTIR spectroscopy revealed significant changes in the secondary structure such as the formation of  $\alpha$ -helices in the antibody.

## 4.4 DISCUSSION

Four different stress methods aiming to generate aggregates of a murine IgG2c antibody were investigated. All methods elicited aggregation of the antibody and thus are evaluated to be suitable for preparative generation of larger amounts of aggregates.

Table 4-5 provides an overview of the classification of physico-chemical changes on the muAb molecule caused by the stress conditions.

**Table 4-5 – Overview of resulting physico-chemical alterations in muAb after stress studies.**

Stress method	Enhanced number of particles	Formation of soluble aggregates	Formation of fragments	Altered secondary structure	Altered tertiary structure / unfolding
Stirring	++	-	-	+	+
Shaking	+	-	-	+	+
Heat	+	+	+	++	++
Light	+	++	+	++	++

- No substantial alterations detected

+ Moderate alterations detected

++ Strong alterations detected

Agitation of muAb by stirring and shaking particularly induces the generation of particulate protein aggregates. At a similar agitation speed stirring with PTFE – coated stir bars was found to be more efficient in aggregation than shaking, resulting in faster formation of higher particle numbers, accompanied by a loss of soluble protein content. Furthermore, no increased particle loading was detected in the buffer formulation (either stirred or shaken). Therefore, it can be concluded that the majority of particles is composed of protein. Though no soluble aggregates were detected by SEC in either sample after agitation modifications in the protein's secondary and tertiary structure were indicated. Again the stirred samples revealed stronger changes after 24 hours than the shaken samples after 48 hours of incubation. After stirring the most severe disparities in the parameters for protein conformation were discovered in the ANS fluorescence spectra. Already after 4 h of stirring a considerable increase in ANS fluorescence was detectable, suggesting the exposure of hydrophobic moieties and thus unfolding of the antibody. At the same time it was found from the 2<sup>nd</sup> derivative FTIR spectra that the unfolding is accompanied by alterations in secondary structure. Interestingly, the shaken muAb samples show similar changes in 2<sup>nd</sup> derivative FTIR spectra, but no differences in ANS fluorescence and 2<sup>nd</sup> derivative UV absorbance spectra were detected at all. Therefore, it can be assumed, that shaking the protein for up to 48 h does not imply substantial unfolding expressed by the enhanced exposure of hydrophobic patches. However, a minor quenching of the tryptophane fluorescence was found which might be considered as precursor for unfolding when shaking is prolonged. Regarding the five aggregation mechanisms widely accepted in biopharmaceutical research [Philo *et al.*, 2009], both stress methods, shaking and stirring, are

assumed to be at least partly based on the interaction between the protein and surfaces. The air-water interface enables an enrichment of protein molecules that potentially can involve unfolding [Chi *et al.*, 2003a; Manning *et al.*, 1995]. During stirring the PTFE surface of the stir bars might additionally serve as areas of protein enrichment. Such resulting assemblings of mostly native antibody molecules in literature are assumed to be weak and might be resolvable. Kiese *et al.* reported that insoluble aggregates of a monoclonal antibody vanished during storage, indicating the reversibility of the assembling [Kiese *et al.*, 2010].

The storage of the murine IgG2c antibody at an elevated temperature of 50°C entails the formation of soluble as well as insoluble aggregates. The distribution of protein species detected by SEC indicates the growth of aggregates gaining an intermediate size of soluble oligomers before exceeding the benchmark and forming insoluble oligomers. Since the monomer content is only slightly reduced during 27 d of incubation, it is suggested that the formation of conformationally altered structures leads to aggregation and later on small oligomers tend assemble to large aggregates. The protein's structure was found to be considerably altered to an increasing extent during storage at 50°C. The characteristic secondary structure of the antibody changed and substantial unfolding including the exposure of hydrophobic moieties to the surface was proven. Hence, the aggregation mechanism based on conformationally altered structures is definitely involved in the formation of aggregates during storage at 50°C [Kendrick *et al.*, 1998; Krishnamurthy *et al.*, 2002; Krishnan *et al.*, 2002; Wang, 2005]. However, the generation of remarkable amounts of aggregates took several weeks which is disadvantageous for the aimed repeated preparation of aggregate samples for *in vivo* studies.

Similar to the human model antibody (see previous Chapter 3) light exposure induces vast structural modifications and strong aggregation in the murine antibody as well. Huge percentages of the total amount of protein were incorporated in aggregates during light exposure. Size exclusion chromatograms showed a strong reduction of monomeric species coincidental with a steady elevation of the amount of soluble oligomers. At the same time the total recovery of soluble protein species drastically decreased. Besides, the exposure to light results in alterations of the histidine containing formulation buffer as well. Presumably the histidine is oxidized by light. The distribution of protein species after light exposure is different to the muAb samples stored at 50°C, where the oligomer content in the soluble fraction is reduced with increasing formation of insoluble species and the monomer content remains rather stable. Therefore, the mechanisms behind differ as well. The nucleation theory reported in literature [Chi *et al.*, 2003b; Philo *et al.*, 2009] is assumed to be part of the underlying aggregation mechanism during light exposure. The soluble oligomers are assumed to serve as nuclei interacting with monomeric antibody. This interaction leads to growth and subsequently the formation of particulate aggregates. At the same time, the amount of oligomers in the remaining soluble fraction does not drop but slightly increase, indicating that no association between oligomers occurred. However, the immense structural modifications proven by spectroscopic

methods indicate the involvement of altered conformations in aggregation too. A combination of several aggregation mechanisms has to be assumed.

Regarding the previous study performed with the model antibody (see Chapter 3), the behavior of both immunoglobulines under similar stress conditions is concluded to be very much comparable. The human IgG1 as well as the murine IgG2c are prone to the formation of subvisible particles by stirring. Both agitation procedures performed during these studies, stirring and shaking, had only minor impact on the conformation of the IgG's, whereas heating and light exposure resulted in significant alterations of their secondary and tertiary structures and unfolding. The most impressive formation of soluble protein aggregates was triggered by light exposure in both cases. However, some substantial differences between both antibodies have to be mentioned as well. Storage at 50°C for several weeks resulted in strong fragmentation of the human antibody but not in the murine antibody. This finding can be explained by the higher susceptibility of the IgG1 isotype to fragmentation as described by Ishikawa *et al.* [Ishikawa *et al.*, 2010]. Instead, in the murine antibody higher amounts of soluble aggregates were detected after storage at 50°C. These discrepancies can be assumed to depend on the different  $T_m$  and thus the unfolding of the proteins. The different formulation buffers also have to be taken into consideration when comparing the aggregation behaviors of both IgG's. It can be concluded that the histidine in muAb formulation is oxidized during light exposure [Huvaere *et al.*, 2009]. The degradation products of histidine have a major impact on the analytical methods to evaluate the modifications appearing in muAb samples during light exposure.

## 4.5 CONCLUSION

A variety of methods to reproducibly generate aggregates in a human model IgG1 antibody was successfully transferred to a murine IgG2c antibody. Furthermore, the analytical tools to detect changes in protein structure were transferred as well.

Comparing the results of the murine IgG2c antibody to the aggregation studies on the model human IgG1 antibody in chapter 3, it can be concluded that the characteristics of the formulations after stressing are very similar. Both molecules form more or less only insoluble aggregates during agitation stress, with stirring being much more efficient than shaking. Both molecules are prone to conformational alterations by light exposure, forming huge amounts of soluble oligomers amongst others. After storage at 50°C some differences can be discriminated between huAb and muAb. The murine antibody seems to be more susceptible for the elevated temperature and revealed more distinct changes. This can be explained by the lower  $T_m$  of the murine molecule.

In the murine antibody formulation, which is aimed to be used in subsequent *in vivo* studies, all investigated stress procedures induced the formation of aggregates. After certain



incubation time all four methods led to the formation of insoluble aggregates, namely subvisible particles. Besides, heavy modifications of protein structure were detected after storage at 50°C and after light exposure. The latter was also found to be the only procedure leading to high amounts of soluble aggregates. The next chapters will deal with the preparative separation of these species from monomer and fragments.

Regarding all analytical results characterizing the muAb samples, tremendous discrepancies between the stress methods were discovered, which was strongly desired concerning the planned *in vivo* studies. However, separation of the aggregated species and an affiliated characterization of these aggregate need to be done prior to animal studies.

## 4.6 REFERENCES

[Chi *et al.*, 2003a], Roles of conformational stability and colloidal stability in the aggregation of recombinant human granulocyte colony-stimulating factor, *Protein Science*, 12, 903-913

[Chi *et al.*, 2003b], Physical Stability of Proteins in Aqueous Solution: Mechanism and Driving Forces in Nonnative Protein Aggregation, *Pharmaceutical Research*, 20, 1325-1336

[Datamonitor, 2010] Monoclonal Antibodies: 2010, [http://www.datamonitor.com/store/Product/monoclonal\\_antibodies\\_2010?productid=HC00029-00002](http://www.datamonitor.com/store/Product/monoclonal_antibodies_2010?productid=HC00029-00002)

[Huvaere *et al.*, 2009], Light-Induced Oxidation of Tryptophan and Histidine. Reactivity of Aromatic N-Heterocycles toward Triplet-Excited Flavins, *Journal of the American Chemical Society*, 131, 8049–8060

[Ishikawa *et al.*, 2010], Influence of pH on heat-induced aggregation and degradation of therapeutic monoclonal antibodies., *Biological and Pharmaceutical Bulletin*, 33, 1413-1417

[Janeway *et al.*, 2004], Immunobiology: The Immune System in Health and Disease, 6th Edition,

[Kendrick *et al.*, 1998], Aggregation of Recombinant Human Interferon Gamma: Kinetics and Structural Transitions, *J. Pharm. Sci.*, 87, 1069-1076

[Kiese *et al.*, 2010], Equilibrium studies of protein aggregates and homogeneous nucleation in protein formulation, *J. Pharm. Sci.*, 99, 632-644

[Krishnamurthy *et al.*, 2002], The stability factor: importance in formulation development, *Current Pharmaceutical Biotechnology*, 3, 361-371

[Krishnan *et al.*, 2002], Aggregation of Granulocyte Colony Stimulating Factor under Physiological Conditions: Characterization and Thermodynamic Inhibition, *Biochemistry*, 41, 6422-6431

[Manning *et al.*, 1995], Approaches for increasing the solution stability of proteins, *Biotechnology and Bioengineering*, 48, 506-512

[PhEur 2.2.1., 2011], Clarity and degree of opalescence of liquids, *European Directorate for the Quality of Medicine (EDQM)*, 7th edition,

[Philo *et al.*, 2009], Mechanisms of protein aggregation, *Current Pharmaceutical Biotechnology*, 10, 348-351

[Roskos *et al.*, 2004], The clinical pharmacology of therapeutic monoclonal antibodies, *Drug Development Research*, 61, 108-120

[Wang, 2005], Protein aggregation and its inhibition in biopharmaceutics, *International Journal of Pharmaceutics*, 289, 1-30

[Wang *et al.*, 2006], Antibody structure, instability, and formulation, *J. Pharm. Sci.*, 96, 1-26

## 5 FRACTIONATION OF PROTEIN AGGREGATES OF A HUMAN MONOCLONAL ANTIBODY BY AF4

---

### 5.1 INTRODUCTION

The aim of this study was to develop a preparative AF4 method to separate soluble aggregates of a monoclonal antibody from the concurrently existing monomeric species and fragments in preparation of an *in vivo* study. A human monoclonal antibody of IgG1 isotype (huAb) should first be utilized for method development and optimization. This step aims to achieve a suitable concentration of a certain protein aggregate that is stable during several days of storage. The final concentration of the protein aggregates after fractionation should at least exceed 250 µg/mL, due to limited volumes that can be administered subcutaneously. The separated fractions were characterized as far as possible. Furthermore, it was checked whether those aggregates separated from concomitant protein species show a tendency to dissociate during storage. Later on, the entire procedure was transferred and reassigned to a mouse monoclonal antibody (muAb) and the immunogenicity of these aggregates was evaluated in an animal study. -80°C and 2-8°C storage were chosen as appropriate conditions for the preparation of *in vivo* studies.

Due to the investigations on various methods capable of inducing aggregation in the model huAb (see chapter 3 of this thesis), light exposure was utilized to provide a suitable distribution of soluble aggregates for this study. It was shown that the conditions of irradiation resulted in abundant amounts of huAb-oligomers that were differentiable by SEC. Therefore, a separation via asymmetrical flow field-flow fractionation seemed to be feasible as well.

#### 5.1.1 The use of asymmetrical flow field-flow fractionation (AF4) to separate protein aggregates

Recently, AF4 is increasingly used as analytical tool to separate different species of various materials according to their size. A major benefit of the technique is the broad size range that can be covered. The field of application starts in the low nanometer range, covers the complete colloidal size range and ends up in the two-digit micrometer range [Giddings, 1993]. Therefore, one feature of this separation technology that is worth it to be highlighted is its great versatility [Fraunhofer *et al.*, 2004; Schimpf, 2000]. It is capable of separating macromolecules such as polysaccharides or proteins [Leeman *et al.*, 2006; Liu *et al.*, 2006] as well as assemblies like viruses, virus-like particles and liposomes [Hupfeld *et al.*, 2006; Kowalkowski *et al.*, 2006; Lang *et al.*, 2009; Sweeney *et al.*, 2010].

AF4 is a valuable analytical method for sizing and quantification of different aggregate species within protein samples [Fraunhofer *et al.*, 2004]. It is distinguished from size exclusion

chromatography (SEC) and reversed phase high performance liquid chromatography (RP-HPLC) by lower pressures, much lower shear forces and very small surface areas, interfering with the analytes. Out of these, the major benefit of AF4 when using to separate and characterize protein aggregates is its separation principle involving no matrices that might absorb or interact with protein aggregates, potentially altering the proteins features. In SEC, the non-specific binding to the column material can even lead to a loss of aggregates [Stulik *et al.*, 2003]. Instead, the field-flow fractionation principle is based on differences in diffusion coefficients, respectively the hydrodynamic radii of the analytes [Giddings *et al.*, 1976]. However, at harsh cross flow conditions, a membrane-protein interaction can still exist. Using a membrane made from regenerated cellulose, these interactions can strongly be reduced, since the material is known to be hydrophilic and non-protein adsorptive. For prevention of enhanced particle – wall interactions and particle – particle interactions due to high concentration in a small area, the cross flow always should be fixed at low values for analyzing protein aggregates [Liu *et al.*, 2006]. A high cross flow implies an enhanced pressure in the separation channel and concentration effects at the membrane which can impact for example the conformation of aggregates. However, a fair separation of different size species strongly depends on a sufficient cross flow and usually there is only little scope of varying this parameter.

Like in SEC, the AF4 system can be connected to refractive index (RI) and ultraviolet (UV) detectors that enable a quantification of the protein species [Reschiglian *et al.*, 2001]. Furthermore light scattering detectors are used to determine the molecular weight of the analytes [Thielking *et al.*, 1995; Wyatt, 1991]. Due to the separation principle in AF4 based on the perpendicular directed flows, the sample is usually diluted in much higher volumes of mobile phase than in SEC. The removal of buffer by the cross flow through the ultrafiltration membrane over the whole channel length finally results in sufficient protein concentrations reaching the detector. To increase the final concentration improvements of the channel were implemented by Postnova Analytics (Salt Lake City, USA). The upper portion of the laminar flow can be discharged by an additional port incorporated close to the detector outlet. This fraction of mobile phase should be free of protein. Therefore, the previous dilution of the sample can be reduced and the sensitivity of the detector can be enhanced. Increasing the loading of the protein can raise the yield only to a limited amount. Overloading can be recognized by loss of resolution, peak broadening and peak skewness [Litzen *et al.*, 1991]. To overcome this, the channel height can easily be increased by using spacers of various thicknesses. However, an increased channel height concurrently entails a higher volume of mobile phase and thus dilution, as well as an altered peak resolution. Alternatively, the channel width can be broadened to improve the sample loading. But again the volume of the mobile phase and hence dilution increase. Furthermore, broadening of the channel can lead to trouble with tightness of the channel.

AF4 can be utilized with various buffers, in many cases allowing the use of the buffer the protein is formulated in. Like in SEC, a separation in a mobile phase substantially differing from the formulation buffer potentially can alter the distribution of weakly associated protein species like non-covalent aggregates [Arakawa *et al.*, 2007]. A fractionation in the formulation

buffer is furthermore advantageous if subsequent *in vivo* studies are planned. No buffer exchange has to be performed before administration to the animals when the formulation buffer can be maintained while fractionation takes place. The typically utilized high salt concentrations in SEC [Wen *et al.*, 1996], would interfere with the adjustment of tonicity for parenteral administration.

## **5.2 MATERIALS AND METHODS**

### **5.2.1 Sample preparation**

A recombinant human monoclonal IgG1 antibody (huAb) was kindly provided by Abbott GmbH & Co. KG and used as a model protein for these separation studies. The antibody solution applied in the experiments was diluted to a concentration of 10 mg/mL in a citrate/phosphate formulation buffer at pH 5.2. The IgG1 stock solution had an initial concentration of 70 mg/mL and was stored at -80 °C in the deep freezer. Prior to use, the formulation buffer was filtrated using a 0.2 µm sterile syringe filter made of cellulose acetate (VWR International, Darmstadt, Germany). The antibody solution was filled into cleaned and sterilized 6 R vials made from glass type 1 (Schott AG, Mainz, Germany), sealed with Teflon-faced rubber stoppers (West Pharmaceuticals Services, Eschweiler, Germany) and crimped. All antibody samples were prepared under aseptic conditions. Highly purified water generated in-house was used for the preparation of samples and buffers (PURELAB Plus instrument (USF Elga, Celle, Germany)). All substances used were of analytical grade.

The generation of aggregates was triggered by 48 h of light exposure, using a Suntest CPS instrument (Heraeus, Hanau, Germany) using the same conditions as in chapters 3 and 4 (see section 3.2.2.4).

### **5.2.2 Asymmetrical flow field-flow fractionation**

AF4 was employed to separate the soluble oligomers generated by 48 h of light exposure from other protein species. The separation was conducted with an Eclipse 2.0 system (Wyatt Technology Europe GmbH, Dernbach, Germany) combined with an auto sampler and an in-line degasser of the Agilent 1100 series (Agilent Technologies, Palo Alto, USA). The system was additionally connected to detectors for refractive index, for ultraviolet spectroscopy (both from Agilent Technologies, Palo Alto, USA) and to a DAWN EOS (Wyatt Technology Europe GmbH, Dernbach, Germany) multi angle laser light scattering detector. For molar mass determination of all proteins, the refractive index increment  $dn/dc$  was set at 0.185 mL/g. A novel semi-preparative channel (SP1, Wyatt Technology Europe GmbH, Dernbach, Germany) of 245 mm length and 350 µm height and equipped with a membrane made of regenerated cellulose with a 10 kDa molecular weight cut off (MWCO) was used for separation. The samples were collected in glass tubes by a Gilson FC 203B Fraction Collector (Gilson Inc., Middleton, USA). The delay of time between UV detector and fraction collector was previously determined using dextrane blue and transparent tubing between detector and collector. The

time between the rising UV absorbance and the visually detected arriving at the fraction collector amounted to 1 minute and 40 seconds. As carrier liquid a phosphate buffered saline (PBS) consisting of 50 mM phosphate and 400 mM sodium chloride at pH 7.0 was employed. The buffer was filtrated through a 0.1 µm cellulose nitrate filter with a diameter of 50 mm (Whatman GmbH, Dassel, Germany) prior to connection the system. The detector flow was set to 1 mL/min, whereas the cross flow was appointed at 3 mL/min for 5 minutes followed by a linear reduction to 0 mL/min over a period of 20 min. Finally, 30 minutes of elution without any cross flow (VX) were added. 100 µL of stressed antibody sample were injected per run, equaling a total amount of 1 mg of protein injected to the channel. The injection volume used for the native huAb was 50 µL, equaling 0.5 mg of protein. The distribution of the species was calculated from the AUC using Astra 5.3 software (Wyatt Technology Europe GmbH, Dernbach, Germany).

**Table 5-1 – Separation methods of AF4 applied to the recombinant human IgG1 antibody (huAb) using the semi-preparative channel SP1 with a constant detector flow of 1.0 mL/min.**

A) Separation method applied to the native huAb    B) Separation method applied to huAb after light exposure

A)	Time [min]	Mode	VX start [mL/min]	VX end [mL/min]	Focus flow [mL/min]
	2	Elution	5.0	5.0	
	1	Focus			3.0
	2	Focus + Injection			3.0
	1	Focus			3.0
	20	Elution	2.0	2.0	
	10	Elution	2.0	0.0	
	17	Elution	0.0	0.0	
	<b>Σ = 53</b>				

B)	Time [min]	Mode	VX start [mL/min]	VX end [mL/min]	Focus flow [mL/min]
	2	Elution	5.0	5.0	
	1	Focus			3.0
	2	Focus + Injection			3.0
	1	Focus			3.0
	5	Elution	3.0	3.0	
	20	Elution	3.0	0.0	
	32	Elution	0.0	0.0	
	<b>Σ = 63</b>				

Both methods described in Table 5-1 could be divided into three major steps. Each run starts with the injection of the sample, followed by a focusing step and the final elution and separation. The detector flow was set to 1 mL/min for all methods. Depending on the volume of

the sample injected, the analytes might diffuse all over the channel, resulting in broad peaks and a very poor resolution. Therefore, a focusing step is carried out prior to separation by the cross flow. This step entails the accumulation of the complete sample within a narrow band inside the channel. Ideally, this band is formed approximately 5 mm downstream from the injection port [Fraunhofer *et al.*, 2004].

### 5.2.3 Protein concentration by centrifugation

The oligomer fractions of several injections were collected in glass tubes and concentrated by centrifugation using disposable centrifugal protein concentration devices. Three different types of protein concentrators were tested and compared. Vivaspin 6 (2 – 6 mL, 5 kDa MWCO, membrane made of polyethersulfone, Sartorius Stedim Biotech S.A., Aubagne Cedex, France) and Vivaspin 15R centrifugal concentrators (2 – 15 mL, 5 kDa MWCO, membrane made of cellulose derivate Hydrosart®, Sartorius Stedim Biotech S.A., Aubagne Cedex, France) as well as Protein Concentrators (7 mL, 9 kDa MWCO, membrane made of regenerated cellulose, Pierce Biotechnology, Rockford, USA) were employed to test whether concentration of the probes was actually possible. Hence, 100 µL of stressed antibody sample were injected to AF4 three times in a row, the aggregate peaks collected pooled and loaded onto either type of the Vivaspin concentrators or Protein Concentrator tubes, respectively. Pre-rinsing was carried out according to the manufacturer's instructions by adding 2 mL of AF4 mobile phase to the tubes, followed by a centrifugation step for 5 min at 4000 x g in order to allow equilibrium and to remove traces of glycerine or sodium azide from the production process that could possibly influence the results. Once the pooled protein solution had been placed in the upper chamber of the concentrators, the tubes were put into swinging buckets and centrifuged at 4000 x g and a temperature of 4 °C for 30 min using a Megafuge 1.0R and the corresponding 7570F rotor (Heraeus Instruments, Santa Clara, USA). The concentration of the resulting fractions was determined via UV absorbance at an excitation wavelength of 280 nm as well as with a Micro BCA Assay according to the manufacturer's instructions (Pierce Biotechnology, Rockford, USA). UV absorbance spectroscopy measurements were performed at 25°C with a Fluostar Omega spectrophotometer (BMG Labtech, Offenburg, Germany) and the Omega Software Version 1.01 together with MARS data analysis, Version 1.01. 200 µL aliquots of native samples were measured in a quartz 96-well plate.

### 5.2.4 Micro BCA™ Protein Assay Kit

To determine very low protein concentrations a Micro BCA assay (µ-BCA) was used from Pierce Biotechnology (Rockford, USA). Bicinchoninic acid reacts with  $\text{Cu}^+$ , which originates from a stoichiometric reduction of  $\text{Cu}^{2+}$ , mediated by peptide bonds. Finally, the absorbance of the resulting coloration is measured at 562 nm in a 96 well plate made of quartz (Hellma, Müllheim, Germany).

### **5.2.5 Sodium dodecyl sulfate – polyacrylamide gel electrophoresis**

Non-reducing denaturing sodium dodecyl sulfate – polyacrylamide gel electrophoresis (SDS-PAGE) was used to additionally investigate the distribution of protein species, such as aggregates and fragments, after light exposure. The electrophoresis was performed in a XCell II Mini cell system (Novex, San Diego, USA). The samples were diluted to a final concentration of 0.05 mg/mL in a Tris-buffer pH 6.8 including 2 % glycerin and 2 % SDS. For reducing conditions dithiothreitol (DTT) was added to the sample buffer. Denaturation was performed by heating at 95°C for 20 minutes. Finally, 20 µl of each sample were loaded into the precast wells in the gel. Electrophoresis was carried out with NuPAGE® Pre-Cast 10 % Bis-Tris gels 1 mm, 12 wells and NuPAGE® MES running buffer (Life Technologies, Grand Island, USA). Separation was accomplished with 40 mA and running time was approximately 45 minutes. After electrophoretic separation the gels were stained with SilverXPRESS® Silver Staining Kit (Life Technologies, Grand Island, USA). A molecular weight standard was analyzed on each gel as well, to determine the molecular weight of the detected protein species (HiMark™ Unstained Standard, Life Technologies, Grand Island, USA).

### **5.2.6 Size exclusion chromatography**

Size exclusion chromatography (SEC) was employed as orthogonal method to AF4 to monitor the distribution of protein species after light exposure. A Superose 6 10/300 GL column (GE Healthcare, Little Chalfont, Great Britain) was utilized as solid phase on a Postnova AF2000 FOCUS system (Postnova Analytics GmbH, Landsberg, Germany). As mobile phase PBS pH 7.4 (12 mM phosphate, 137 mM sodium chloride, 2.7 mM potassium chloride) with a flow rate of 0.5 mL/min was used. The protein recovery was calculated using UV absorbance signal at 280 nm. The area under the curve (AUC) of the unstressed sample was defined 100%.

## **5.3 RESULTS**

### **5.3.1 Characterization of the samples**

Non-reduced SDS-PAGE showed no bands originated from aggregates in the native protein sample. The height of the most prominent band in line 2 of the gel (Figure 5-1, A) is around 160 kDa and thus originates from the monomer. No species larger than the monomer and its isoforms are detected in SDS-PAGE. Two light bands referring to species smaller than 100 kDa are detected in the native sample as well. They resemble fragments of the antibody that were generated by the harsh conditions of denaturing SDS-PAGE. Comparing the resulting pattern of native and light exposed sample, they look similar in the majority of bands, though the intensity of the bands differs. However, after light exposure additional stains above the 160



kDa band arise. These weak areas probably derived from covalently aggregates within the sample, though no clear band can be detected.

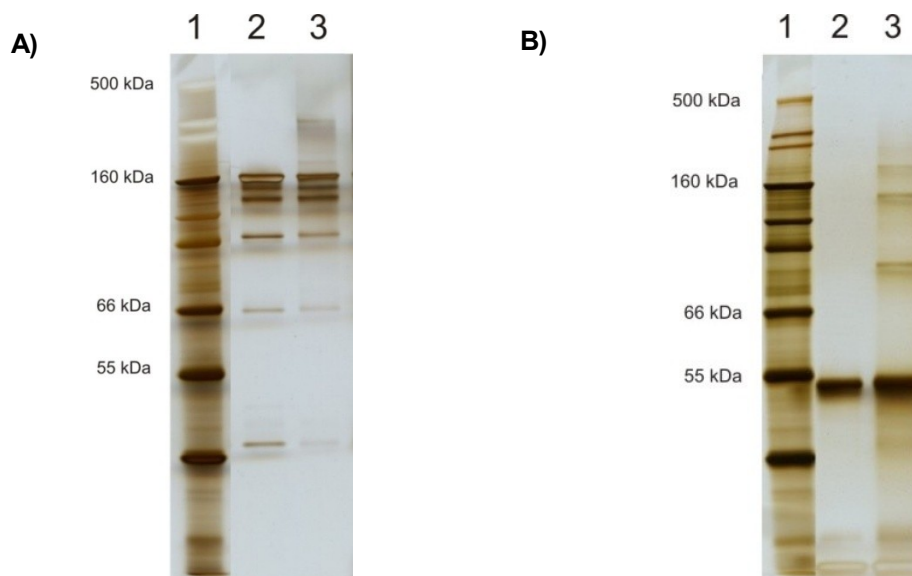


**Figure 5-1 – Silver-stained SDS-PAGE gels of huAb.**

**A)** SDS-PAGE under non-reducing conditions

**B)** SDS-PAGE under reducing conditions

In line 1 the resulting bands of the HiMark™ Unstained Protein Standard are shown and some dedicated molecular weight values are labelled on the left side. Line 2 represents the native huAb molecule and line 3 represent the huAb after 48 h of light exposure.

Under reducing conditions (Figure 5-1, B) the native huAb sample is completely cut in pieces through disulfide-cleavage, resulting in one intense band around 50 kDa. Instead, the light exposed sample reveals three additional bands of larger molar mass, that derived from new formed species within the sample and that are not linked by disulfide bonds.

To confirm the formation of aggregates the sample were analyzed by SEC as well. The chromatograms obtained of a single run of the native or stressed sample by SEC are shown in Figure 5-2. 200 µg of each material were injected into the system. For better comparison of the distribution of the species, the chromatogram of the native huAb is displayed in another scale. The area under the curve (AUC) of the UV 280 nm chromatogram was used to calculate the percentage of the different species separated by SEC. The native huAb (see Figure 5-2, black line) results in one sharp peak eluting after 32 minutes. The recovery determined by Astra software was 97.0 % and the molecular weight determined by a 3-angle MALLS detector was 166 kDa. The red line depicts the chromatogram of the stressed huAb sample, with a total recovery of 79.2 % compared to the unstressed sample. The separation resulted in 3 different species eluting prior to the monomer at 32 minutes. Referring to the molecular weight behind these peaks (see Table 5-2), they are defined as high molecular weight aggregates (HMW) eluting at 15 minutes, intermediate molecular weight aggregates (IMW) eluting between 17 and 25 minutes and dimers/trimers eluting at 27.5 minutes.

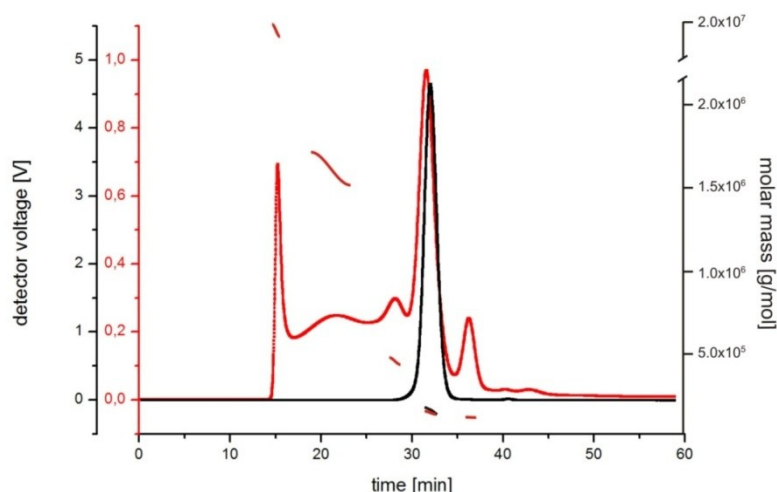


**Figure 5-2 – SEC separation of the human IgG1 before and after light exposure.**

Time dependent UV detector voltage at 280 nm and molar mass detection by MALLS after SEC separation of light exposed huAb (red line) and native huAb (black line). The UV chromatograms are scaled on the y-axes on the left side. The red y-axis refers to the stressed sample and the black y-axis refers to the native sample. The right y-axis represents the molar mass scale for both samples.

The samples of the recombinant human IgG1 antibody after 48 h of light exposure showed four different peaks in UV 280 nm detection after field-flow fractionation (see Figure 5-3).

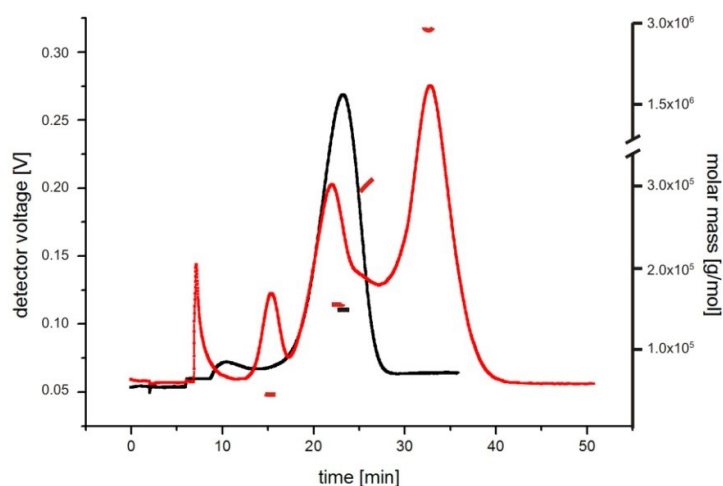


**Figure 5-3 – AF4 separation of the human IgG1 before and after light exposure.**

Time dependent UV detector voltage at 280 nm and molar mass detection by MALLS of light exposed huAb (red line) and native huAb (black line) after separation by Eclipse 2.0.

The area under the curve (AUC) of the UV 280 nm fractogram was used to calculate the percentage of the different species separated by AF4. The native huAb (see Figure 5-3, black line) results in one single peak eluting between 17 and 27 minutes, with a peak maximum at ~23.5 minutes. The determination of the molecular weight light scattering of the overall peak yielded in 131 kDa, which is reasonable for the expected molecular weight of ~ 144 kDa for this specific antibody. Due to the nearly monodispers composition of that sample only a limited amount of 500 µg protein was injected into the channel, since overloading would result in a poor peak shape and fronting or tailing effects. However, the slightly elevated baseline prior to the main peak is attributed to the high injection mass. The calculated total recovery was 96.8 %. To maximize the amount of protein aggregates fractionated and collected after elution, 100 µl of the sample after light exposure was injected into the system. The concentration of the sample was 10 mg/mL, thus a maximum recovery of 1 mg protein was procurable. The total recovery detected by UV spectroscopy at 280 nm was 88.4 % of protein, compared to the unstressed sample. The fractogram was subdivided into four different peaks and one shoulder shown in Figure 5-3. Using the 18-angle MALLS detector the molecular weights (MW) of these species were determined. The three major eluting peaks represent fragments of the IgG1 (elution maximum at 15.5 minutes), the monomeric protein (elution maximum at 22 minutes), and oligomeric structures (elution maximum at 33 minutes). Furthermore, a shoulder eluted directly after the monomeric species between 24.5 and 27.5 minutes. Additionally a void peak arose when analyzing this sample. The elution time of this novel peak was at 7 – 7.5 minutes. Determination of the MW of this void peak with Astra 5.3 software was not possible. This peak most likely represents large aggregates that elute prior to all other species due to the so called steric mode of field-flow fractionation (see Chapter 2).

The results of both orthogonal methods are summarized in Table 5-2.

**Table 5-2 – Comparison of SEC and AF4 analysis of huAb after light exposure.**

Overview of molecular weight determination as well as the content of the separated protein species in SEC (MW<sub>SEC</sub>, Content<sub>SEC</sub>) and in AF4 (MW<sub>AF4</sub>, Content<sub>AF4</sub>) measurements.

Protein species	MW <sub>SEC</sub>	MW <sub>AF4</sub>	Content <sub>SEC</sub>	Content <sub>AF4</sub>
<b>Fragments</b>	n/a	37 kDa	8.6 %	6.7 %
<b>Monomer</b>	162 kDa	166 kDa	35.2 %	25.4 %
<b>Dimer / Trimer</b>	415 kDa	295 kDa	15.6 %	9.5 %
<b>Oligomers</b>	1867 kDa (IMW) 6620 kDa (HMW)	2771 kDa	30.0 % (IMW) 10.6 % (HMW)	54.7 %
<b>Total recovery</b>	---	---	79.2 %	88.4 %

The overall recovery is pretty much comparable within both methods. After separation with AF4, 88.4 % of the original protein content was detected, whereas the analysis by SEC resulted in only 79.2 %. The difference is at least in part due to the missing void peak in SEC, representing large aggregates. However, the AUC of this peak in AF4 amounted only 3.7 %, not

completing the entire difference of 9 %. Since the total recovery in both methods is not 100 %, the formation of large insoluble species that precipitated prior to injection is expected. The percentages of the various protein species differ as well. Using SEC the content of fragments, monomer and small aggregates like dimers/trimers is higher than in AF4, in exchange the recovery of oligomers is lower. Comparing the determination of the molecular weights of the species very similar results were determined for the monomer peak. For the fragment peak in AF4 37 kDa were found, whereas no value was available in SEC. The comparison of molecular weight of species larger than the monomer is flawed, because of the totally differing distribution. For example small aggregates like dimers and trimers are separated well in SEC, forming a peak. Instead, the separation by AF4 shows only a shoulder representing these species, compromising a distinct determination of MW and AUC. Anyway, the resolution in both methods is poor and does not reach the baseline within the peaks. Therefore, all values are only approximations.

### 5.3.2 Collection of protein species after field-flow fractionation

The fractions separated by AF4 were collected by elution time using a Gilson fraction collector. Directly after fractionation the protein concentration of each fraction was determined by Micro BCA assay ( $\mu$ -BCA assay). Before injecting the light exposed sample to the field-flow fractionation channel, the sample concentration of 10 mg/mL was confirmed by this assay too. After injection of 100  $\mu$ L, fractionation and collection of one sample over the entire elution time an amount of 1.053 mg total protein was determined using the  $\mu$ -BCA assay as well.

All protein species incorporated in the stressed sample except the shoulder resembling the dimer were gathered in glass tubes. The collection times comprised only the peak maxima and are shown in Table 5-3. The collected fractions covered only portions of the eluting peaks to achieve the highest possible protein concentrations.

**Table 5-3 – Elution times and collection times of protein species in huAb sample after light exposure.**

The collection times were always defined narrower than the elution to reduce potential cross-contamination of two fractions. A collection time of 1 minute implies a volume of 1 mL, since the detector flow was set to 1 mL/min.

Protein species	Elution time	Collection time
<b>Void Peak / Large aggregates</b>	7.0 – 7.5 minutes	7.0 – 7.5 minutes
<b>Fragments</b>	12.0 – 17.5 minutes	13.0 – 17.0 minutes
<b>Monomers</b>	18.0 – 24.0 minutes	18.5 – 23.5 minutes
<b>Oligomers</b>	28.0 – 40.0 minutes	31.0 – 38.0 minutes

The single void peak fraction covered only  $7.2 \pm 0.33$   $\mu$ g/mL and the fractions containing fragments covered  $20.2 \pm 1.3$   $\mu$ g/mL. The recovery of the monomer was  $42.1 \pm 4.4$   $\mu$ g/mL of total protein, whereas  $58.8 \pm 3.9$   $\mu$ g/mL of soluble oligomers were

determined in the fraction. Due to the remarkable dilution effect occurring in AF4 measurements, these concentrations are far below the expected 1 mg/mL. However, regarding the volumes of the collected fractions, 707  $\mu\text{g}$  of protein were recovered in the fractions comprising only the peak maxima. That means, approximately 30 % of the injected amount of protein was not collected and got lost.

To make sure that the aggregates did not disintegrate after collection due to dilution within the AF4 buffer or other side effects, 100  $\mu\text{L}$  of the collected aggregate fraction were re-injected using the same separation mode again. Proving that aggregates were still present in the sample, a peak was observed in light scattering signal as well as in UV absorbance at the same retention time found before for the aggregate peak in the stressed sample between 28 and 36 minutes. However, the low concentration of the sample accounts for the very small peak in UV absorbance (see Figure 5-4). The other collected fractions were not re-injected, since the concentrations were even less and the study focused on the large oligomer peak.

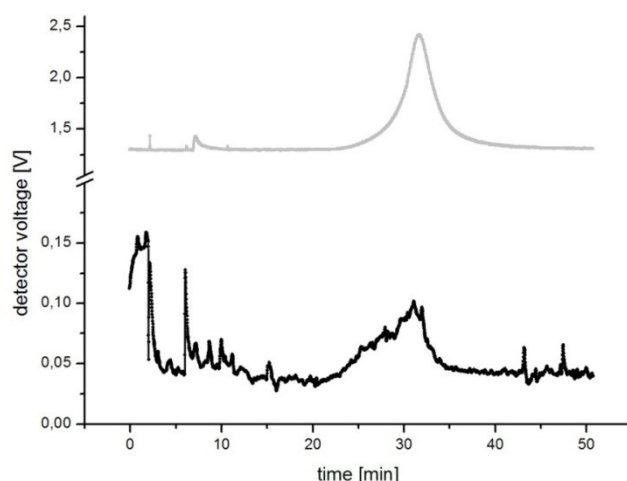


**Figure 5-4 – AF4 fractogram of re-injected oligomeric fraction of huAb after 48 h of light exposure.**

After collection of the fraction containing the oligomeric species, 100  $\mu\text{L}$  of that sample were re-injected. The black line displays the UV absorbance at 280 nm. The grey line displays the light scattering signal at 90°.

The stability of the samples after fractionation was investigated after storage at 2 – 8 °C since it is already known that protein species like aggregates tend to change their size distribution during storage [Kiese *et al.*, 2010]. The fractionation by AF4 implicates a new buffer composition the protein species exist in, which might have an impact on the stability of the species as well. Two consecutive runs injecting 100  $\mu\text{L}$  of the stressed sample were fractionated by AF4 as described above. The collection of both runs was pooled in clean and sterilized 6 R glass vials (Schott AG, Mainz, Germany). Concentration was measured at day 0, day 3, day 7, day 14 and after three weeks by  $\mu\text{-BCA}$ . For each time point a separate vial was utilized. The samples were centrifuged for 5 min at 4000 x g before analysis, and Figure 5-5

displays the determined protein concentrations over time. The fractions containing fragments, monomers or oligomers maintain their total protein concentrations over 21 days of storage at 2 – 8 °C. Precipitation was neither visually detected nor did the concentration in the supernatants decrease over time. Only the fraction containing the void peak shows a constant decrease in protein concentration. Due to the marginal protein concentration < 10 µg/mL only a slight precipitation was detected visually after 21 days.

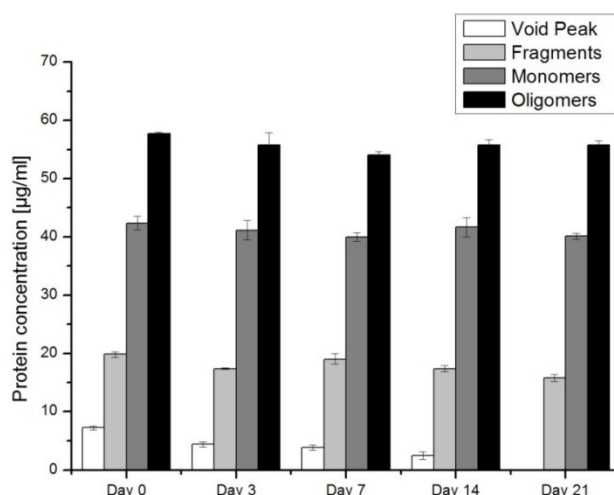


**Figure 5-5 – Fractions collected during AF4 analysis of the huAb after 48 h of light exposure.**

Stability investigated over a period of three weeks storage at 2 – 8 °C by determination of protein concentration via a Micro BCA assay.

Parts of the samples were also stored in the deep freezer at -80 °C, gently thawed over night at 2 – 8 °C and subsequently the concentration was analyzed by µ-BCA assay as well. The concentration of soluble species remained stable when thawed after three weeks and no precipitation was apparent (data not shown).

### 5.3.3 Increasing protein concentration within the fractions

As the aggregates collected after the separation via asymmetrical flow field-flow fractionation were supposed to be administered to mice and a significant dilution occurred during fractionation, samples had to be concentrated and adjusted to a certain protein concentration. Disposable ultracentrifugation centrifugal devices appeared to be the most applicable and time-effective means to achieve satisfactory protein concentrations. The membranes inserted into the centrifugal tubes consisted of hydrophilic substances such as high-performance regenerated cellulose, polyethersulfone or Hydrosart® which guarantee low protein binding and could retain molecules bigger than the molecular weight cut off claimed by the manufacturer. Besides the membrane material, precipitation, aggregation and adsorption to the filter material could have a strong impact on concentration efficiency and can entail sample

loss. Those interactions to some extent are based on the surface characteristics of the protein which again are highly dependent on its aggregation state.

Using the collection schedule shown in Table 5-3 the aggregate peak of each run comprises 7 mL. Hence, 21 mL of AF4 mobile phase including ~1260 µg aggregated protein were collected within three runs. The fractions of three runs first were pooled. Then, the volume was split into thirds of 7.0 mL and each was loaded onto a Vivaspin 6, Vivaspin 15 R or a Protein Concentrator tube and centrifuged for 30 min at 4000 x g and a temperature of 4 °C. Afterwards, protein content was determined and compared as shown in Table 5-4. The whole procedure was carried out twice.

**Table 5-4 – Concentration of oligomeric fractions separated by AF4.**

Comparison of the effectiveness of three different types of centrifugal protein concentration devices, concerning the resulting concentration after 30 minutes of spinning at 4000 x g and 4 °C. Protein content was determined via a Micro BCA assay.

Type of disposable concentrator	Concentration before ( $c_0$ ) and after centrifugation ( $c_{conc}$ )	1	2
<b>Vivaspin 6</b>	$c_0$	59.0 µg/mL	55.1 µg/mL
	$c_{conc}$	111.0 µg/mL	102.3 µg/mL
<b>Vivaspin 15 R</b>	$c_0$	59.0 µg/mL	55.1 µg/mL
	$c_{conc}$	140.5 µg/mL	138.8 µg/mL
<b>Protein Concentrator</b>	$c_0$	59.0 µg/mL	55.1 µg/mL
	$c_{conc}$	197.7 µg/mL	198.2 µg/mL

Protein Concentrators from Pierce Biotechnology were assumed to be best suited for enriching the concentration of the aggregates. The concentration process using those devices was subsequently further improved and the efficiency was evaluated. Promising protein contents of more than 1 mg/mL for the aggregate fraction could be achieved (data not shown).

The reproducibility and reliability of the process was ensured by the repetitive fractionation and concentration of three consecutive runs. Each repetition based on two injections of 100 µL of the stressed huAb sample to the AF4 system. Both collected fractions were pooled before the total volume and the initial protein content were determined. Then the pooled sample was divided in two halves and applied to two Protein Concentrators. Centrifugation was carried out as described above and a µ-BCA assay was performed and the remaining volume was recorded too (see Table 5-5).

**Table 5-5 - Results of reproducibility study.**

Protein concentrations at various intermediate steps during fractionation and concentration. The concentration was determined in AF4 mobile phase by  $\mu$ -BCA assay.

Preparation step	1	2	3
<b>Collection of aggregate peak</b>			
<b>Protein mass at injection</b>	2000 $\mu$ g	2000 $\mu$ g	2000 $\mu$ g
<b>Concentration of collected aggregate peak</b>	63.2 $\mu$ g/mL	63.0 $\mu$ g/mL	55.3 $\mu$ g/mL
<b>Volume of collected aggregate peak</b>	14.5 mL	14.5 mL	14.5 mL
<b>Protein mass in collected aggregate peak</b>	916.4 $\mu$ g	913.5 $\mu$ g	801.9 $\mu$ g
<b>Total amount of aggregates in the sample</b>	45.8 %	45.7 %	40.1 %
<b>Concentration step</b>			
<b>Volume prior to concentration</b>	14.0 mL	14.0 mL	14.0 mL
<b>Protein mass prior to concentration</b>	884.8 $\mu$ g	882.0 $\mu$ g	774.2 $\mu$ g
<b>Concentration after 30 min centrifugation</b>	328.6 $\mu$ g/mL	330.5 $\mu$ g/mL	391.6 $\mu$ g/mL
<b>Volume after 30 min centrifugation</b>	2.0 mL	2.0 mL	1.7 mL
<b>Protein mass after 30 min centrifugation</b>	657.2 $\mu$ g	661.0 $\mu$ g	665.72 $\mu$ g
<b>Total recovery of protein</b>	74.3 %	74.9 %	86.0 %

The collection of the aggregate peak provided an aggregate content varying between 800 and 916  $\mu$ g, implying that 40 to 46 % of the total protein in the stressed sample could be collected. During the concentration step, the protein content of the samples was increased by a factor of 5.2 for the first two runs. A higher factor was found for the third run, reaching a 7.0 fold increase in protein concentration. Furthermore, the total recoveries of protein achieved by the concentrating procedure were approximately 74 % for runs 1 and 2, and 86 % in the more effective third run. The filtrate was checked by  $\mu$ -BCA assay for accidental passing of protein through the membrane. No significant amount of protein appeared in the filtrate. Hence, the low recoveries indicate a loss of protein by adsorption to the membrane material.

The stability of the concentrated aggregate samples was investigated as described above in section 5.3.2. New samples were prepared and stored at 2 – 8 °C and –80 °C in clean and sterilized 6 R glass vials (Schott AG, Mainz, Germany) for 21 days. Before performing a



$\mu$ -BCA assay, potentially generated precipitates were separated by centrifugation. The protein concentration over storage time at 2 – 8 °C is shown in Figure 5-6.

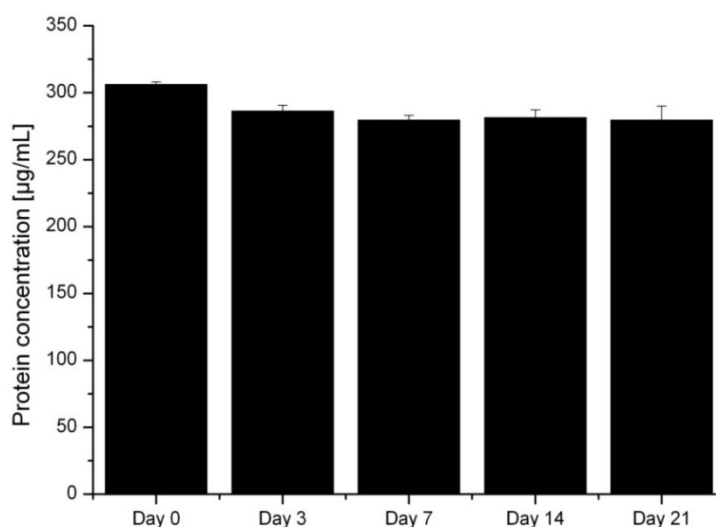


**Figure 5-6 – Protein content in concentrated aggregate peak.**

Stability of the concentrated aggregate fraction in AF4 mobile phase investigated over a period of three weeks storage at 2 - 8 °C by determination of protein concentration via a Micro BCA assay.

No important loss of protein concentration was determined over 21 days of storage at 2 – 8 °C. For -80°C storage the concentration of soluble species remained stable over three weeks of time and including one freeze-thaw cycle and no precipitation was apparent (data not shown). Besides the overall protein content in solution, the stability of the aggregates was checked by re-injection to the AF4 system and detection at 214 nm. 100  $\mu\text{L}$  of sample were injected to AF4 system either directly after concentration or after 21 days of storing. Both storage conditions of 2 – 8 °C and -80 °C were tested. The resulting fractograms are displayed in Figure 5-7. Directly after concentration the fractogram shows mainly the peak representing the aggregates, eluting around 30 minutes. After storage at -80 °C for three weeks and subsequent thawing at 2 – 8 °C overnight, slight fronting effects were found in peak shape, and a growth of peaks that can be assumed to consist of fragments and monomer due to their elution times. This instability of the aggregates is dramatically higher when storing several days at 2 – 8 °C. After 21 days storage in the refrigerator, nearly no aggregates are found anymore, though the amount of species eluting early significantly increased. The molar mass determination of this shifted elution profile revealed 155 kDa in the main peak and confirmed the assumption of the presence of monomeric antibody species. The distribution of the species cannot clearly be defined, because of the poor resolution between the peaks. The storage at 2 - 8 °C leads to dissociation of the aggregates in fragments and monomeric species.

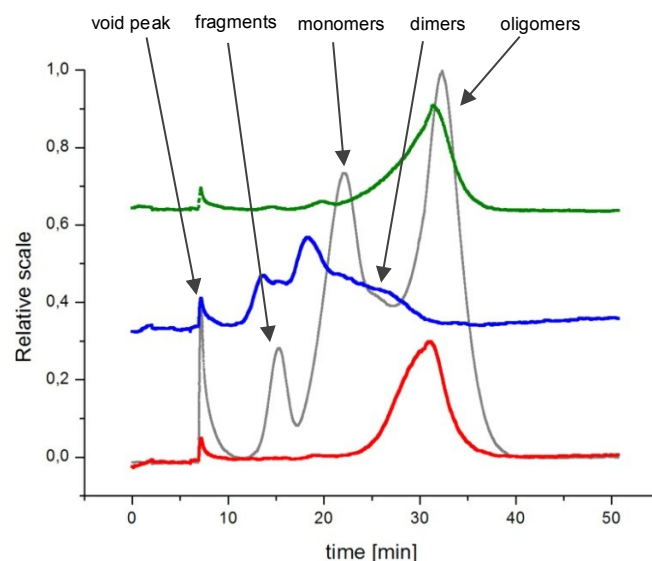


**Figure 5-7 – UV 214 nm AF4 fractograms after re-injection of aggregate fractions.**

The concentrated aggregate fraction was re-injected directly after concentration (red line), after 21 days storage at 2 – 8 °C (blue line) and after 21 days storage at -80 °C (green line). The UV 280 nm fractogram of the original sample of huAb after 48 h of light exposure is shown in grey.

Identical samples were also analyzed by size exclusion chromatography and revealed similar results (see Figure 5-8). Directly after finishing the concentration using the disposable devices, the sample consists of mostly aggregates. These aggregates can be subdivided in two species with SEC. During storage at 2 – 8 °C the aggregate content drastically decreases and the chromatogram shows monomer and fragments again. In comparison, storage at -80 °C leads only to a slight dissociation of the aggregates represented by a slight increase in height of the monomer peak.

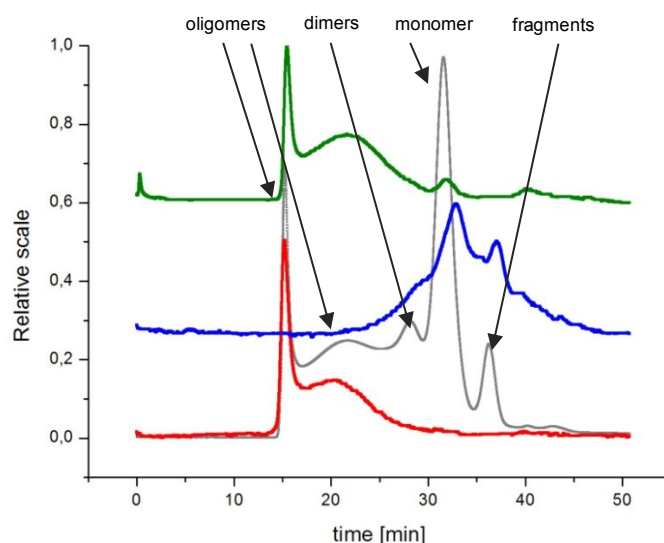


**Figure 5-8 – UV 214 nm SEC chromatograms after re-injection of aggregate fractions.**

The concentrated aggregate fraction was re-injected directly after concentration (red line), after 21 days storage at 2 – 8 °C (blue line) and after 21 days storage at -80 °C (green line). The UV 280 nm fractogram of the original sample of huAb after 48 h of light exposure is shown in grey.

These results were furthermore confirmed by non-reducing SDS-PAGE, showing weak bands representing fragments as well as monomeric species, besides diffuse stains representing aggregates (data not shown).

## 5.4 DISCUSSION

Light exposure can occur to biopharmaceuticals during multiple stages in formulation and subsequent inspection as long as the primary containers are not yet packaged and labeled. Furthermore, many recently developed therapeutic proteins are aimed for self-administration to improve the compliance of the patient. The advancement involves increasing possibility of undesigned exposure to room light or even sun light. Thus light exposure has to be considered as relevant extrinsic stress condition a protein therapeutic can encounter.

The high amount of soluble protein species generated by light exposure was in the focus of this study. Asymmetrical flow field-flow fractionation served as analytical method for the separation and fractionation of the distinct protein species and was first of all compared to the separation by the “gold-standard” size exclusion chromatography. Discrepancies in the distribution of the protein species within identical samples either analyzed by SEC or analyzed by AF4 were found.

In SEC a lower amount of protein was recovered in total. Besides, the pattern of huAb protein species displayed in the chromatograms and fractograms of this study differ a lot. In AF4 but not in SEC a void peak eluting before any other protein species was detected. The resolution between the monomer and small aggregates is much better in SEC, whereas the AF4 fractogram shows only a shoulder following the monomer peak impeding an accurate area definition. Therefore, also the MW determination is affected and influenced by the overlay with monomeric species. In SEC a MW of 415 kDa was determined for these small aggregates, representing dimers and trimers. However, an improvement of resolution in the AF4 method was not the ambition of this study. Another obvious difference is the elution of oligomers. In AF4 only one oligomeric species, eluting after all other protein species was detected. Instead, the size exclusion chromatograms revealed two species of higher molecular weight eluting several minutes prior to the small aggregates: a sharp peak eluting very early, representing high molecular weight (HMW) aggregates, and a broad peak that represents intermediate molecular weight (IMW) aggregates.

As described in literature, these differences are first and foremost related to the varying separation principles [Litzen *et al.*, 1993]. In general, during the focusing step in AF4, the protein sample is pushed towards the ultrafiltration membrane and concentrated in a narrow band within the channel. This might alter the conformation and structure of the species and an artificial aggregation can be triggered, potentially leading to higher recoveries of soluble aggregates [Liu *et al.*, 2006]. The incidence of interaction to a solid phase is much higher in

SEC, which first and foremost induces protein losses and might modify the aggregate distribution as well.

Another reason for the reduced protein recovery in SEC is the separation range of the Superose 6 column, which is narrower than the range of molar masses AF4 is capable to separate.  $5 \times 10^3$  to  $5 \times 10^6$  Da is the designated molar mass range the Superose column can cope with, whereas AF4 was shown to separate also large protein complexes in the higher Mega-Dalton range [Veesler, 2010]. Considering the extended separation range, it can be concluded, that the void peak detected by AF4 comprises large protein species or even insoluble aggregates which elude from separation by the cross flow due to their size. This inverse elution profile, the so called steric operation mode of AF4, has been reported in literature several times [Gottschalk *et al.*, 2006; Litzen *et al.*, 1993]. This void peak, which only appears in the fractogram, also contributes to the higher total protein recovery in AF4 compared to SEC.

The detected HMW species in SEC found to be larger than  $6 \times 10^6$  Da in size already exceeded the limit of detection of the column and thus eluted very early in a very sharp peak. However, they are clearly separated from IMW species that resulted in a broad peak, probably representing numerous different aggregates of similar size. The oligomer peak in AF4 fractogram also represents aggregates of different sizes, which obtain similar hydrodynamic radii and thus diffuse in close areas in the channel and elute simultaneously. Since the recovery of this peak was 54.7 % it can be assumed, that both, the peak representing HMW aggregates and the peak representing IMW aggregates in SEC with a total recovery of 40.6 % are incorporated in that single peak in AF4. The MW determination supports this hypothesis, since the value found in AF4 (2771 kDa) is in between the MW values of the peaks found in SEC (1867 kDa and 6620 kDa).

Both methods entail a significant dilution to the sample, which potentially leads to the dissociation of weak, non-covalently linked aggregates [Liu *et al.*, 2006]. In addition, the utilization of different mobile phases can also bias the mass distribution of the protein species. Furthermore, differences in shear force and adsorption the protein encounters in AF4 and SEC could have an impact on aggregates [Demeule *et al.*, 2009].

The AF4 studies described, for the first time used a semi-preparative channel, a prototype that was kindly provided by Wyatt Technology Europe. However, the final concentration of the collected aggregate peak was quite low. Challenges in construction accompanied with leakage are problems involved in the enlargement of the separation channel. Besides, protein loading is limited, due to poor resolution and thus overlapping of the various species, and the dilution of the sample is still very high. Hence, an aggregate fraction containing approximately 60 µg/mL of protein was achieved.

A variety of disposable centrifugal devices were tested for their ability to concentrate these aggregate samples. All three tested tools were feasible to concentrate the sample.

However, the efficiency differed and the Protein concentrators<sup>®</sup> turned out to be best suited. The molecular weight cut off of 9 kDa, compared to 5 kDa within the both Vivaspin tubes, might account for the more effective enhancement of the protein concentration. Slight differences in membrane materials were not investigated and can play a role as well. An up to seven-fold increase of the protein content was achieved, though further improvement of the method could provide even higher concentrations.

By re-injection of this fraction the composition and size of the concentrated fractions of aggregates was confirmed. The stability studies conducted with the aggregates after fractionation indicate the formation of weakly linked, reversible aggregates that tend to re-dissociate when separated from monomer and fragments. Non-reducing as well as reducing SDS-PAGE showed the formation of covalently linked aggregates. However, the harsh conditions of denaturing at 90 °C can tamper with the original aggregation and fragmentation pattern in the sample [Hunt *et al.*, 1999]. But, since non-covalent aggregates are not detectable with denaturing SDS-PAGE, it can be concluded that the light exposed sample consists of a versatile mixture of fragments and covalently linked aggregates. Interestingly, the aggregation process is not stopped when turning off the light, but proceeds in the sample. Removing the smaller species within the mixture destabilizes the aggregates and leads to dissociation of the aggregates. During storage of the entire huAb sample in formulation buffer at the same conditions directly after light exposure, no dissociation of the oligomers back to fragments and monomers was detected (data not shown). Thus, a stabilizing effect of the smaller species, such as monomer and fragments, on the cohesion of the aggregates can be concluded. The resulting species exist in a balance, though influences of the buffer composition cannot be excluded. Kiese *et al.* already showed that protein aggregates of a monoclonal IgG1 antibody tend to gain equilibrium during storage [Kiese *et al.*, 2010]. When storing the collected aggregate fraction of huAb at –80°C almost complete absence of other peaks, e.g. fragment or monomer, was found, confirming that the soluble aggregates remained stable. Disintegration occurred only to a negligible extent, which might emerge during thawing overnight at 2 – 8 °C and the time in the auto sampler at 4 °C prior to injection to SEC or AF4.

Looking at these results, it was shown that acceptable concentration of separated soluble aggregates of the applied human IgG1 antibody can be achieved by the AF4 technique. For the first time, the stability of antibody oligomers after separation from accompanying protein species and concentration was shown. Thus, the field-flow fractionation is a promising tool for preparation of samples for the prospective *in vivo* studies.

## 5.5 CONCLUSIONS

AF4 is a valuable method to analyze and characterize protein aggregates. Using the new semi-preparative channel and combining it with a fraction collector, FFF is now applicable as a semi-preparative system as well, maintaining its advantages compared with SEC. The major benefit of AF4 is the separation principle, which is independent of a packed stationary phase. That implicates minor shear stress and marginal interactions of the analytes with solid phases. The semi-preparative channel enables separation of protein in the upper  $\mu\text{g/mL}$  range and no complex upgrading of the instrumentation for standard AF4 is necessary for this approach. The described procedure of light exposure, fractionation by semi-preparative AF4 and concentration by disposable concentration devices is suitable to generate large amounts of a pure aggregate fraction. Storage at  $-80\text{ }^{\circ}\text{C}$  in combination with gentle thawing and short-term storage at  $2 - 8\text{ }^{\circ}\text{C}$  is recommended to maintain the aggregated structure of the monoclonal antibody. The good reproducibility and reliability of the method guarantee for consistent amounts of aggregates and are promising results for the planned transfer to a mouse antibody. The aggregates formed by light exposure definitely need to be further characterized to understand the mechanisms behind the disintegration behavior. The reversibility of even covalent linked aggregates should be investigated in more detail by, for example, experts in mass spectrometry and peptide mapping. Furthermore, it would also be of interest to investigate the secondary and tertiary structure of the separated fractions.

The studies described in this chapter are only dealing with the separation of the most abundant oligomer peak of one monoclonal antibody by light exposure. Further investigations are useful to transfer the method to other proteins and other aggregate species as well, generated under varying stress conditions. Since for an *in vivo* study a certain buffer composition is required, the fractionation by AF4 should be performed within the final buffer to avoid destabilizing dialysis prior to administration.

## 5.6 REFERENCES

[Arakawa *et al.*, 2007], Aggregation analysis of therapeutic proteins, part 3: principles and optimization of field-flow fractionation (FFF), *BioProcess International*, 5, 52-70

[Demeule *et al.*, 2009], New methods allowing the detection of protein aggregates: a case study on trastuzumab, *mAbs*, 1, 142-150

[Fraunhofer *et al.*, 2004], The use of asymmetrical flow field-flow fractionation in pharmaceuticals and biopharmaceuticals, *European Journal of Pharmaceutics and Biopharmaceutics*, 58, 369-383

[Giddings, 1993], Field-flow fractionation: analysis of macromolecular, colloidal, and particulate materials, *Science (Washington, DC, United States)*, 260, 1456-1465

[Giddings *et al.*, 1976], Flow field-flow fractionation: a versatile new separation method, *Science*, 193, 1244-1245

[Gottschalk *et al.*, 2006], Quantification of Insoluble Monoclonal Antibody Aggregates, *Application Note on www.wyatt.com*,

[Hunt *et al.*, 1999], Capillary electrophoresis sodium dodecyl sulfate nongel sieving analysis of a therapeutic recombinant monoclonal antibody: A biotechnology perspective, *Analytical Chemistry*, 71, 2390-2397

[Hupfeld *et al.*, 2006], Liposome size analysis by dynamic/static light scattering upon size exclusion-/field flow-fractionation, *Journal of Nanoscience and Nanotechnology*, 6, 3025-3031

[Kiese *et al.*, 2010], Equilibrium studies of protein aggregates and homogeneous nucleation in protein formulation, *J. Pharm. Sci.*, 99, 632-644

[Kowalkowski *et al.*, 2006], Field-flow fractionation: theory, techniques, applications and the challenges, *Critical Reviews in Analytical Chemistry*, 36, 129-135

[Lang *et al.*, 2009], Asymmetrical flow FFF as an analytical tool for the investigation of the physical stability of virus-like particles, *LCGC North America*, 27, 844-852

[Leeman *et al.*, 2006], Programmed cross flow asymmetrical flow field-flow fractionation for the size separation of pullulans and hydroxypropyl cellulose, *Journal of Chromatography, A*, 1134, 236-245

[Litzen *et al.*, 1991], Effects of temperature, carrier composition and sample load in asymmetrical flow field-flow fractionation, *Journal of Chromatography*, 548, 393-406

[Litzen *et al.*, 1993], Separation and quantitation of monoclonal antibody aggregates by asymmetrical flow field-flow fractionation and comparison to gel permeation chromatography, *Analytical Biochemistry*, 212, 469-480

[Liu *et al.*, 2006], A critical review of analytical ultracentrifugation and field flow fractionation methods for measuring protein aggregation, *AAPS Journal*, 8, E580-E589

[Reschiglian *et al.*, 2001], Quantitative analysis by UV-Vis detection in flow-assisted separation techniques for dispersed samples Part I: Theory part II: Experimental tests with applications to field-flow fractionation, *Reviews in Analytical Chemistry*, 20, 239-269

[Schimpf, 2000], Field Flow Fractionation Handbook, 1st Edition, *Wiley-Interscience*, 560 pp,

[Stulik *et al.*, 2003], Some potentialities and drawbacks of contemporary size-exclusion chromatography, *Journal of Biochemical and Biophysical Methods*, 56, 1-13

[Sweeney *et al.*, 2010], Field flow fractionation with multiangle light scattering for measuring particle size distributions of virus-like particles, *Formulation and Process Development Strategies for Manufacturing Biopharmaceuticals*, 253-268, 252 plates

[Thielking *et al.*, 1995], Online Coupling of Flow Field-Flow Fractionation and Multiangle Laser Light Scattering for the Characterization of Polystyrene Particles, *Analytical Chemistry*, 67, 3229-3233

[Veesler, 2010], Mega-Dalton protein complexes characterization, *LCGC North America*, 16

[Wen *et al.*, 1996], Size-exclusion chromatography with on-line light-scattering, absorbance, and refractive index detectors for studying proteins and their interactions, *Anal Biochem*, 240, 155-166

[Wyatt, 1991], Absolute measurements with FFF and light scattering: particles, *Polymeric Materials Science and Engineering*, 65, 198-199



## 6 THE PREPARATIVE USE OF AF4 TO OBTAIN ENDOTOXIN-FREE PROTEIN SPECIES

---

### 6.1 INTRODUCTION

The immunogenic potential of therapeutic proteins is a serious problem for their application. The formation of antibodies against the drug depends on numerous factors such as the route of administration, formulation properties, and patient characteristics [Schellekens, 2002]. Several studies showed that aggregates present in a biopharmaceutical formulation enhance the immunogenicity of the therapeutic protein [Hermeling *et al.*, 2006; Moore *et al.*, 1980; Palleroni *et al.*, 1997; Schernthaner, 1993]. Since proven methods for the prediction of immunogenicity are not available, *in vivo* studies have to be conducted for detailed investigations. Two general approaches, usually conducted in mice, can be pursued. Transgenic mice are immune tolerant to a certain human protein, closely resembling the therapeutic situation. However, the immune system of these animals is artificially altered, which might bias its response. Wild-type mice, instead, will recognize all human proteins as foreign molecules and induce a classical immune response. The use of wild-type mice is only reasonable when a protein generated in mice is investigated. Due to the versatile potential immunogenic stimuli mentioned above, a proper implementation is crucial for all immunogenicity studies *in vivo*, to eliminate all potentially biasing factors, such as endotoxins.

Endotoxins are toxic molecules that typically can be found in the membrane of gram-negative bacteria and are capable of being recognized by the immune system [Magalhães *et al.*, 2007]. The most common endotoxins are lipopolysaccharides (LPS) consisting of a lipid and a polysaccharide chain [Williams, 2007]. Since the existence of even small amounts of endotoxins within a parenteral drug product can induce inflammation in patients or even septic shock, they must be removed from formulations and containers [Hurley, 1995]. Sterilization does not sufficiently destroy endotoxins, because they are released during bacterial cell lysis. Depyrogenation processes have to be performed to remove endotoxins from containers and formulations. Glass containers can easily be exposed to temperatures above 250 °C for at least 30 minutes to inactivate LPS [USP/NF, 2008]. Sodium hydroxide can as well be used to inactivate endotoxins, for example for container materials susceptible to heat like plastics. Ion exchange chromatography is one method utilized to remove endotoxins from protein samples [Dembinski *et al.*, 1986].

Because of the severe effects of endotoxins inadvertently administered to patients the European Pharmacopoeia strictly limits the endotoxin levels for parenteral formulations to 0.25 EU/mL, for “Water for injections”, which usually represents the main “excipient” in all parenteral products [PhEur 0169, 2011]. The maximum endotoxin level for a product depends

on the delivered volume and body weight of the patient and is specified in the individual monographs. A benchmark of 5 EU/kg body weight is mentioned in USP <85> to be the limit for intravenous application [USP/NF, 2008]. According to the pharmacopoeias all parenterals have to be tested with regards to bacterial endotoxins. The Limulus Amebocyte Lysate (LAL) test is the most prominent method to quantify endotoxins. It is based on the blood of horseshoe crabs, *Limulus polyphemus*, clotting when exposed to endotoxins. Detection can either be performed by measuring turbidity, coloration or by gel formation [Bang, 1956]. The currently available and approved test kits have a limit of detection of 0.005 EU/mL and quickly provide the results within 30 minutes.

In preparation of an *in vivo* study to investigate the immunogenicity of protein aggregates, the benchmark of 0.25 EU/ml was predefined and should not be exceeded. Therefore, the formulations have to be checked for their endotoxin levels. Hence, utilizing asymmetrical flow field-flow fractionation (AF4) as preparative tool to separate protein aggregates (see Chapter 5) requires the separation of fractions with low endotoxin levels. The aim of this study was to use the AF4 instrument for fractionation of aggregates of a mouse monoclonal antibody in preparation of an *in vivo* study and thus to establish a protocol to clean the entire instrument from microbial and endotoxin contaminants. The fractionation and concentration procedures established before using a human monoclonal IgG1 antibody had to be transferred to a mouse monoclonal IgG2c antibody and final endotoxin concentrations below 0.25 EU/mL had to be guaranteed.

## 6.2 MATERIALS AND METHODS

### 6.2.1 Sample preparation

A mouse monoclonal IgG2c antibody (muAb) was kindly provided by Abbott GmbH & Co. KG. The antibody solution applied in the experiments was diluted to a concentration of 10 mg/mL in a 20 mM histidine formulation buffer at pH 6.0. The IgG2c stock solution had an initial concentration of 33 mg/mL and was stored at -80 °C in the deep freezer. Prior to use, the formulation buffer was filtrated using a 0.2 µm sterile syringe filter out of cellulose acetate (VWR International, Darmstadt, Germany). The antibody solution was filled into cleaned and sterilized 2 R vials made from glass type 1 (Schott AG, Mainz, Germany), sealed with Teflon®-faced rubber stoppers (West Pharmaceuticals Services, Eschweiler, Germany) and crimped. All antibody samples were prepared under aseptic conditions. Highly purified water generated in-house was used for the preparation of samples and buffers (PURELAB Plus instrument (USF Elga, Celle, Germany)). All substances used were of analytical grade.

The generation of aggregates was triggered by light exposure, using a Suntest CPS instrument (Heraeus, Hanau, Germany). The light source was a xenon lamp with a wavelength spectrum from 200 to 1000 nm. The irradiance was fixed at  $55 \pm 5$  W/m<sup>2</sup>. A filter made of sheet

glass was installed, to obtain a radiation close to the real light exposure. The samples were exposed to light for 48 h.

### **6.2.2 Asymmetrical flow field-flow fractionation**

AF4 was employed to separate the soluble oligomers generated by 48 h of light exposure from other protein species. The separation was conducted with an Eclipse 2.0 system (Wyatt Technology Europe GmbH, Dernbach, Germany) combined with an auto sampler and an in-line degasser of the Agilent 1100 series (Agilent Technologies, Palo Alto, USA). The system was additionally connected to detectors for refractive index, for ultraviolet spectroscopy (both from Agilent Technologies, Palo Alto, USA) and to a DAWN EOS (Wyatt Technology Europe GmbH, Dernbach, Germany) multi angle laser light scattering detector. For molar mass determination of all proteins, the refractive index increment  $dn/dc$  was set at 0.185 mL/g. A semi-preparative channel (SP1, Wyatt Technology Europe GmbH, Dernbach, Germany) of 245 mm length and 350  $\mu$ m height and equipped with a membrane made of regenerated cellulose with a 10 kDa molecular weight cut off (MWCO) was used for separation. The samples were collected in glass tubes by a Gilson FC 203B Fraction Collector (Gilson Inc., Middleton, USA). The delay of time between UV detector and fraction collector was previously determined using dextran blue and transparent tubing between detector and collector. The time between the rising UV absorbance and the visually detected arriving at the fraction collector amounted to 1 minute and 40 seconds. As carrier liquid the formulation buffer consisting of 20 mM histidine buffer at pH 6.0 was employed. The buffer was filtrated through a 0.1  $\mu$ m cellulose nitrate filter with a diameter of 50 mm (Whatman GmbH, Dassel, Germany). The detector flow was set to 1 mL/min, whereas the cross flow was appointed at 3 mL/min for 5 minutes followed by a linear reduction to 0 mL/min over a period of 20 min. Finally, 30 minutes of elution without any cross flow (VX) were added. 100  $\mu$ L of stressed antibody sample were injected per run, equaling a total amount of 1 mg of protein injected to the channel. The injection volume of the native muAb was limited to 50  $\mu$ L, equaling 0.5 mg of protein. The distribution of the species was calculated from the AUC using Astra 5.3 software (Wyatt Technology Europe GmbH, Dernbach, Germany).

### **6.2.3 Protein concentration by centrifugation**

The oligomer fractions of several injections were collected in glass tubes and concentrated by centrifugation using Protein Concentrators (7 mL, 9 kDa MWCO, membrane made of regenerated cellulose, Pierce Biotechnology, Rockford, USA). Hence, 100  $\mu$ L of stressed antibody sample were injected to AF4 several times in a row, the aggregate peaks collected, pooled and loaded onto Protein Concentrator tubes, respectively. Pre-rinsing was carried out according to the manufacturer's instructions by adding 4 mL of 20 mM histidine buffer pH 6.0 to the tubes, followed by a centrifugation step for 10 min at 4000 x g in order to allow equilibrium and to remove traces of glycerin or sodium azide from the production process that could possibly influence the results. Once the pooled protein solution had been placed in

the upper chamber of the concentrators, the tubes were put into swinging buckets and centrifuged at 4000 x g and a temperature of 4 °C for 90 min using a Megafuge 1.0R and the corresponding 7570F rotor (Heraeus Instruments, Santa Clara, USA). The concentration of the resulting fractions was determined via UV absorbance at an excitation wavelength of 280 nm. UV absorbance spectroscopy measurements were performed at 25°C with a Fluostar Omega spectrophotometer (BMG Labtech, Offenburg, Germany) and the Omega Software Version 1.01 together with MARS data analysis, Version 1.01. Aliquots of 200 µL of the samples were measured in a quartz 96-well plate and concentrations between 0.0625 mg/mL and 1 mg/mL were used for calibration.

#### **6.2.4 Determination of endotoxin level**

To assure that the amount of endotoxins in the samples is lower than 0.25 EU/mL as required by the European Pharmacopoeia in monograph “water for injections”, a Limulus Amebocyte Lysate (LAL) test (Endosafe™-PTS Portable Test System by Charles River Laboratories International Inc., Wilmington, USA) was used. The principle of this FDA-licensed test bases on an enzyme cascade in which serine proteases are activated by endotoxins. The activated enzymes cleave a peptide from the substrate coagulogen that subsequently produces gelatin and turbidity. The latter is optically quantified at 395 nm. 4 times 25 µL of the samples of interest were added to the disposable cartridge and quantitation results were obtained in 15 minutes. The sensitivity of the cartridges used was  $\geq 0.005$  EU/mL.

### **6.3 RESULTS**

#### **6.3.1 Preparation of instrument, samples and buffer solutions**

To assure low endotoxin levels in the final protein fractions a meticulous cleaning and disinfection program had to be established for the AF4 instrument and all equipment needed for sample preparation. For glass containers, such as vials, collection tubes and buffer reservoirs, the depyrogenation at 250 °C for  $\geq 30$  minutes was chosen. All other container materials like stoppers and Teflon®-coated stir bars were first of all rinsed with highly purified water and subsequently sterilized by hot steam in an autoclave. All samples and the buffer solution were prepared under the laminar air flow hood to minimize all new contamination. In addition the buffers were sterile filtered using 0.2 µm sterile filters made of cellulose acetate (VWR International, Darmstadt, Germany). For the preparation of the protein samples sterile and endotoxin-free reaction vessels and pipette tips were utilized (all from Eppendorf Biopur® quality, Eppendorf AG, Hamburg, Germany).

The entire AF4 instrument (including all valves, online filter, injection loop and waste tubing, and the fraction collector) was first washed with highly purified water (HPW), which was shown to be free of endotoxins (data not shown), for at least one hour at 1 mL/min, to remove

potential salt residues from previous used buffers. Subsequently the whole procedure was repeated with 70 % (v/v) ethanol for disinfection, before again rinsing with highly purified water.

The SP1 separation channel was treated separately. Steam sterilization of the ultrafiltration membrane made of regenerated cellulose lead to shrinkage and thus was not an option. Instead the membrane was treated in the same manner as the channel components. All single components were stored in 70 % (v/v) ethanol for one hour, except the upper wall. The upper wall consists of Plexiglas® and thus is not compatible to organic solvents. Hence, it was thoroughly cleaned with Light-Duty tissue wipers (VWR International, Darmstadt, Germany) impregnated with 70 % ethanol. All channel components were rinsed with HPW before reassembling under the aseptic conditions of the laminar air flow hood.

After installation of the clean channel to the meticulously rinsed system HPW was connected as fluent and the eluate collected in a glass tube was tested for endotoxins. An endotoxin level below the limit of detection (LOD) 0.005 EU/mL was detected, proving the rinsing protocol was successful. Using 20 mM histidine buffer as fluent, the eluate had to be diluted 1:20 for the determination of endotoxins, due to interference of histidine with the test principle. On that account the LOD of the test cartridges increased to 0.1 EU/mL and the histidine buffer eluting resulted in an endotoxin level below this LOD. After these preliminary tests the separation of the mouse antibody started.

### **6.3.2 Field-flow fractionation of mouse IgG2c**

The samples of the mouse IgG2c antibody after 48 h of light exposure showed four different peaks in UV 280 nm detection after field-flow fractionation (see Figure 6-1). The area under the curve (AUC) of the UV 280 nm fractogram was used to calculate the percentage of the different species separated by AF4. The native muAb (see Figure 6-1, black line) results in one single peak eluting between 16 and 25 minutes, with a peak maximum at ~21.5 minutes. The determination of the molecular weight was performed by MALLS and UV absorbance detection. The overall monomer peak yielded in 150 kDa, perfectly matching to the expected molecular weight for an antibody. The monomer peak is accompanied by a small void peak. A limited amount of 500 µg protein was injected into the channel, since overloading would result in a poor peak shape and fronting or tailing effects. The total recovery was 93 %. To maximize the amount of protein aggregates fractionated and collected after elution, 100 µL of the sample after light exposure was injected into the system. The concentration of the sample was 10 mg/mL, thus a maximum recovery of 1 mg protein was procurable. The total recovery detected by UV spectroscopy at 280 nm was  $96 \pm 2.8$  % of protein, subdivided into four different peaks shown in Figure 6-1. Using the 18-angle MALLS detector the molecular weights (MW) of these species were determined. A huge and sharp void peak elutes first (elution maximum at 7.0 minutes) and the 5669 kDa of molar mass were detected for this peak. The three following eluting peaks represent fragments of the IgG2c (elution maximum at 15.5 minutes), the monomeric protein (elution maximum at 21 minutes), and oligomeric structures (elution

maximum at 32 minutes). No molecular weight was determined for the fragments portion. The monomer peak resulted in 182 kDa and the oligomer peak resulted in 3224 kDa. The distribution of the species was calculated by analysis of the area under the curve (AUC). The light exposed sample consisted of 19.3 % void peak, 4.8 % fragments, 10.1 % monomers and 65.9 % oligomers. The resolution between the monomer peak and the oligomer peak is poor. Hence there might be some overlay and lack of definition between those species.

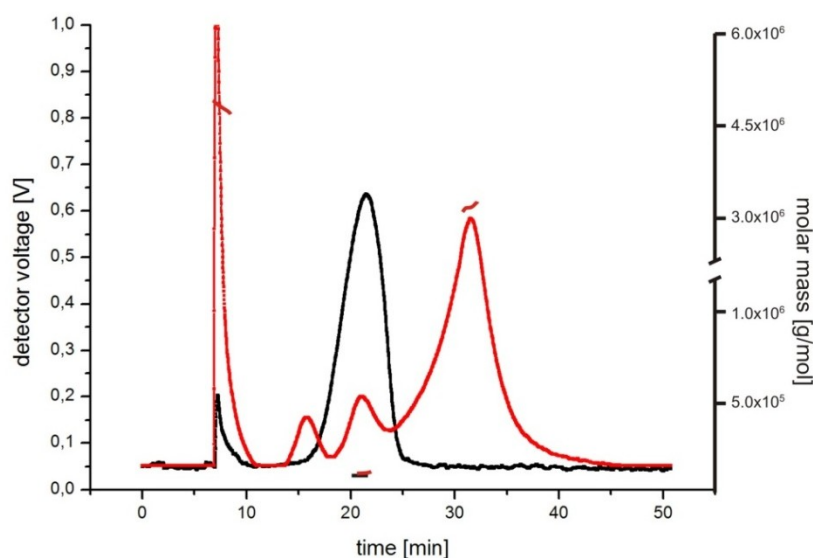


**Figure 6-1 – AF4 separation of the mouse IgG2c before and after light exposure.**

Time dependent UV detector voltage at 280 nm and molar mass detection by MALLS of light exposed muAb (red line) and native muAb (black line) after separation by Eclipse 2.0.

### 6.3.3 Collection and concentration of protein species after AF4 separation

The protein fractions separated by AF4 were collected in glass tubes using the Gilson fraction collector. In preparation of an *in vivo* study, facing the immunogenicity of protein aggregates, only the void peak and the oligomeric peak were further investigated. Due to earlier investigations and the molar mass detection, those fractions are known to represent aggregates. For the void peak, collection time was set to 6.5 to 8.0 minutes and that of the large oligomer peak was set to 28.0 to 34.0 minutes. The concentrations of the collected fractions were subsequently determined by UV absorbance at 280 nm, since the histidine buffer interfered with the Micro BCA assay.

Within three consecutive runs  $105.6 \pm 3.6$  µg/mL of protein were detected in the oligomer fractions before pooling them. The duration of the centrifugation using Protein concentrators to enhance the concentration in the pooled fraction was prolonged to 90 minutes. A final concentration of 593.4 µg/mL protein within the oligomer fraction was achieved. Within the void peak fraction very low protein concentrations of approximately 10 µg/mL were determined. An accurate determination in that range was not possible by UV 280 nm detection. Using Protein concentrators and the extended centrifugation procedure the final concentration

could not be significantly increased, though the volume of the sample was slightly narrowed (data not shown). However, the investigations were continued only for the oligomer peak eluting at the end.

The stability of the oligomer fraction was confirmed by storage at -80 °C for seven days, thawing at 2 – 8 °C overnight and re-injection to the AF4 system. 100 µL of the peak representing the oligomers was re-injected to the instrument after concentration and storage. Detection was performed by UV absorbance at 214 nm. The distribution in Figure 6-2 shows a prominent peak eluting between 25 and 34 minutes, perfectly matching with the original elution schedule of the oligomer peak. Besides, a void peak and a very small peak eluting around 20 minutes were detected. The latter probably represents marginal amounts of monomer within the fraction.

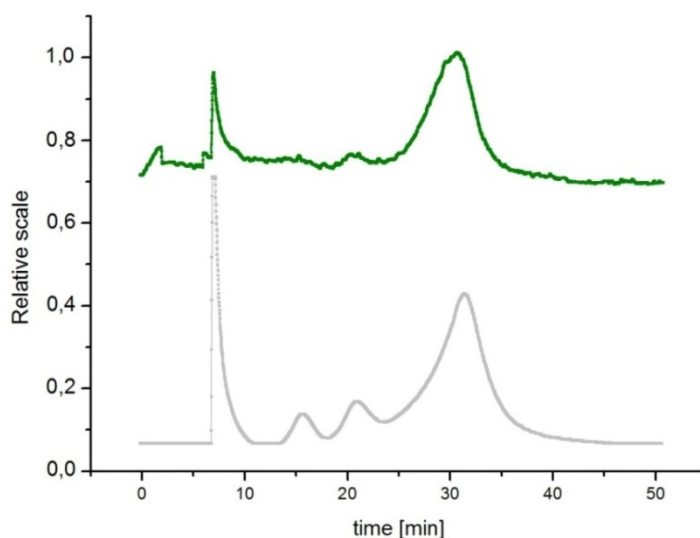


**Figure 6-2 – UV 214 nm AF4 fractograms after re-injection of aggregate fractions.**

The concentrated aggregate fraction was re-injected directly after concentration and storage at -80 °C (green line). The UV 280 nm fractogram of the original sample of muAb after 48 h of light exposure is shown in grey.

Directly after collection both fractions were tested for the endotoxin burden in a 1:20 dilution. Both resulted in < 0.1 EU/mL endotoxin levels after fractionation. Furthermore, the endotoxin measurements were repeated after the centrifugation step and again, both concentrated fractions showed similar values. The filtrates were tested as well, to detect potential contaminations by the cellulose membrane, but they resulted in values below 0.1 EU/mL as well.

## 6.4 DISCUSSION

The separation of a mouse monoclonal IgG2c antibody after 48 h of light exposure was performed by utilizing a semi-preparative channel in asymmetrical flow field-flow fractionation. The resulting distribution of protein species in the fractogram showed four main portions, which is excellently comparable to the results obtained from the human model antibody (see previous chapter of this thesis) separated with the same method. The light exposure triggered fragmentation of the immunoglobulin as well as the formation of aggregates. The extent of aggregate formation within 48 hours of light exposure differs between both antibodies. The tremendous peak height of the void peak eluting directly after the focusing step narrowing all analytes in a band near the sample inlet, is noticeable in the muAb sample. As the size determination by MALLS implies, oligomers larger than 5000 kDa elute within that peak, deducing that a steric separation mode existed [Fraunhofer *et al.*, 2004; Qureshi *et al.*, 2011]. The total recovery determined by AUC certainly includes the void peak and compared to the unstressed muAb sample  $96 \pm 2.8$  % of the overall protein content were retrieved. In reverse, a marginal amount of protein formed insoluble species, eluding from AF4 separation. Another peak, representing aggregates as well, terminates the separation profile. The average molecular weight of those analytes was determined to be around 3000 kDa. The threshold of size defining whether an oligomer is eluted in the void peak or regularly after the fragments and monomers, presumably lies in between 3000 kDa and 5000 kDa. However, crossovers cannot be excluded. Large species that range in areas of high velocity within the laminar channel flow, might also entrain other species to pass the channel.

The determination of the molecular weight by MALLS is proportional to the molar mass times the concentration of the species [Larkin *et al.*, 2010]. This implicates that for low molar mass species the concentration needs to be very high to achieve a proper determination of the molecular weight. The concentration and light scattering signals of the fragment peak were thus too low to calculate the molecular weight of this species. The MW of 182 kDa determined for the peak representing the monomer of the mouse IgG2c is approximately 20 % higher than the expected ~150 kDa for a monoclonal antibody. The overestimation indicates an overlay of hidden species like dimers and trimers, though at first sight the peak seems to derive from one species. When looking back to chapter 5, a shoulder representing dimers and trimers was detected in the human model antibody after light exposure. The formation of small aggregates can thus be anticipated as well, since the fractograms in general look very similar. The separation of high concentrations in the SP1 channel is not capable of resolving the monomer from these small aggregates. However, the overall ambition was the preparative use of AF4 and thus large amounts of protein are required, though at the cost of resolution.

Including the void peak, two species of oligomeric aggregates of the mouse antibody were generated by light exposure. Both are worth to be investigated *in vivo* concerning their immunogenicity. Unfortunately, it was not possible to obtain satisfactory amounts of the



aggregates eluting with the void peak in the collected fractions. The concentration step well working for the concomitant aggregate species eluting later, did not significantly increase the protein concentration of the species in the void peak. The efficiency of volume reduction was quite low. The huge aggregates might have interacted with the ultrafiltration membrane in the concentrators and thus clogged the pores. Thus the *in vivo* study focused on the preparation of the slightly smaller oligomers. Nicely comparable to the previous stability study performed with the human model antibody, the concentrated fraction of oligomers maintained its composition during storage at -80 °C in most parts. Hence, a proper handling of the formulation prior to administration to animals is assured and the final distribution within the sample is well-known.

The overall study was performed in the formulation buffer of the antibody, consisting of 20 mM histidine buffer at pH 6.0. This consistency implies a simplification of the handling of the aggregate fraction prior to animal administration, since the buffer can be maintained and no dialysis has to be installed later on which potentially alters the aggregate behavior. Only minor adaptations concerning tonicity and pH might be required, but should not have an influence as big as a complete buffer exchange.

The determination of endotoxins within a formulation for parenteral use is of great concern, since endotoxins are known to induce severe immune responses or even septic shock in patients [Morrison *et al.*, 1979]. The United States Pharmacopoeia and the European Pharmacopoeia require endotoxin levels below 0.25 EU/mL in their monographs “water for injections”. The planned animal studies will include mice usually having a body weight of approximately 20 g. Regarding the 5 EU/kg endotoxin level described in USP <85>, this ends up in a tolerable dose of 0.1 EU/mouse per injection. Since the designated injection volume will be 200 µl, an endotoxin level of  $\leq 0.25$  EU/ml will finally entail  $\leq 0.05$  EU/injection to the mice. This benchmark was thus defined to be valid for the preparation of protein formulations for *in vivo* studies. The Endosafe™-PTS Portable Test System by Charles River Laboratories used in this study has a high sensitivity of up to 0.005 EU/mL and quickly provides the results. A downside of the method is its susceptibility to interference by buffer components. A high dilution might be necessary increasing the limit of detection. For example, the 20 mM histidine buffer used throughout this study entailed a 1:20 dilution with highly purified water for the endotoxin determination. However, the resulting limit of detection of 0.1 EU/mL is still sufficiently below the predefined benchmark of 0.25 EU/mL.

The use of a field-flow fractionation instrument to prepare samples for preclinical studies is critical in terms of the endotoxin burden within the separated fractions. For our purpose the instrument cannot be placed under sterile conditions and even more the device is used for diverging analytical purposes. Hence a reliable method was established to purge the instrument and simultaneously clean and disinfect it. The extensive rinsing with highly purified water, 70 % (v/v) ethanol and again HPW in combination with the aseptic preparation of samples, sterilization of buffers, and heat depyrogenation of containers successfully provided fractionation conditions with very low endotoxin levels. The later on required concentration step,

using disposable concentrators, did also not contaminate the samples with endotoxins. Therefore, the overall procedure of meticulous cleaning, fractionation and concentration turned out to be applicable for the generation of protein fractions for preclinical studies.

## 6.5 CONCLUSIONS

Asymmetrical flow field-flow fractionation is a very useful preparative tool to generate samples for preclinical *in vivo* studies. The fractionation of valuable amounts of a certain protein species was shown and the concentration protocol established in a previous study worked very well for the aggregates of interest of a mouse antibody. The use of the formulation buffer instead of PBS for separation was successfully implemented, simplifying the subsequent handling of the fraction for the *in vivo* studies. For the intended animal studies the final fraction in formulation buffer can easily be stored at -80 °C, gently thawed prior to use and finally administered to the animals. Establishing a meticulous cleaning procedure accompanied by a thorough preparation of samples, buffers, and containers under aseptic conditions provides a proper possibility to keep the endotoxin levels far below the requested 0.250 EU/mL for parenteral administration. The entire cleaning procedure is very simple and thus should easily be transferable to similar instruments and different analytes. For regular preparations of samples for *in vivo* studies the entire AF4 system and all steps have to be located and run in a sterile facility.

## 6.6 REFERENCES

- [Bang, 1956], A bacterial disease of *Limulus polyphemus*, *Bulletin of the Johns Hopkins Hospital*, 98, 325-351
- [Dembinski *et al.*, 1986], Improved large scale purification procedure of natural human fibroblast interferon, *Preparative Biochemistry*, 16, 175-186
- [Fraunhofer *et al.*, 2004], The use of asymmetrical flow field-flow fractionation in pharmaceuticals and biopharmaceuticals, *European Journal of Pharmaceutics and Biopharmaceutics*, 58, 369-383
- [Hermeling *et al.*, 2006], Antibody response to aggregated human interferon alpha2b in wild-type and transgenic immune tolerant mice depends on type and level of aggregation, *J. Pharm. Sci.*, 95, 1084-1096
- [Hurley, 1995], Endotoxemia: methods of detection and clinical correlates, *Clinical microbiology reviews*, 8, 268-292
- [Larkin *et al.*, 2010], Light-scattering techniques and their application to formulation and aggregation concerns, *Formulation and Process Development Strategies for Manufacturing Biopharmaceuticals*, 269-305, 263 plates

[Magalhães *et al.*, 2007], Methods of Endotoxin Removal from Biological Preparations: a Review, *Journal of pharmacy & pharmaceutical sciences*, 10, 388-404

[Moore *et al.*, 1980], Role of aggregated human growth hormone (hGH) in development of antibodies to hGH, *The Journal of clinical endocrinology and metabolism*, 51, 691-697

[Morrison *et al.*, 1979], Bacterial endotoxins and host immune responses, *Advances in Immunology*, 28, 293-450

[Palleroni *et al.*, 1997], Interferon immunogenicity: preclinical evaluation of interferon- $\alpha$ 2a, *Journal of Interferon and Cytokine Research*, 17, S23-S27

[PhEur 0169, 2011], Monograph "Water for injections", *European Directorate for the Quality of Medicine (EDQM)*, 7th edition,

[Qureshi *et al.*, 2011], Application of flow field-flow fractionation for the characterization of macromolecules of biological interest: a review, *Analytical and Bioanalytical Chemistry*, 399, 1401-1411

[Schellekens, 2002], Bioequivalence and the immunogenicity of biopharmaceuticals, *Nature Reviews Drug Discovery*, 1, 457-462

[Scherthaner, 1993], Immunogenicity and allergenic potential of animal and human insulins, *Diabetes care*, 16 Suppl 3, 155-165

[USP/NF, 2008], general chapter <85> Bacterial Endotoxins Test, *Ed. Rockville, MD: United States Pharmacopoeial Convention*,

[Williams, 2007], Endotoxins: Pyrogens, LAL Testing and Depyrogenation (Drugs and the Pharmaceutical Sciences), *Informa Healthcare*, 3



## 7 THE NEED FOR IMMUNE COMPLEX DISSOCIATION IN ANTI-DRUG ANTIBODY DETECTION

---

### 7.1 INTRODUCTION

When exploring the immunogenic potential of aggregates of a given biopharmaceutical three main challenges must be considered. First, representative test aggregates must be reproducibly generated in the laboratory. Second, the composition of test aggregates must be characterized. Finally, the test aggregates must be tested in a suitable *in vivo* model.

The current study investigates for the first time the immunogenicity of aggregates of a murine monoclonal antibody in wild-type mice. A murine monoclonal antibody (hereafter referred to as muAb) of isotype IgG2c was generated in C57BL/6 mouse cells. Formulations of muAb were stressed by exposure to controlled amounts of light or by agitation to produce suspensions of aggregated antibody, and these suspensions subsequently were injected subcutaneously in C57BL/6 mice. Serum samples were collected from the mice and analyzed for antibodies that were cross-reactive with the native muAb molecule.

At the onset of the study, it was unknown whether administration of aggregates of the antibody could provoke an immune response that would be cross-reactive with muAb, but it was anticipated that aggregated antibodies might present a variety of epitopes, and that immune responses would likely be polyclonal. As such, one of the challenges in using standard ELISA-based methods to analyze immune response was the lack of reference standards for positive responses. Furthermore, because of their relatively large size (approximately 150 kDa) it was anticipated that binding of ADAs to muAb coated on ELISA plates might result in steric overlay and hindrance. Depending on the orientation of the ADAs after binding to the capturing antigen, other binding sites might then become inaccessible. Finally, monoclonal antibodies have a very long half-life (up to several months) as compared to other therapeutic proteins [Carpenter *et al.*, 2009]. This makes it very challenging to detect anti-drug antibodies in serum samples, because immune complexes between the circulating drug and anti-drug antibodies potentially may form.

Two different ELISA methods were used to test identical serum samples and the results were compared. Both set-ups were of sandwich ELISA format, meaning that the antigen of interest (anti-drug antibody) is fixed by two antibodies that specifically bind to the antigen. The detection mode was varied. One method relied on a bridging over the two Fab fragments of the anti-drug antibodies, whereas the other method was based on a bridging over the Fc fragment and one Fab fragment of the ADAs [Janeway *et al.*, 2004]. Using the two ELISA set-ups

surprisingly lead to completely different results in the detection of ADAs. The limitations and results of each method will be discussed and possible advantages and drawbacks of each method will be pointed out.

Subvisible particles are currently under suspicion to be related to enhanced immune responses to biopharmaceuticals, though (up to now) for approval only the size classes  $\geq 10\ \mu\text{m}$  and  $\geq 25\ \mu\text{m}$  are of concern [PhEur 2.9.19., 2008; Singh et al., 2010; USP/NF, 2008]. These specifications entail a huge gap of aggregates below these benchmarks which might impact product quality [Carpenter et al., 2009]. However, all conditions that enhanced the loading of subvisible particles in the samples were especially found to contain numerous particles smaller than  $10\ \mu\text{m}$ , accompanied with structural changes. These initial alterations might be missed within the current release specifications.

## **7.2 MATERIALS AND METHODS**

### **7.2.1 Generation of protein aggregate test items**

MuAb, a murine IgG2c antibody directed against murine TNF- $\alpha$ , was kindly provided by Abbott Bioresearch Center (Worcester, USA) in a formulation comprising 20 mM histidine, pH 6.0, and a protein concentration of 33 mg/mL. The initial preparation was diluted under aseptic conditions to a protein concentration of 4 mg/mL in 20 mM histidine buffer. The pH was adjusted to 5.7 using hydrochloric acid. Three milliliters of the solution were filled in 6 R vials, glass type 1 (Schott AG, Mainz, Germany) closed with Teflon<sup>®</sup>-coated rubber stoppers (West Pharmaceutical Services, Inc., Lionville, PA, USA). Aliquots were stressed either by stirring at 400 rpm, 25°C for 48 h using Teflon<sup>®</sup>-coated magnetic stir bars, 6 x 3 mm in size (VWR International, Darmstadt, Germany), or by light exposure using a xenon lamp in a Suntest CPS (Heraeus Holding, Hanau, Germany) radiation chamber at a radiation intensity of  $55 \pm 5\ \text{W/m}^2$  for 48 h. Samples were placed horizontally in the irradiation chamber. The xenon lamp emitted light of the whole sunlight spectrum including ultraviolet (UV) radiation. The emitted light was filtered by sheet glass to obtain a radiation spectrum close to that to which an antibody formulation might be exposed to during storage and handling. The light-exposed samples were analyzed by size exclusion chromatography and showed a soluble protein concentration of about 85% of the muAb initially present. Accordingly, 15 % of the total protein content formed insoluble species. Subsequently, the insoluble species in the samples were removed from the suspension by centrifugation ( $10,000 \times g$ , 10 min). The soluble fraction present in the supernatant was diluted further to obtain a concentration of 250  $\mu\text{g/mL}$  soluble protein species (including  $\sim 56\%$  soluble aggregates). To adjust tonicity, 8% (w/v) sucrose was added. If necessary, the pH was adjusted to 5.7 with hydrochloric acid or sodium hydroxide.

Stirring resulted in the formation of visible particles that were subsequently collected by centrifugation ( $10,000 \times g$ , 10 min). The resulting pellet was collected and resuspended in

buffer. Particles in the resulting suspension were counted by light obscuration using a Pamas SVSS instrument (PAMAS GmbH, Rutesheim, Germany). Each sample was measured in triplicate.

Finally, two different formulations containing either 25 µg/mL or 250 µg/mL protein were prepared from the light-exposed samples. These formulations were spiked with ~4000 particles (of a size  $\geq 1$  µm) per ml that previously had been generated by stirring and counted by light obscuration. With this approach two dosages of a combination of soluble and insoluble aggregates of different kinds and sizes together were used for injection. All reagents used were of analytical grade.

### **7.2.2 Size exclusion chromatography**

Concentrations of soluble aggregates and monomeric protein were measured by size exclusion chromatography (SEC) on an Agilent 1100 system with RI, MALLS and UV detection (Agilent Technologies, Palo Alto, USA). A Superose 6 10/300 GL column (GE Healthcare, Little Chalfont, UK) was used as the solid phase. Phosphate buffered saline (PBS) at pH 7.4 (12 mM phosphate, 137 mM sodium chloride, 2.7 mM potassium chloride) with a flow rate of 0.5 mL/min was used as a mobile phase. The protein recovery was calculated using the UV absorbance signal at 214 nm. The area under the curve (AUC) of the unstressed sample was defined as 100%.

### **7.2.3 Light obscuration**

Light obscuration (LO) measurements were conducted with a PAMAS-SVSS-C Sensor HCB-LD 25/25 (Partikelmess- und Analysensysteme GmbH, Rutesheim, Germany) to quantify particles  $\geq 1$  µm. Three aliquots of 0.3 mL of each sample were analyzed. Between the sample measurements the system was rinsed with highly purified water (Millipore Corporation, Billerica, USA) until the system was free of particles. Before each measurement, 0.3 mL of the sample was flushed through the system and discarded.

### **7.2.4 Endotoxin testing**

The samples were checked for endotoxins using a FDA-licensed Endosafe-PTS instrument (Charles River Laboratories, Wilmington, USA) with a limit of detection of 0.005 EU/mL. All samples were diluted 1:50 with endotoxin-free highly purified water, due to interference of the buffer with the measurement. All samples were found to be free of endotoxins ( $< 0.25$  EU/mL).

### **7.2.5 Animals**

Male and female (3 of each per test group) C57BL/6 mice were obtained from Charles River Laboratories, Wilmington, USA. All mice were used from approximately 9 weeks of age, and had access to tap water (autoclaved, acidified, pH 2.5-2.8) and food (R/M-H pellets rodent diet, Ssniff, Soest, Germany) available *ad libitum*. Mice were allowed at least five days to

acclimate before the dosing period commenced. Mice were housed individually in U-Temp™ Type II long cages, barriered conditions with bedding. The environmental conditions were set at a room temperature of  $22 \pm 2^\circ\text{C}$ , humidity of  $55 \pm 10\%$  and 15 to 18 air changes per hour. Rooms were set on a 12-hour daily light cycle (light from 6 a.m. to 6 p.m.) except as required for sample collection or other study procedures.

All animals were observed each day for the duration of the study, and none of the animals died or showed abnormalities. Injection sites, body weight and food intake were examined for each animal and did not show abnormalities (data not shown).

All experiments were conducted in the laboratories of Abbott GmbH & Co. KG (Ludwigshafen, Germany) in accordance with the following international regulations: International Conference on Harmonization of Technical Requirements for Registration of Pharmaceuticals for Human Use (ICH): Non-Clinical Safety Studies for the Conduct of Human Clinical Trials for Pharmaceuticals, ICH M3(M), (CPMP/ICH/286/95, modification), November 2000 and the Committee for Proprietary Medicinal Products (CPMP): Note for Guidance on Repeated Dose Toxicity, CPMP/SWP/1042/99 corr., October 2000.

#### **7.2.6 Immunization protocol**

200  $\mu\text{L}$  injections of various muAb or placebo formulations were administered subcutaneously into the scruff of the neck to male and female C57BL/6 mice. Four different test groups were previously defined. Serving as negative control, the first group of animals ("Group A") received a placebo formulation of 20 mM histidine buffer with 8% (w/v) sucrose, pH 5.7. The verum formulations contained either 250  $\mu\text{g/mL}$  of native muAb ("Group B"), or light exposed, aggregate-spiked muAb aggregates at a total concentration of 25  $\mu\text{g/mL}$  of protein ("Group C"), light exposed, aggregate-spiked muAb aggregates at a total concentration of 250  $\mu\text{g/mL}$  of protein ("Group D"). Injections were carried out on days 1, 2, 4, 6, 13, 20, 27 followed by a six week recovery period.

#### **7.2.7 Collection of blood samples**

Blood sampling was performed postmortem during necropsy from the *Vena cava* on day 1 (before any injection), day 15, day 29 or day 71. The whole blood was collected in polypropylene tubes without anticoagulant and kept at room temperature for 30 to 60 minutes until centrifugation ( $10000 \times g$ , 5 minutes) at approximately  $5^\circ\text{C}$ . The serum was separated from the blood cells and divided in two halves. The aliquots were stored at  $-80^\circ\text{C}$  before analysis.

#### **7.2.8 Determination of Anti-Drug Antibodies (ADAs)**

Anti-drug antibodies towards muAb were determined from serum samples using sandwich enzyme-linked immuno sorbent assays (ELISA's) in polystyrene MaxiSorp 96-well plates (Nunc, Roskilde, Denmark) according to either Method A or Method B below (see Figure



7-2). In both methods, 150  $\mu$ L/well of muAb solution (concentration 750 ng/mL in PBS) were used as capture-antibodies for potential anti-muAb antibodies in serum samples. The wells were coated with muAb solution overnight at 4°C. Blocking subsequently was performed by incubating each well for 1 h at room temperature with 200  $\mu$ L 1% BSA (Sigma Aldrich, Steinheim, Germany) solution in Dulbecco's PBS (Invitrogen, Darmstadt, Germany). Between the incubation steps the wells were washed with PBS (12 mM phosphate, 137 mM sodium chloride, 2.7 mM potassium chloride), containing 0.05% Tween-20. All substances were of analytical grade and all buffers and solutions were prepared in highly purified water (Purelab Plus, USF Elga GmbH, Celle, Germany).

#### 7.2.8.1 Method A

Serum samples (100  $\mu$ L) were added to the muAb-coated wells at 1:10 dilution in a solution containing 14.4 mM tri-sodium citrate dihydrate, 1.1 M sodium chloride and 0.1 % polysorbate 20. After incubating 90 minutes and washing, 62.5 ng/mL of biotinylated muAb was added, incubated for 90 minutes and subsequently after five washing steps 1:16,000 fold diluted streptavidin peroxidase-conjugated anti-biotin antibody fragment (Sigma Aldrich, Steinheim, Germany) was added and the plate was washed. The bound peroxidase reacted with a substrate containing 0.65 mM hydrogen peroxide (Merck, Darmstadt, Germany) and 0.05 mg/mL 3,3',5,5'-tetramethylbenzidine (Fluka, Taufkirchen, Germany) dissolved in dimethylsulfoxide (Merck, Darmstadt, Germany). The reaction of peroxidase and substrate was stopped by the addition of 0.5 M sulfuric acid (Mallinckrodt Baker, Deventer, Netherlands) prior to measuring the absorbance with a FLUOstar Omega at 450 nm (BMG Labtech GmbH, Offenburg, Germany). Each serum sample was measured in duplicate. Serum samples were declared positive for ADAs when the mean absorbance values were at least three times higher than the upper 95<sup>th</sup> percentile value for negative control serum samples from a total of 24 mice that had received either no injections (3 male and 3 female mice) or injections of placebo formulations containing only buffer (3 male and 3 female mice sacrificed on each of days 15, 29, and 71).

The suitability of method A to detect anti-muAb antibodies was validated by using a reference polyclonal rabbit antiserum (Biotrend Chemicals GmbH, Cologne, Germany) raised against native muAb. Rabbits were hyper-immunized with muAb and the induced rabbit anti-muAb antibodies were chromatographically purified and spiked into to serum from naïve C57BL/6 mice, which was then analyzed as described above.

#### 7.2.8.2 Method B

The presence of antibody-antigen complexes in serum presents a challenge for detection of ADAs in standard ELISA assays. Shomali *et al.* showed that addition of an acid dissociation step reduced interference from immune complexes and increased the amount of ADAs that could be detected in mice that had been immunized with ovalbumin as a model drug [Shomali *et al.*, 2010]. In the present study, an additional acid dissociation step was added to

the ELISA protocol to dissociate potential antibody-muAb complexes prior to ADA analysis. In this step, 1:20 diluted serum samples were incubated in 300 mM acetic acid (resulting pH 2.5-3.0) for one hour to dissociate potential immune complexes, after which time the pH was adjusted to 7.4 using 1 M Tris base pH 9.5. Under this low pH environment dissociation of immune-complexes is favored, but antibodies do not appear to lose their binding capacity [Patton *et al.*, 2005].

In this method, the ELISA analysis was conducted as described in Method A, except that 1:15,000 diluted isotype-specific HRP-conjugated goat anti-mouse isotype (anti-IgM, anti-IgG1, anti-IgG2b or anti-IgG3) antibodies (Jackson ImmunoResearch, West Grove, USA) were used for detection.

### **7.2.9 Determination of drug levels in serum (pharmacokinetics, PK)**

For the determination of muAb in serum samples, an ELISA was developed using MaxiSorp 96-well plates. A volume of 150  $\mu$ L/well of murine TNF- $\alpha$  (eBioscience Inc., San Diego, USA) at a concentration of 100 ng/mL in PBS was used as capture-antigen for muAb in serum samples. After blocking with 1% BSA in PBS and washing the plates, 1:80,000 diluted biotinylated goat anti-mouse-IgG2c (Southern Biotech, Birmingham, AL, USA) was used as primary detection antigen. As a secondary detection antigen a streptavidin peroxidase conjugated anti-biotin fragment in 1:16,000 dilution was added, after further washing steps. The bound peroxidase was measured by addition of 0.65 mM H<sub>2</sub>O<sub>2</sub> and 0.05 mg/ml 3,3',5,5'-tetramethylbenzidine. After 15 minutes of incubation, the reaction was quenched by addition of 0.5 M sulfuric acid and, the reaction product detected by absorbance at 450 nm using a BMG FLUOStar. For calibration muAb spiked to C57BL/6 serum (LPT - Laboratory of Pharmacology and Toxicology, Hamburg, Germany) was used. The serum samples were diluted individually in a solution containing 14.4 mM tri-sodium citrate dihydrate, 1.1 M sodium chloride and 0.1 % polysorbate 20 until the linear range of a calibration curve was reached. Each serum sample was measured in duplicate.

## **7.3 RESULTS**

### **7.3.1 SEC Analysis of murine IgG2c after light exposure**

Prior to exposure to light, muAb samples were largely monomeric, with a small amount ( $1.20 \pm 0.19$  %) of the sample present as lower molecular weight species. After 48 hour exposure to light muAb samples formed roughly 15% insoluble aggregates. Furthermore, the populations of both higher molecular weight species and low molecular weight fragments increased dramatically, with a concomitant decrease in the amount of monomer present (see Figure 7-1).

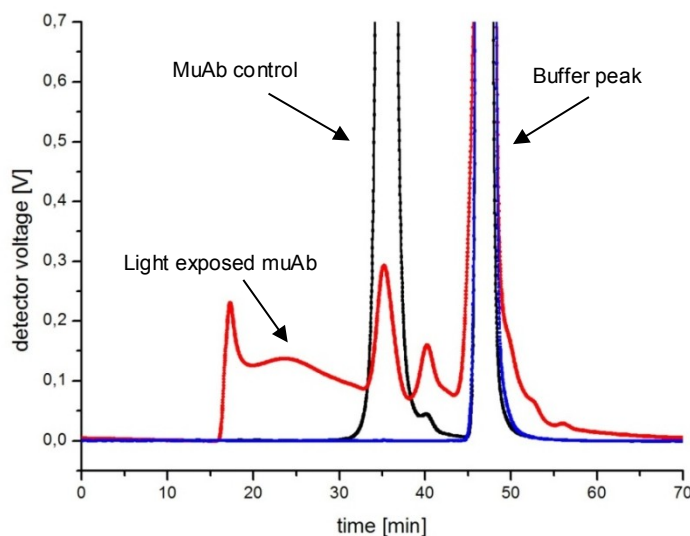


**Figure 7-1 – UV-size exclusion chromatograms at 214 nm of muAb.**

The blue line represents the placebo formulation, revealing a large peak at 47 minutes caused by histidine. The unstressed muAb formulation is displayed by the black line, and the muAb sample after 48 h of light exposure is shown by the red line. The light exposed sample shows a strong decrease of monomer peak (retention time 36 min) as well as an increase of aggregates and fragments.

After centrifugation to remove insoluble aggregates, the remaining  $\sim 85\%$  of initially present muAb contained  $15.3 \pm 1.7\%$  of monomer, accompanied by  $55.9 \pm 2.6\%$  aggregates and  $28.7 \pm 4.3\%$  fragments.

### 7.3.2 Analysis of anti-drug antibody levels using two ELISA formats

Figure 7-2 provides the schematic mode of operation of the utilized ELISA formats. All samples were first analyzed using method A, which did not include an acid dissociation step. Furthermore, this set-up relied on the availability of a second free Fab part of the anti-drug antibodies in the samples. The performance of the assay was tested by the reference antibody generated in hyper-immunized rabbits.

The sensitivity of the method depends on the concentration of the reference antibody (see Figure 7-3). The limit of detection of the reference antibody was determined to be  $\sim 27$  ng ( $3 \times \delta$ ) and the limit of quantification was determined to be  $\sim 41$  ng ( $10 \times \delta$ ).

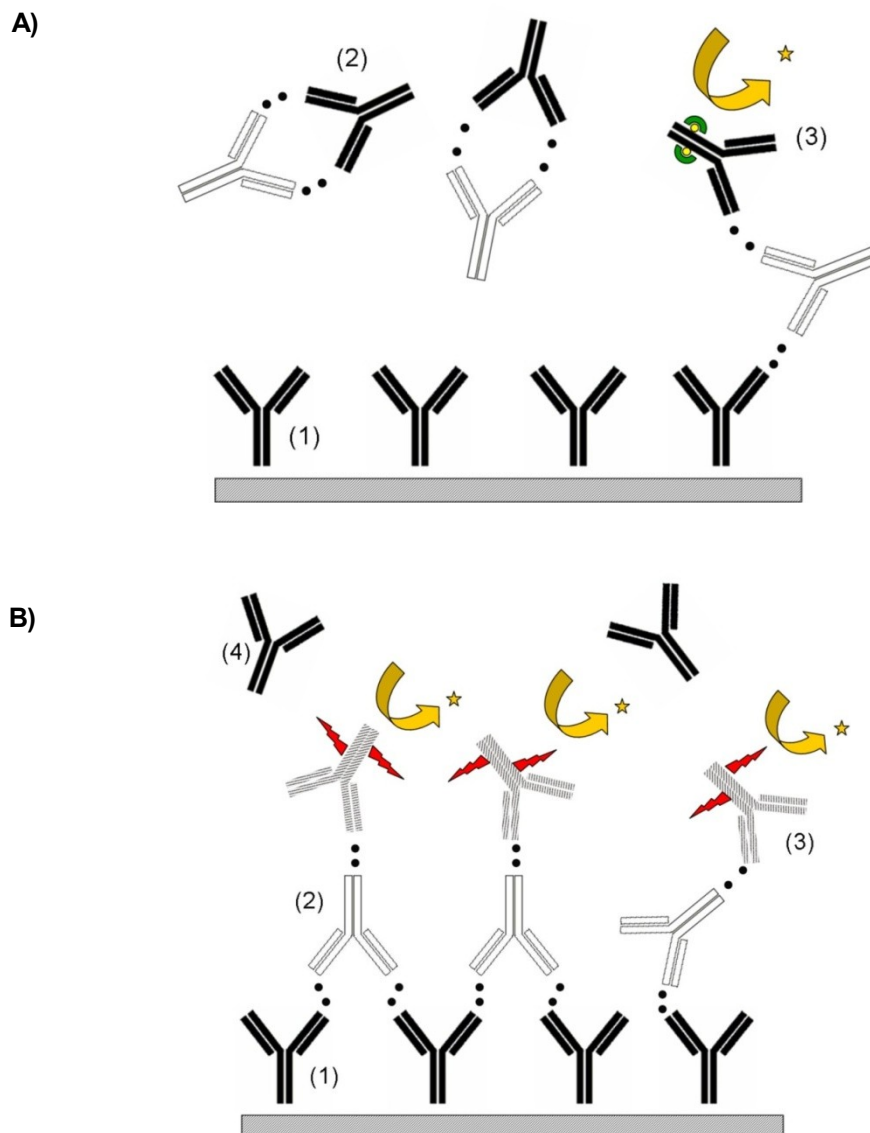


**Figure 7-2 – Schematic representation of the two ELISA formats used.**

The enzymatic reaction for detection resulting in coloration is pictured by the arrow. **A)** Design of method A: muAb (shown in solid black) was coated on the surface of the well plate (1), the serum contains muAb as well as anti-muAb antibodies (shown in solid white), which form immune complexes (2). Bridging reactions of anti-muAb antibody between muAb coated and muAb labeled with biotin (●) are displayed in (3). **B)** Design of method B: muAb (shown in solid black) was coated on the surface of the well plate (1). In method B, immune complexes are dissociated by incubation with acetic acid prior to applying to the well plate. Therefore the circulating muAb molecules are free (4) and not complexing anti-muAb antibodies and hence these are able to bind via Fab fragments to the coated muAb (2). Detection was performed with HRP – labeled (🔪) goat anti-mouse antibodies (grey dashed antibody draft), binding to the Fc domain of anti-muAb antibodies.

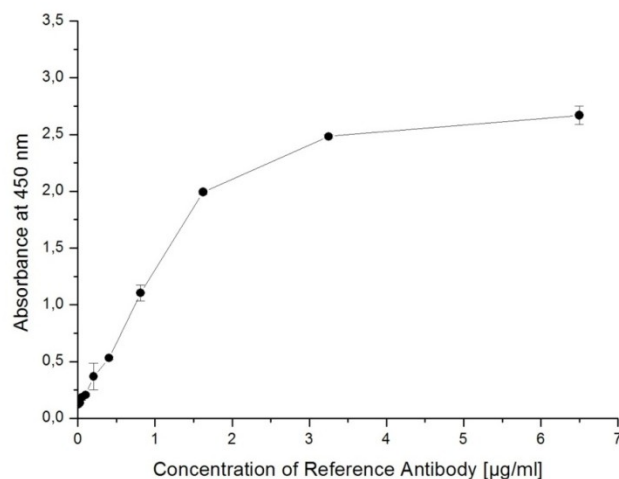


**Figure 7-3 – Absorbance results of different concentrations of the reference antibody using method A.**

The reference material was generated in rabbits. The error bars represent the standard deviation of measurements in triplicate.

In contrast, method B included an additional incubation step wherein the serum samples were incubated with a weak acid to dissociate immune complexes that might have formed between muAb and the anti-muAb in serum. Instead of using biotinylated muAb as a detection antibody, which would require free Fab arm of ADA for binding, the detection in method B was based on goat anti-mouse isotype-specific antibodies binding to the Fc portion of potential ADAs.

The results obtained from these two ELISA setups were compared within this study. The ADA detection by method A was performed at LMU Munich, Department of Pharmacy, whereas ELISA method B was conducted by our academic cooperation partner at University of Colorado in Boulder. The group of Theodore W. Randolph and especially Maliheh Shomali performed this part of the studies. After completion of the *in vivo* studies and analysis of serum samples using method A, the left-over serum samples were shipped to Colorado. They kindly provided the results for better comprehension of the entire thesis. However, this small part is property of the University of Colorado and was not conducted on my own.

For each setup a background absorbance was averaged from the values determined in the sera of 6 naïve mice and 18 mice that received the placebo formulation. Due to the diverging number of repetitions of sample measurements performed either by method A (triplicates) or method B (duplicates), the standard error of the mean was calculated, which refers to the sample size.

The results of the measurement of the serum samples from the mice that were injected with the placebo formulation are shown in Figure 7-4 A-E. Each bar represents an individual animal, since the mice were sacrificed for bleeding. Analysis of sera from mice injected with buffer only showed a constant background response when analyzed by Method A

(Figure 7-4 A). A similar result was obtained when the sera were analyzed for IgG1, IgG3 and IgM by Method B (Figures 7-4 B, D and E, respectively). However, background responses against IgG2b detected by Method B increased over time, particularly for females (Figure 7-4 C). The reason(s) for this apparent increase in background signal over time are unclear.

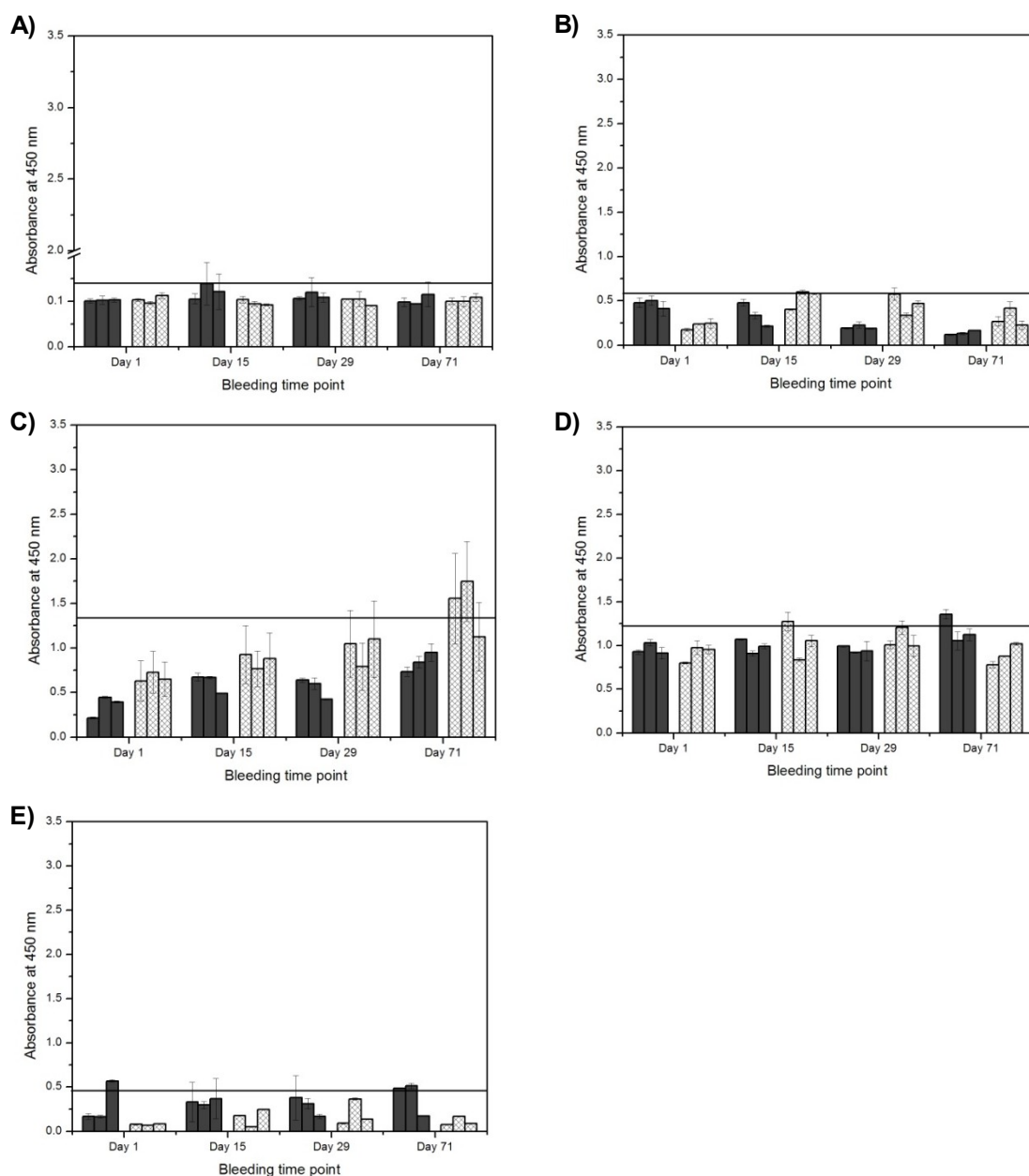


**Figure 7-4 - Absorbance measurements of ELISA for detection of anti-drug antibodies in mice having obtained the placebo formulation.**

**A)** detection of ADA by method A (n=3, error bars represent standard error of the mean) **B)** detection of IgG1 directed against muAb by method B **C)** detection of IgG2b directed against muAb by method B **D)** detection of IgG3 directed against muAb by method B **E)** detection of IgM directed against muAb by method B (n=2, error bars represent standard error of the mean). The plain grey bars represent the data obtained from 3 male mice, and the checkered bars represent the data obtained from 3 female mice. The horizontal line represents the predefined benchmark of non-responders and responders for each assay set-up (the upper 95<sup>th</sup> percentile of background absorbance values from 24 mice). Because animals were sacrificed for blood collection, each bar represents a separate animal.

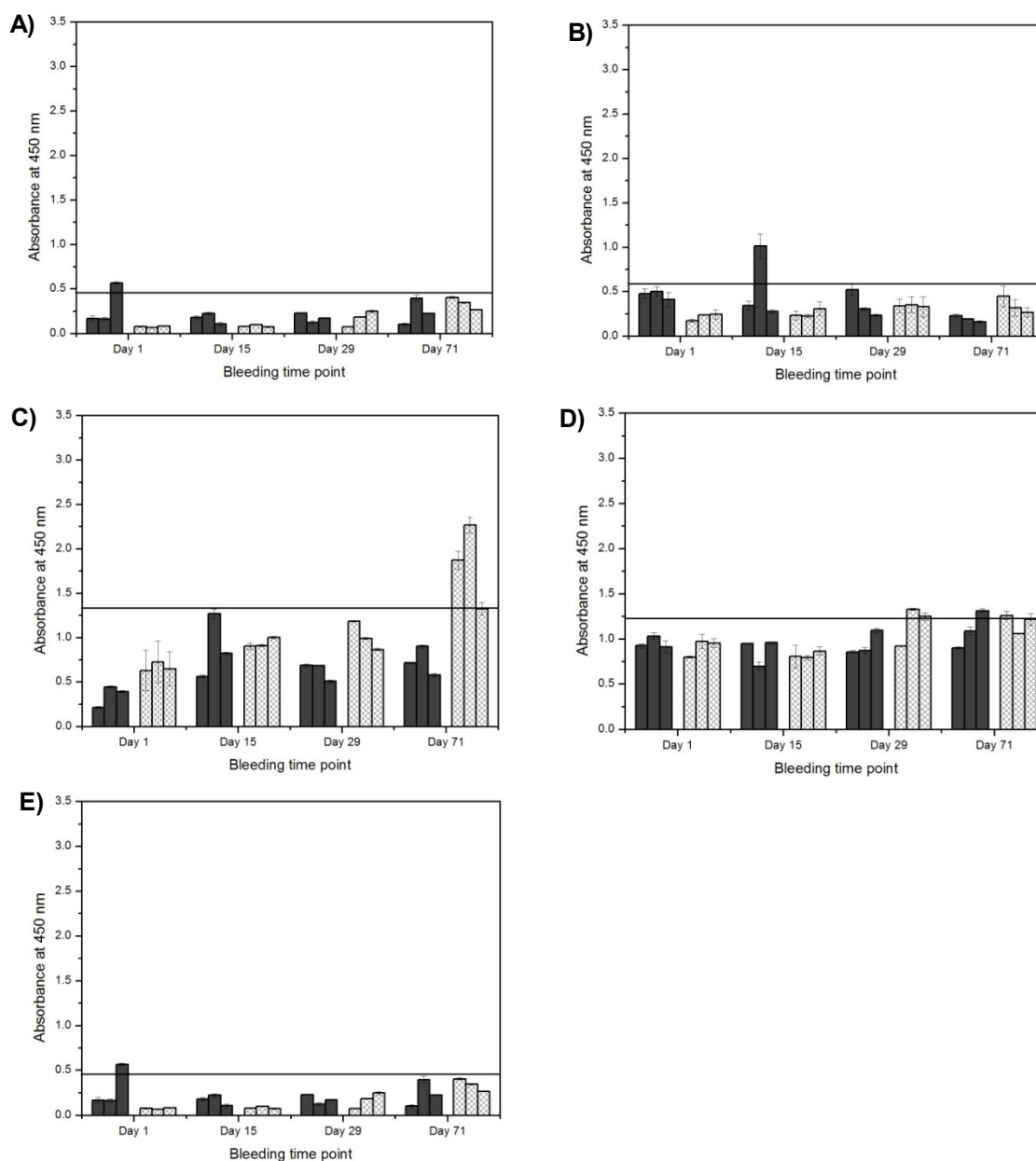


**Figure 7-5 - Absorbance measurements of ELISA for detection of anti-drug antibodies in mice having obtained the formulation containing native muAb.**

**A)** detection of ADA by method A (n=3, error bars represent standard error of the mean) **B)** detection of IgG1 directed against muAb by method B **C)** detection of IgG2b directed against muAb by method B **D)** detection of IgG3 directed against muAb by method B **E)** detection of IgM directed against muAb by method B (n=2, error bars represent standard error of the mean). The plain grey bars represent the data obtained from 3 male mice, and the checkered bars represent the data obtained from 3 female mice. The horizontal line represents the predefined benchmark of non-responders and responders for each assay set-up (the upper 95<sup>th</sup> percentile of background absorbance values from 24 mice). Because animals were sacrificed for blood collection, each bar represents a separate animal.

The results of the measurement of the serum samples from the mice that were injected with the formulation containing native muAb are shown in Figure 7-5 A-E. Method A did not detect ADA for mice sacrificed on day 15 or day 29, and detected only very low positive ADA levels in one mouse that was sacrificed on day 71 (Figure 7-5 A). The detection of anti-muAb IgG1 levels with the comparative Method B shows a positive response in a single male mouse

on day 15 (Figure 7-5 B). In contrast, two IgG2b absorbance values from female mice were higher than the upper 95% confidence level for the mean of controls (Figure 7-5 C), but these IgG2b levels cannot be definitively classified as positive responses, because the placebo also showed similar increases, which were also more pronounced in female mice. The results of anti-muAb IgG3 in Group B are shown in Figure 7-5 D. In 2/6 samples from day 29 and 3/6 samples from day 71 positive responses were detected. No increased anti-muAb IgM response was detected (Figure 7-5 E) in any serum sample of Group B.

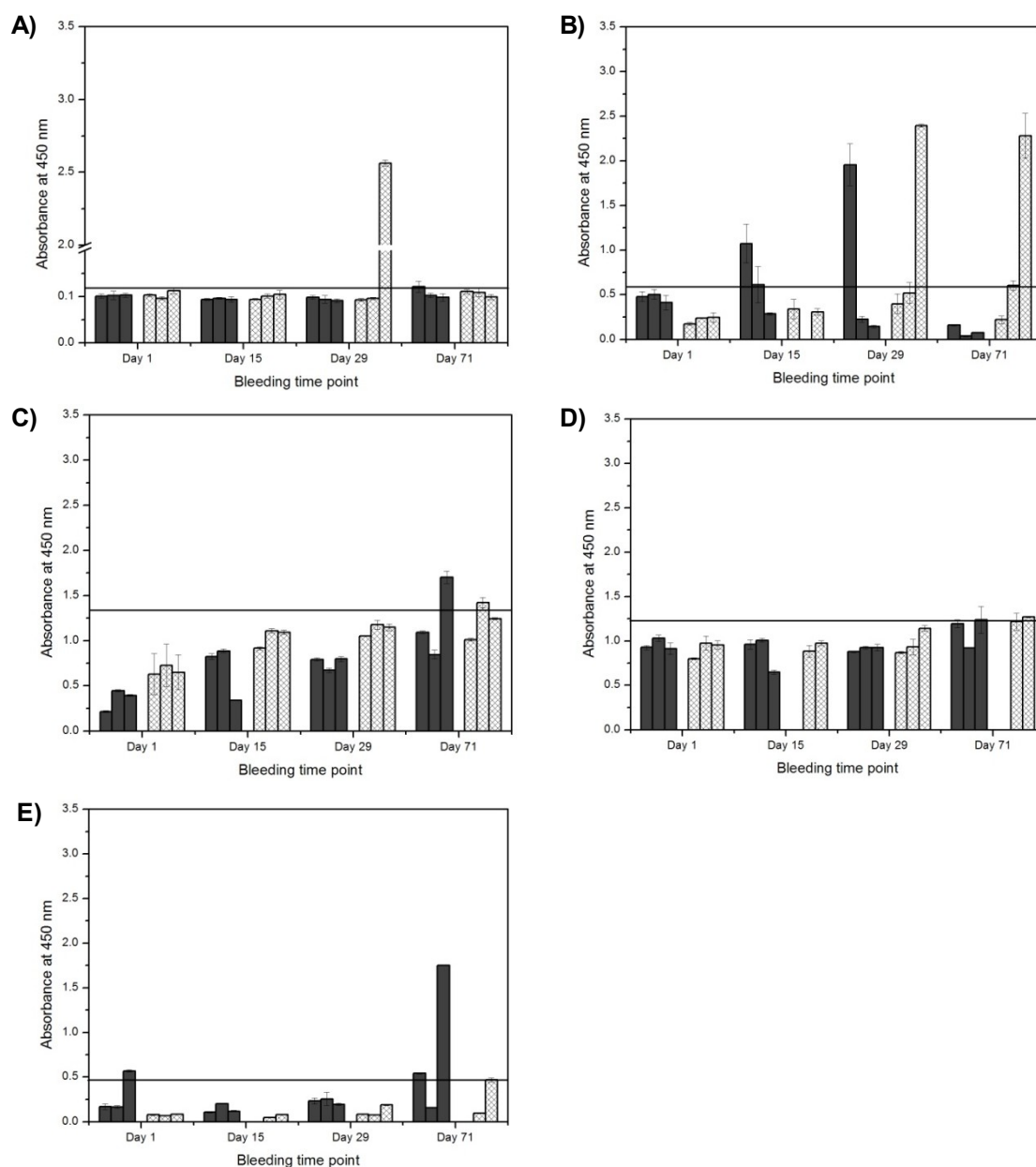


**Figure 7-6 - Absorbance measurements of ELISA for detection of anti-drug antibodies in mice having obtained the formulation containing a low dose of aggregated muAb.**

**A)** detection of ADA by method A (n=3, error bars represent standard error of the mean) **B)** detection of IgG1 directed against muAb by method B **C)** detection of IgG2b directed against muAb by method B **D)** detection of IgG3 directed against muAb by method B **E)** detection of IgM directed against muAb by method B (n=2, error bars represent standard error of the mean). The plain grey bars represent the data obtained from 3 male mice, and the checkered bars represent the data obtained from 3 female mice. The horizontal line represents the predefined benchmark of non-responders and responders for each assay set-up (the upper 95<sup>th</sup> percentile of background absorbance values from 24 mice). Because animals were sacrificed for blood collection, each bar represents a separate animal.



ADA levels in serum samples from the mice injected with the low dose of aggregated protein (5 µg protein in total per injection) are shown in Figure 7-6 A-E. Using method A, ELISA analysis of the majority of the samples (17 out of 18) from mice that received the low dose of aggregated protein resulted in absorbance values that were near or below the defined response cutoff value. Only one serum sample from a female mouse bled on day 29 shows a substantial anti-drug antibody response under these circumstances (Figure 7-6 A). Serum from the same female also showed a high anti-muAb IgG1 response when method B was used (see below). In other mice tested by Method B for IgG1, responses were detected in 2/6, 2/6, and 2/6 mice sacrificed on days 15, 29, and 71, respectively (Figure 7-6 B). Two mice (one male and one female) showed moderate IgG2b responses to low-dose aggregates (Figure 7-6 C), but as discussed above this could not be unequivocally assigned to an ADA response because the increased anti-IgG2b response seen at later time was also observed in the placebo samples (Figure 7-4 C). The results of anti-muAb IgG3 detection using method B show 2/5 weakly positive serum samples at day 71 (Figure 7-6 D). Finally, two serum samples obtained on day 71 show also positive responses in the IgM assay of method B (Figure 7-6 E).

The fourth dosing Group D received the formulation containing the high dose of light exposed muAb (50 µg of protein in total per injection), spiked with the same number of aggregated protein particles as were administered to the low-dose group. Figure 7-7 shows the results of the measurement of anti-muAb antibodies in the serum samples from those mice. No mice that received the high dose of muAb show positive ADA responses when using detection method A (Figure 7-7 A). In contrast, strong positive responses for Anti-muAb IgG1 levels were detected using method B. On day 15, four out of six sera showed positive anti-muAb IgG1 responses (Figure 7-7 B). On day 29, the blood of one male mouse clotted immediately during bleeding, hence no serum could be produced and investigated. All of the remaining samples (5/5) resulted in positive IgG1 responses directed against muAb, comparable to the 4/6 responding mice on day 71. The absorbance of the sera from responders on days 29 and 71 were higher than those on day 15. Analysis of the sera for anti-muAb IgG2b levels showed 2 responders on day 71 (Figure 7-7 C), but was inconclusive for reasons discussed above. When tested for anti-muAb IgG3 levels, 2/6 serum samples obtained on day 71 were positive and both were received from female mice (Figure 7-7 D). Substantial IgG3 responses against muAb were not detected at earlier time points. None of the mice that received the high dose of muAb generated substantial amounts of anti-muAb IgM (Figure 7-7 E).

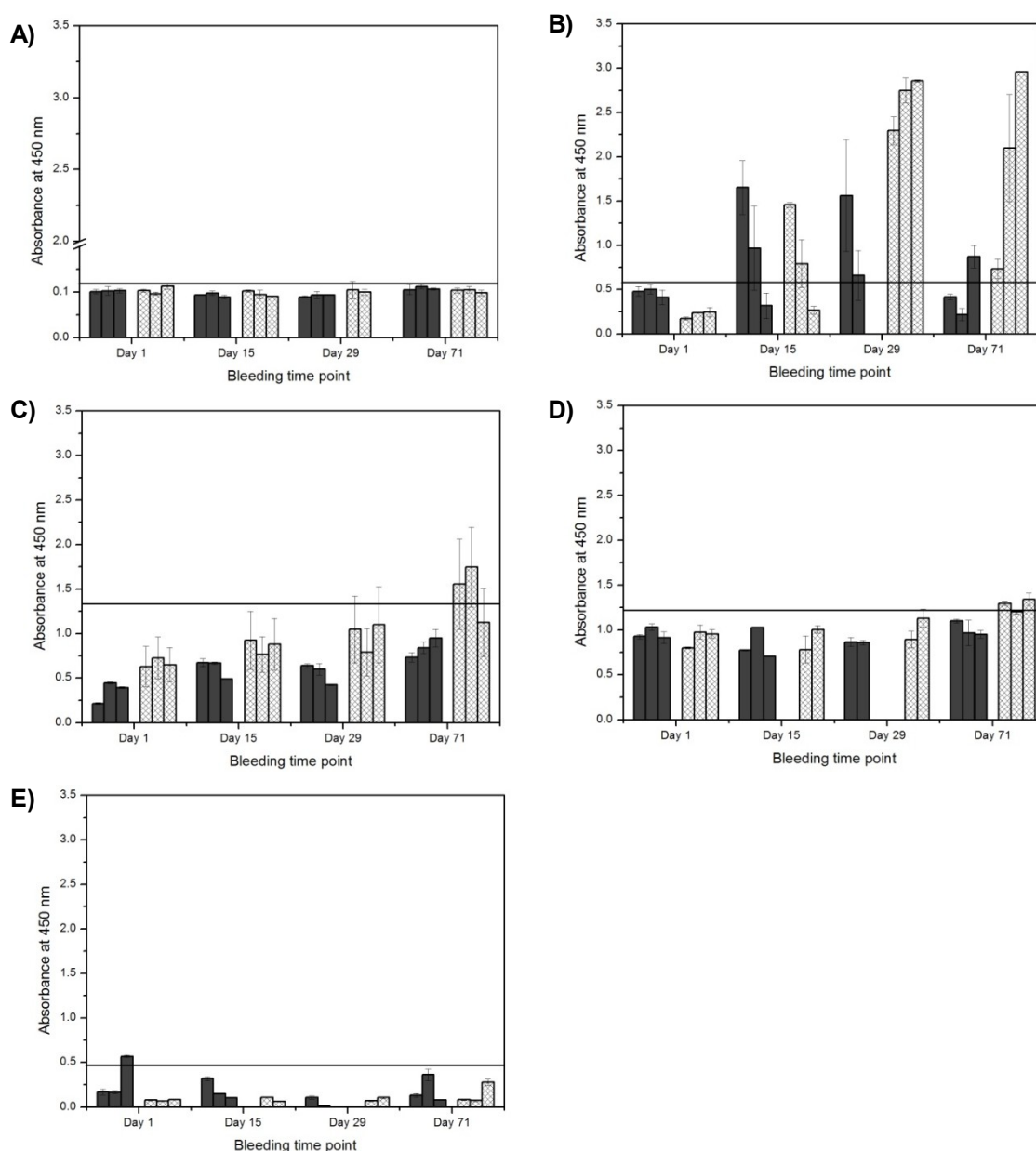


**Figure 7-7 – Absorbance measurements of ELISA for detection of anti-drug antibodies in mice having obtained the formulation containing the high dose of aggregated muAb.**

**A)** detection of ADA by method A ( $n=3$ , error bars represent standard error of the mean) **B)** detection of IgG1 directed against muAb by method B **C)** detection of IgG2b directed against muAb by method B **D)** detection of IgG3 directed against muAb by method B **E)** detection of IgM directed against muAb by method B ( $n=2$ , error bars represent standard error of the mean). The plain grey bars represent the data obtained from 3 male mice, and the checkered bars represent the data obtained from 3 female mice. The horizontal line represents the predefined benchmark of non-responders and responders for each assay set-up (the upper 95<sup>th</sup> percentile of background absorbance values from 24 mice). Because animals were sacrificed for blood collection, each bar represents a separate animal.

As noted above, using method A, ADA levels well above the positive response cutoff were detected in only one of 36 sera of mice that received the formulations containing muAb aggregates (Figure 7-6 A, Figure 7-7 A). This animal had received the low dose aggregated antibody formulation (5  $\mu\text{g}$  per time point). To assure that the one positive sample detected with method A (later on referred to as mouse serum C29+) was truly an ADA against muAb, a

duplicate of the serum sample was spiked with 100 ng/ml of the native protein (muAb). True anti-muAb antibodies would bind to added muAb molecules in solution and thus not bind to muAb coated in wells and washed away, leading to loss of signal at the end of the assay.

Addition of 100 ng/ml muAb to the serum sample, C29+, resulted in a complete inhibition of the response (Figure 7-8). The formation of immune complexes between muAb and specific anti-muAb antibodies in C29+ inhibited the binding of ADA to the coated muAb molecules. The high absorbance signal of this specific animal thus was proven to originate from ADAs. Additionally, the strong influence of free drug circulating in the serum was shown. As expected, when analyzed by method B, this same sample was also positive for anti-muAb ADAs.

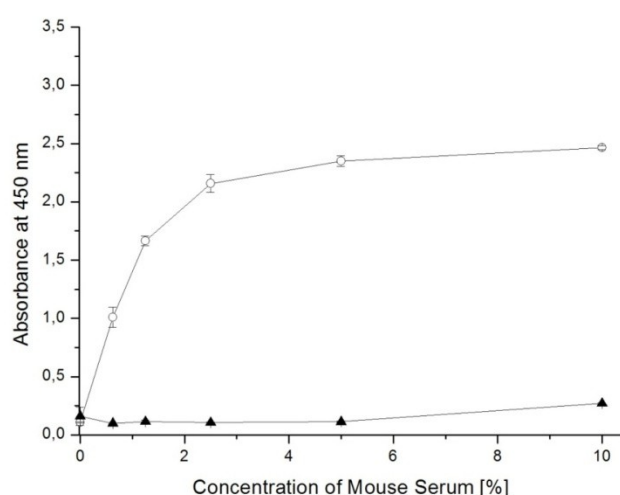


**Figure 7-8 – Inhibition of positive ADA response in serum of mouse C29+ by adding native muAb.**

Absorbance results of the positive serum sample (white circles) using method A and after adding 100 ng/mL muAb to the serum (black triangles). (Error bars = standard deviation of three measurements)

### 7.3.3 Detection of serum levels of muAb – pharmacokinetics

In addition to the determination of ADAs, the pharmacokinetics (PK) of the murine antibody was of great importance in this study. It was important to determine how fast the antibody was cleared in the animal and if the presence of unbound antibody in the blood could result in false negative results regarding the ADAs. Each serum sample was analyzed in duplicate. No muAb was detected in the PK assay in the serum samples of the mice that received the placebo formulation (Group A) at all sampling times (data not shown). Similar results were observed in the sera of mice which received the low dose formulation. A different result was observed in the samples of the mice that received the native antibody muAb (see Figure 7-9). The levels of the muAb in the serum were quite high for the group that received the native protein formulation. Even after a six week recovery period (with no additional muAb injection), concentrations in the upper nanogram per ml range were determined. The long half

life is a well known quality of monoclonal antibodies [Carpenter *et al.*, 2009]. Therefore, the high levels of muAb detected in Group B are not very surprising. On day 15 the measured amounts of muAb in Group B reach up to about 100 µg/ml. On day 29 the amounts showed stable values of around 50 µg/ml before the values decreased by day 71.

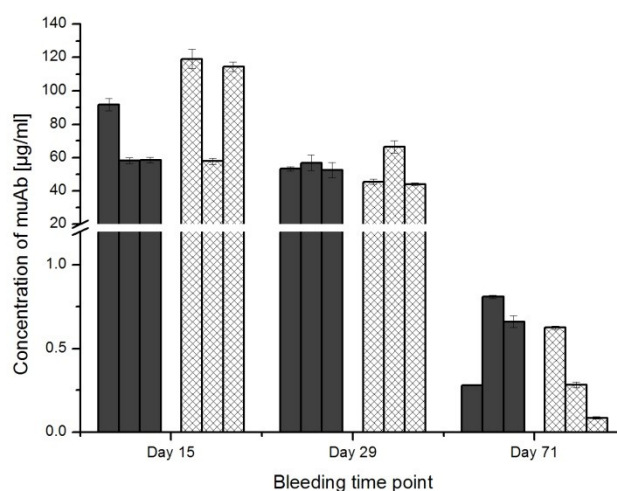


**Figure 7-9 – Results of ELISA determining the concentration of muAb in the serum samples of mice that obtained 50 µg of the native antibody per injection.**

The plain grey bars represent the data obtained from 3 male mice, and the checkered bars represent the data obtained from 3 female mice. (Triplicate measurements per sample, error bars represent standard deviation)

The formulation containing aggregates still consisted of considerable amounts of monomeric muAb (see Figure 7-1) and is thus expected to result in detectable muAb levels in serum. Figure 7-10 shows the results for sera of the mice that received the high dose formulation. The calculation of the amount of muAb within the aggregated formulations was made using the aggregated formulation as calibration standard. In the sera obtained on day 71 no muAb was detected and on days 15 and 29 the recovery was much lower compared to the native Group B. The levels detected in these sera were about 10 times lower than the serum levels of mice in Group B. The results of Group A and Group C are not shown, because these were below the limit of detection.

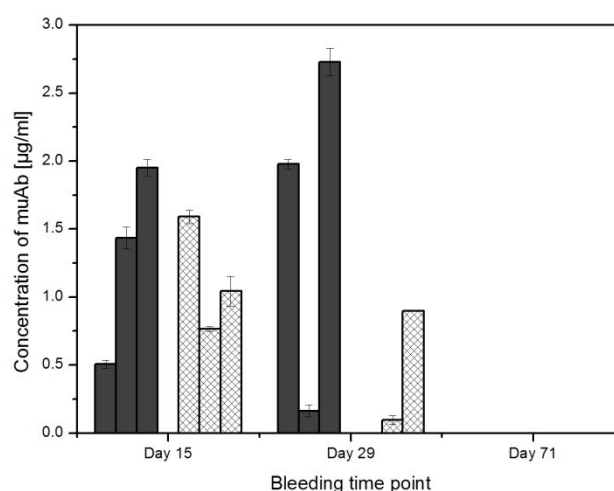


**Figure 7-10 – Results of ELISA determining the concentration of muAb in the serum samples of mice that obtained 50 µg of the aggregated antibody per injection.**

The plain grey bars represent the data obtained from 3 male mice, and the checkered bars represent the data obtained from 3 female mice. (Triplicate measurements per sample, error bars represent standard deviation)

## 7.4 DISCUSSION

The study was initiated to establish a bioanalytical method for prospective *in vivo* studies concerning the immunogenicity of aggregates of a murine antibody (muAb) in mice. Two different ELISA protocols were designed for the detection of anti-muAb antibodies, whose generation was strongly expected after the repeated administration of various kinds of aggregates of muAb in contrast to the repeated administration of native muAb.

The data from two ELISA methods showed significant differences. After analyzing the serum samples using method A, one might think the negative results could either mean that no anti-muAb antibodies were generated in most animals, that mainly false negative samples were obtained due to a lack of detection, or that the antibodies generated were not directed against muAb. Looking only at these results, it is not possible to clarify whether ADAs were produced against the administered samples or not.

Since the native muAb is a self-protein for C57BL/6 mice, the mice in Group B (native muAb) showed the formation of only very few positive anti-muAb antibodies. Using method A, only very weak immune response to native muAb could be detected. However, method B showed increased levels of anti-muAb antibodies of various subclasses.

Administering the ten-times higher amount of aggregated protein considerably increased the incidence of anti-muAb IgG1 formation, though this dose concomitantly failed to induce an ADA response detectable by method A. A difference between the responses of both

genders was determined in anti-muAb IgG1 levels (Figure 7-7 B). Two female mice on day 15 and all female mice on days 29 and 71 responded, whereas only two male mice each on days 15 and 29 and one on day 71 resulted in minor formation of IgG1 towards muAb. Differences between the higher and the lower dose of aggregated protein were not significant for IgG3 class ADAs.

No strong responses of IgG3 directed against muAb were observed over time in any group. IgG3 responses are frequently associated with T-cell independent immune responses [Swanson *et al.*, 2010]. The lack of IgG3 response is thus consistent with a T-cell dependent mechanism for immune response to muAb, although more detailed immunological studies beyond the scope of the current work would be required to provide conclusive evidence.

Anti-muAb IgM was only generated in mice to which low-dose aggregates were administered. Interestingly, these response were observed only at the last bleed point on day 71. IgM responses to soluble antigens are typically short-lived [Murphy *et al.*, 2008]. It is speculated that a possible depot effect of the aggregated protein may have led to the delayed IgM response. However, a detailed investigation of IgM response towards muAb would have required the inclusion of several bleeds within the first two weeks and is outside the scope of the present study.

The most probable reason for not detecting existing ADAs when method A was used is the formation of complexes between free drug (muAb) and ADAs circulating in the blood. The definitive influence of small amounts of circulating drug was shown by the complete inhibition of the only positive response by adding muAb to the respective serum sample. Furthermore, the immune complexes formed may be eliminated quickly from the blood stream [Murphy *et al.*, 2008]. Using method B leads to different results: ADAs could be detected in most of the animals treated with aggregates of muAb. This set-up of ELISA included an acid dissociation step in order to break immune complexes. Therefore, the interference of circulating drug is presumably reduced, resulting in diminished interference of immune complexes with the ELISA assay. Furthermore, the biotinylated muAb as a detection reagent was replaced by HRP-labelled goat anti-mouse immunoglobulins of isotypes IgM, IgG1, IgG2b and IgG3. This approach added to the data interpretation by supplying additional information about the isotypes of ADAs generated. Whether the acid dissociation step in method B, the exchange of detection antibodies, or both is the reason for these differences was not investigated in this study. The mode of detection seems not to be crucial to the differences between the methods. This assumption is supported by the single highly positive result obtained using Method A. It is most likely that this single animal showed enhanced metabolic kinetics and/or an accelerated clearance of the drug and thus not enough muAb was left circulating in the blood stream to form complexes with the ADAs. Presumably this is the reason for the strongly positive response detected.

One must be careful about the baseline reactivity of immunoglobulins in the mouse sera for the test antigen, muAb. This could be differentiated by testing the pre-bleeds from each mouse. Some immunoglobulins in pre-bleeds might bind to muAb and could give rise to false positives. Since the study design scheduled bleedings by necropsy, no initial level for each animal can be determined, but the serum of three naïve animals of each gender was included in the calculation of a background.

The results were complemented by the pharmacokinetics assays that were used to determine the amount of muAb present in the sera that was capable of binding TNF- $\alpha$ . The detected drug levels in Group D in the  $\mu\text{g/ml}$  range at days 15 and 29 support the assumption of immune complex formation in these samples. This would imply that all anti-drug antibodies being generated in the animals are complexed to circulating drug molecules and could not be detected using method A. Since monoclonal antibodies usually offer a half-life of 10-21 days in plasma, an excess of circulating drug molecules is presumably available.

In conclusion, there probably were plenty of drug molecules circulating, much more than anti-drug antibodies generated. The high levels of up to 100  $\mu\text{g/ml}$  drug detected in serum samples of Group B prove the long lasting availability of numerous free drug molecules. This imbalance caused the lack of detection of ADAs if no dissociation step was included. One animal showed a strong ADA response that was detected using method A even without the dissociation step. As discussed before, we assume that to be a statistical outlier with an accelerated clearance of the drug and free ADA molecules.

Several obstacles were encountered when the serum samples of the mouse study were analyzed. First was the lack of a positive control. The immunogenicity of aggregates was anticipated and some of the epitopes exposed in protein aggregates might provoke antibodies that cross-react with native muAb. Furthermore, it was expected that samples from the formulation that contained both a variety of aggregate types and the highest concentrations of aggregates would be most immunogenic. Unexpectedly, when using method A, no strong positive ADA response from this formulation was detected, likely because immune complexes interfered with the analysis. Finally, the alternative method B, including the acid dissociation step to dissociate immune complexes, was able to detect significant increases in anti-muAb IgG1 levels in the majority of mice of test Group D. These IgG1 responses towards muAb were clearly more pronounced and appeared with higher incidence than in those samples obtained from the mice that received only one-tenth of the same formulation which included both monomer and soluble aggregates. These results confirmed the hypothesis that the immune response generated in the animals depends on the amount of aggregates administered and increases with the application of more aggregates of the same type.

## 7.5 CONCLUSION

To some degree, all therapeutic proteins are potentially immunogenic, and their aggregated forms are of great concern for immunogenicity. Singh *et al.* reviewed package inserts of approved biopharmaceuticals and literature and stated that ADAs were seen in almost all cases [Singh, 2011].

The investigation of different aggregates is of great interest, because it is still unclear whether aggregates in general or only aggregates with specific structural properties have an impact on immune response. Supported by the European Medicines Agency (EMA) “Guideline on Immunogenicity assessment of biotechnology-derived therapeutic proteins” animal models are often used to evaluate the safety of protein drugs leading to the question which species should be used to predict immunogenicity in humans [Pendley *et al.*, 2003; Roskos *et al.*, 2004]. The use of transgenic animals is quite common but very expensive and their immune system is artificially altered. The use of naïve animals without any alteration in the immune system is an advantage compared to transgenic mice, and this is an approach very close to the therapeutic situation of human antibodies in human patients. This study in principal proves the suitability of using wild type mice to investigate murine antibodies compared to the transgenic approach.

This study shows that the detection of anti-drug antibodies depends on a thorough development of a proper assay format. It can be concluded that including an acid dissociation step to the ELISA results in the detection of anti-drug antibodies that could not be detected in serum samples without the acid dissociation step. Dissociation of immune complexes is thus essential for an adequate detection of ADAs; otherwise potential immune reactions could be missed or overlooked. Therefore, it is recommended to include this approach in the analysis of *in vivo* studies as well as in clinical studies when immunogenicity is assessed.

The mode of detection, either based on free Fab arms of the ADAs or on a binding to the Fc part of the ADAs, was not investigated in more detail. The use of subtype specific detection antibodies is recommended and entails the advantage of additional information about the subclass of ADAs generated.

The pharmacokinetic behaviour of the drug should be investigated in parallel. Monoclonal antibodies have an especially long half-life in blood and therefore have a chance to have a significant impact on the formation of immune complexes. The strong binding between small amounts of circulating drug and anti-drug antibodies emphasizes the relevance of ADAs *in vivo*. If ADAs are generated during a drug therapy they can potentially bind the drug and strongly reduce its activity.

Considerable efforts still have to be undertaken to extend the knowledge of the relation between immunogenicity and various types of aggregates that might be generated in biopharmaceuticals for an improved safety and efficacy of this growing class of drugs.



## 7.6 REFERENCES

[Carpenter *et al.*, 2009], Overlooking subvisible particles in therapeutic protein products: gaps that may compromise product quality, *J. Pharm. Sci.*, 98, 1201-1205

[Janeway *et al.*, 2004], Immunobiology: The Immune System in Health and Disease, 6th Edition,

[Murphy *et al.*, 2008] Janeway's Immunobiology, 7th Edition, 887 pp

[Patton *et al.*, 2005], An acid dissociation bridging ELISA for detection of antibodies directed against therapeutic proteins in the presence of antigen, *J Immunol Methods*, 304, 189-195

[Pendley *et al.*, 2003], Immunogenicity of therapeutic monoclonal antibodies, *Current Opinion in Molecular Therapeutics*, 5, 172-179

[Roskos *et al.*, 2004], The clinical pharmacology of therapeutic monoclonal antibodies, *Drug Development Research*, 61, 108-120

[Shomali *et al.*, 2010] Acid dissociation ELISA assay in measuring anti-drug antibodies (ADA) in the presense of excess drug, *Colorado Protein Stability Conference (poster session)*, Breckenridge, Colorado, USA

[Singh, 2011], Impact of product-related factors on immunogenicity of biotherapeutics, *J. Pharm. Sci.*, 100, 354-387

[Swanson *et al.*, 2010], Type I IFN enhances follicular B cell contribution to the T cell-independent antibody response, *Journal of Experimental Medicine*, 207, 1485-1500



## 8 INVESTIGATIONS ON THE IMMUNOGENICITY OF PROTEIN AGGREGATES OF A MURINE MONOCLONAL ANTIBODY IN WILD-TYPE MICE

---

### 8.1 INTRODUCTION

Besides many other factors, immunogenicity is particularly supposed to be related to aggregates and particles which are suspected to activate the immune system and to initiate the elicitation of antibodies by B cells [Braun *et al.*, 1997; Carpenter *et al.*, 2009; Hermeling *et al.*, 2005]. However, it is still unknown, if aggregates in general, or only some particular structures are responsible for this activation of the immune system. This study focuses on the aggregates of a murine monoclonal antibody, whose immunogenic potential was investigated in wild type mice. Using that approach, foreignness of the antibody to the *in vivo* model can be excluded and additionally the therapeutic situation of administering a human monoclonal antibody to human is imitated well.

The current method to determine immunogenicity of protein aggregates is the measurement of anti-drug antibody (ADA) levels in the serum. These ADAs can either bind to the drug molecule, leading to an accelerated elimination, or neutralize the effect of the drug. Both mechanisms entail a loss in efficacy of the drug. In more severe circumstances, the ADAs can even neutralize endogenous human proteins, which might lead to life-threatening complications [Schellekens, 2005; Schernthaner, 1993].

In this study, five different types of aggregates of a murine monoclonal antibody of IgG2c subtype were prepared from pure protein by stirring, shaking, light exposure and exposure to heat. All four mechanisms represent relevant stress factors that can potentially occur during protein manufacturing and might lead to protein aggregation [Schoeneich, 2010; Wang, 2005]. The aggregates were analyzed using different analytic techniques and separated either by centrifugation or by AF4. Subsequently, all samples were administered to C57BL/6 and BALB/c mice and antibodies directed against the drug as well as the pharmacokinetic profile of the drug were investigated by serum sample analysis.

The purpose of the study was to detect immune responses in the mice that received aggregates of the murine antibody. The detection of discrepancies in the quality of the immune responses after administration of different aggregates within one mouse strain would be an indication that aggregate features influence the response of the immune system. Furthermore, the experiment aimed to detect differences in the immune response of two mouse strains to similar aggregates.

## 8.2 MATERIALS AND METHODS

### 8.2.1 Materials

#### 8.2.1.1 Murine IgG2c antibody (muAb)

A murine monoclonal anti-mouse TNF- $\alpha$  IgG2c antibody (muAb) produced in C57BL/6 mice was kindly provided by Abbott Bioresearch Center (Worcester, USA) in a formulation comprising 20 mM histidine, pH 6.0, and a protein concentration of 33 mg/mL. Histidine, sucrose and hydrochloric acid were purchased from Sigma-Aldrich Chemie GmbH (Steinheim, Germany). Highly purified water was generated in-house using a PURELAB Plus instrument from USF Elga (Celle, Germany). All reagents were of analytical grade.

#### 8.2.1.2 Animals

Female C57BL/6J and female BALB/c mice were obtained from Janvier, Le Genest-Saint-Isle, France. All mice were used from approximately 6-8 weeks of age and had access to tap water (autoclaved, acidified, pH 2.5-2.8) and food (R/M-H pellets rodent diet, Ssniff, Soest, Germany) *ad libitum*. Mice were allowed at least two weeks to acclimate (predosing period) before the dosing period commenced. Mice were maintained under specific pathogen free (SPF) conditions in groups of 3 to 4 animals in M2-L cages with bedding and enrichment. The environmental conditions were set at a room temperature of 22°C and humidity of 60% RH. Rooms were set on a 12-hour daily light cycle (light from 7 a.m. to 7 p.m.) except as required for sample collection or other study procedures. Ten animals were investigated for each formulation group.

All animal experiments were carried out at the LMU Munich in accordance with the international ethical guidelines for the care and use of laboratory animals and were approved by the local animal ethics committee of the Regierung von Oberbayern (Reference number Az.55.2.1.53-2532.12.11).

### 8.2.2 Methods

#### 8.2.2.1 Sample preparation

The formulation buffer for the preparation of all dosing groups was a sterile filtered 20 mM histidine buffer pH 5.7. The protein concentration used for preparation of aggregates was 10 mg/mL and the pH was adjusted to 5.7 using hydrochloric acid. One milliliter of this solution was filled in 2 R vials, glass type 1 (Schott AG, Mainz, Germany) which were closed using Teflon<sup>®</sup>-coated rubber stoppers from West Pharmaceutical Service, Inc. (Lionville, USA).

In total eight different formulations were prepared. The placebo formulation included histidine buffer and 8% (w/v) sucrose to adjust tonicity. All protein formulations were diluted to a final protein concentration of 25  $\mu$ g/mL by the histidine-sucrose buffer. For the preparation of an

adjuvant containing formulation, aluminum hydroxide gel (Alu-Gel-S suspension, Serva Electrophoresis GmbH, Heidelberg, Germany) was added in 40 fold excess to the protein solution. This protein containing suspension was gently stirred at 200 rpm for 13 hours before injection to provide sufficient time for the protein to adsorb to the aluminum hydroxide. The final concentration was 25 µg/mL of total protein and 8% sucrose (w/v) at pH 5.7. The adjuvant containing protein suspension was freshly prepared due to the instability of alum suspensions during freezing.

Six vials containing 10 mg/mL muAb solution were exposed to light. Three vials were irradiated for 48 h and three vials for 120 h using a Suntest CPS (Heraeus Holding, Hanau, Germany). A xenon lamp with a wavelength spectrum from 200 to 1000 nm was used for light exposure and the radiation was fixed at  $55 \pm 5 \text{ W/m}^2$ . A filter made of sheet glass was installed, to obtain a radiation close to the real light.

Soluble oligomers in the sample exposed to light for 48 h were separated by asymmetrical flow field-flow fractionation (AF4). The oligomer fractions of 10 injections were collected in glass tubes and concentrated by centrifugation using disposable Protein concentrators<sup>®</sup> (Thermo Scientific, Pierce Biotechnologies, Rockford, USA). The membrane inside was made of regenerated cellulose with a molecular weight cut-off (MWCO) of 9 kDa. Centrifugation was performed at 4000 x g and the concentration of the resulting fractions was determined by UV absorbance spectroscopy in a quartz cuvette at 25°C using an Agilent 8453 UV-visible spectrophotometer (Agilent Technologies, Waldbronn, Germany). Finally, samples were diluted to 25 µg/mL total protein concentration and subsequently stored at -80°C.

Aggregates were obtained by stirring for 48 h at 25°C and 400 rpm using Teflon<sup>®</sup>-coated stirring bars of 6 x 3 mm in size (VWR International, Darmstadt, Germany). To obtain aggregates from shaking, samples were shaken in horizontal circles for 48 h at 25°C and 800 rpm. To obtain aggregates by heating the protein solution was stored at 60°C for 48 h. Each process (stirring, shaking, and heating) was conducted in three different vials that were pooled directly after termination of the incubation step. All samples were diluted at a 1:1 ratio with placebo buffer before centrifugation at 4000 x g for 10 minutes using a Megafuge 1.0 R and the corresponding 7570F rotor (Heraeus Instruments, Santa Clara, USA). The pellets formed by centrifugation were re-suspended in the placebo buffer to a final concentration of approximately 25 µg/mL protein. This calculation was based on the concentration of protein determined in the supernatant and the volume of supernatant. The amount of protein in the supernatant was subtracted from the original protein concentration of 10 mg/mL and the residual mass of protein had to be present in the insoluble pellets after centrifugation. All samples except the alum-containing sample were stored at -80°C prior to injection. Prior to injection into animals each group was analyzed in triplicate by light obscuration using a Pamas SVSS instrument (Pamas, Rutesheim, Germany) to determine the particle loading.

#### 8.2.2.2 Size exclusion chromatography (SEC)

Size exclusion chromatography to determine concentration and size of soluble protein species in the muAb samples was conducted as described in section 7.2.2.

#### 8.2.2.3 Asymmetrical flow field-flow fractionation (AF4)

The set-up of the AF4 measurements was previously described in chapter 6 (see section 6.2.2). A sample volume of 100  $\mu\text{L}$  was injected into the system and the fractions of ten single runs were collected.

#### 8.2.2.4 Light obscuration (LO)

Light obscuration measurements were conducted as described in section 7.2.3.

#### 8.2.2.5 Turbidity measurements

Turbidity was analyzed according to section 3.2.3.3.

#### 8.2.2.6 Endotoxin testing

The endotoxin load in the samples was analyzed as described in section 7.2.4.

#### 8.2.2.7 Fourier transform infrared spectroscopy (FTIR)

For the determination of changes in secondary structure of the protein, native and aggregated formulation samples except the alum-containing formulation were analyzed directly after preparation at 10 mg/mL by FTIR in attenuated total reflection (ATR) mode. 20 mM histidine buffer at pH 5.7 served as background. A Bio-ATR II unit of a Tensor 27 spectrometer (Bruker Optics GmbH, Ettlingen, Germany) at 20°C was used. Spectra were collected from 4000  $\text{cm}^{-1}$  to 850  $\text{cm}^{-1}$  with a resolution of 4  $\text{cm}^{-1}$ . 120 scans were averaged for each sample measurement. Each spectrum was background corrected and vector normalized on the amide I band. Finally, the second derivatives of the spectra were calculated and smoothened on 17 points according to the Savitzky-Golay algorithm.

#### 8.2.2.8 Ultraviolet (UV) absorbance spectroscopy at 280 nm

UV absorbance spectroscopy to determine protein concentration was either performed in a quartz cuvette at 25°C using an Agilent 8453 UV-visible spectrophotometer (Agilent Technologies, Waldbronn, Germany) or in a 96 well-plate made of quartz at 25°C using a FLUOstar Omega (BMG Labtech GmbH, Offenburg, Germany). For each measurement a linear calibration curve including at least three different concentrations of muAb was prepared and the concentration of the samples was calculated based on the Lambert-Beer-law. Each measurement was background corrected.

#### 8.2.2.9 Immunization protocol

All formulations were administered subcutaneously into the scruff of the neck at a dose of 5  $\mu\text{g}$  of protein drug. Each time 200  $\mu\text{L}$  of the formulations containing 25  $\mu\text{g/mL}$  of protein

were injected. Histidine buffer (20 mM, pH 5.7, containing 8% (w/v) sucrose) served as formulation buffer and negative control. Injections were carried out on days 1, 2, 4, 6, 13, 20, 27 of the study followed by a six week recovery period.

#### 8.2.2.10 Collection of blood samples

Blood were obtained from the tail vein by collecting 120  $\mu$ L of blood on days 1 (prior to any injection), 6, 13, 20, and 27. All mice were sacrificed on day 71 of the study using a lethal dose of anesthetic (Ketamine/Xylazine) and blood was withdrawn from the *Vena cava*. Blood samples were collected in polypropylene tubes (no anticoagulant) and immediately centrifuged for 5 minutes at 4000 x g (Eppendorf MiniSpin<sup>®</sup>, Eppendorf AG, Hamburg, Germany) at room temperature. The serum was separated and stored at -80°C before analysis.

#### 8.2.2.11 Determination of anti-drug antibodies (ADAs)

The detection of anti-drug antibodies towards muAb was performed based on the method established in the previous study. Please refer to section 7.2.8.2 for details. In this study only the concentration of the detection antibodies (HRP-labeled goat anti-mouse immunoglobulines) was adjusted. A 1:75,000 dilution of isotype-specific (anti-IgG1, anti-IgG2a, anti-IgG2b and anti-IgG3) antibodies was used throughout this study.

Each serum sample was measured in triplicate in a 1:100 dilution. The results were normalized by calculating the absorbance ratio of each animal by dividing the absorbance measured on each day by the absorbance of day 1 (before any injection).

#### 8.2.2.12 Determination of drug levels in serum (pharmacokinetics, PK)

For the determination of muAb in serum samples triplicate measurements of each serum sample according to the method described in section 7.2.9 were performed.

#### 8.2.2.13 Statistical analysis

Each dosing groups had ten replicates and where applicable, the results are expressed as mean  $\pm$  standard error of the mean. Statistical analysis was carried by an analysis of variance (ANOVA) and the probability (p) was calculated. A probability of > 95 % ( $p < 0.05$ ) was defined as significant.

## 8.3 RESULTS

The aim of this study was to investigate the immunogenic potential of protein aggregates of a murine monoclonal antibody in mice. As the aggregates were artificially prepared in the lab, a number of complementary analytical techniques were employed to analyze if and how the native murine monoclonal antibody was affected by the applied stress.

### 8.3.1 Preparation and analysis of aggregates

The native protein stock solution contained 33 mg/mL of the monoclonal murine antibody (muAb). Size exclusion chromatography revealed  $97.98 \pm 0.40$  % monomer,  $0.91 \pm 0.22$  % fragments and  $1.08 \pm 0.21$  % aggregates in the native protein stock solution (data not shown).

After 48 h of light exposure soluble oligomers were separated by AF4. A total protein amount of 1 mg of the light exposed sample and 0.5 mg of the native muAb was injected, respectively. The fractograms of the irradiated samples and the native muAb are shown in Figure 8-1. At concentrations higher than 0.5 mg or 1 mg, overloading effects were observed. The irradiated sample was composed of  $17.4 \pm 3.9$  % monomer,  $4.0 \pm 0.3$  % fragments and  $74.4 \pm 3.9$  % oligomers with a total recovery of  $86.9 \pm 4.6$  %, meaning that some insoluble aggregates had also been formed which cannot be detected by AF4. The fraction eluting between 29.5 minutes and 35.5 minutes (illustrated by the green lines) was collected (see Figure 8-1). Previous studies revealed a mean approximate size of the soluble aggregates of 20 – 100 nm determined by dynamic light scattering (data not shown).

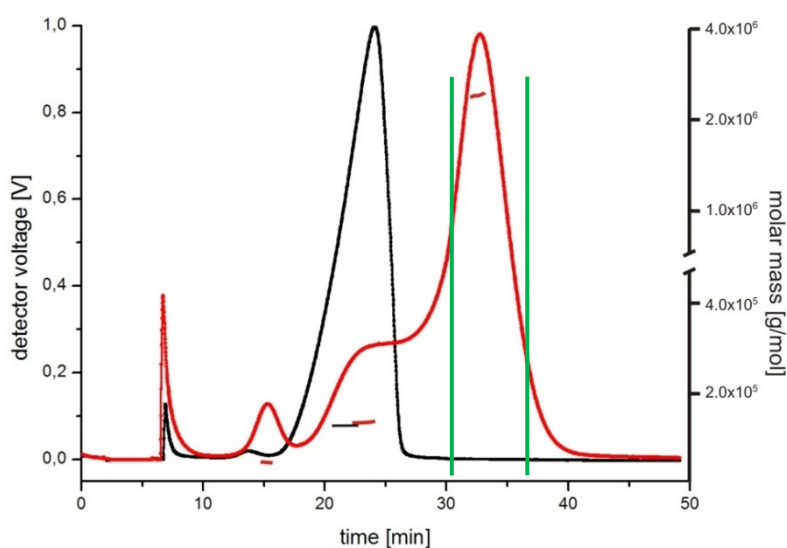


**Figure 8-1 – UV 280 nm fractograms and molar mass of murine IgG2c samples.**

Time dependent UV detector voltage at 280 nm and molar mass detection by MALLS of light exposed muAb (red line) and native muAb (black line) after separation by Eclipse 2.0. The collection period is displayed by the green lines.

Light obscuration measurements were carried out immediately after completion of the generation of the aggregates and after a storage time of at least 7 days at  $-80^{\circ}\text{C}$ . No differences were observed in the particle size distribution and total particle numbers (data not shown) between the samples immediately after preparation and the stored samples.

The by far highest numbers of subvisible particles were counted in the stirred samples, which contained more than 100,000 particles  $\geq 1 \mu\text{m}$ . The total particle numbers per mL of



species  $\geq 1 \mu\text{m}$  (see Table 8-1) in the other protein containing samples analyzed by light obscuration ranged from  $\sim 1000$  (native muAb) to  $\sim 21000$  (insoluble species from light exposure). The fractionated soluble aggregates generated by light exposure were smaller than  $1 \mu\text{m}$  in size and low numbers of particles in the micrometer range were detected within that sample. None of the formulations contained more than 300 particles larger than  $10 \mu\text{m}$ . The light obscuration measurements were conducted at the final concentration of  $25 \mu\text{g/ml}$  and after several days of storage at  $-80^\circ\text{C}$ .

Turbidity measurements were carried out in triplicate and are summarized in Table 8-1. Slightly increased turbidity values were obtained in the dosing groups containing aggregates. Stirring leads to the strongest elevation of turbidity, whereas the turbidity of the sample containing insoluble aggregates generated by light exposure is comparable to the solution containing native muAb.

**Table 8-1 – Summary of turbidity measurements and particle counts per ml of the different formations investigated in this study.**

Dosing group	Description	Turbidity [FNU]	Particle counts $\geq 1 \mu\text{m}$ per mL	Particle counts $\geq 10 \mu\text{m}$ / $\geq 25 \mu\text{m}$
1	Placebo	0.60	170	21 / 5
2	Native muAb	0.80	900	5 / 2
3	Native muAb + Adjuvant	N/A	N/A	N/A
4	Soluble aggregates from light exposure	2.20	5000	27 / 1
5	Insoluble aggregates from light exposure	0.84	21000	59 / 2
6	Insoluble aggregates from stirring	3.97	107000	292 / 2
7	Insoluble aggregates from shaking	2.25	9000	4 / 1
8	Insoluble aggregates from heating	1.77	8000	14 / 1

The formulations were investigated by FTIR to observe changes in the secondary structure of the antibody after the different stress conditions. Figure 8-2 displays the 2<sup>nd</sup> derivative FTIR spectra of the muAb containing formulations (except the formulation containing native muAb plus Alum) directly after preparation.

The analysis of the FTIR spectra obtained from the different formulation shows that processing conditions such as stirring and shaking do not lead to a substantial alteration of the secondary structure of the antibody (Figure 8-2) as the spectra are very similar to those of the native muAb. In contrast, light exposure as well as storage at elevated temperatures of  $60^\circ\text{C}$  implied strong modifications in the conformation of the muAb and resulted in a strong decrease of the intramolecular  $\beta$ -sheet band at around  $1638 \text{ cm}^{-1}$ . At the same time, the absorbance of the intermolecular  $\beta$ -sheet band around  $1622 \text{ cm}^{-1}$  showed a strong increase in light exposed and heated samples.

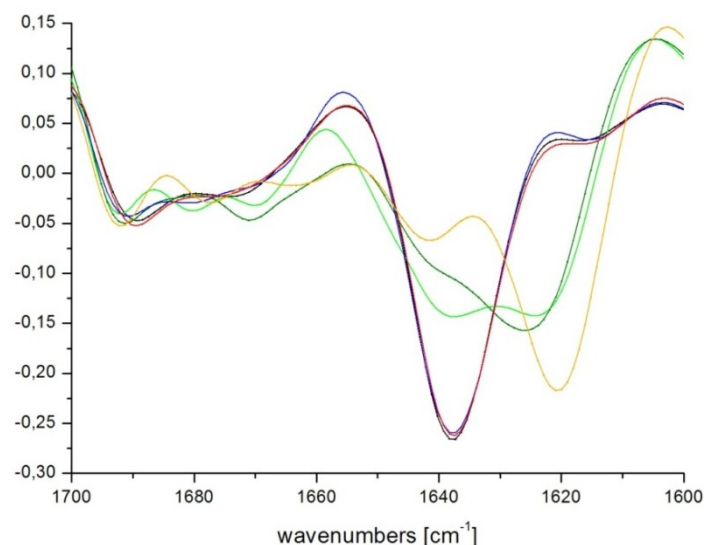


**Figure 8-2 – 2<sup>nd</sup> derivative FTIR spectra of the muAb samples for *in vivo* use directly after stressing.**

The black line represents the spectrum of the native muAb, the blue line represents the spectrum of the stirred sample, and the red line represents the spectrum of the shaken sample. The light green line represents the secondary structure of the protein after 48 h light exposure, the dark green line represents the sample after 120 h light exposure, and the yellow line represents the muAb sample after storage at 60°C.

### 8.3.2 Preparation and analysis of the adjuvant samples

For the preparation of the adjuvant containing samples, the murine monoclonal antibody was adsorbed to aluminum hydroxide. The supernatant of the adjuvant containing sample after centrifugation was analyzed and  $3.0 \pm 0.01$  µg/mL of muAb were detected by UV absorbance spectroscopy. In conclusion, approximately 22 µg/mL (approximately 90 %) of protein had been adsorbed to the surface of the aluminum hydroxide particles.

### 8.3.3 Testing of the samples for the presence of endotoxins

Prior to the study, all formulations except the adjuvant sample were analyzed for the presence of endotoxins, and endotoxin levels below 0.25 EU/mL. Therefore, the generation of undesirable immune responses triggered by pyrogens which may have biased the results of this study can be excluded. Due to the high turbidity of the adjuvant sample, no endotoxin determination was feasible.

### 8.3.4 Detection of immune response – Anti-drug antibodies towards muAb

In this study, a murine monoclonal antibody was investigated in C57BL/6 and BALB/c mice. No cross-reactive antibodies against the native molecule were expected in the C57BL/6 animals. A minor response to the administered muAb was expected in BALB/c mice [Martin *et al.*, 1998]. Nonetheless, the generation of anti-drug antibodies directed against aggregates is assumed to be stronger compared to the immune response of BALB/c mice that received the native muAb. Different IgG subtypes were analyzed and the results of the three control groups

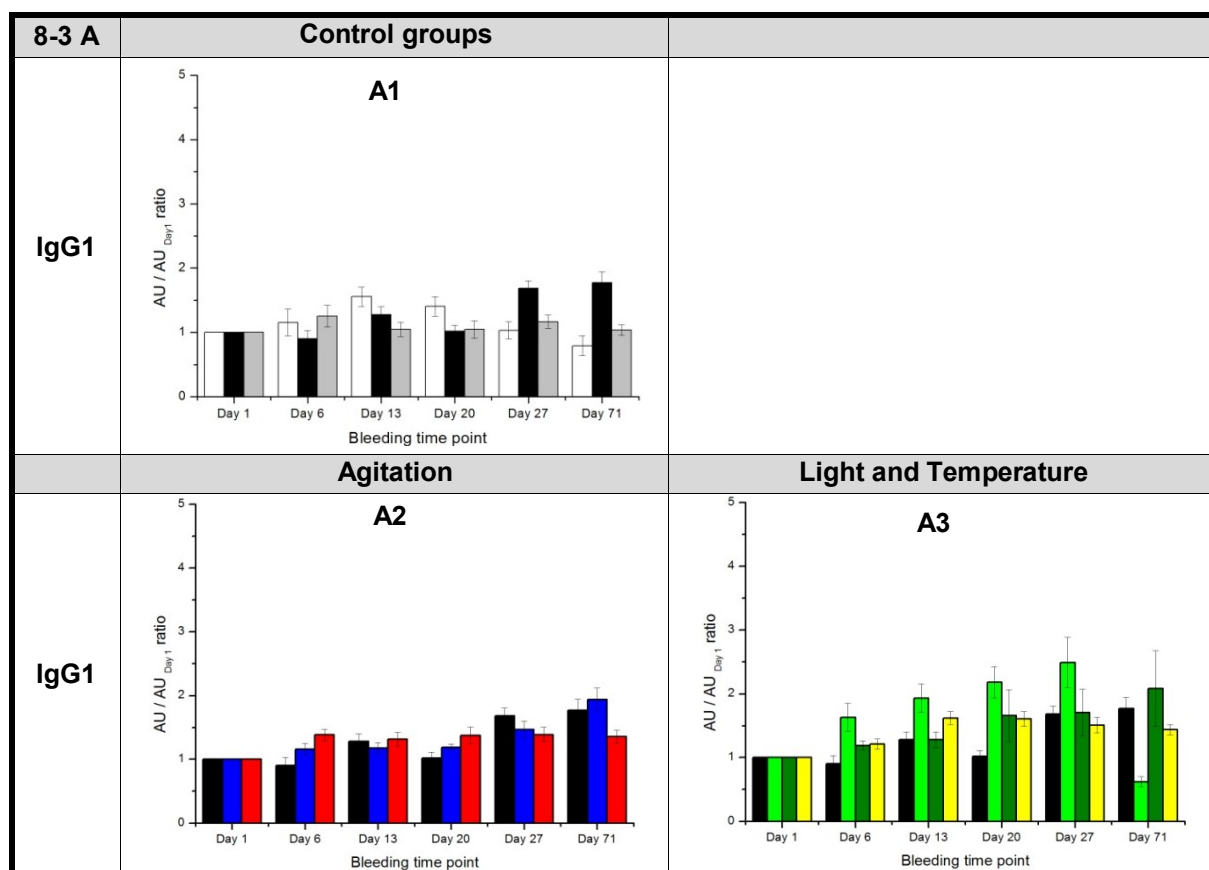
in both mouse strains are shown in Figure 8-3. The placebo and the native muAb group served as negative control groups, whereas the adjuvant-containing formulation served as a positive control for the generation of anti-drug-antibodies, as alum has been described in literature to induce a reliable antibody ( $T_H2$ ) response [Petrovsky *et al.*, 2004].

#### 8.3.4.1 anti-muAb antibodies in C57BL/6 mice

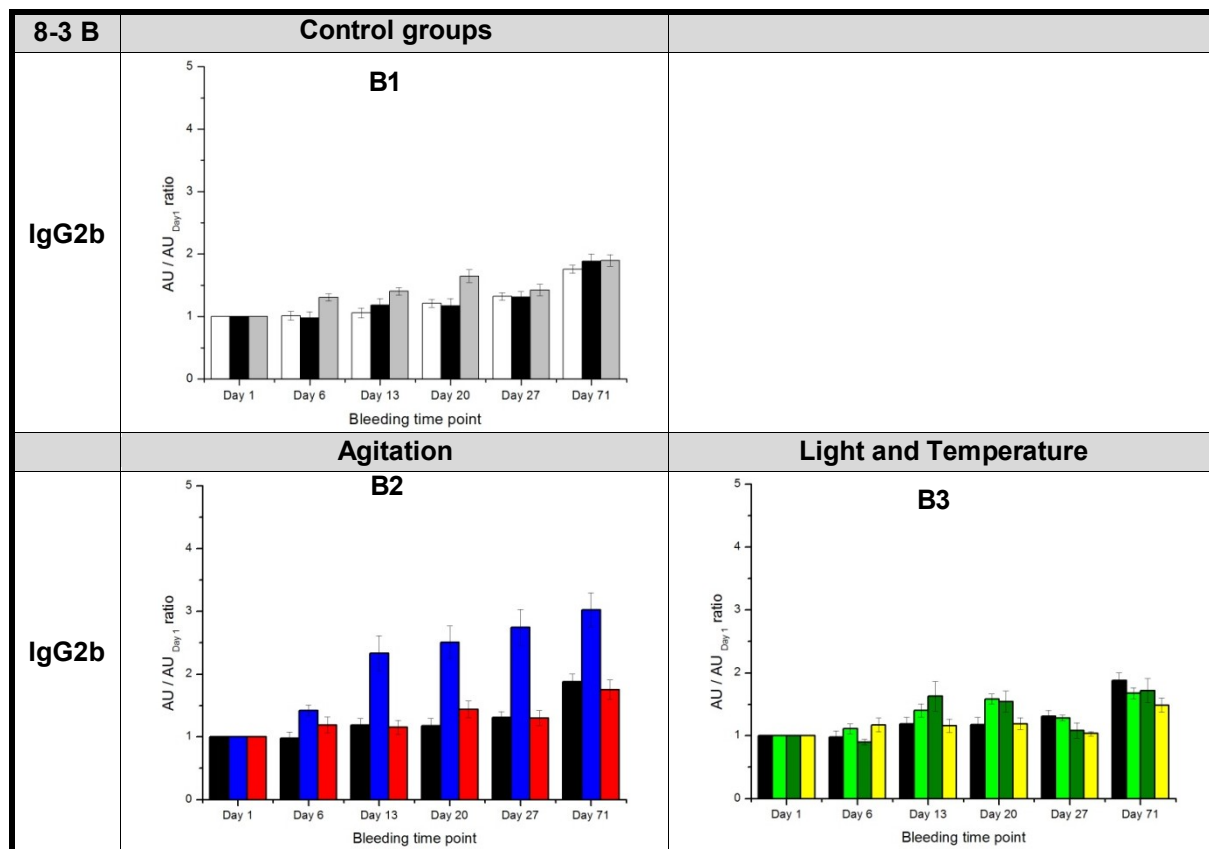
Figure 8-3 provides an overview of different IgG isotype results from anti- muAb antibody detection in C57BL/6 mice. Figures 8-3, A1 to A3 represent the results of anti-IgG1 muAb antibodies, B1 to B3 the results of anti-IgG2b muAb antibodies and C1 to C3 represent the results of anti-IgG3 muAb antibodies.

In C57BL/6 mice, the placebo formulation as well the formulations containing the native muAb or the native muAb plus adjuvant induced a rather weak immune response which was detectable by the generation of anti-muAb antibodies of IgG1, IgG2b and/or IgG3 isotype. In IgG1 isotype only the native muAb shows a response on days 27 and 71. The absorbance ratios of IgG2b detection show a very similar minor increase of all three control groups throughout the study. Significantly ( $p < 0.05$ ) increasing absorbance ratios were detected for group 3 (adjuvant plus native muAb) on days 20, 27 and 71 and for group 2 (native muAb) on days 27 and 71 in IgG3 ELISA. Confirming the expectations, after administration of the placebo formulation to C57BL/6 mice, the absorbances relative to day 1 (prior to any injection) were not substantially enhanced in any of the anti-muAb isotype assays.

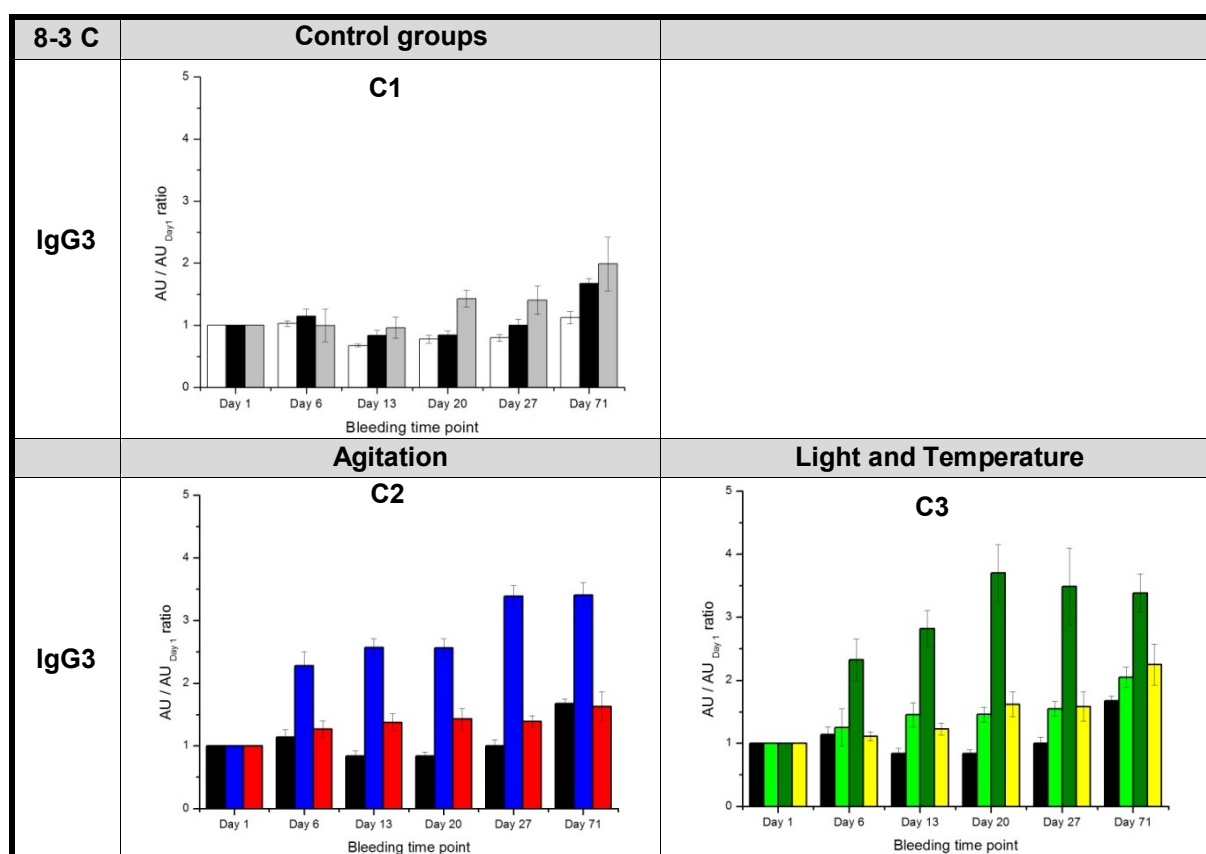
Increased IgG1 levels in C57BL/6 mice directed towards muAb were detected after the administration of the soluble aggregates generated by light exposure and fractionated by AF4. The results showed steadily increasing anti-muAb IgG1 levels from day 6 to day 27 that drop back to the base level or even below that after the recovery of 6 weeks on day 71 (Figure 8-3, A3). A maximum absorbance ratio of 2.5 was observed on day 27. Subsequently, the IgG1 levels directed towards muAb decrease within the 6 week recovery phase. On day 71, the absorbance ratio was below the basic value of day 1, before any injection. The IgG1 immune response directed towards muAb after administration of the soluble aggregates was significantly enhanced compared to the response after administration of all other investigated formulations including the native muAb, serving as reference. The insoluble aggregates (Groups 5-8) failed to induce a significantly higher immune response of IgG1 antibodies than the native muAb in C57BL/6.



Figures 8-3 A – Absorbance unit ratios of anti-IgG1 muAb detection in C57BL/6



Figures 8-3 B – Absorbance unit ratios of anti-IgG2b muAb detection in C57BL/6



**Figures 8-3 C – Absorbance unit ratios of anti-IgG3 muAb detection in C57BL/6**

Figures 8-3 A-C:

The results of the control groups are shown in A1, B1 and C1: placebo in white, native muAb in black and native muAb + alum in grey. Figures A2, B2 and C2 represent the anti-muAb results for the mice that received aggregates generated by agitation (stirring in blue and shaking in red) compared to the native muAb (black). And Figures A3, B3 C3 represent the anti-muAb results of the mice that received aggregates from light stressed (soluble aggregates in light green, and insoluble aggregates in dark green) or heated muAb (yellow). The error bars represent the standard error of the mean of ten animals per group.

However, these aggregated species resulted in immune responses expressed by the increases of other IgG isotypes. The aggregates generated by stirring were capable of eliciting antibodies of anti-muAb IgG2b isotype in C57BL/6 starting on day 6 which constantly increased until day 71. The other aggregates, either soluble or insoluble, and the native muAb resulted in increased absorbance ratios especially on day 71, though the anti-muAb IgG2b release in those animal groups was on a similar level and none of the aggregates exceeded the induction of ADAs by the native protein.

Considering the IgG3 isotype levels all aggregate containing formulations resulted in a significant increase in C57BL/6 mice starting on day 6 ( $p < 0.05$ ). Slightly higher anti-muAb IgG3 levels were detected after administration of the formulation containing soluble aggregates when the results were compared to the administration of native muAb from day 13 onwards. Strongly elevated absorbance ratios were detected for anti-muAb IgG3 after administration of insoluble aggregates generated by light exposure or stirring. On days 27 and 71 the highest

ratios were observed within both groups. The aggregates generated by shaking and those generated by storage at 60°C show only a minor IgG3 response towards muAb.

In summary, the C57BL/6 mice showed minor immune responses to the native muAb (Group 2) after repeated administration, expressed in slightly enhanced IgG1, IgG2b and IgG3 levels on day 71. The response to the adjuvant group (Group 3) was not significantly higher compared to the native muAb group (Group 2). Regarding the aggregate containing test formulations the insoluble aggregates obtained either by stirring or by light exposure revealed the highest anti-muAb antibody levels, especially of IgG3 isotype, compared to the administration of native muAb. Additionally, the soluble aggregates obtained by light exposure resulted in enhanced IgG1 levels concomitant to repetitive administration of these species, that not persist throughout the recovery phase.

#### 8.3.4.2 anti-muAb antibodies in BALB/c mice

Figure 8-4 provides an overview of the different anti-muAb IgG isotypes results in BALB/c mice. In BALB/c mice, the administration of the placebo formulation did not result in enhanced anti-muAb IgG1 generation ( $p < 0.01$ ) whereas formulations containing the native muAb or native muAb plus adjuvant resulted in strongly enhanced anti-muAb IgG1 levels (Figure 8-4, A1), commencing on day 13. This level of anti-muAb IgG1 remained on a stable level until day 71. The level of anti-muAb IgG1 was significant higher ( $p < 0.01$ ) in mice that received the adjuvant containing formulation (Group 3) than in the mice that obtained the native muAb (Group 2).

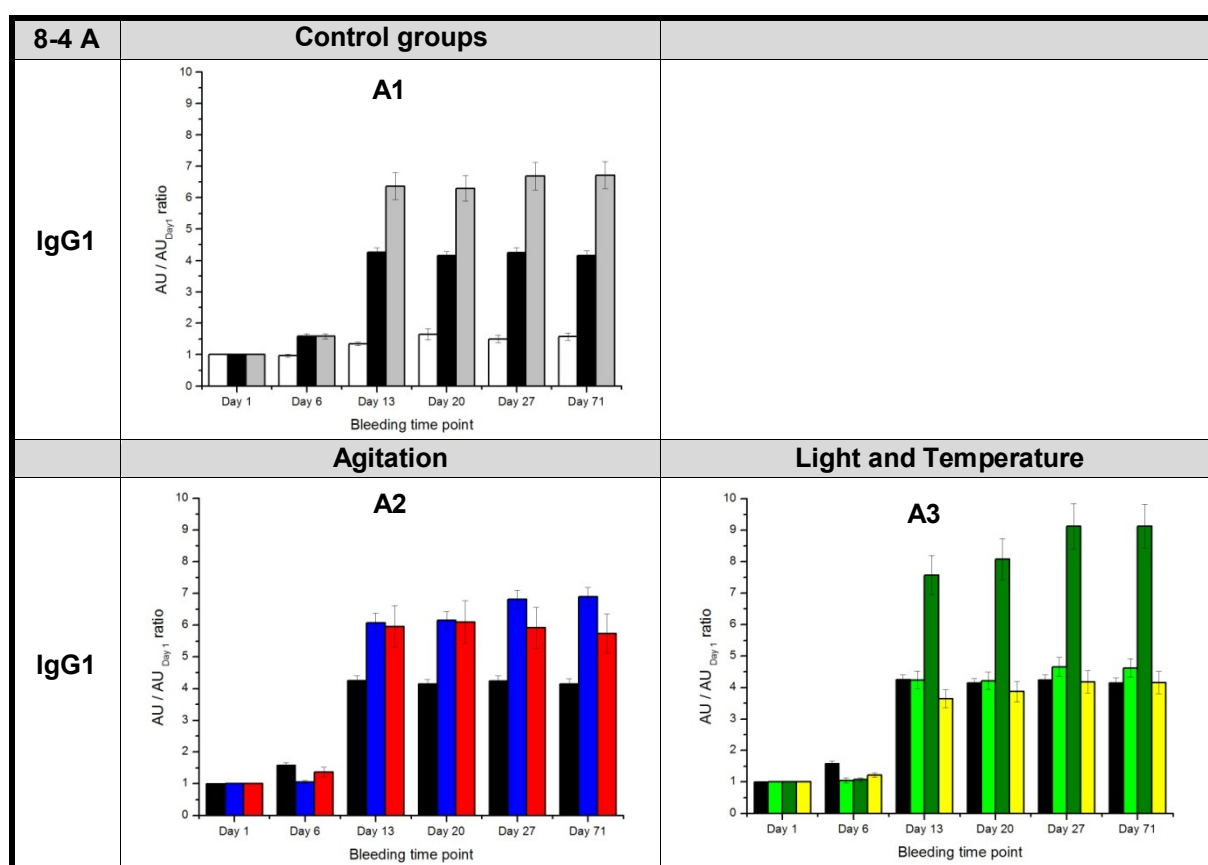


Figure 8-4 A – Absorbance unit ratios of anti-IgG1 muAb detection in BALB/c

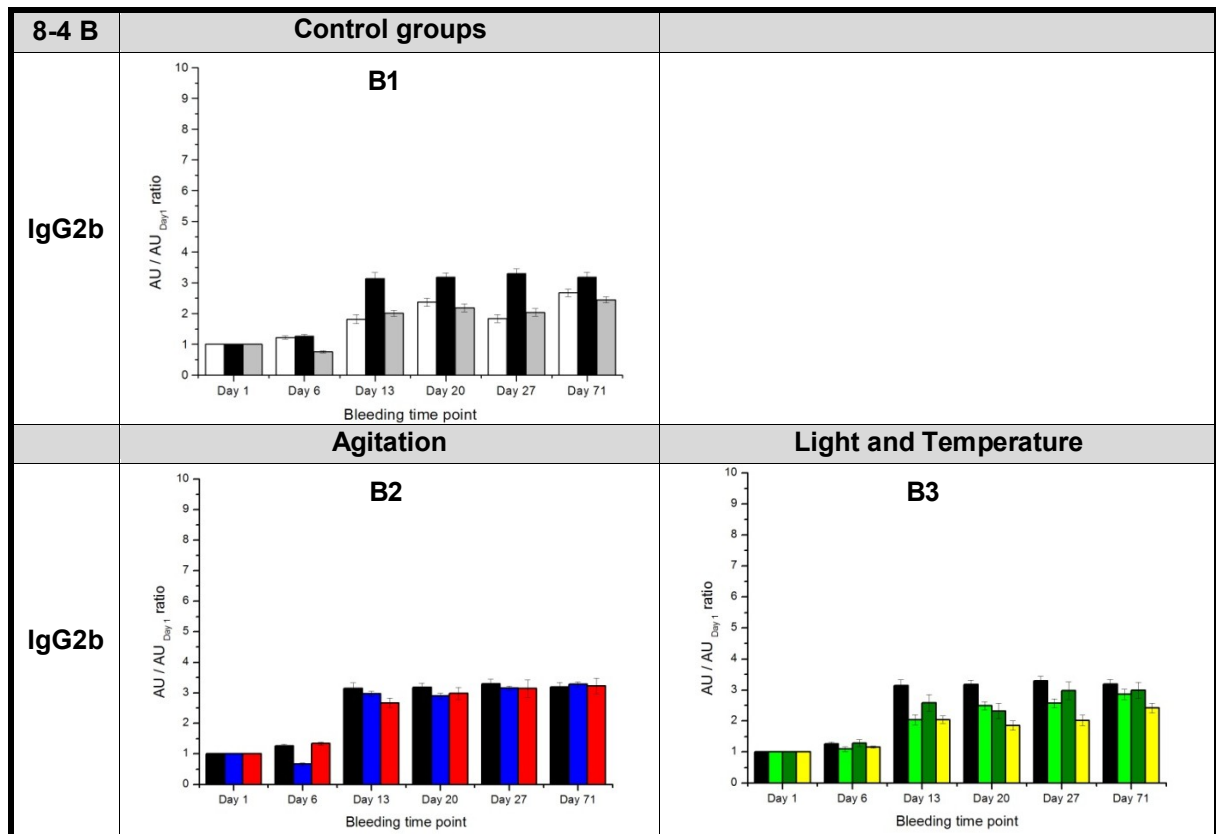


Figure 8-4 B – Absorbance unit ratios of anti-IgG2b muAb detection in BALB/c

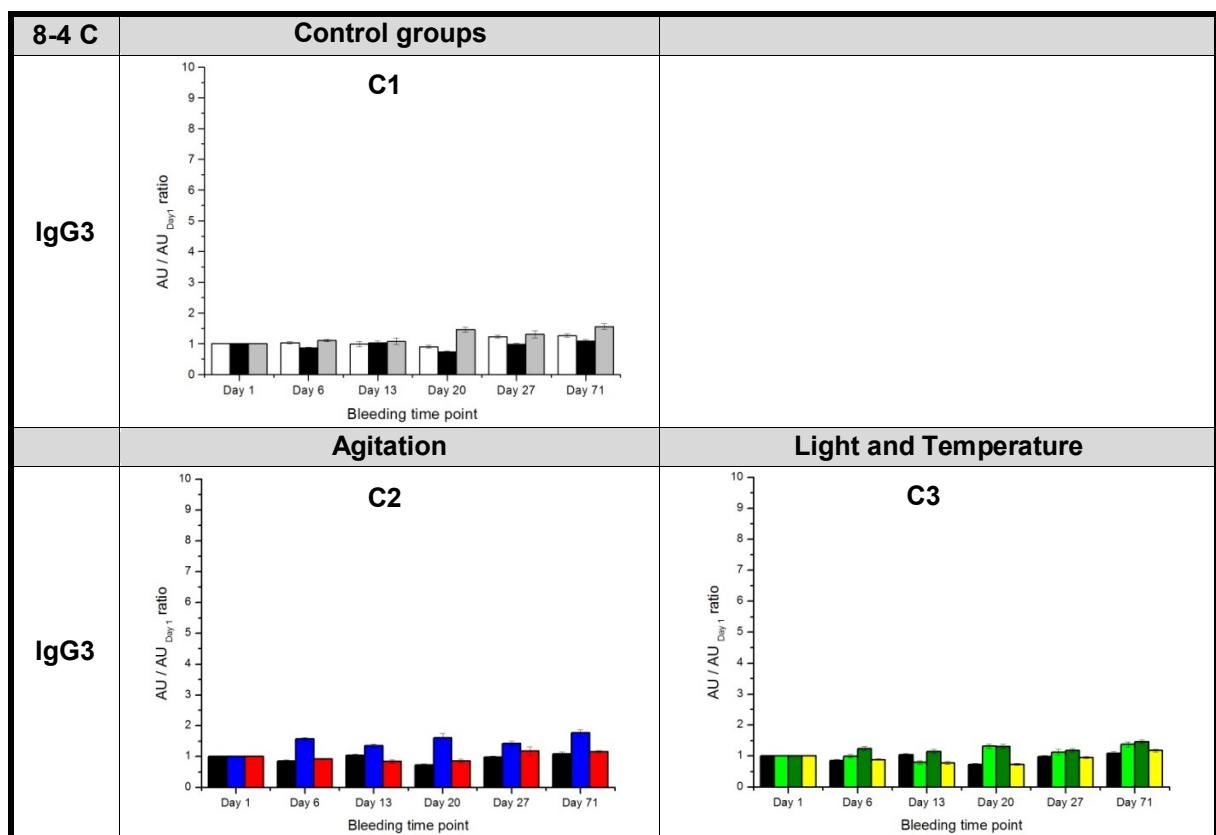
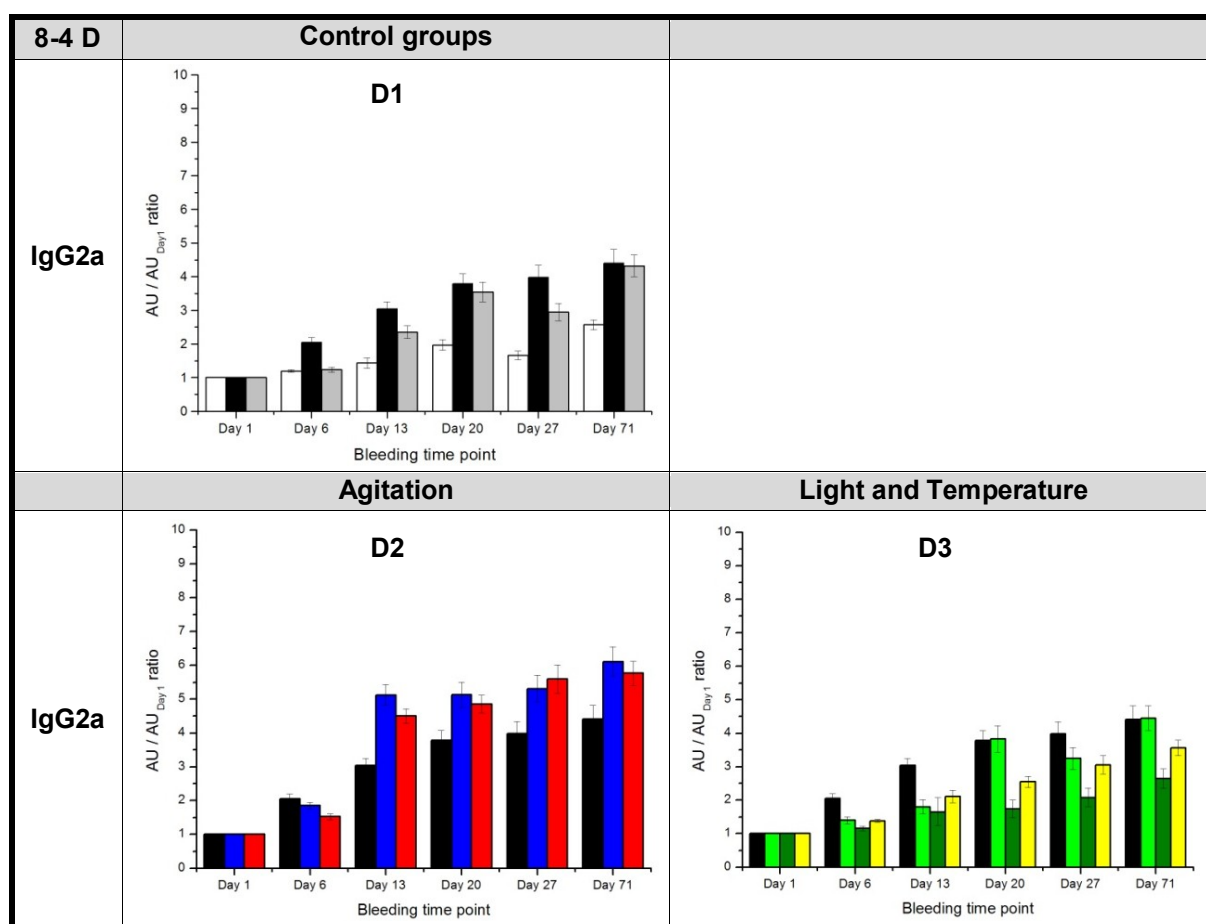


Figure 8-4 C – Absorbance unit ratios of anti-IgG3 muAb detection in BALB/c



**Figure 8-4 D – Absorbance unit ratios of anti-IgG2a muAb detection in BALB/c**

Figures 8-4 A-D:

The results of the control groups are shown in A1, B1, C1 and D1: placebo in white, native muAb in black and native muAb + alum in grey. Figures A2, B2, C2 and D2 represent the anti-muAb results for the mice that received aggregates generated by agitation (stirring in blue and shaking in red) compared to the native muAb (black). And Figures A3, B3, C3 and D3 represent the anti-muAb results of the mice that received aggregates from light stressed (soluble aggregates in light green and insoluble aggregates in dark green) or heated muAb (yellow). The error bars represent the standard error of the mean of ten animals per group.

A slight but significant enhancement in the generation of ADAs of IgG2b isotype in BALB/c was initiated by native muAb samples, starting on day 13 (Figure 8-4, B1). Instead, the anti-muAb IgG2b responses to the placebo formulation and the adjuvant-containing formulation did not significantly increase over the duration of the study. None of those three formulations resulted in anti-muAb IgG3 release in BALB/c mice (Figure 8-4, C1). As shown in Figure 8-4, D1 a continuous increase of anti-muAb IgG2a levels in BALB/c mice from day 6 onwards was observed, resulting from the administration of the native muAb. From day 13 onwards also anti-muAb IgG2a levels were observed after administration of the adjuvant-containing formulation.

It is important to note that, in BALB/c mice, the two formulations consisting either of native muAb or of soluble aggregates did not differ in the generation of anti-muAb antibodies. After administration of this aggregate species IgG1, IgG2a and IgG2b isotypes directed towards muAb were generated in BALB/c mice, all of them starting on day 13 and steadily increasing



over time and maintaining high absorbance ratios on day 71. The magnitude of the absorbance ratios achieved was comparable to that of the mice that received the native muAb formulation. In this respect no increased immunogenicity of these soluble aggregates compared to the native protein could be determined in BALB/c mice.

The animals that received insoluble aggregates from light exposure (Figure 8-4, A3), stirring or shaking (Figure 8-4, A2), showed significantly higher absorbance ratios in their serum samples compared to those that received the native protein ( $p < 0.05$ ), whereas the other aggregate containing formulations (soluble aggregates from light exposure or insoluble aggregates from heating (Figure 8-4, A3)), did not show any enhancement compared to the native muAb formulation. The highest ratios (around 10) were detected in IgG1 levels after administration of the insoluble species generated by light irradiation (Group 5), followed by those generated by stirring (Group 6) and shaking (Group 7). Both latter groups of insoluble aggregates generated by agitation predominate the response of IgG2a isotype as well (Figure 8-4, D2). On day 13, these groups showed approximately five times higher absorbance values compared to day 1. The mean values slowly increased until day 71. The other groups that obtained aggregates (Groups 4, 5 and 8, Figure 8-4, D3)) showed a slow increase over time as well, though never outreaching the response to the native muAb. Regarding ADAs of isotype IgG2b, the administration of none of the aggregates initiated a stronger generation compared to the native muAb. Finally, all eight formulations investigated did not induce an IgG3 response directed towards muAb in BALB/c mice.

In summary, the anti-muAb antibody response in BALB/c was dominated by significant antibody levels elicited by the administration of native muAb. Comparing the different ADA isotypes incorporated in this study, the IgG1 response is the most important in BALB/c mice. The adjuvant containing formulation as well as three out of five aggregate containing formulations resulted in higher IgG1 responses compared to the native muAb formulation: insoluble aggregates from light exposure, stirring, and shaking. Insoluble aggregates from stirring and shaking but not from light exposure additionally exceed the IgG3 response to native muAb. In none of the ADA isotypes the soluble aggregates obtained by light exposure or the insoluble aggregates obtained by storage at elevated temperatures ever top the immune response to the native muAb molecule. Furthermore, in BALB/c mice no alteration in the IgG3 levels were detected at all.

#### 8.3.4.3 Comparison of C57BL/6 mice and BALB/c mice

The repetitive administration of the muAb formulations revealed completely different ADA responses in C57BL/6 and BALB/c mice. The anti-drug antibody responses towards the control groups substantially differ between the two mouse strains. No substantial immune response against the placebo formulation was detected in either mouse strain, but the responses towards the native muAb formulation (Group 2) and adjuvant containing formulation (Group 3) significantly differ between the two strains: BALB/c mice show strongly elevated

immune responses (especially of IgG1 isotype) to the native muAb and adjuvant containing formulations compared to the C57BL/6 mice. Interestingly, the alum containing positive control sample resulted only in an increase of IgG1 ADAs in the BALB/c mice, though a high immune response in both species and more IgG subtypes was expected. Figure 8-5 provides a summary of the diverging IgG1 responses against native muAb in both mouse strains.

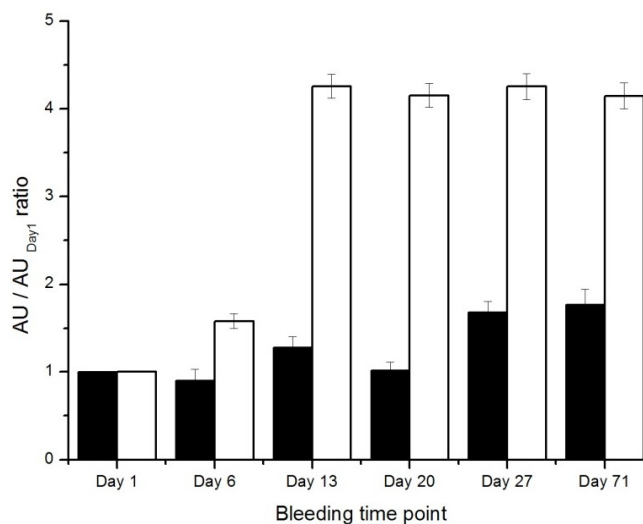


**Figure 8-5 – IgG1 absorbance unit ratios of Group 2 at the different blood sampling time points.**

The black bars represent the results of C57BL/6 mice and the white bars represent the results of BALB/c mice. The error bars represent the standard error of the mean of ten animals per group.

The enhanced absorbance ratios pursued in the IgG1 responses towards the test groups of BALB/c mice that received aggregate containing formulations. In these mice, three test groups exceeded the IgG1 immune response of the native muAb group: insoluble aggregates from light exposure, stirring, and shaking. In none of these groups an IgG1 immune response was detected in C57BL/6 mice. The latter mouse strain only revealed slightly enhanced IgG1 ADA levels to soluble aggregates from light exposure. However, the insoluble aggregates from light exposure and stirring elicited ADAs of IgG3 isotype in C57BL/6 mice, whereas no IgG3 response was detectable in BALB/c (see Figure 8-6).

Diverging immune responses were also detected for IgG2b antibody levels. Compared to the administration of native muAb the aggregates from stirring induced significantly higher numbers of anti-muAb antibodies of IgG2b isotype in C57BL/6 mice but not in BALB/c mice.

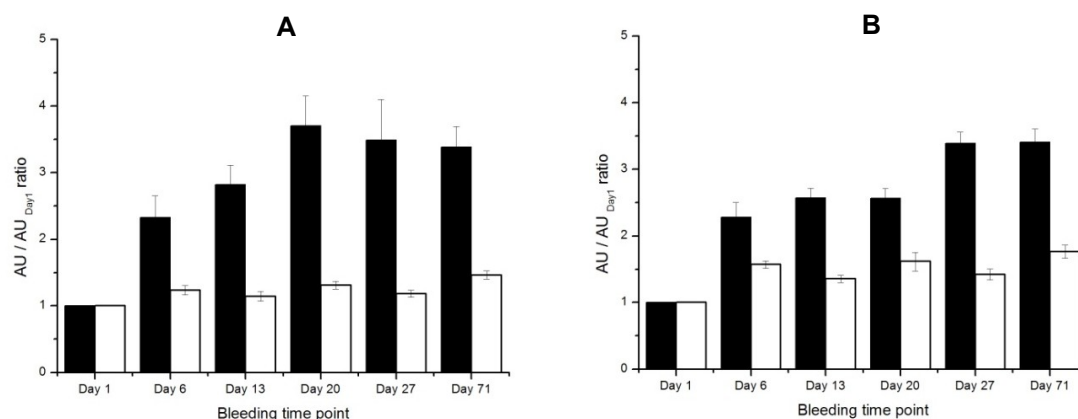


**Figure 8-6 – IgG3 absorbance unit ratios of groups 5 and 6 at the different blood sampling time points.**

A shows the results for group 5 (insoluble aggregates from light exposure) and B shows the results from group 6 (insoluble aggregates from stirring). The black bars represent the results of C57BL/6 mice and the white bars represent the results of BALB/c mice. The error bars represent the standard error of the mean of ten animals per group.

### 8.3.5 Detection of muAb circulating in the blood stream – pharmacokinetics

The determination of the pharmacokinetics is of great importance since it is crucial to determine how fast the drug is cleared from the blood stream in the presence and absence of ADAs. It can be assumed that significant amounts of ADAs could strongly reduce circulation time and serum concentration of the monoclonal antibody. An ELISA based on murine TNF- $\alpha$ , the antigen to the monoclonal antibody, was performed. The recovery of muAb in the formulations prior to injection was determined. In all formulation, except for the formulation containing only insoluble aggregates after light exposure, substantial amounts of muAb were quantified with the ELISA (data not shown). Figure 8-7 provides an overview of the results obtained for muAb pharmacokinetics.

The mice that received the placebo formulation or the formulations containing the insoluble aggregates showed no quantifiable amounts of muAb in the serum samples, neither in C57BL/6 nor in BALB/c mice (data not shown). In C57BL/6 mice both, the native muAb formulation and the native muAb plus adjuvant formulation, show serum levels that do not point to the generation of ADAs. The maximum serum levels of muAb were measured on day 6, after three booster injections on days 1, 2 and 4. Later on, when only administered weekly, the levels decreased slowly reaching the basic level after 6 weeks washing out phase. Since monoclonal antibodies are characterized by half-lives of several days to weeks the results obtained for those groups are reflecting a regular, undisturbed pharmacokinetic profile.

However, the results for the native muAb formulation and the adjuvant formulation were considerably different in BALB/c mice, where muAb was only detected on day 6. This is similar in mice of groups 2 and 3 (see Figure 8-7, A2 and B2). Neither after administration of native muAb formulation nor after administration of native muAb plus adjuvant circulating muAb molecules were detectable at any other bleeding time point than day 6.

The repetitive administration of the formulation containing soluble aggregates resulted in no detectable free circulating muAb molecules in C57BL/6, whereas levels of muAb were detectable in BALB/c. The absorbance ratios in group 4 of BALB/c were lower compared to those on day 6 in animals of groups 2 or 3 and had a maximum on day 13 that was constantly decreasing until on day 27 the basic value was achieved again.

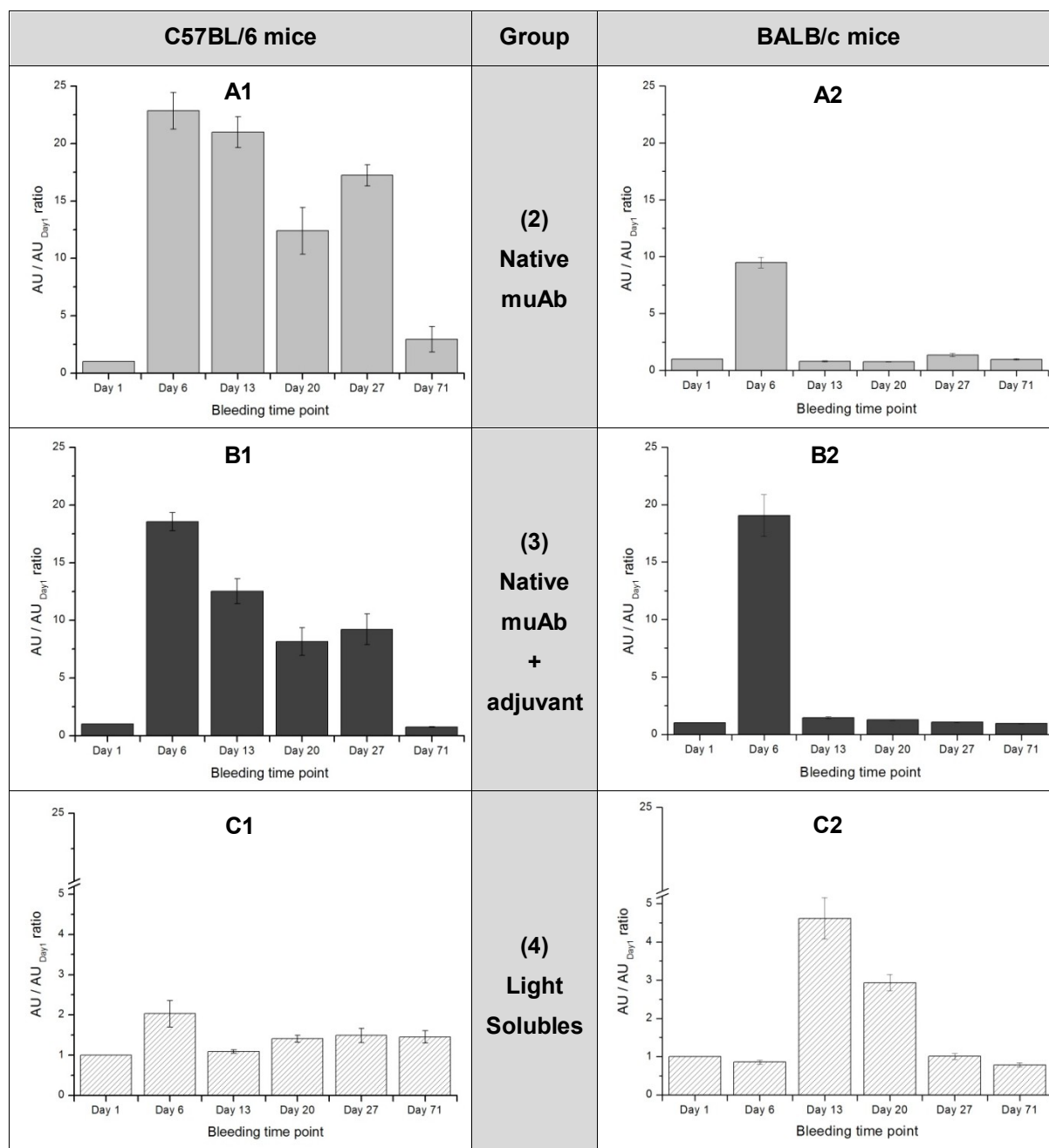


**Figure 8-7 – Absorbance unit ratios of PK ELISA in C57BL/6J and BALB/c mice.**

**A)** After receipt of the native muAb formulation. **B)** After receipt of the formulation consisting of native muAb + adjuvant. **C)** After receipt of the soluble aggregates after 48 h of light exposure.

## 8.4 DISCUSSION

The study for the first time investigates the immune response to protein aggregates in two different wild-type mouse strains. The C57BL/6 animals were selected, since the monoclonal antibody investigated in this study was generated in this strain. Additionally BALB/c mice were selected, because of their well-known strong  $T_H2$  immune response, resulting in strong antibody elicitation [Watanabe *et al.*, 2004]. The subcutaneous route of administration was chosen as this is commonly used in patient's therapy using monoclonal antibodies besides the intravenous administration [Berger *et al.*, 2002]. Also, the subcutaneous administration is, in general, thought to be more immunogenic than other administration routes [Wierda *et al.*, 2001].

The antibody elicitation after administration of five different aggregate formulations of muAb was investigated. Those formulations were prepared under different conditions and consisted of aggregates differing in size and structural properties. According to the immunon model hypothesized by Dintzis *et al.*, aggregates of large sizes and repeating epitopes on their surface are capable to induce an immune response [Dintzis *et al.*, 1976]. The mechanisms behind immune responses to protein aggregates have not yet been clarified. Currently, administrative organizations and industrial research focus on anti-drug antibodies that potentially can have an impact on the efficacy of the drug, altering pharmacokinetics and thus the success of the therapy. Thus, it is supposed, that aggregates with structural properties close to the native protein are foremost crucial in the formation of ADAs. However, it is entirely conceivable that antibodies towards aggregate-specific structures can be generated as well, which probably do not have a large impact on the pharmacokinetics of the therapeutic protein, but might lead to adverse effects such as allergic reactions.

The structure and size of the administered species was investigated beforehand. The secondary structure of the native and the aggregated muAb samples was investigated by FTIR after the completion of the stress procedure, but not of the final injection samples, since the final concentration of 25  $\mu\text{g/mL}$  of total protein is too low for FTIR analysis. Of the five formulations containing aggregates, three contained protein species with a strongly modified secondary structure (Groups 4, 5 and 8). Exposure to light (Groups 4 and 5) as well as storage at elevated temperatures (Group 8) resulted in strong changes of the protein as indicated by unfolding, whereas after shaking (Group 7) and stirring (Group 6) the protein mostly maintained its secondary structure.

Unfolding and structural modifications might imply the formation of antibodies that are not capable of binding to muAb. In this case, the ADAs will not be detected in this assay. Therefore, in theory the subcutaneously injected formulations of aggregated antibody in this study should still be able to bind to the antigen, indicating a native-like structure and ensuring the generation of antibodies directed towards the original native structure of the drug molecule.

For the duration of the study, the animals were maintained in SPF conditions. Despite the repetitive administration of the native muAb to the host strain, the meticulous cleaning and preparation of all instruments and samples was suggested to keep constantly low background levels of immunoglobulins. The results detected in C57BL/6 mice indicated the absence of pathogens; however these mice are known to elicit fewer antibodies when compared to other mouse strain [Mills *et al.*, 2000]. The study only determined the generation of antibodies directed against the native muAb, but not towards the aggregates administered to the mice. Therefore, the results do not reflect the total levels of IgG isotype in the serum samples, but the levels specifically directed towards the muAb molecule.

#### **8.4.1 Pharmacokinetics of muAb**

After administration of the placebo formulation no muAb was detectable in the serum of the mice. The discrepancies between the pharmacokinetics profiles of the native drug in the control groups 2 and 3 of both mouse strains are obvious (see Figure 8-7). The C57BL/6 mice reveal the expected undisturbed profile possessing a maximum on day 6 and subsequently decreasing until day 71. In BALB/c, the maximum serum levels of muAb were reached on day 6 due to the repeated administration, although the absorbance ratios were lower than in C57BL/6. On day 13 no drug molecules were circulating any more in BALB/c mice of these dosing groups (Figure 8-7, A2 and B2). This profile strongly suggests the formation of anti-muAb antibodies after administration of native muAb and native muAb + adjuvant. The generated ADA molecules obviously captured the circulating muAb molecules and the resulting immune complexes were rapidly eliminated. The generation of antibodies by the human immune system is known to last several days [Vollmar, 2005] and to be similar to the murine immune system [Haley, 2003]. Thus the formation of ADAs is the reason for the inability to detect muAb after day 6.

The high recoveries of muAb in the sera of C57BL/6 mice that received the native muAb formulation or the native muAb plus adjuvant formulation indicate no substantial ADA formation. If ADAs would have been present, the immune complex formation would interfere with the detection of muAb in C57BL/6 mice. The slowly decreasing muAb levels in both groups (2 and 3) point in the same direction.

Interestingly, within each mouse strain the profiles are rather similar between the animals that received the native muAb and the animals that received the adjuvant plus native muAb. The expected “positive control” was not capable to induce ADA formation in C57BL/6 mice, presumably due to their preferred  $T_H1$  response. In BALB/c mice both formulations elicited ADAs. However, on day 6, the recovery of muAb in the serum was higher in the adjuvant group than in the native group. This finding suggests, that the progress of generation of ADAs started earlier in the native group. A slower absorption of the protein adsorbed to the aluminum hydroxide particles from the s.c. injection site and thus a sustained recognition by the immune system can be assumed.

Within the test groups, only the formulation containing soluble aggregates from light exposure resulted in low but detectable amounts of muAb circulating in the blood. Interestingly, the BALB/c mice that received this formulation revealed a slowly decreasing pharmacokinetic profile indicating that these aggregates did not induce an ADA generation as fast as after administration of native muAb or adjuvant plus native muAb. In C57BL/6 mice these aggregates induce fast ADA formation and thus minor muAb levels were detected on day 6.

#### **8.4.2 Immunogenicity of muAb in the control groups**

The administration of the formulation buffer did not induce significant levels of ADAs, neither in C57BL/6 nor in BALB/c mice. Since C57BL/6 has been reported as a mouse strain typically showing cellular immune responses, with only minor elicitation of antibodies, the anti-drug antibody responses to the aggregate containing formulations are anticipated to be low. Confirming the results from pharmacokinetic ELISA, the ADA levels detected in animals that received native muAb or adjuvant plus native muAb remained close to the baseline values. The intended positive control consisting of the native muAb plus an adjuvant did not result in the expected strongly increasing levels of IgG1, IgG2b or IgG3 directed towards muAb.

Anti-muAb IgG2a levels were determined in BALB/c but not in C57BL/6 mice, because the latter are known to be incapable to generate this isotype [Martin *et al.*, 1998]. BALB/c mice were assumed to recognize the native muAb as foreign molecule, but were included in this study because of the typically strong generation of antibodies. The exclusive administration of the native muAb served as a reference in these animals, since the aim was to detect increased immunogenicity of formulations containing aggregates, compared to those of the native drug molecule. Therefore, a significant immune response to an aggregate always related to the response of mice of the same strain, on the same bleeding time point, that received the native muAb formulation. This assumption was supported by the increased levels of IgG1, IgG2a and IgG2b after administration of the formulation containing the native muAb. They were significantly higher than those after administration of placebo formulation ( $p < 0.01$ ). The positive control including alum as an adjuvant resulted in increased levels of IgG1 and IgG2a as well. For anti-muAb IgG1 they were even higher than after administration of the native muAb ( $p < 0.01$ ), whereas for IgG2a they were on a similar level. The animals receiving the adjuvant resulted in anti-muAb IgG2b levels comparable to the animals receiving placebo. It can be concluded that the effect of the adjuvant Alum on the formation of anti-muAb antibodies is weak.

#### **8.4.3 Soluble aggregates of muAb**

The oligomers that were formed after light exposure and separated by field-flow fractionation (Group 4) were stored at  $-80^{\circ}\text{C}$  prior to injection. The stability of those aggregates during storage was shown in previous studies [Freitag *et al.*, 2011]. These aggregates are also known to be of reversible constitution and tend to dissociate back into monomeric species when

stored in an unfrozen state. It can be assumed, that such weakly associated (dissociable) aggregates will not exist for a long time after subcutaneous injection. However, the exposure to light induced some chemical alterations and oxidation processes to the molecules that will still be present after dissociation. Interestingly, the application of soluble aggregates after light exposure resulted in an IgG1 ADA profile deviating from all other dosing groups in C57BL/6 mice. The progressively increasing absorbance ratio tremendously dropped during the six-week recovery phase. In comparison, all other immune responses determined throughout this study resulted in the generation of persistent levels of ADAs. This observation suggests the generation of IgG1 ADAs that are rapidly eliminated when the antigen is not present anymore. The elimination presumably was accelerated by immune complex formation with native muAb released from the soluble aggregates. Considering the reversibility of these soluble aggregates, an enhanced availability of native muAb several days after the last administration is supposed. However, in the FTIR spectra of the muAb sample containing these aggregates substantial alterations of the secondary structure were detected, suggesting that also after dissociation non-native structures are present. If no additional aggregates are applied, the muAb content can either level or even exceed the ADA content, and no more positive IgG1 ADA results are obtained anymore because of immune complex formation. The ADA profiles of IgG2b and IgG3 induced by the same aggregate species did not show these tendencies. The increases within the first four weeks of the study were slower than for IgG1 and no drop was detectable after the recovery phase.

#### **8.4.4 Insoluble aggregates of muAb**

Insoluble aggregates are very large particles composed of associated protein molecules. They can be either visible or subvisible and some tend to precipitate, while others do not. The insoluble aggregates investigated in this study were all separated from soluble species by centrifugation. Four different stress factors lead to the rapid formation of considerable amounts of such large particles.

The absorption or degradation of subcutaneously administered aggregates, especially the particulate structures, has not yet been reported in literature. The differences in the immunoglobulin profiles (regarding e.g. IgG isotypes, time and strength of immune response) observed after administration of insoluble aggregates for example after stirring and shaking in our study, might arise from the sustained absorption to the lymphatic system and are probably not directly related to a lower or higher immunogenicity. The resulting absorbance unit read out of the ELISA related to the value before any injection of each individual animal cannot easily be converted into total concentrations of anti-drug antibodies, since no appropriate reference was available. This lack of appropriate references is a disadvantage of using a murine antibody in a wild-type mice model instead of using a human antibody in transgenic mice. In a transgenic animal model the process of creating tolerance against the human protein would meanwhile entail the formation of mouse anti-human protein antibodies before tolerance is achieved. These immunoglobulines will later on serve as reference for antibodies elicited e.g. by protein



aggregates. However, using the wild-type model one can distinguish between the magnitudes of the absorbance ratios to rank the immunogenic potential of those aggregates. The most relevant aggregates in this study seem to be insoluble aggregates. Especially those generated by light exposure are able to rapidly induce the generation of ADAs.

#### 8.4.4.1 Aggregation by light exposure

The insoluble aggregates after light exposure showed substantial alterations in secondary structure. The results of the ELISA which was used to determine the recovery of muAb in the injected samples indirectly confirmed these changes, since the muAb in this formulation was the only one of the stressed protein species that was not at all able to bind TNF- $\alpha$  within the pharmacokinetics ELISA. It can be suggested that the complementarity determining region (CDR) was structurally modified due to light irradiation and therefore the elicited ADAs are not directed towards CDR. Results from mass spectrometry furthermore indicate that those aggregates possess chemically altered sequences and oxidized patches in the CDR region of the antibody (data not shown). Hence, other insoluble aggregates with a more native-like structure were expected to be more immunogenic in the sense that they induce ADAs directed towards the native muAb.

Surprisingly, the insoluble aggregates generated by light exposure rapidly induced the formation of ADAs, even significantly exceeding the formation of ADAs after administration of the positive control on days 20, 27 and 71 ( $p < 0.01$ ). These results indicate that aggregates from light exposure with chemical and structural changes induce binding antibodies towards muAb, and thus can also have a strong impact on pharmacokinetics and efficacy. Compared to the soluble aggregates generated by light exposure, all generated ADAs persisted over the entire study. That suggests an influence of the size of the aggregates or the more pronounced structural changes on the mechanisms of ADA formation.

#### 8.4.4.2 Aggregation by mechanical stress

Two other formulations that induced ADA release of many IgG isotypes are those consisting of aggregates from stirring or shaking (Groups 6 and 7). In both formulations the native structure of muAb is maintained, but subvisible particle formation occurred. The formulation obtained by stirring included the highest numbers of subvisible particles compared to all other formulations. The administration of these aggregates induced significant ADA levels of at least two isotypes in each mouse strain. This indicates a relation between the loading of subvisible particles in a formulation and the immune response. The aggregates generated by shaking resulted in lower numbers of subvisible particles detectable by light obscuration and induced significant amounts of anti-muAb antibodies in BALB/c mice but not in C57BL/6 mice. Overall and cautiously, a qualitative correlation of the number of particles and ADA generation can be assumed. However, the enhanced IgG1 and IgG2a levels in BALB/c induced by those

aggregates are on a very similar level and thus no ranking between the immune response of both aggregate species is possible in this species.

#### 8.4.4.3 Aggregation by elevated temperature

The aggregates generated by storage at 60°C possess the most distinct altered secondary structure of all muAb formulations. At the same time, this formulation shows less subvisible particles  $\geq 1 \mu\text{m}$  than all other insoluble aggregate formulations. The heated species failed to induce an immune response exceeding the response to the native muAb in BALB/c. In C57BL/6 mice slightly enhanced IgG3 levels were detected after administration of aggregates obtained from heating. The strong structural changes within the aggregates might have impeded the formation of antibodies directed towards the native structure of muAb and thus only minute ADAs were detected. Within the ELISA format to determine the recovery of muAb in the formulations a marginal binding to TNF- $\alpha$  was detected. This was not surprising due to the heavy structural changes discovered in those aggregate species.

#### 8.4.5 Species differences

It was already reported, that immune responses of C57BL/6 and BALB/c mice differ between the strains [Mills *et al.*, 2000]. The most obvious reason is the known preferential  $T_H2$  response in BALB/c mice. Hence, there may be more than one explanation for the varying IgG profiles detected in the two strains. The foreignness of muAb to BALB/c is probably one reason for the higher absorbance ratios in the ADA assays and the completely modified pharmacokinetic profile. The differences discovered in the isotypes of generated ADAs within one mouse strain are well-known phenomena. Interestingly, the IgG1 isotype is the one with the highest incidence in BALB/c mice (the preferential  $T_H2$  responders), whereas C57BL/6 (the preferential  $T_H1$  responders) primarily elicit ADAs of IgG3 isotype. Coutelier *et al.* reported in 1988 the dependence of IgG subclass generation on the present antigen in mice. Antibodies towards proteins and carbohydrates were found to be restricted to the IgG1 and IgG3 subclass, whereas antiviral antibodies predominantly belonged to the IgG2a subclass [Coutelier *et al.*, 1988]. A predominant mechanism of the  $T_H1$  immune response implies the release of IFN- $\gamma$  and enhances the secretion of IgG2a [Stevens *et al.*, 1988]. However, since C57BL/6 are not able to generate IgG2a subclass [Martin *et al.*, 1998], these immunoglobulins were not investigated in this study. Instead, IgG3 preponderated in this mouse strain. In BALB/c mice, being predominantly  $T_H2$  responders, the cytokine IL-4 is mainly secreted leading to strong IgG1 responses [Ramakrishna *et al.*, 2003]. Although the  $T_H2$  mechanism is preferred, a minor  $T_H1$  response will be present as well, inducing the IgG2a subclass. In BALB/c the dominating IgG ADA subclass was also shown to be dependent on the route of administration [Feltquate *et al.*, 1997]. However, throughout this study, the samples were administered subcutaneously and therefore no impact on the IgG subclass was expected.

None of the investigated aggregate formulations was capable to induce each of the investigated IgG isotypes of ADAs, though each formulation induced at least one immunoglobulin isotype. The differences in the aggregate features therefore seem to result in different profiles of immunogenicity and in diverging immunoglobulin patterns. Significant differences were detected between the insoluble aggregate species mostly consisting of micron-sized particles. These aggregates were characterized by diverging numbers of subvisible particles per ml and by distinct secondary structures, determined by FTIR spectroscopy. Additionally, the immune responses to the aggregates obtaining a substantially altered secondary structure of the protein vary a lot. Especially the aggregates generated by light exposure were capable to induce a strong immune response, whereas the aggregates generated by heating revealed only minor formation of IgG ADAs. The aggregates from stirring and shaking, revealing a native-like structure, resulted in similar responses in BALB/c mice, but the ADA levels in C57BL/6 did not resemble each other. Therefore, more detailed information on the aggregates is preferably needed to explain the differences in their immunogenic potential.

In this study, only 5 µg of protein were injected at each time point. Otherwise, with high doses of a potentially immunogenic material tolerance might have been induced, leading to false negative results and covering the responses. However, the injected formulations consisted of almost pure aggregates. This finally implied the administration of very high doses of aggregates to each animal, compared to only trace amounts in typically administered liquid formulations of therapeutic proteins. This high dose of immunogenic material resulted in an altered pharmacokinetic profile in BALB/c mice and probably would have entailed a complete loss of efficacy of the drug. The dose dependency was not subject of this study but has to be investigated in future. It would be of interest to get more information if low amounts of only a few percent of aggregates in the presence of > 90% native drug within a formulation can have such a dramatic impact as well. However, this first study aimed to see whether aggregates have an immunogenic effect in wild-type animals at all and therefore based on high doses.

## **8.5 CONCLUSION**

This study for the first time proves the immunogenicity of various well-defined aggregates of a monoclonal antibody (muAb) in a wild-type animal model. All selected aggregates might potentially occur during protein manufacturing and are thus defined as relevant for immunogenicity testing. Compared to many other recently published in vivo studies a murine monoclonal antibody (muAb) was investigated in wild-type mice. The selection of the mouse strain to investigate the immune response to a murine protein has an impact on the results. Though the genetic background of C57BL/6 and BALB/c mice differs only marginally, the immune responses in terms of the generation of anti-drug antibodies is substantially different. A murine protein can even be foreign to mice. The same aspect might hold true for

human proteins globally administered to various human races, leading to diverging incidences of immunogenic side reactions to therapeutic proteins.

All aggregates incorporated show increasing ADA levels of one or another immunoglobulin isotype. The exposure to light and elevated temperatures, stirring, and shaking are therefore relevant parameters that can entail immunogenicity to a therapeutic protein due to aggregation. However, the resulting immune response strongly depends on the type of aggregate that is administered and cannot be generalized for all aggregates of a certain protein. It was already expected beforehand, that there is a relation between features of the aggregate species and the kinetics of elicitation of ADAs and the resulting IgG isotype. This study clearly approved this assumption. For example the results indicate that weak/reversible aggregates can result in completely different ADA profiles compared to the situation for more stable aggregates. However, little is known what happens to aggregates after subcutaneous injection. Thus, detailed studies tracking protein aggregates *in vivo*, for example by labeling them, have to be conducted, if one wants to determine possible relations between the duration of aggregate uptake and the immune response. The divergence in aggregate uptake and metabolism might also be a reason for some aggregates not reaching the same absorbance ratios in IgG ADA assays at the same time as the native muAb in BALB/c mice.

An interesting novelty the results of this study reveal is that the most critical aggregates seem to be of large insoluble nature and these aggregates do not necessarily have to maintain a native-like structure. Especially insoluble aggregates from light exposure and stirring lead to rapid formation of high ADA levels. Both species can be considered to be a particular contamination potentially occurring during production and handling of the drug, presented to the immune system. The light exposed samples possess an oxidized amino acid sequence, whereas the stirred samples preserve a native-like structure but consist of much higher particle numbers. The evident improvements in quality and purity of therapeutic protein production can largely exclude these impurities. Purification steps can be extended to reduce the amount of oxidized molecules. Several new techniques to improve the detection of subvisible particles in protein formulations emerged within the last years [Zoells *et al.*, 2012]. Based on this progress, a limitation of the numbers of subvisible particles in the range from 1 - 10  $\mu\text{m}$  for approval is currently under debate in industry, academics and authorities [Carpenter *et al.*, 2009; Singh *et al.*, 2010].

However, the smaller and soluble aggregates generated by light exposure that were preliminary shown to be dissociable, were immunogenic as well. Therefore, the size of aggregates is not exclusively responsible for ADA formation. The detection of such soluble aggregates during production by size-exclusion chromatography is rather simple, though no fixed limits for the maximum percentage of soluble aggregates in a therapeutic protein formulation have yet been set. Interestingly, these aggregates resulted in non-persistent IgG1 ADAs in C57BL/6 mice, indicating another mechanism of antibody elicitation.

Chromatographic purification is suitable to separate soluble aggregates from a formulation (though only throughout production but not after storage), whereas especially subvisible particles are difficult to remove. Regarding the strong detected immune responses towards particulate (insoluble) aggregates, the discussion on analytical techniques to quantify small subvisible particles in therapeutic protein formulations is justified [Carpenter *et al.*, 2009; Singh *et al.*, 2010].

The obtained immunogenic differences between two inbred wild-type mouse strains that possess rather similar genetic characteristics are considered to be another important outcome of this study.

## 8.6 REFERENCES

[Berger *et al.*, 2002], Therapeutic applications of monoclonal antibodies, *The American journal of the medical sciences*, 324, 14-30

[Braun *et al.*, 1997], Protein aggregates seem to play a key role among the parameters influencing the antigenicity of interferon alpha (IFN-alpha ) in normal and transgenic mice, *Pharmaceutical Research*, 14, 1472-1478

[Carpenter *et al.*, 2009], Overlooking subvisible particles in therapeutic protein products: gaps that may compromise product quality, *J. Pharm. Sci.*, 98, 1201-1205

[Coutelier *et al.*, 1988], Virally induced modulation of murine IgG antibody subclasses, *Journal of Experimental Medicine*, 168, 2373-2378

[Dintzis *et al.*, 1976], Molecular determinants of immunogenicity: The immunon model of immune response, *Proceedings of the National Academy of Sciences of the United States of America*, 73, 3671-3675

[Feltquate *et al.*, 1997], Different T helper cell types and antibody isotypes generated by saline and gene gun DNA immunization, *Journal of immunology (Baltimore, Md. : 1950)*, 158, 2278-2284

[Freitag *et al.*, 2011], The preparative use of flow field-flow fractionation, *LC-GC Europe*, 24, 134, 136, 138, 140

[Haley, 2003], Species differences in the structure and function of the immune system, *Toxicology*, 188, 49-71

[Hermeling *et al.*, 2005], Structural Characterization and Immunogenicity in Wild-Type and Immune Tolerant Mice of Degraded Recombinant Human Interferon Alpha2b, *Pharmaceutical Research*, 22, 1997-2006

[Martin *et al.*, 1998], The need for IgG2c specific antiserum when isotyping antibodies from C57BL/6 and NOD mice, *Journal of Immunological Methods*, 212, 187-192

[Mills *et al.*, 2000], M-1/M-2 macrophages and the Th1/Th2 paradigm, *Journal of Immunology*, 164, 6166-6173

[Petrovsky *et al.*, 2004], Vaccine adjuvants: current state and future trends, *Immunology and Cell Biology*, 82, 488-496

[Ramakrishna *et al.*, 2003], T helper responses to japanese encephalitis virus infection are dependent on the route of inoculation and the strain of mouse used, *Journal of General Virology*, 84, 1559-1567

[Schellekens, 2005], Immunologic mechanisms of EPO-associated pure red cell aplasia, *Best Practice & Research, Clinical Haematology*, 18, 473-480

[Schemthaner, 1993], Immunogenicity and allergenic potential of animal and human insulins, *Diabetes care*, 16 Suppl 3, 155-165

[Schoeneich, 2010] Light-induced oxidation and aggregation of proteins: potential immunogenicity consequences, *Workshop on Protein Aggregation and Immunogenicity, Breckenridge, CO, July 20-22, 2010*

[Singh *et al.*, 2010], An industry perspective on the monitoring of subvisible particles as a quality attribute for protein therapeutics, *J. Pharm. Sci.*, 99, 3302-3321

[Stevens *et al.*, 1988], Regulation of antibody isotype secretion by subsets of antigen-specific helper T cells, *Nature (London, United Kingdom)*, 334, 255-258

[Vollmar, 2005], Immunologie - Grundlagen und Wirkstoffe, 1st Edition, *Wissenschaftliche Verlagsgesellschaft mbH Stuttgart*, 455 pp,

[Wang, 2005], Protein aggregation and its inhibition in biopharmaceutics, *International Journal of Pharmaceutics*, 289, 1-30

[Watanabe *et al.*, 2004], Innate immune response in Th1- and Th2-dominant mouse strains, *Shock*, 22, 460-466

[Wierda *et al.*, 2001], Immunogenicity of biopharmaceuticals in laboratory animals, *Toxicology*, 158, 71-74

[Zoells *et al.*, 2012], Particles in therapeutic protein formulations, Part 1: Overview of analytical methods, *J. Pharm. Sci.*, 101, 914 - 935

## 9 FINAL SUMMARY AND CONCLUSIONS

---

The overall aim of this thesis was to investigate the immunogenicity of protein aggregates *in vivo*. The objectives of this work originate from consolidated findings reported in earlier studies that protein aggregates can induce immunogenicity [Braun *et al.*, 1997; Fradkin *et al.*, 2009; Hermeling *et al.*, 2006; Rosenberg, 2006]. However, the previous studies all utilized transgenic animal models that artificially were made tolerant towards foreign (especially human) proteins. This study was initiated to use for the first time wild-type animals and a protein originated from the same species: a murine monoclonal antibody was investigated in mice. Additional motivation of the thesis was the separation of aggregates from non-aggregated protein species before application to the animals. This approach would imply a close correlation between a certain aggregate species and an immune response – independent from potentially accompanying species such as fragments. Due to the increasing importance of monoclonal antibodies in therapeutic perspectives, the study focused on a monoclonal antibody as model protein. Finally, the ambiguity whether all aggregates or only a certain species exhibiting specific characteristics can trigger immunogenicity, was a major question that should be addressed during the studies in this project.

The thesis can be subdivided in two major parts: First, the generation and characterization of the aggregates was carried out. These studies include a detailed physicochemical characterization of the protein and the separation of the generated aggregates from concomitant protein species. The second part of the thesis presents animal studies that investigate the effect of aggregates *in vivo*. A proper assay format to determine the immunogenicity was required and established. The immunogenicity of various aggregates was investigated using the implemented methods.

Chapter 1 describes the objectives of the thesis.

In chapter 2 a general introduction into the topic of protein aggregation and immunogenicity is given. A focus of the discussion is put on the currently accepted pathways of protein aggregation. Five major mechanisms are discriminated by the most important scientific reviews [Chi *et al.*, 2003; Philo *et al.*, 2009; Wang, 2005]. The pathways are generally classified firstly according to the structure of the protein species involved in aggregation, being conformationally altered, chemically modified or native, and secondly according to external triggers that can provoke aggregation, such as surfaces and “critical nuclei” that arise in the formulation. The most common techniques to characterize protein aggregates of different type are described in chapter 2 as well. A special focus during the analytical part is put on field-flow fractionation, since this technique represents a crucial part of the overall work. Furthermore, the introduction discusses factors that potentially influence immunogenicity of protein therapeutics

and a rough overview of the mechanisms of immune responses in human. The elicitation of antibodies that are directed towards the protein are the main focus of the immunogenicity studies in this work. Finally, a short introduction in structure and pharmacokinetics of monoclonal antibodies (mAbs) is given as well, since this thesis bases on mAbs as model proteins.

Chapter 3 describes a first aggregation study using a human model protein. The aim of this chapter is to prepare for the following chapters. Information on the aggregation of the mAb is collected and analytical methods to characterize the aggregates are developed, that subsequently (chapter 4) are transferred to the protein of interest.

A human IgG1 antibody was stressed by a variety of methods that were defined to be relevant conditions reflecting different steps during production, shipment and handling of biopharmaceuticals. The mechanical stress methods stirring and shaking first and foremost induce particulate aggregates that are detectable by increasing turbidity and generation of subvisible particles. Light exposure and storage at elevated temperatures induce the generation of soluble protein species like aggregates and fragments, detected by size exclusion chromatography. Repetitive freeze-thaw cycles did not result in substantial formation of aggregates or substantial changes in the protein structure. Thus, this approach to generate aggregates is not followed up throughout this work. A variety of physicochemical methods to evaluate the protein structure and aggregate content are described and compared. The methods complement one another and give a broad overview about the consequences of the stress methods on protein stability. The most striking modifications in protein structure are induced by exposure to light.

In chapter 4 the previously developed methods to generate and analyze protein aggregates are transferred to a murine monoclonal IgG2c antibody. The aggregation behavior of this protein is similar to the human protein investigated in the previous chapter: (i) Stirring and shaking induce particulate aggregates but no soluble species. (ii) Light exposure and storage at elevated temperatures result in the formation of soluble aggregates and fragments. (iii) Light exposure induces drastic structural alterations in the murine antibody as well. Concerning the later *in vivo* studies all four stress methods are considered to be relevant and suitable to induce a sufficient amount of aggregates from the murine antibody. Light exposure turned out to be the only incubation method that reveals huge amounts of soluble aggregates. Therefore, this type of stress will be utilized to implement a method to preparative use asymmetric flow field-flow fractionation (AF4) to separate soluble aggregates from monomeric protein.

In chapter 5 a preparative AF4 method using the human model antibody after light exposure was developed. The key point is the successful implementation of a semi-preparative channel prototype and a fraction collector to the system. Subsequently, a method to collect large amounts of aggregates generated by light exposure is developed. The dilution in



consequence of the fractionation principle limits the directly achievable protein concentration in the collected aggregate fraction. Therefore, a concentration step is necessary. Different disposable concentrators are evaluated in chapter 5. Protein aggregate concentrations up to ~650 µg/mL were achieved. The stability of these fractions during storage at 2 – 8°C and at -80°C was found to be sufficient for supporting an *in vivo* study.

In the following chapter 6 the preparative use of AF4 was successfully transferred to the murine antibody. The focus of this chapter is put on the low endotoxin level in the final aggregate fraction. A meticulous cleaning procedure of the entire AF4 instrument and all devices used was established. The collected and subsequently concentrated fractions meet the requirements of the European Pharmacopoeia (< 0.25 EU/mL) [PhEur 0169, 2011]. A sufficient protein concentration of approximately 600 µg/mL was achieved in the final aggregate fraction. The low endotoxin level of < 0.1 EU/ml and the proper stability during storage at -80°C prove the applicability of the developed fractionation procedure of the murine antibody in preparation of an *in vivo* study.

The conducted animal studies are described in chapters 7 and 8. First of all, in chapter 7, two different ELISA set-ups are described. Both were used to detect the immunogenicity of anti-drug antibodies towards the murine monoclonal antibody used. It has to be mentioned that one part of this study was performed at the University of Colorado in the research group of Theodore W. Randolph. The entire sample preparation and animal handling for this first study was performed at the site of an industrial partner under command and responsibility of the Department of Pharmaceutical Technology and Biopharmaceutics at the LMU Munich by myself. Solely the analytics using a second ELISA method were conducted abroad in Colorado after shipping the left-over serum samples to our colleagues. However, for better understanding and comprehension of the second animal studies, these results are provided as well. The assay design was found to be crucial for reliable results in immunogenicity investigations. The need of acid dissociation of immune complexes in the serum samples is proven in chapter 7. The long half-life of monoclonal antibodies implies the circulation of native drug molecules that capture Anti-drug antibody molecules and thus elude them from detection by ELISA. The ADA detection without an acid dissociation step revealed no immunogenicity of the mixture of muAb aggregates used throughout this study. Two different doses of soluble and insoluble aggregates generated by light exposure and stirring were included in this study to cover a broad range of aggregate features. The inclusion of an acid dissociation step can be used to overcome that effect. Dissociating the immune complexes enables the detection of ADAs in the animals that received muAb aggregates.

Besides the method development, this study shows that the murine antibody sample containing various types of aggregates and fragments induces a substantial immune response in wild-type mice. This immunogenic potential is concluded to be related to the presence of muAb aggregates and/or fragments, since no foreignness of muAb in the mice is expected.

Furthermore, the higher dose of aggregates applied to the mice results in higher ADA levels showing the dose dependency of immunogenicity of protein aggregates.

The study described in this chapter for the first time investigated the immunogenicity of protein aggregates (murine) in wild-type animals (mice) and proves the suitability of this approach closely resembling the therapeutic situation of human proteins in human patients.

The final and pivotal animal studies are described and discussed in chapter 8. A variety of different well-defined aggregates from the murine IgG2c antibody were separated from the monomer and fragments to the extent possible. The detection of anti-drug antibodies of different IgG isotypes based on the assay set-up developed in the previous section. The ELISA results prove that protein aggregates can elicit an immune response in terms of anti-drug antibodies.

Two different mouse strains are included in this study. Though the genetic background of C57BL/6 and BALB/c mice differs only marginally, the immune responses in terms of the generation of anti-drug antibodies is substantially different. A murine protein can even be foreign to mice. This is an interesting aspect with regards to the different human races. Different incidences of immunogenic side reactions to therapeutic proteins triggered by protein aggregates in various populations might be the consequence.

All aggregates included in this study induced an immune response. Since only aggregates relevant for production and handling of therapeutic proteins are investigated, it has to be concluded that in general all aggregates and particles determined in a drug product should be reduced to the extent possible before release of the drug.

However, the experiments also prove that different aggregates result in different immune responses. The responses for example differ in strength, duration as well as in the IgG isotypes preferentially generated by the individuals. Two features of the aggregates are concluded to be crucial for immunogenic reactions: the size and chemical modifications in the molecule. A high and persisting immune response is detected after repeated application of insoluble aggregates obtained from light exposure, from stirring and from shaking. In conclusion, large protein aggregates and subvisible particles can induce strong immune response. As far as investigated in this study smaller soluble aggregates result in a weaker and short-term increase of ADAs. Interestingly, aggregates possessing strong structural alterations due to chemical modifications reveal high ADA levels. Against all expectations aggregates that failed to bind the desired antigen because of a heavily altered structure induced immense immune responses in mice. Thus the generation of anti-drug antibodies not necessarily requires unmodified CDR regions of the monoclonal antibody molecules incorporated in the aggregate.

The generated immunoglobulin isotype of ADAs towards the aggregates strongly differ between C57BL/6 mice and BALB/c mice. As expected, BALB/c mice preferably generate antibodies of IgG1 isotype, whereas C57BL/6 mice show the highest levels in IgG3 isotype. The

generated immunoglobulin isotypes differ also within one mouse strain. This aspect might be related to variations in kinetics and mechanisms of absorption of the aggregates after subcutaneous injection but is not subject of this study.

This thesis touches the huge topic of the relation of protein aggregates and immunogenicity. For the first time, this study has shown the suitability of using wild type mice to investigate murine antibodies compared to the transgenic approach. The immunogenicity of a variety of aggregates of a monoclonal antibody was proven and revealed remarkable differences between the aggregates, with regards to strength and type of ADAs generated. Besides these major findings the work showed, that a proper assay format is crucial for the detection of anti-drug antibodies and that the immune response differs between different mouse strains. Based on the established assay format, further investigations should be conducted to gain a more detailed understanding of the immunogenicity of protein aggregates in wild type animals.

## 9.1 REFERENCES

- [Braun *et al.*, 1997], Protein aggregates seem to play a key role among the parameters influencing the antigenicity of interferon alpha (IFN-alpha ) in normal and transgenic mice, *Pharmaceutical Research*, 14, 1472-1478
- [Chi *et al.*, 2003], Physical Stability of Proteins in Aqueous Solution: Mechanism and Driving Forces in Nonnative Protein Aggregation, *Pharmaceutical Research*, 20, 1325-1336
- [Fradkin *et al.*, 2009], Immunogenicity of aggregates of recombinant human growth hormone in mouse models, *J Pharm Sci*, 98, 3247-3264
- [Hermeling *et al.*, 2006], Antibody response to aggregated human interferon alpha2b in wild-type and transgenic immune tolerant mice depends on type and level of aggregation, *J. Pharm. Sci.*, 95, 1084-1096
- [PhEur 0169, 2011], Monograph "Water for injections", *European Directorate for the Quality of Medicine (EDQM)*, 7th edition,
- [Philo *et al.*, 2009], Mechanisms of protein aggregation, *Current Pharmaceutical Biotechnology*, 10, 348-351
- [Rosenberg, 2006], Effects of protein aggregates: an immunologic perspective, *The AAPS Journal* 2006, 8, E501-E507
- [Wang, 2005], Protein aggregation and its inhibition in biopharmaceutics, *International Journal of Pharmaceutics*, 289, 1-30



## LIST OF ABBREVIATIONS

---

ADA	-	Anti-drug antibody
AF4	-	Asymmetrical flow field-flow fractionation
ANS	-	8-Anilinonaphthalene-1-sulfonate
APC	-	Antigen presenting cell
ATR	-	Attenuated total reflectance
AU	-	Absorbance units
a.u.	-	arbitrary units
AUC	-	Area under the curve
BALB/c	-	Inbred mouse strain BALB/c
$\mu$ -BCA	-	Micro bicinchoninic acid assay
BCR	-	B cell receptor
BSA	-	Bovine serum albumin
C57BL/6	-	Inbred mouse strain C57BL/6
CD4+	-	T-helper cells
CDR	-	Complementarity determining region
C <sub>H</sub>	-	Constant region of heavy chain
CHO	-	Chinese hamster ovary
C <sub>L</sub>	-	Constant region of light chain
CPMP	-	Committee for Proprietary Medicinal Products
DC	-	Dendritic cell
DLS	-	Dynamic light scattering
DMSO	-	Dimethylsulfoxide
DNA	-	Deoxyribonucleic acid

dn/dc	-	Refractive index increment
μ-DSC	-	Micro differential scanning calorimetry
DTT	-	Dithiothreitol
ECD	-	Equivalent circle diameter
ELISA	-	Enzyme-linked immuno sorbent assay
EMA	-	European Medicines Agency
EU	-	Endotoxin units
Fab	-	Antigen-binding fragment
Fc	-	Crystallizable fragment
FcRn	-	Neonatal Fc receptor
FDA	-	U.S. Food and Drug Administration
FFF	-	Field-flow fractionation
FIM	-	Flow Imaging Microscopy
F <sub>In</sub>	-	Channel inlet flow
FNU	-	Formazine nephelometric units
F <sub>out</sub>	-	Channel outlet flow
FTIR	-	Fourier transform infrared spectroscopy
F <sub>x</sub>	-	Cross-flow
G-CSF	-	Granulocyte colony-stimulating factor
GI	-	Gastrointestinal tract
GM-CSF	-	Granulocyte macrophage colony-stimulating factor
GPC	-	Gel permeation chromatography
HAMA	-	Human anti-mouse antibody
HMW	-	High molecular weight
H <sub>2</sub> O <sub>2</sub>	-	Hydrogen peroxide
HP-SEC	-	High performance size exclusion chromatography

HPW	-	Highly purified water
HRP	-	Horseradish peroxidase
huAb	-	human monoclonal antibody
ICH	-	International Conference on Harmonization
Ig	-	Immunoglobulin
IgG	-	Immunoglobulin class G
IM	-	Intramuscular
IMW	-	Intermediate molecular weight
IV	-	Intravenously
kDa	-	Kilo Dalton
LAL	-	Limulus amebocyte lysate
LMW	-	Low molecular weight
LO	-	Light obscuration
LOD	-	Limit of detection
LPS	-	Lipopolysaccharide
mAb	-	monoclonal antibody
MALLS	-	Multi angle laser light scattering
mg	-	Milligram
MHC-II	-	Major histocompatibility complex class II
ml	-	Milliliter
µm	-	Micrometer
µM	-	Micromolar
muAb	-	murine monoclonal antibody
MW	-	Molecular weight
MWCO	-	Molecular weight cut-off
n/a	-	not applicable

nm	-	Nanometer
NTA	-	Nanoparticle tracking analysis
PAGE	-	Polyacrylamide gel electrophoresis
PAMP	-	Pathogen-associated molecular pattern
PBS	-	Phosphate buffered saline
PCS	-	Photon correlation spectroscopy
PDI	-	Polydispersity index
PES	-	Polyethersulfone
PhEur	-	European Pharmacopoeia
PK	-	Pharmacokinetics
PTFE	-	Polytetrafluoroethylene
QELS	-	Quasi-elastic light scattering
RI	-	Refractive index
RP-HPLC	-	Reversed phase high performance liquid chromatography
rpm	-	rounds per minute
SC	-	Subcutaneously
S.D.	-	Standard deviation
S.E.	-	Standard error of the mean
SDS	-	Sodium dodecyl sulfate
SEC	-	Size exclusion chromatography
SP1	-	Semi-preparative channel Prototype 1
SPF	-	Specific pathogen free
SV-AUC	-	Sedimentation velocity analytical ultracentrifugation
TCR	-	T cell receptor
TEM	-	Transmission electron microscopy
T <sub>h</sub> 1/T <sub>h</sub> 2	-	T-helper cells Type 1 and Type 2



$T_m$	-	Melting temperature
TMB	-	3,3',5,5'-Tetramethylbenzidine
$TNF\alpha$	-	Tumor necrosis factor $\alpha$
Trp	-	Tryptophane
Tyr	-	Tyrosine
USP	-	United States Pharmacopoeia
UV	-	Ultraviolet
$V_H$	-	Variable region of heavy chain
$V_L$	-	Variable region of light chain
VX	-	Cross flow
$W/m^2$	-	Watt per square meter
$Z_{ave}$	-	Z-average diameter



# LIST OF PRESENTATIONS AND PUBLICATIONS

---

## ARTICLES

Angelika J. Freitag, Maliheh Shomali, Stylianos Michalakis, Martin Biel, Michael Siedler, John F. Carpenter, Theodore W. Randolph, Gerhard Winter, Julia Myschik: *Are different protein aggregates equally immunogenic? – Investigation of the immunogenicity of protein aggregates of a murine monoclonal antibody in wild-type mice*: in preparation.

Angelika J. Freitag, Maliheh Shomali, Zehra Kaymakcalan, Ralf Löbbert, Angelika M. Vollmar, Michael Siedler, John F. Carpenter, Gerhard Winter, Julia Myschik, Theodore W. Randolph: *Detection of Anti-Drug Antibodies in Murine Serum Samples: The Need for Immune Complex Dissociation*: in preparation.

Angelika Juliane Freitag, Katharina Wittmann, Laura Isabell Immohr, Gerhard Winter and Julia Myschik: *Asymmetrical flow field-flow fractionation. A preparative tool to obtain endotoxin-free protein species for preclinical studies*: G.I.T. Laboratory Journal Europe 11-12/2011, Pages 17 - 19

Angelika Juliane Freitag, Laura Isabell Immohr, Gerhard Winter and Julia Myschik: *The Endotoxin-free Separation of Protein Species via Asymmetrical Flow Field-Flow Fractionation (AF4)*. Winner of Wyatt Application Note Contest Santa Barbara 2011, published online in October 2011

Angelika Juliane Freitag, Katharina Wittmann, Gerhard Winter and Julia Myschik: *The Preparative Use of Flow Field-Flow Fractionation (AF4)*. Wyatt Application Note, published online in July 2012

Angelika Juliane Freitag, Katharina Wittmann, Gerhard Winter and Julia Myschik: *The Preparative Use of Flow Field-Flow Fractionation (AF4)*. LC GC Europe Volume 24, Number 3, March 2011, Pages 134 – 140

## POSTER PRESENTATIONS

Freitag AJ, Myschik J, Schulze S, Winter G: *Preparative methods to reproducibly generate aggregates of monoclonal antibodies*. 7<sup>th</sup> World meeting on Pharmaceutics, Biopharmaceutics and Pharmaceutical Technology, 2010, Valletta/Malta

Freitag AJ, Myschik J, Schulze S, Winter G: *Immunogenicity of Protein Aggregates*. Science to Market Conference, Hannover, 6.-7.10.2009

Freitag AJ, Immohr LI, Winter G, Myschik J: *The Endotoxin-free Separation of Protein Species via Asymmetrical Flow Field-Flow Fractionation (AF4)*. 22<sup>nd</sup> Annual International Light Scattering Colloquium - October 31<sup>st</sup> – November 1<sup>st</sup> 2011, Santa Barbara, California, USA



# CURRICULUM VITAE

---

Angelika Juliane Freitag

## PERSONAL DATA

---

Date of birth: March 11<sup>th</sup>, 1984

Place of birth: Zwickau, Germany

Nationality: German

## PROFESSIONAL EXPERIENCE

---

Since 01 / 2012                      Project leader

Coriolis Pharma Research GmbH, Martinsried, Germany

## EDUCATION

---

04 / 2008 – 01 / 2012              Ph.D. thesis

Department of Pharmacy, Pharmaceutical Technology  
and Biopharmaceutics, Ludwig-Maximilians-University /  
München, Germany  
Supervisor: Prof. Dr. Gerhard Winter

11 / 2010 – 12 / 2010              Research stay at the University of Colorado, USA

Center for Pharmaceutical Biotechnology  
Supervisor: Prof. Dr. Theodore W. Randolph

02 / 2008                              License to practice as a Pharmacist ("Approbation")

01 / 2008 – 02 / 2008              Internship at Schwarz Pharma Produktions-GmbH in Zwickau

05 / 2007 – 10 / 2007              Internship at Glückauf-Apotheke in Zwickau

11 / 2006 – 04 / 2007              Internship at Boehringer Ingelheim Pharma GmbH & Co. KG in  
Biberach

10 / 2002 – 12 / 2007              Study of Pharmacy at University of Leipzig